nature chemistry

Article

https://doi.org/10.1038/s41557-024-01462-8

Tandem catalysis enables chlorine-containing waste as chlorination reagents

In the format provided by the authors and unedited

Contents

Materials and Methods

Materials

Inorganic salts including Cu salts, Pd salts and nitrates, solvents, alkyl chlorides and arene (if not specified) were purchased from Sigma-Aldrich and used directly unless specified otherwise. Pure polymers including polyvinylidene chloride (PVDC) M_w ~50,000/100000/250000, polychloroprene (chloroprene rubber, CR), polyepichlorohydrin (PECH) M_w ~700,000, poly(epichlorohydrin-co-ethylene oxide) (PECHEO, epichlorohydrin 64-69 wt.%) and poly(epichlorohydrin-co-CO_2) (PECHC) were purchased from Sigma-Aldrich. Compressed air, N_2 and O_2 was purchased from Carbagas. PVC or neoprene-based water pipe, electrical conduit, electric wire and vacuum tube were obtained from the chemical store at EPFL. PVDC blisters (Ibuprofen N Zentiva) was purchased from SUN STORE Pharmacies in Lausanne.

Typical reaction (standard condition)

Typical reaction using PVC water pipe as the chlorination reagent:

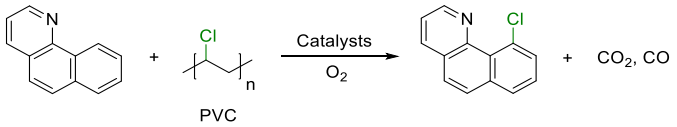

7,8-Benzoquinoline **1a** (0.25 mmol), PVC water pipe (1.5 equiv., 0.375 mmol), $Cu(NO_3)_2$•$3H_2O$ (20%, 0.05 mmol), PdO (5%, 0.0125 mmol), $NaNO_3$ (20%, 0.05 mmol), biphenyl (0.2 mmol, internal standard) and DMSO (2 mL) were added into glass insert vial of autoclave and charged with O_2 (3 bar). The reactor was heated to 140 ºC for 15 h. After cooling to room temperature, the gas products were collected with a Tedlar® gas sampling bag (Sigma-Aldrich) for analysis by gas chromatography (GC). Ethyl acetate (EA, 3×3 mL) and an aqueous saturated brine solution (5 mL) was added to the reaction mixture to extract the organic products. The combined organic phase was used for analysis. Further purification was achieved using silica gel chromatography (Hexane/ethyl acetate as eluent if not specified) when required.

Process mass intensity (PMI) = Total mass in process / Mass of products = [M(substrate) + M(PVC) + M($Cu(NO_3)_2$•$3H_2O$) + M(PdO) + M($NaNO_3$) + M(O_2)] / [M(product) + M(CO)]

Environmental factor (E-factor) = Mass of waste / Mass of products = [M(substrate) + M(PVC) + M($Cu(NO_3)_2$•$3H_2O$) + M(PdO) + M($NaNO_3$) + M(O_2) − M(product) − M(CO)] / [M(product) + M(CO)]

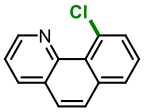

1b, 10-Chlorobenzoquinoline

^{1}H NMR (400 MHz, DMSO) δ 9.07 (dd, *J* = 4.3, 1.9 Hz, 1H), 8.46 (dd, *J* = 8.0, 1.9 Hz, 1H), 8.07 (dd, *J* = 7.9, 1.4 Hz, 1H), 8.01 (d, *J* = 8.8 Hz, 1H), 7.95 (d, *J* = 8.8 Hz, 1H), 7.87 (dd, *J* = 7.7, 1.3 Hz, 1H), 7.77 – 7.66 (m, 2H). ^{13}C NMR (101 MHz, DMSO) δ 148.31, 145.85, 136.59, 136.53, 131.83, 131.51, 128.64, 128.50, 127.76, 127.48, 126.97, 122.76.

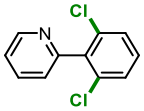

2b, 2-(2,6-dichlorophenyl)pyridine

^{1}H NMR (400 MHz, DMSO) δ 8.73 – 8.68 (m, 1H), 7.94 (t, *J* = 7.7 Hz, 1H), 7.59 (d, *J* = 8.1 Hz, 2H), 7.46 (dt, *J* = 17.0, 8.3 Hz, 3H). ^{13}C NMR (101 MHz, DMSO) δ 155.29, 149.96, 138.66, 137.32, 134.07, 131.23, 128.82, 125.31, 123.86.

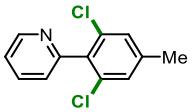

3b, 2-(2,6-dichloro-4-methylphenyl)pyridine

^{1}H NMR (400 MHz, DMSO) δ 8.70 (m, *J* = 4.9, 1.8, 1.0 Hz, 1H), 7.91 (td, *J* = 7.7, 1.8 Hz, 1H), 7.47 – 7.34 (m, 4H), 2.35 (d, *J* = 0.9 Hz, 3H). ^{13}C NMR (101 MHz, DMSO) δ 155.35, 149.91, 141.48, 137.15, 135.81, 133.65, 129.13, 125.45, 123.67, 20.65.

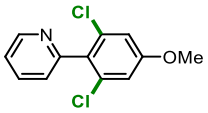

4b, 2-(2,6-dichloro-4-methoxyphenyl)pyridine

^{1}H NMR (400 MHz, DMSO) δ 8.68 (dt, *J* = 4.8, 1.4 Hz, 1H), 7.91 (td, *J* = 7.7, 1.9 Hz, 1H), 7.47 – 7.35 (m, 2H), 7.19 (s, 2H), 3.85 (s, 3H). ^{13}C NMR (101 MHz, DMSO) δ 160.08, 155.22, 149.89, 137.19, 134.56, 131.19, 125.84, 123.65, 114.63, 56.62.

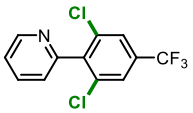

5b, 2-(2,6-dichloro-4-(trifluoromethyll)phenyl)pyridine

^{1}H NMR (400 MHz, DMSO) δ 8.74 (m, *J* = 4.8, 1.8, 1.1 Hz, 1H), 8.03 (d, *J* = 0.8 Hz, 2H), 7.98 (td, *J* = 7.7, 1.8 Hz, 1H), 7.49 (m, *J* = 7.7, 5.6, 1.1 Hz, 2H). ^{13}C NMR (101 MHz, DMSO) δ 154.24, 150.17, 142.50, 137.53, 135.34, 132.08, 131.74, 131.41, 131.08, 127.06, 125.82, 125.78, 125.75, 125.71, 125.03, 124.34, 124.27, 121.63, 118.91.

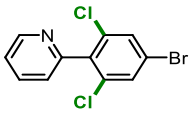

6b, 2-(2,6-dichloro-4-bromophenyl)pyridine

^{1}H NMR (400 MHz, DMSO) δ 8.71 (m, *J* = 4.9, 1.9, 1.0 Hz, 1H), 7.95 (td, *J* = 7.7, 1.8 Hz, 1H), 7.91 (s, 2H), 7.51 – 7.40 (m, 2H). ^{13}C NMR (101 MHz, DMSO) δ 154.48, 150.10, 138.03, 137.45, 135.09, 131.27, 125.32, 124.09, 122.46.

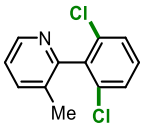

7b, 2-(2,6-dichloro-phenyl)-3-methyl-pyridine

^{1}H NMR (400 MHz, DMSO) δ 8.52 (m, *J* = 4.8, 1.6, 0.7 Hz, 1H), 7.80 (m, *J* = 7.7, 1.7, 0.9 Hz, 1H), 7.62 (dd, *J* = 8.0, 0.8 Hz, 2H), 7.50 (dd, *J* = 8.8, 7.3 Hz, 1H), 7.39 (dd, *J* = 7.8, 4.8 Hz, 1H), 2.03 (s, 3H). ^{13}C NMR (101 MHz, DMSO) δ 154.91, 147.55, 138.41, 137.99, 133.91, 132.09, 131.24, 128.81, 124.12, 18.05.

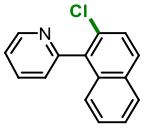

8b, 2-(2-chloronaphthalen-1-yl)pyridine

^{1}H NMR (400 MHz, $CDCl_3$) δ 8.76 (m, *J* = 4.9, 1.8, 1.0 Hz, 2H), 7.79 (m, *J* = 8.5, 6.9, 4.9 Hz, 6H), 7.48 (d, *J* = 8.8 Hz, 2H), 7.45 – 7.24 (m, 10H). ^{13}C NMR (101 MHz, $CDCl_3$) δ 156.66, 149.83, 136.41, 136.10, 133.24, 132.12, 130.70, 129.76, 128.04, 127.18, 126.01, 125.69, 122.67,

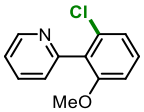

9b, 2-(2-chloro-6-methoxyphenyl)pyridine

^{1}H NMR (400 MHz, $CDCl_3$) δ 8.65 (m, *J* = 4.9, 1.8, 1.0 Hz, 1H), 7.67 (td, *J* = 7.7, 1.8 Hz, 1H), 7.27 – 7.16 (m, 3H), 7.01 (dd, *J* = 8.1, 1.0 Hz, 1H), 6.81 (dd, *J* = 8.4, 1.0 Hz, 1H), 3.64 (s, 3H). ^{13}C NMR (101 MHz, $CDCl_3$) δ 158.25, 154.97, 149.47, 136.05, 134.13, 129.79, 129.20, 125.67, 122.36, 121.82, 109.53, 77.31, 56.11.

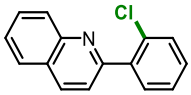

10b, 3-(2-chlorophenyl)isoquinoline

^{1}H NMR (400 MHz, $CDCl_3$) δ 8.19 – 8.07 (m, 2H), 7.81 (dd, *J* = 8.0, 1.5 Hz, 1H), 7.72 – 7.64 (m, 2H), 7.66 – 7.58 (m, 1H), 7.51 (m, *J* = 8.2, 6.9, 1.2 Hz, 1H), 7.44 (dd, *J* = 7.2, 2.0 Hz, 1H), 7.33 (pd, *J* = 7.4, 1.8 Hz, 2H). ^{13}C NMR (101 MHz, $CDCl_3$) δ 157.45, 148.11, 139.70, 135.67, 132.39, 131.71, 130.11, 129.89, 129.72, 129.69, 127.57, 127.19, 127.15, 126.79, 122.79, 77.23.

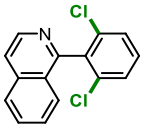

11b, 1-(2,6-dichlorophenyl)isoquinoline

^{1}H NMR (400 MHz, $CDCl_3$) δ 8.61 (d, *J* = 5.7 Hz, 1H), 7.86 (dt, *J* = 8.3, 1.1 Hz, 1H), 7.72 – 7.59 (m, 2H), 7.51 – 7.38 (m, 4H), 7.32 (dd, *J* = 8.9, 7.2 Hz, 1H). ^{13}C NMR (101 MHz, $CDCl_3$) δ 156.70, 142.49, 136.96, 136.36, 135.20, 130.45, 130.24, 128.18, 127.80, 127.16, 126.04, 121.01, 77.23.

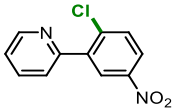

12b, 2-(2-chloro-5-nitrophenyl)pyridine

^{1}H NMR (500 MHz, $CDCl_3$) δ 8.79 (dd, *J* = 4.3, 2.6 Hz, 1H), 8.54 (d, *J* = 2.7 Hz, 1H), 8.22 (dt, *J* = 8.8, 1.8 Hz, 1H), 7.86 (td, *J* = 7.7, 1.8 Hz, 1H), 7.75 – 7.70 (m, 1H), 7.68 (d, *J* = 8.7 Hz, 1H), 7.40 (m, *J* = 7.6, 5.0, 1.3 Hz, 1H). ^{13}C NMR (126 MHz, $CDCl_3$) δ 154.60, 150.03, 146.74, 140.45, 139.09, 136.34, 131.22, 126.78, 124.73, 124.08, 123.40.

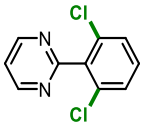

13b, 2-(2,6-dichlorophenyl)pyrimidine

^{1}H NMR (400 MHz, DMSO) δ 9.01 (d, *J* = 5.0 Hz, 2H), 7.66 – 7.59 (m, 3H), 7.54 (dd, *J* = 9.0, 7.1 Hz, 1H). ^{13}C NMR (101 MHz, DMSO) δ 163.64, 158.35, 137.82, 133.32, 131.65, 128.78, 121.38.

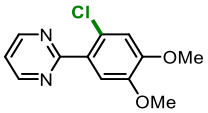

14b, 2-(2-chloro-4,5-dimethoxyphenyl)pyrimidine

^{1}H NMR (400 MHz, $CDCl_3$) δ 8.89 (d, *J* = 4.9 Hz, 2H), 7.39 (s, 1H), 7.28 (t, *J* = 4.9 Hz, 1H), 7.01 (s, 1H), 3.96 (d, *J* = 1.8 Hz, 6H). ^{13}C NMR (101 MHz, $CDCl_3$) δ 165.34, 157.23, 157.01, 150.39, 147.83, 129.50, 124.69, 118.95, 114.06, 113.52, 77.23, 56.28, 56.18.

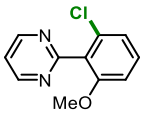

15b, 2-(2-chloro-6-methoxyphenyl)pyrimidine

^{1}H NMR (400 MHz, $CDCl_3$) δ 8.83 (d, *J* = 4.9 Hz, 2H), 7.30 – 7.17 (m, 2H), 7.02 (dd, *J* = 8.1, 0.9 Hz, 1H), 6.84 (dd, *J* = 8.4, 0.9 Hz, 1H), 3.68 (s, 3H). ^{13}C NMR (101 MHz, $CDCl_3$) δ 164.23, 158.11, 157.31, 133.54, 130.30, 128.29, 121.77, 119.55, 109.60, 77.23, 56.16.

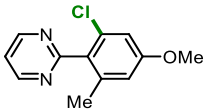

16b, 2-(2-chloro-4-methoxy-6-methylphenyl)pyrimidine

^{1}H NMR (400 MHz, $CDCl_3$) δ 8.80 (d, *J* = 4.9 Hz, 2H), 7.21 (t, *J* = 4.9 Hz, 1H), 6.79 (d, *J* = 2.5 Hz, 1H), 6.66 (dd, *J* = 2.4, 0.9 Hz, 1H), 3.74 (s, 3H), 2.03 (s, 3H). ^{13}C NMR (101 MHz, $CDCl_3$) δ 166.22, 159.75, 157.24, 139.05, 133.27, 131.14, 119.27, 114.77, 112.23, 55.52, 20.34.

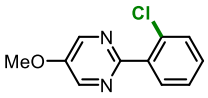

17b, 2-(2-chlorophenyl)-5-methoxypyrimidine

^{1}H NMR (500 MHz, $CDCl_3$) δ 8.56 (s, 3H), 7.72 (dd, *J* = 6.1, 3.4 Hz, 2H), 7.55 – 7.48 (m, 2H), 7.45 – 7.28 (m, 4H), 4.01 (s, 5H). ^{13}C NMR (126 MHz, $CDCl_3$) δ 158.22, 151.90, 143.53, 143.20, 137.44, 132.63, 131.55, 130.51, 130.03, 128.08, 126.79, 56.03.

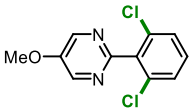

17b', 2-(2,6-dichlorophenyl)-5-methoxypyrimidine

^{1}H NMR (500 MHz, $CDCl_3$) δ 8.58 (s, 2H), 7.42 (d, *J* = 8.0 Hz, 2H), 7.30 (dd, *J* = 14.8, 6.5 Hz, 1H), 4.02 (s, 3H). ^{13}C NMR (126 MHz, $CDCl_3$) δ 156.51, 152.19, 143.52, 137.29, 134.49, 130.12, 128.08, 56.03.

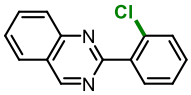

18b, 2-(2-chlorophenyl)quinazoline

^{1}H NMR (500 MHz, $CDCl_3$) δ 9.58 (d, *J* = 16.0 Hz, 1H), 8.16 (d, *J* = 8.2 Hz, 1H), 8.09 – 7.96 (m, 3H), 7.89 – 7.82 (m, 1H), 7.82 – 7.70 (m, 1H), 7.60 – 7.53 (m, 1H), 7.50 – 7.33 (m, 3H). ^{13}C NMR (126 MHz, $CDCl_3$) δ 162.02, 160.29, 150.38, 138.30, 134.64, 134.44, 132.92, 131.81, 130.58, 130.36, 130.25, 128.71, 128.68, 128.54, 128.19, 128.11, 127.31, 127.19, 126.93, 123.31.

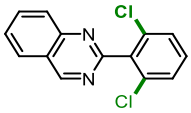

18b', 2-(2,6-dichlorophenyl)quinazoline

^{1}H NMR (500 MHz, $CDCl_3$) δ 9.59 (s, 1H), 8.18 (d, *J* = 8.5 Hz, 1H), 8.09 – 7.99 (m, 2H), 7.78 (m, *J* = 8.1, 6.9, 1.1 Hz, 1H), 7.47 (d, *J* = 8.1 Hz, 2H), 7.36 (dd, *J* = 8.7, 7.5 Hz, 1H). ^{13}C NMR (126 MHz, $CDCl_3$) δ 160.86, 160.38, 150.35, 137.90, 134.64, 134.26, 130.25, 128.71, 128.53, 128.19, 127.30, 123.61.

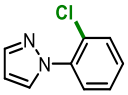

19b, 1-(2-chlorophenyl)-1H-pyrazole

^{1}H NMR (400 MHz, $CDCl_3$) δ 7.81 (d, *J* = 2.4 Hz, 3H), 7.68 (d, *J* = 1.9 Hz, 3H), 7.56 – 7.47 (m, 3H), 7.47 – 7.35 (m, 3H), 7.35 – 7.21 (m, 6H), 6.47 – 6.37 (m, 3H). ^{13}C NMR (101 MHz, $CDCl_3$) δ 140.93, 131.30, 130.66, 130.63, 129.00, 128.68, 128.37, 127.82, 127.67, 106.69, 106.66.

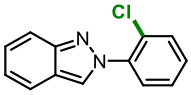

20b, 2-(2-chlorophenyl)-2H-indazole

^{1}H NMR (400 MHz, $CDCl_3$) δ 8.27 (d, *J* = 1.0 Hz, 1H), 7.76 – 7.58 (m, 3H), 7.57 – 7.46 (m, 1H), 7.44 – 7.24 (m, 3H), 7.07 (m, *J* = 8.5, 6.6, 0.9 Hz, 1H). ^{13}C NMR (101 MHz, $CDCl_3$) δ 149.43, 138.64, 130.70, 129.97, 129.00, 128.59, 127.71, 126.95, 125.23, 122.45, 122.02, 120.53, 117.95, 77.23.

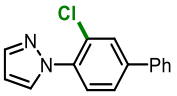

21b, 1-(3-chloro-[1,1'-biphenyl]-4-yl)-1H-pyrazole

^{1}H NMR (400 MHz, $CDCl_3$) δ 7.86 (dd, *J* = 2.4, 0.6 Hz, 1H), 7.69 (dd, *J* = 11.4, 1.9 Hz, 2H), 7.63 – 7.48 (m, 4H), 7.46 – 7.29 (m, 3H), 6.43 (dd, *J* = 2.5, 1.9 Hz, 1H). ^{13}C NMR (101 MHz, $CDCl_3$) δ 142.22, 141.01, 138.79, 137.13, 131.32, 129.11, 129.06, 128.40, 128.27, 127.92, 127.12, 126.30, 106.75, 77.23.

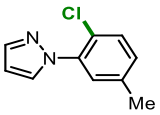

22b, 1-(2-chloro-5-methylphenyl)-1H-pyrazole

^{1}H NMR (400 MHz, $CDCl_3$) δ 7.90 (d, *J* = 2.5 Hz, 1H), 7.76 (d, *J* = 1.8 Hz, 1H), 7.46 – 7.38 (m, 2H), 7.16 (dd, *J* = 8.4, 2.2 Hz, 1H), 6.49 (t, *J* = 2.2 Hz, 1H), 2.40 (s, 3H). ^{13}C NMR (101 MHz, $CDCl_3$) δ 140.79, 138.01, 137.79, 131.29, 130.27, 129.72, 128.26, 124.97, 106.55, 77.23, 20.77.

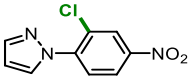

23b, 1-(2-chloro-4-nitrophenyl)-1*H*-pyrazole

^{1}H NMR (500 MHz, $CDCl_3$) δ 8.69 (d, *J* = 2.5 Hz, 3H), 8.55 (dd, *J* = 9.1, 2.5 Hz, 3H), 8.42 (d, *J* = 2.7 Hz, 3H), 8.15 (d, *J* = 9.1 Hz, 3H), 7.92 (d, *J* = 1.7 Hz, 3H), 6.67 (t, *J* = 2.1 Hz, 3H), 1.37 – 1.26 (m, 2H), 0.93 – 0.83 (m, 1H). ^{13}C NMR (126 MHz, $CDCl_3$) δ 145.64, 145.05, 143.91, 130.42, 129.60, 128.88, 124.21, 115.54, 110.33, 104.28.

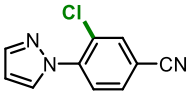

24b, 3-chloro-4-(1H-pyrazol-1-yl)benzonitrile

^{1}H NMR (400 MHz, $CDCl_3$) δ 8.01 (dd, *J* = 2.6, 0.6 Hz, 1H), 7.80 – 7.70 (m, 3H), 7.61 (dd, *J* = 8.4, 1.8 Hz, 1H), 6.47 (dd, *J* = 2.6, 1.8 Hz, 1H). ^{13}C NMR (101 MHz, $CDCl_3$) δ 142.15, 141.55, 134.60, 131.41, 131.24, 127.86, 127.55, 116.90, 112.18, 107.93, 77.23.

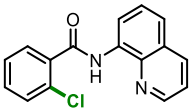

25b, 2-chloro-N-(quinolin-8-yl)benzamide

^{1}H NMR (400 MHz, $CDCl_3$) δ 10.61 (s, 1H), 8.85 – 8.78 (m, 2H), 8.52 (dd, *J* = 8.6, 1.7 Hz, 1H), 8.04 – 7.96 (m, 2H), 7.58 (d, *J* = 8.4 Hz, 1H), 7.56 – 7.43 (m, 4H). ^{13}C NMR (101 MHz, $CDCl_3$) δ 165.44, 148.79, 139.34, 134.91, 133.90, 133.50, 132.03, 128.87, 127.34, 127.30, 126.04, 124.51, 122.44, 116.49, 77.24.

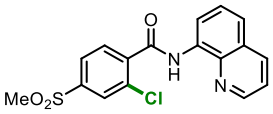

26b, 2-chloro-4-(methylsulfonyl)-N-(quinolin-8-yl)benzamide

^{1}H NMR (500 MHz, $CDCl_3$) δ 10.51 (s, 1H), 8.93 (p, *J* = 4.5 Hz, 1H), 8.81 (dd, *J* = 4.1, 1.9 Hz, 1H), 8.22 (dd, *J* = 8.2, 1.9 Hz, 1H), 8.11 (d, *J* = 1.8 Hz, 1H), 8.03 – 7.95 (m, 2H), 7.63 (d, *J* = 4.5 Hz, 2H), 7.50 (dd, *J* = 8.2, 4.1 Hz, 1H), 3.14 (d, *J* = 1.7 Hz, 3H). ^{13}C NMR (126 MHz, $CDCl_3$) δ 163.16, 148.60, 143.21, 140.64, 138.51, 136.50, 133.87, 132.60, 131.02, 129.54, 128.00, 127.35, 126.09, 122.81, 121.95, 117.17, 44.48.

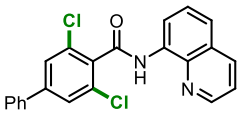

27b. 3,5-dichloro-N-(quinolin-8-yl)-[1,1'-biphenyl]-4-carboxamide

^{1}H NMR (500 MHz, $CDCl_3$) δ 10.13 (s, 1H), 9.01 (dd, *J* = 7.2, 1.8 Hz, 1H), 8.81 (dd, *J* = 4.3, 1.6 Hz, 1H), 8.22 (dd, *J* = 8.3, 1.7 Hz, 1H), 7.69 – 7.58 (m, 6H), 7.53 (d, *J* = 7.4 Hz, 1H), 7.53 – 7.44 (m, 3H). ^{13}C NMR (126 MHz, $CDCl_3$) δ 162.69, 148.45, 144.51, 138.49, 137.92, 136.43, 134.58, 134.01, 132.83, 129.21, 128.88, 128.03, 127.45, 127.15, 126.84, 122.51, 121.81, 117.22.

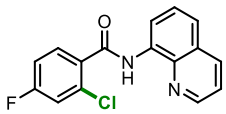

28b', 2-chloro-4-fluoro-N-(quinolin-8-yl)benzamide

^{1}H NMR (500 MHz, $CDCl_3$) δ 10.38 (s, 1H), 9.31 (dt, *J* = 8.9, 1.5 Hz, 1H), 9.07 – 9.01 (m, 1H), 8.98 – 8.89 (m, 1H), 8.64 (dd, *J* = 8.8, 1.6 Hz, 1H), 8.61 (s, 0H), 7.80 – 7.74 (m, 1H), 7.30 – 7.17 (m, 4H). ^{13}C NMR (126 MHz, $CDCl_3$) δ 163.43, 162.44, 149.29, 139.81, 139.59, 137.60, 133.64, 133.41, 127.51, 124.83, 121.75, 116.49, 116.29, 114.51, 77.25.

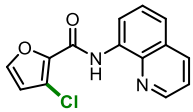

29b, 3-chloro-N-(quinolin-8-yl)furan-2-carboxamide

^{1}H NMR (500 MHz, $CDCl_3$) δ 10.75 (s, 1H), 8.95 (dd, *J* = 4.1, 1.6 Hz, 1H), 8.84 (d, *J* = 8.3 Hz, 1H), 8.61 (dd, *J* = 8.6, 1.8 Hz, 1H), 7.69 – 7.63 (m, 2H), 7.62 (dd, *J* = 8.5, 4.2 Hz, 1H), 7.33 (d, *J* = 3.5 Hz, 1H), 6.62 (dd, *J* = 3.5, 1.7 Hz, 1H). ^{13}C NMR (126 MHz, $CDCl_3$) δ 156.35, 148.91, 148.17, 144.66, 139.21, 133.50, 133.43, 127.28, 126.04, 124.65, 122.47, 116.57, 115.40, 112.55.

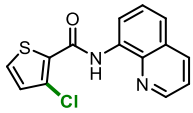

30b, 3-chloro-N-(quinolin-8-yl)thiophene-2-carboxamide

^{1}H NMR (400 MHz, $CDCl_3$) δ 11.29 (s, 1H), 8.85 (dd, *J* = 4.2, 1.6 Hz, 1H), 8.77 (d, *J* = 8.4 Hz, 1H), 8.53 (dd, *J* = 8.6, 1.6 Hz, 1H), 7.61 – 7.46 (m, 3H), 7.02 (d, *J* = 5.2 Hz, 1H). ^{13}C NMR (101 MHz, $CDCl_3$) δ 158.69, 149.02, 139.47, 133.96, 133.82, 133.37, 130.20, 129.86, 127.27, 126.04, 125.02, 124.24, 122.46, 117.25, 77.23.

Substrate preparation

Synthesis of (3-chlorobutyl)benzene, **C13**:[1]

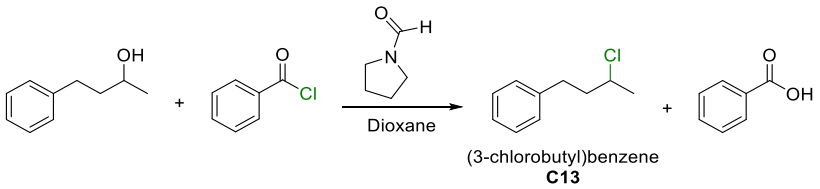

4-Phenyl-2-butanol (2 mmol), benzoyl chloride (1.2 equiv., 2 mmol), formyl pyrrolidine (20 mol%, 0.4 mmol) and dioxane (2 mL) were added to a cylindrical pressure vessel and heated at 80 ºC for 24 h. The reaction mixture was concentrated under vacuum and purified with silica gel chromatography to afford pure **C13** (yield: 80%).

Synthesis of 2,4-dichloropentane **5c**:[2]

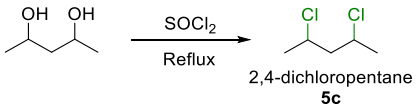

Thionyl chloride ($SOCl_2$, 50 g) was slowly added to a solution of pyridine (1 g) and 2,4-pentanediol (8 g) at -10 ºC. After addition, the reaction mixture was heated at reflux for 3 h. After cooling to room temperature, ice water (200 mL) was added to the reaction mixture and the product extracted with diethyl ether (3×200 mL). The organic phase was washed with aqueous $NaHCO_3$ and water and dried with Na_2SO_4. Pure product was obtained by fractional distillation (b.p. 140 ºC, yield: 63%).

Synthesis of (chloro(cyclopropyl)methyl)benzene **9c**:[3]

Trimethylchlorosilane (30.0 mmol, 5.0 equiv.) was added dropwise into a solution of 1-phenyl-1-cyclopropylmethanol (6.0 mmol) in dry dichloromethane (DCM, 6 mL) at 0 ºC under N_2. The reaction was stirred at 0 ºC for 1 h, then quenched with water (20 mL) and the product extracted with DCM (3×20 mL). The organic phase was washed with brine, dried and concentrated in vacuo to give a colorless oil. The product was purified using silica gel chromatography.

Synthesis of pyridine and pyrimidine directing arenes:[4]

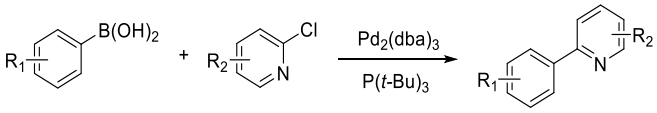

Aryl chloride (2 mmol), boronic acid (2.4 mmol), tris(dibenzylideneacetone)dipalladium(0) ($Pd_2(dba)_3$, 0.03 mmol. 1.5 mol%), P(*t*-Bu)$_3$ (0.08 mmol. 4 mol%), Cs_2CO_3 (5 mmol) and dioxane (5 mL) were added to a Schlenk tube charged with N_2 and heated at 80 ºC for 5 h. After cooling to room temperature, the reaction mixture was concentrated under vacuum and the product purified using silica gel chromatography.

Synthesis of pyrazol directing arenes:[5]

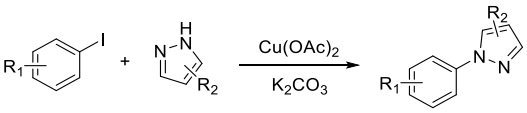

Aryl iodide (2.4 mmol), pyrazol (2.0 mmol), Cs_2CO_3 (4 mmol) and DMF (5 mL) were added to a Schlenk tube charged with N_2 and heated at 110 ºC for 24 h. After cooling to ambient temperature, a saturated aqueous NH_4Cl solution (20 mL) was added and the product extracted with EA (3×20 mL). The organic phase was washed with brine and water, dried with Na_2SO_4 and purified using silica gel chromatography.

Synthesis of 8-aminoquinoline directing arenes:[6]

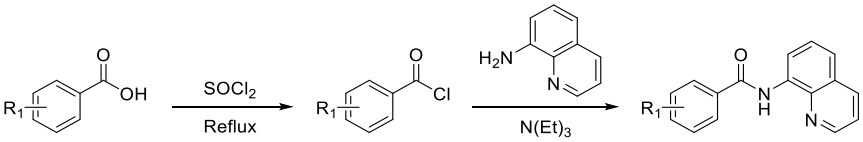

The carboxylic acid (12 mmol) and $SOCl_2$ (11 mL) were added heated under reflux for 3 h at 85 ºC. After cooling to ambient temperature, the reaction mixture was concentrated under vacuum to afford the crude acyl chloride. Dry DCM (20 mL) was added under a N_2 atmosphere and 8-aminoquinoline (10 mmol) and NEt_3 (11 mmol) were dissolved in DCM (20 mL), and slowly added dropwise to the acyl chloride solution.

The reaction was stirred at room temperature for 6 h. After reaction, the mixture was concentrated under vacuum and purified using silica gel chromatography.

Synthesis of benzo[h]quinolinyl Pd(II) chloride dimer:[7]

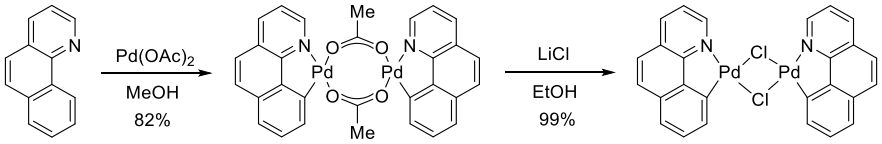

$Pd(OAc)_2$ (6 mmol, 1 equiv.) and benzo[h]quinoline **1a** (6 mmol, 1 equiv.) was added into a MeOH (80 mL) solution, stirred at RT for 8 h. The yellow precipitate was isolated by filtration and washed with MeOH (3×20 mL) and Et_2O (3×20 mL), giving benzo[h]quinolinyl Pd(II) acetate dimer in 82% yield. LiCl (20 mmol, 20 equiv.) was added into a benzo[h]quinolinyl Pd(II) acetate dimer (1 mmol, 1 equiv.) and EtOH (10 mL) suspension at 0 ºC. Then the ice-water bath was removed and the suspension was stirred at RT for another 1 h. The pale yellow precipitate was isolated by filtration and washed with water (3×20 mL), MeOH (3×20 mL), and Et_2O (3×20 mL), giving the benzo[h]quinolinyl Pd(II) chloride dimer in 99% yield.

Analytical Methods

Qualitative and quantitative analysis of gas phase products was performed by gas chromatography (GC) using an Agilent 7890B instrument equipped with a hydrogen flame-ionization detector (FID) and a thermal conductivity detector (TCD). The GC yield was determined based on standard gas mixtures and integrated peak areas. Qualitative and quantitative analysis of crude liquid products was performed using an Agilent 7000C GCMS equipped with a hydrogen flame-ionization detector (FID), electron ionization mass detector (EI-MS) and HP-5 nonpolar column. The GC yield was determined based on internal standard curves and integrated peak areas.

Determination of the molecular weight and polydispersity of the polymers was performed using Gel Permeation Chromatography (GPC, Agilent 390-MDS), equipped with refractive index detector (RI), and Dual-Angle Light Scattering detector. THF was used as eluent. For the measurement after reaction, to the DMSO solution (2 mL) brine (10 mL) was added and the organic components extracted with THF (3×5 mL). The THF extract was used for GPC.

^1H and ^{13}C NMR spectra recorded on a Bruker Avance III HD 400 instrument equipped with a 5 mm BBFO probe. DMSO-d_6 or $CDCl_3$ were used as solvent. DMSO-d_6 was used as the reaction solvent for the reaction that was monitored by ^1H NMR spectroscopy. After centrifuging to remove the PdO catalyst, the crude reaction mixture (0.2 mL) was diluted with DMSO-d_6 or THF-d_8 (0.4 mL) and directly used for ^1H NMR experiment.

Supplementary Figures

Supplementary Table 1. Summary of recent approaches reported for the destruction of PVC.

Year	Catalyst	Solvent	Product	Temp. (ºC)	Yield (%)	Fate of Cl	Ref.
			Homogeneous catalysts				
2000	NaOH	NaOH	Oxalic acid	250	40	Neutralization by base	8
2008	Ammonia	Ammonia	Polyene compounds	230	80	Neutralization by base	9
2010	[Bmim]Cl	[Bmim]Cl	Polyene compounds	220	90	Post-neutralization	10
2010	TBAB	Na_2S/ethylene glycol	Polyene compounds	170	58	Post-neutralization	11
2011	$Ca(OH)_2$	Ethylene glycol	Polyene compounds	190	86	Neutralization by base	12
2014	$[P_{4444}][Cl]$	$[P_{4444}][Cl]$	*Trans*-polyacetylene	180	98	Post-neutralization	13
2020	Ionic liquids	Ionic liquids	Polyene compounds	160	85	HCl emissions	14
2023	$[Ph_3C][B(C_6F_5)_4]$	Benzene	Polyene compounds	110	77	Et_3SiCl	15
2023	Bu_4PCl and $H(CO)Rh(PPh_3)_3$	2-Butanone	Polyene compounds	180	81	HCl emissions	16
			Heterogeneous catalysts				
2007	La-MgO	-	Polyene compounds	400	30	HCl, HOCl, emissions	17
2016	Al-modified graphitic-C_3N_4 (10 wt% Al)	Polyethylene glycol	Dechlorinated PVC	170	75	HCl emissions	18
2018	CuAl-layered double hydroxide	-	Solid	600	81	HCl, HOCl, emissions	19
2020	ZnFeAl-layered double hydroxide	-	Solid	300-800	98	HCl, HOCl emissions	20
2021	Benzimidazole modified layered double hydroxide	-	Solid	300-600	95	HCl, HOCl emissions	21
2023	Mg/Al mixed oxide	-	Dechlorinated PVC	250	100	HCl emissions	22

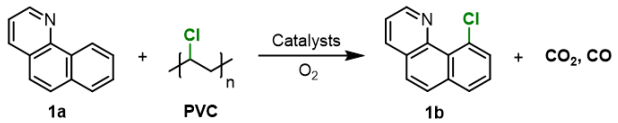

Entry	[Cu]	$NaNO_3$ (%)	Yield of **1b** (%)
1	CuO	100	4
2	$CuSO_4$	100	0
3	$Cu(OAc)_2 \cdot H_2O$	100	0
4	$Cu(NO_3)_2 \cdot 3H_2O$	100	15
5	$Cu(NO_3)_2 \cdot 3H_2O$	50	16
6	$Cu(NO_3)_2 \cdot 3H_2O$	20	19
7	$Cu(NO_3)_2 \cdot 3H_2O$	0	3

Supplementary Figure 1. Cu catalyzed aerobic chlorination using PVC as a chlorination reagent (without a Pd catalyst). Reaction conditions: 7,8-benzoquinoline **1a** (0.25 mmol), PVC (1.5 equiv., 0.375 mmol), Cu catalyst (20 mol%, 0.05 mmol), $NaNO_3$ (0-100 mol%), biphenyl (0.2 mmol, internal standard), DMSO (2 mL), O_2 (3 bar), 140 ºC, 15 h

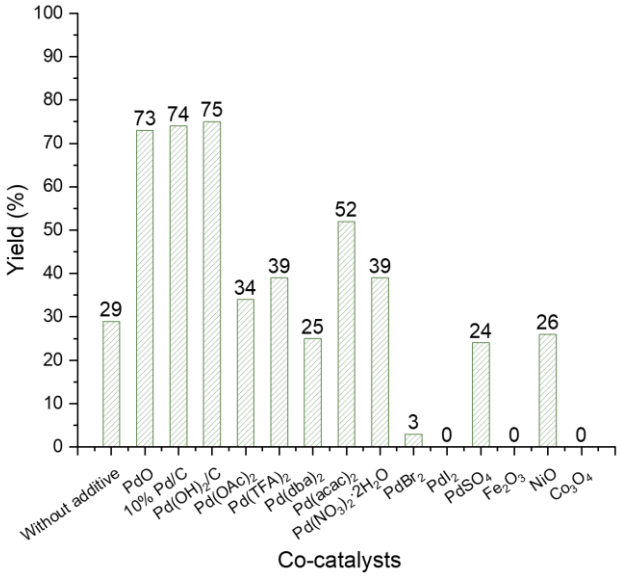

Supplementary Figure 2. Screening of Pd catalysts. Reaction conditions: 7,8-benzoquinoline **1a** (0.25 mmol), PVC (1.5 equiv., 0.375 mmol), $Cu(NO_3)_2 \bullet 3H_2O$ (20 mol%, 0.05 mmol), **Pd catalyst** (10 mol%, 0.025 mmol), $NaNO_3$ (100 mol%, 0.25 mmol), biphenyl (0.2 mmol), DMSO (2 mL), O_2 (3 bar), 140 ºC, 15 h.

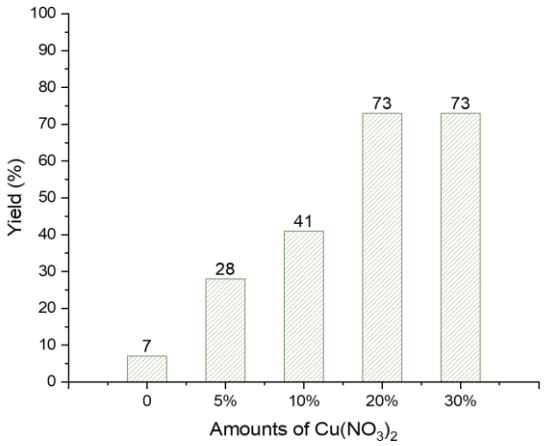

Supplementary Figure 3. Optimization of the $Cu(NO_3)_2$ concentration. Reaction conditions: 7,8-benzoquinoline **1a** (0.25 mmol), PVC (1.5 equiv., 0.375 mmol), **$Cu(NO_3)_2$•$3H_2O$ (0-30 mol%)**, PdO (10 mol%, 0.025 mmol), $NaNO_3$ (100 mol%, 0.25 mmol), biphenyl (0.2 mmol), DMSO (2 mL), O_2 (3 bar), 140 ºC, 15 h.

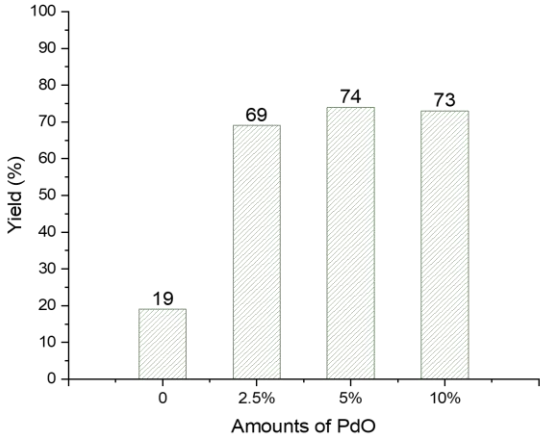

Supplementary Figure 4. Optimization of the PdO concentration. Reaction conditions: 7,8-benzoquinoline **1a** (0.25 mmol), PVC (1.5 equiv., 0.375 mmol), $Cu(NO_3)_2$•$3H_2O$ (20 mol%, 0.05 mmol), **PdO (0-10 mol%)**, $NaNO_3$ (100 mol%, 0.25 mmol), biphenyl (0.2 mmol), DMSO (2 mL), O_2 (3 bar), 140 ºC, 15 h.

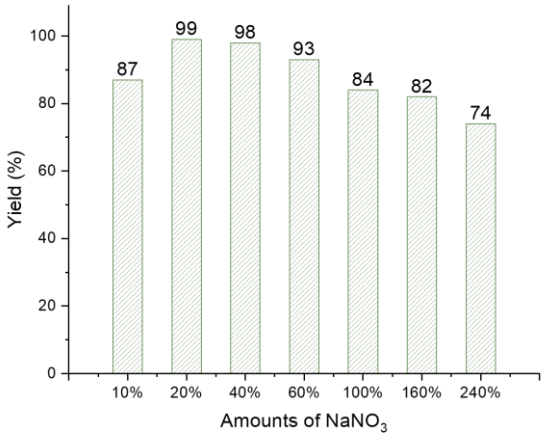

Supplementary Figure 5. Optimization of the $NaNO_3$ concentration. Reaction conditions: 7,8-benzoquinoline **1a** (0.25 mmol), PVC (1.5 equiv., 0.375 mmol), $Cu(NO_3)_2$•$3H_2O$ (20 mol%, 0.05 mmol), PdO (5 mol%, 0.0125 mmol), **$NaNO_3$ (10-240 mol%)**, biphenyl (0.2 mmol), DMSO (2 mL), O_2 (3 bar), 140 ºC, 15 h.

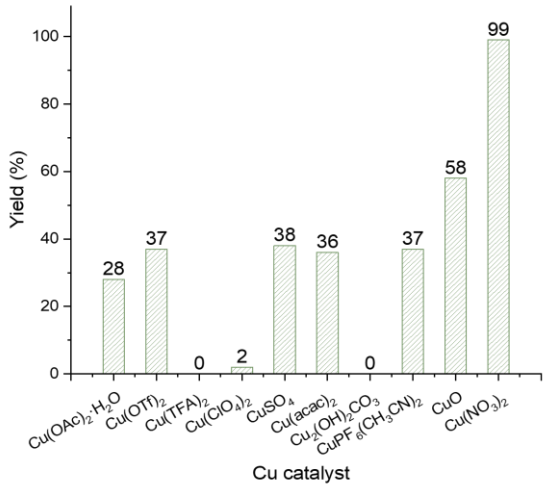

Supplementary Figure 6. Screening of Cu catalysts. Reaction conditions: 7,8-benzoquinoline **1a** (0.25 mmol), PVC (1.5 equiv., 0.375 mmol), **Cu catalyst (20 mol%, 0.05 mmol)**, PdO (5 mol%, 0.0125 mmol), $NaNO_3$ (20 mol%, 0.05 mmol), biphenyl (0.2 mmol), DMSO (2 mL), O_2 (3 bar), 140 ºC, 15 h.

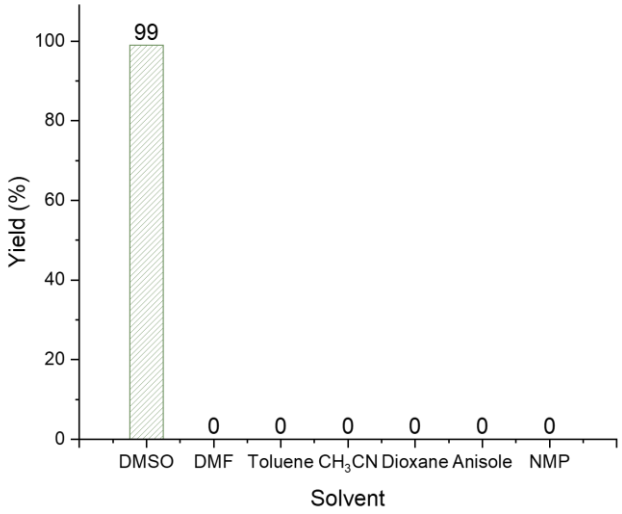

Supplementary Figure 7. Screening of the solvent. Reaction conditions: 7,8-benzoquinoline **1a** (0.25 mmol), PVC (1.5 equiv., 0.375 mmol), $Cu(NO_3)_2$•$3H_2O$ (20 mol%, 0.05 mmol), PdO (5 mol%, 0.0125 mmol), $NaNO_3$ (20 mol%, 0.05 mmol), biphenyl (0.2 mmol), **solvent (2 mL)**, O_2 (3 bar), 140 ºC, 15 h.

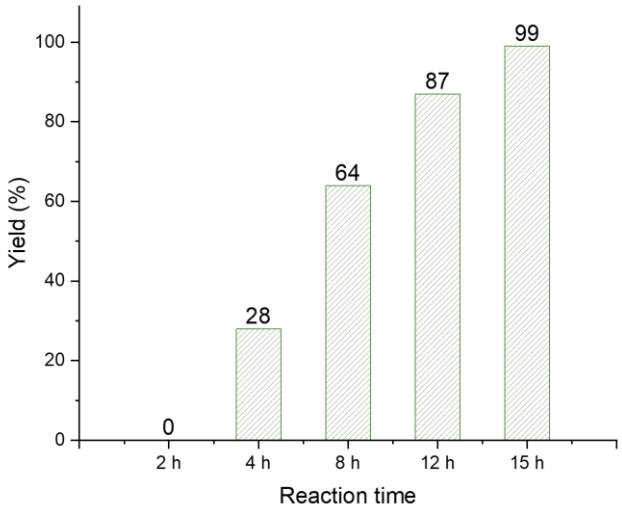

Supplementary Figure 8. Optimization of reaction time. Reaction conditions: 7,8-benzoquinoline **1a** (0.25 mmol), PVC (1.5 equiv., 0.375 mmol), $Cu(NO_3)_2$•$3H_2O$ (20 mol%, 0.05 mmol), PdO (5 mol%, 0.0125 mmol), $NaNO_3$ (20 mol%, 0. 5 mmol), biphenyl (0.2 mmol), DMSO (2 mL), O_2 (3 bar), 140 ºC, **2-15 h**.

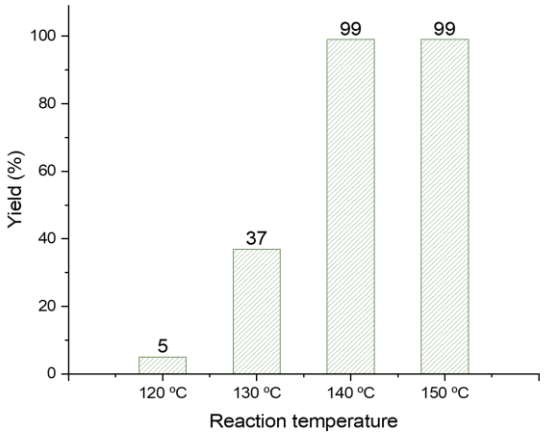

Supplementary Figure 9. Optimization of reaction temperature. Reaction conditions: 7,8-benzoquinoline **1a** (0.25 mmol), PVC (1.5 equiv., 0.375 mmol), $Cu(NO_3)_2$•$3H_2O$ (20 mol%, 0.05 mmol), PdO (5 mol%, 0.0125 mmol), $NaNO_3$ (20 mol%, 0.05 mmol), biphenyl (0.2 mmol), DMSO (2 mL), O_2 (3 bar), **120-150 ºC**, 15 h.

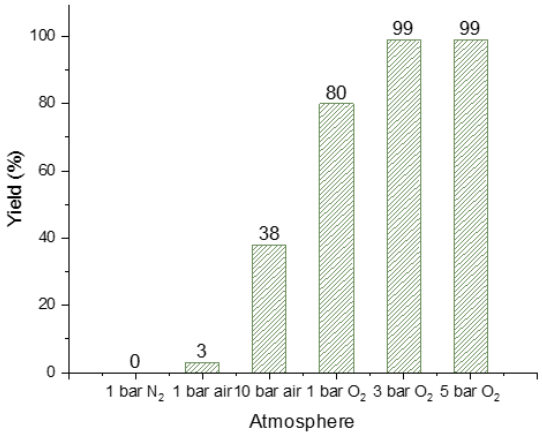

Supplementary Figure 10. Optimization of gas and pressure. Reaction conditions: 7,8-benzoquinoline **1a** (0.25 mmol), PVC (1.5 equiv., 0.375 mmol), $Cu(NO_3)_2$•$3H_2O$ (20 mol%, 0.05 mmol), PdO (5 mol%, 0.0125 mmol), $NaNO_3$ (20 mol%, 0.05 mmol), biphenyl (0.2 mmol), DMSO (2 mL), **gas**, 140 ºC, 15 h.

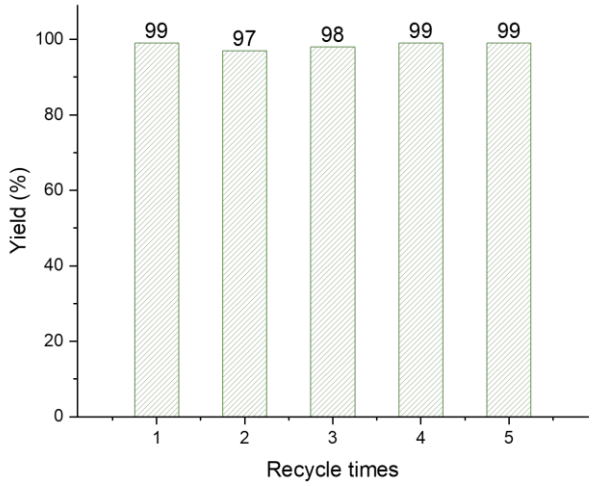

Supplementary Figure 11. Recycling of the PdO catalyst. Reactions were performed using the standard reaction conditions. PdO was recovered by filtration, and was washed with water, acetone, ethyl acetate and diethyl ether, dried under vacuum at 30 ºC for 18 h.

Supplementary Table 2. Optimization of CO production.

Entry	Variation from standard conditions		Yield of 1b (%)	Yield of CO (%)	Yield of CO_2 (%)
1	Standard conditions		99	15	81
2	With additives	50 mol% bis(benzene)chromium	72	48	50
3		50 mol% $Cr(CO)_6$	68	33	65
4		50 mol% Cr_2O_3	65	20	80
5		50 mol% Cr_2O_3·CuO	66	25	72
6		50 mol% $PbCl_2$	98	10	90
7		50 mol% $CaCO_3$	99	10	89
8		50 mol% Na_2SO_4	45	30	66
9		50 mol% Na_2HPO_4	92	16	83
10		50 mol% $MgCl_2$	55	32	67
11		20 equivalent H_2O	54	24	76
12	Other Pd catalysts	Lindlar catalyst instead of PdO	32	37	60
13		5% Pd/$CaCO_3$ instead of PdO	99	11	89
14		10% Pd/C instead of PdO	99	15	85
15		10% Pd/Al_2O_3 instead of PdO	99	9	90
16		5% Pd/$BaSO_4$ instead of PdO	95	5	90
17	Other gases	1 bar O_2	80	16	81
18		1 bar air	3	15	85
19		5 bar air	30	16	83
20	No PdO catalyst		12	83	17

Reaction conditions are the same as those given in Fig. 2a, entry 7.

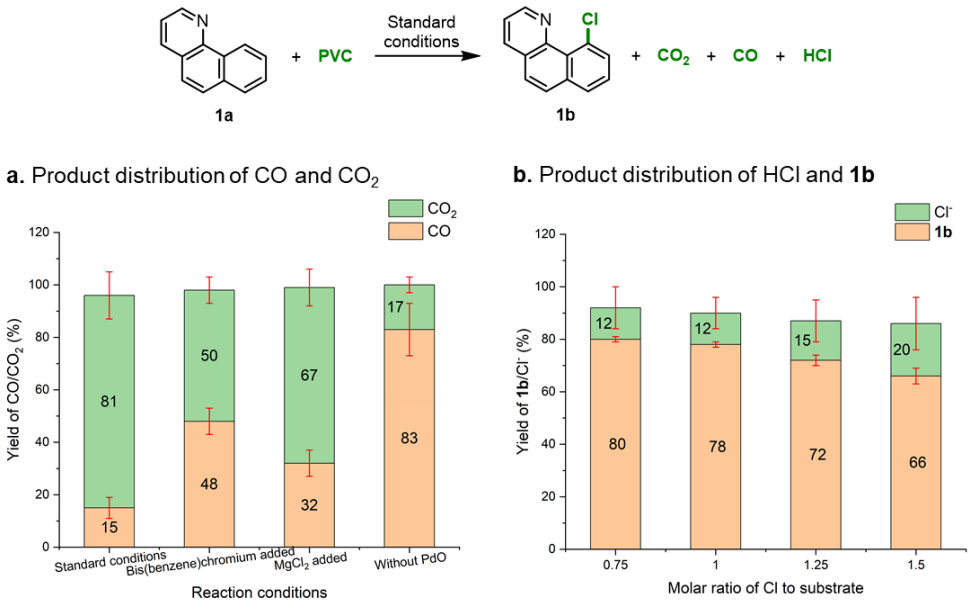

Supplementary Figure 12. Quantification of products. Each reaction was repeated three times to obtain the standard errors (n = 3). The bar graph with labels represents the mean value of reaction yield. Reaction yield were expressed as mean values ± standard error. (**a**) Product distribution of CO and CO_2. Reaction conditions are the same as those given in Supplementary Table 2, entries 1, 2, 10 and 20. (**b**) Product distribution of **1b** and HCl. The chloride concentration in the aqueous phase was determined by ion chromatography. Reaction conditions are the same as those given in Supplementary Table 2, entry 1, but with different amount of PVC (molar ratio of Cl to substrate range from 0.75 to 1.5). Note, HCl is volatile and some is lost during sample preparation (e.g. transfer, dilution).

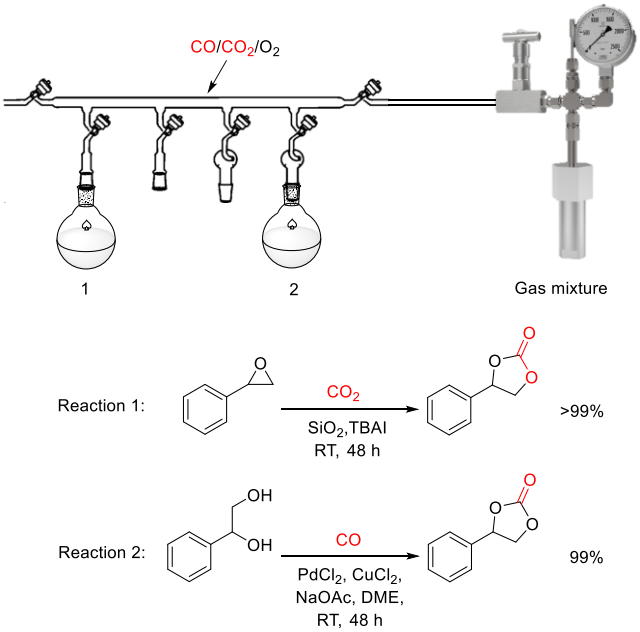

Supplementary Figure 13. Reaction of the CO/CO_2 containing gas produced. Reaction conditions: (**1**) Styrene oxide (2 mmol), SiO_2 (100 mg), tetrabutylammonium iodide (TBAI, 0.06 mmol), RT, 48 h. (**2**) 1-

Phenylethane-2,3-diol (0.2 mmol), $PdCl_2$ (0.02 mmol), $CuCl_2$ (0.4 mmol), NaOAc (0.04 mmol), dichloromethane (DME, 5 mL), RT, 48 h.[23] Yields were determined by GC.

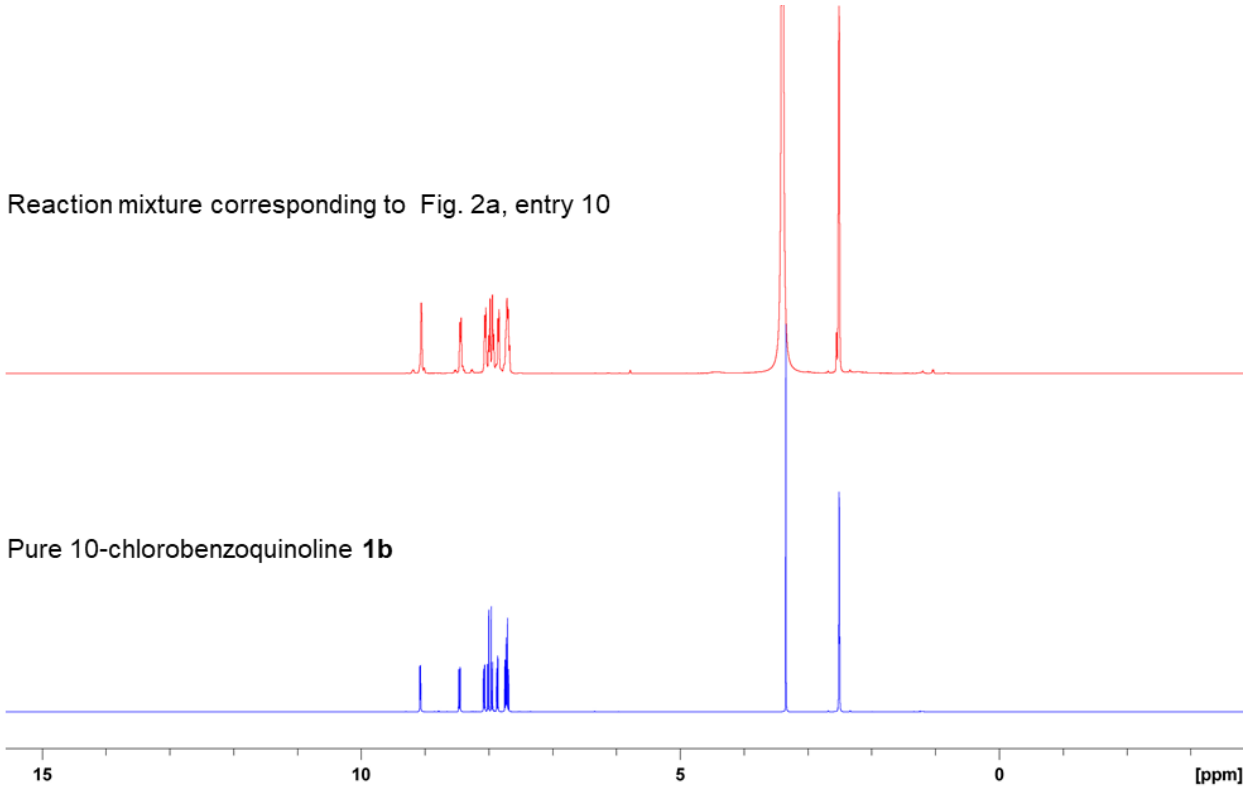

Supplementary Figure 14. Comparison of the ^{1}H NMR spectra of crude product **1b** and pure **1b**. Crude product **1b** is the unpurified reaction mixture corresponding to Fig. 2a, entry 7. Pure **1b** was obtained by purification using silica gel chromatography.

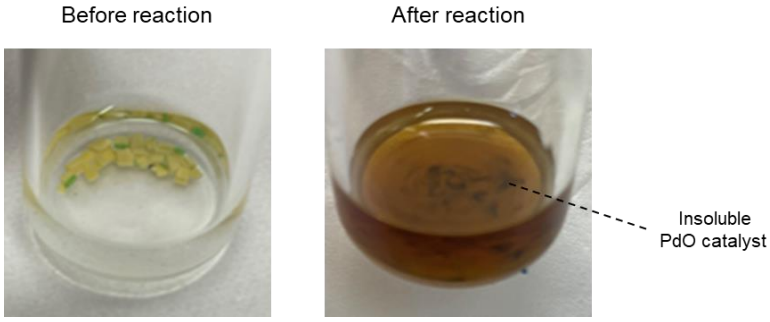

Supplementary Figure 15. Photographs showing the reaction using electric wire before and after reaction.

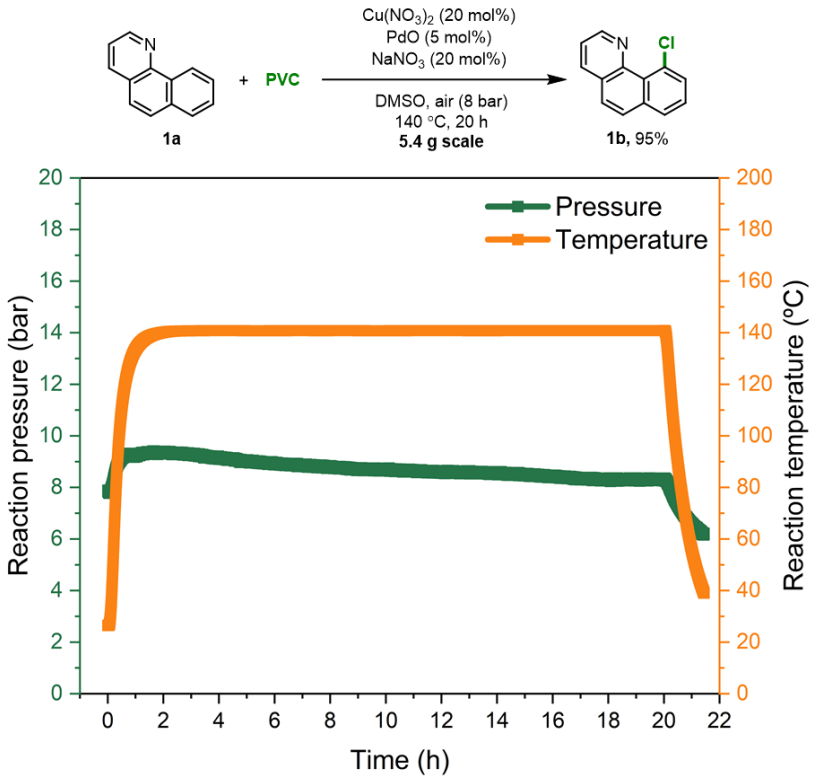

Supplementary Figure 16. Monitoring of the pressure and temperature for the reaction of **1a** on a 5.4 g scale.

Supplementary Table 3. Additive screening to demonstrate functional group compatibility.

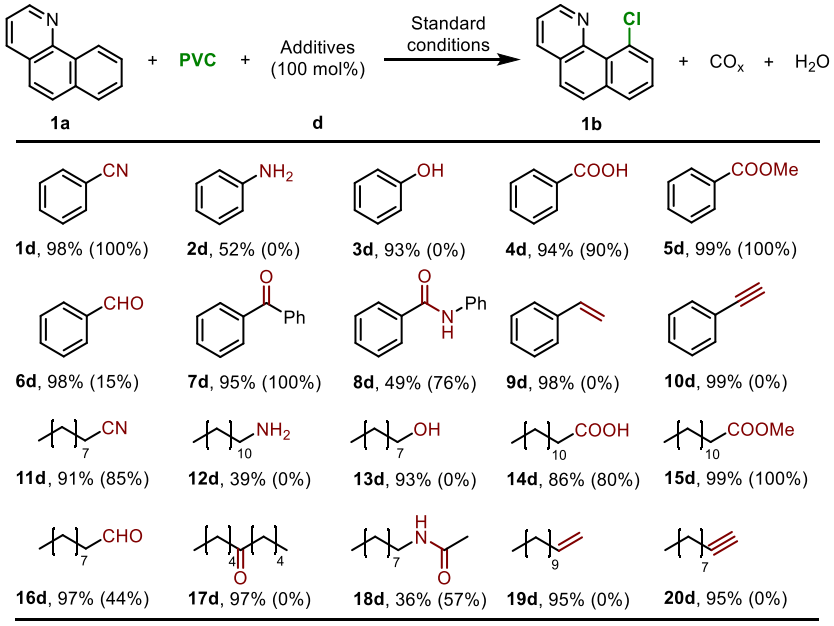

Reaction conditions are the same as those reported in Supplementary Table 2, entry 1. The remaining additive is given in parenthesis.

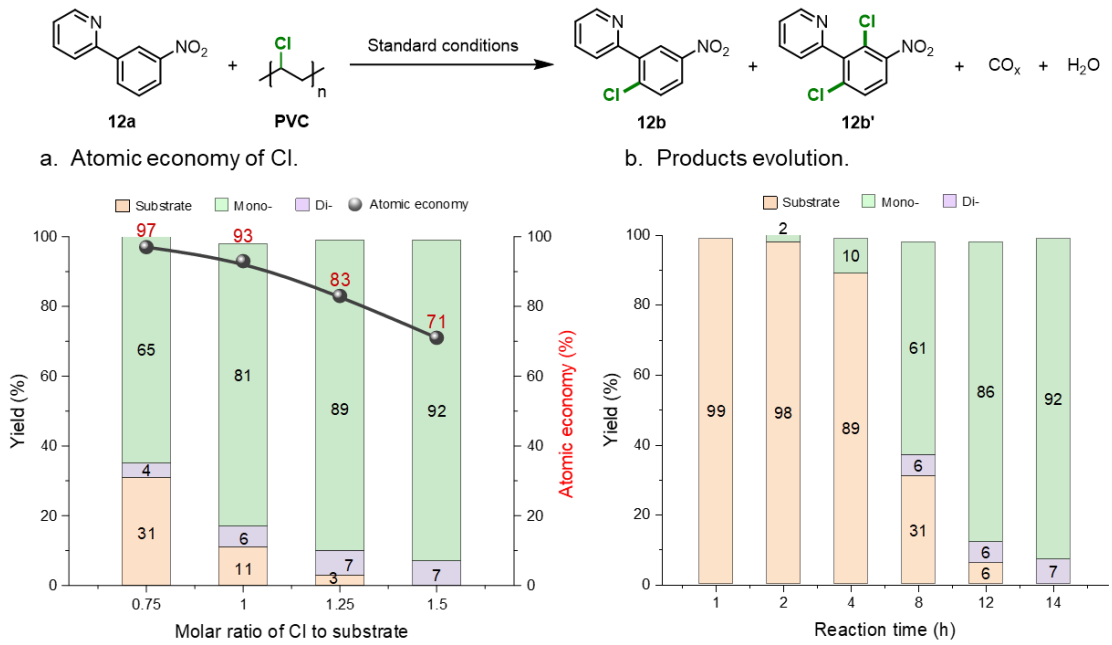

Supplementary Figure 17. Effect of PVC loading and Cl atom economy on yield and selectivity of *ortho*-di and monochloride products in the reaction between **12a** and PVC under the standard reaction conditions. (**a**) Cl atom economy and selectivity to the monochloride product **12b** with different PVC loadings (0.75 to 1.5 equiv. based on **12a**). Reactions were performed using the standard conditions: **12a** (0.25 mmol), PVC water pipe (0.75-1.5 equiv.), $Cu(NO_3)_2$•$3H_2O$ (20 mol%, 0.05 mmol), PdO (5 mol%, 0.0125 mmol), $NaNO_3$ (20 mol%, 0.05 mmol), DMSO (2 mL), O_2 (3 bar), 140 ºC, 15 h. (**b**) Evolution of the reaction with time. The bar graph with labels represents the mean value of reaction yield.

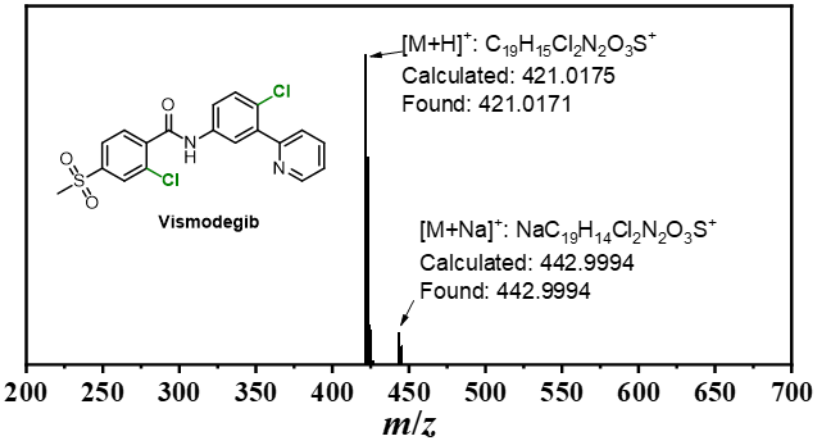

Supplementary Figure 18. Electrospray ionisation mass spectrum (ESI-MS) of vismodegib in THF (0.001 mmol/mL).

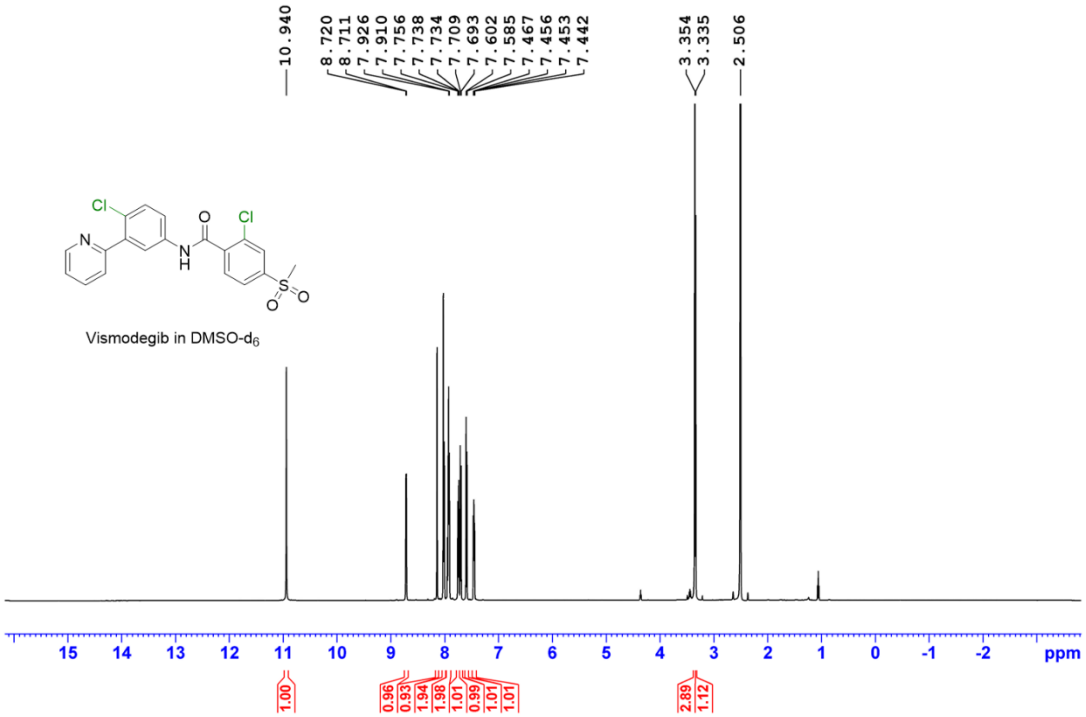

Supplementary Figure 19. ^{1}H NMR spectrum of vismodegib in DMSO-d_6.

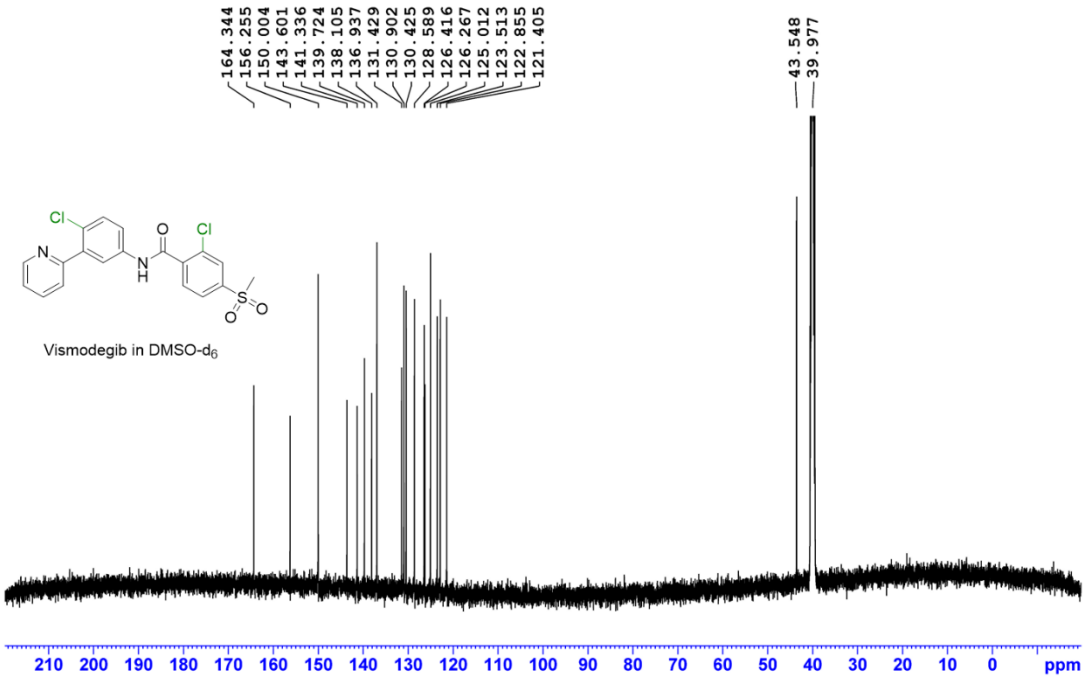

Supplementary Figure 20. ^{13}C NMR spectrum of vismodegib in DMSO-d_6.

Supplementary Table 4. Elemental analysis of vismodegib.

Elemental composition	Calculated (wt%)	Found-1 (wt%)	Found-2 (wt%)	Found-3 (wt%)
C	54.17	54.10	54.10	54.11
H	3.35	3.48	3.44	3.45
N	6.65	6.48	6.68	6.60
S	7.61	7.43	7.22	7.60

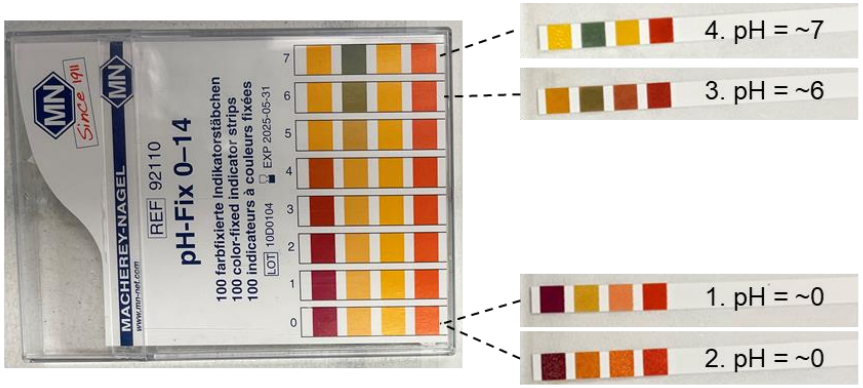

Reaction 1: PVC (2 mmol), THF (2 mL), O_2 (3 bar)

Reaction 2: Standard reaction conditions (Fig. 2a, entry 10)

Reaction 3: PVC (2 mmol), DMSO (2 mL), O_2 (3 bar)

Reaction 4: 1-phenylethyl chloride (**4c**) (2 mmol), DMSO (2 mL), O_2 (3 bar)

Supplementary Figure 21. pH tests of the reaction mixture. Reaction mixture was diluted with H_2O (1:1).

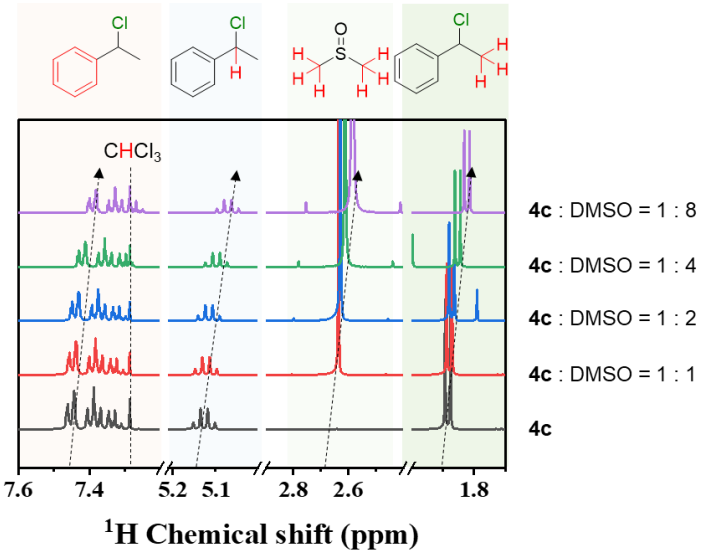

Supplementary Figure 22. ^{1}H NMR spectra of 1-phenylethyl chloride (**4c,** concentration: 1 mmol/mL) and DMSO (concentration: 1-8 mmol/mL) in $CDCl_3$. The peak at 7.26 ppm corresponding to the proton in $CHCl_3$

(present in the $CDCl_3$ solvent) does not change with the DMSO concentration and may be considered as an internal standard. As the concentration of DMSO increases the characteristic peaks of **4c** shift to lower frequencies, indicative of non-covalent interactions between the DMSO and **4c**, activating the C−Cl bond.[24]

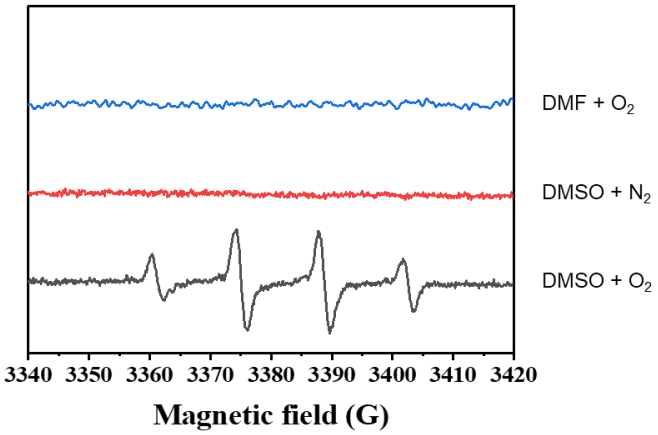

Supplementary Figure 23. Electron paramagnetic resonance (EPR) spectrum of the DMSO/O_2 promoted dehydrochlorination of **4c**. Reaction conditions: 1-phenylethyl chloride **4c** (0.5 mmol), DMSO (5 mL), O_2 or N_2, 140 °C, 0.5 h. The crude reaction mixture (200 μL) was mixed with 5,5-dimethyl-1-pyrroline N-oxide (DMPO, 3 M in DMSO, 200 μL) and an EPR spectrum was recorded at room temperature. An EPR signal (g_0= 2.007) corresponding to DMPO-$^{\bullet}$OH was identified from the reaction of O_2, DMSO and **4c**, confirming the formation of hydroxyl radicals during the reaction.

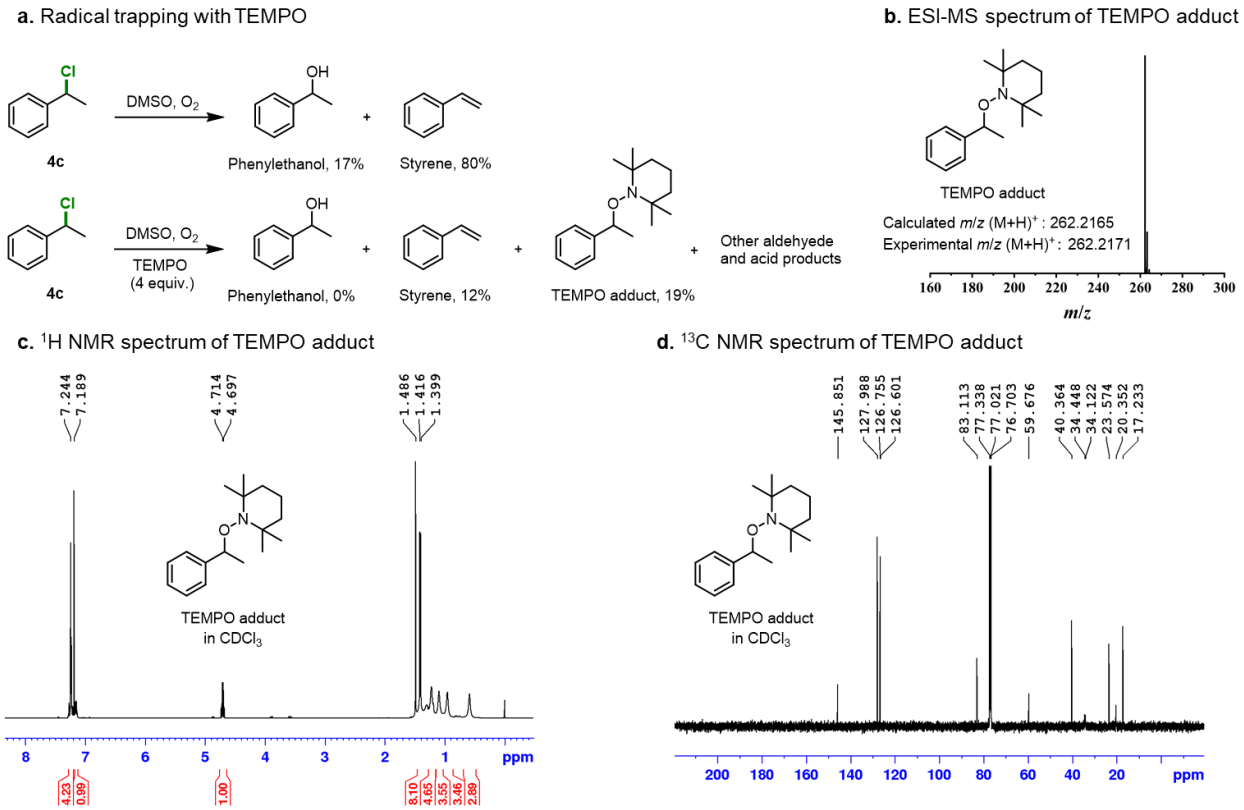

Supplementary Figure 24. Radical trapping experiments. Radical trapping with 4 equiv. 2,2,6,6-tetramethylpiperidin-1-yl)oxyl (TEMPO). Reaction conditions are the same those reported in Extended Data Fig. 2, entry 4. The TEMPO radical adduct was isolated by silica gel chromatography (hexane was used as the mobile phase). (**b**) ESI-MS of the TEMPO radical adduct. (**c**) ^{1}H and (**d**) ^{13}C NMR spectra of the TEMPO radical adduct.

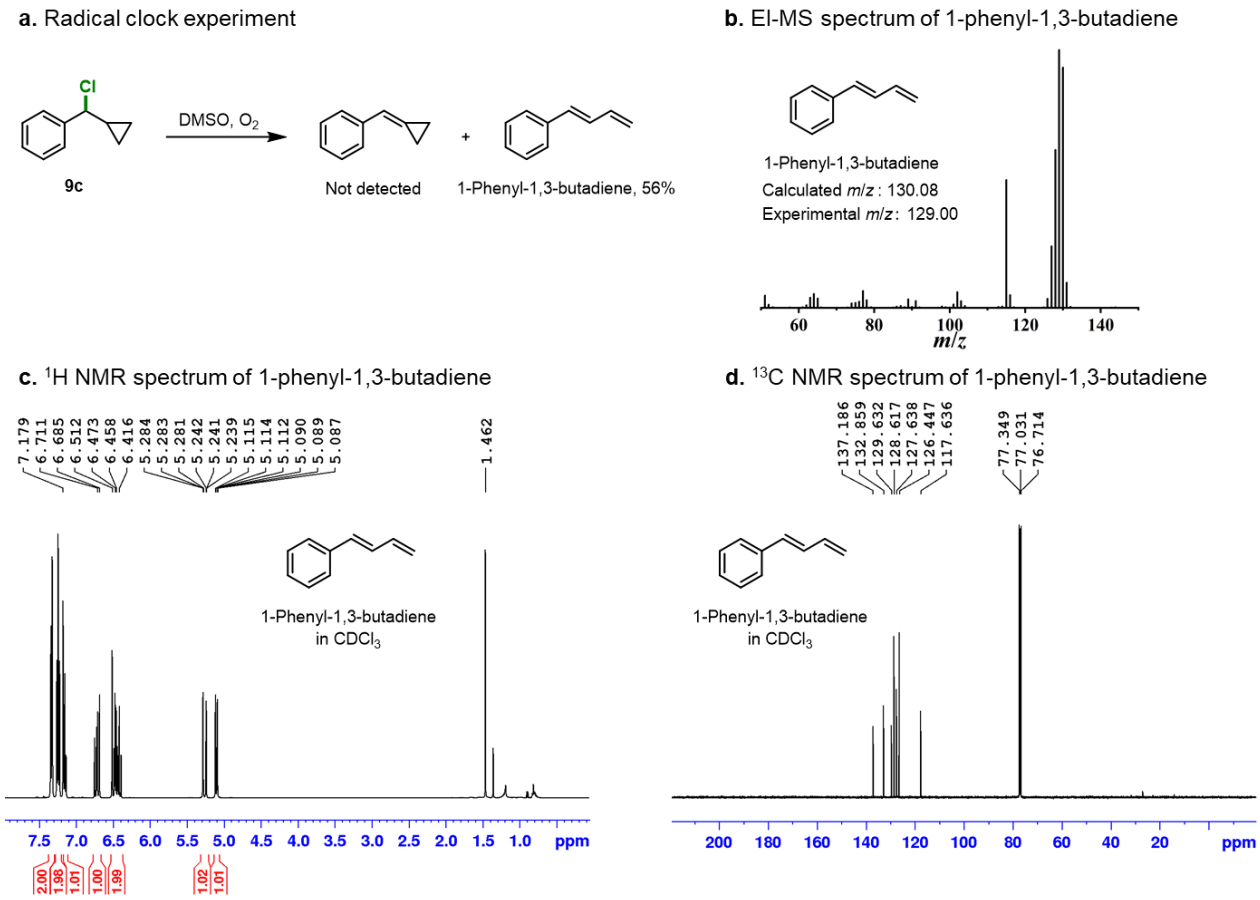

Supplementary Figure 25. Radical clock experiment. (**a**) Radical clock experiment employing (chloro(cyclopropyl)methyl)benzene **9c** as substrate. Reaction conditions are the same as those reported in Extended Data Fig. 2, entry 4. 1-Phenyl-1,3-butadiene was isolated as the main product by silica gel chromatography (hexane was used as the mobile phase). (**b**) EI-MS of 1-phenyl-1,3-butadiene. (**c**) ^{1}H (**d**) ^{13}C NMR spectra of 1-phenyl-1,3-butadiene.

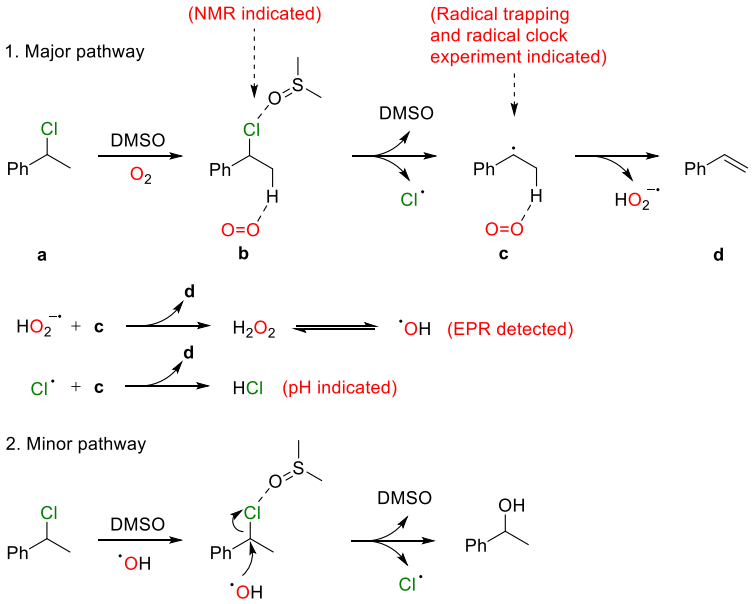

Supplementary Figure 26. Proposed pathways for the DMSO/O_2 catalyzed dechlorination reaction (**a** to **d**). 1,2-Elimination is the major pathway for the thermal dehydrochlorination (>300 ºC) of PVC to produce HCl and polyenes.[10, 13, 17, 19, 25-26] In the reaction reported here, DMSO[27] and O_2[25-26, 28] act as electrophilic Cl^- and nucleophilic H^+ adsorbents, respectively. DMSO is expected to activate the chloride atom in **a** (confirmed by NMR spectroscopy, see Supplementary Figure 22) and O_2 may simultaneously adsorb the β-H, to generate styrene and a $Cl^•$ radical (Major pathway),[25-26] evidenced by the dehydrochlorination product, styrene, not being observed in the absence of O_2 or DMSO (Extended Data Fig. 2, entries 5-7). In addition, O_2 converts into a superoxide radical and the generation of highly active $Cl^•$ radicals and superoxide radicals propagate the continuous dehydrochlorination of **a**, giving HCl (indicated by a decrease in pH, see Supplementary Figure 21) and (hydroxyl radicals, indicated by EPR spectroscopy, see Supplementary Figure 23). A dechloro-hydroxylation product, 1-phenylethanol, was also detected in low yield irrespective of whether the reaction was performed in the absence or presence of O_2 (Extended Data Fig. 2, entries 3-5). A tentative mechanism involving nucleophilic attack of hydroxyl radicals is shown (Minor pathway).[29-31]

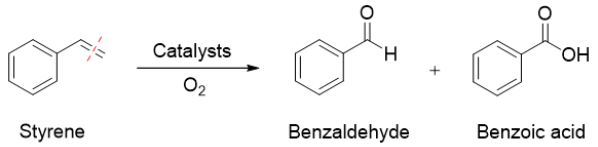

Entry	Catalyst	Benzaldehyde (%)	Benzoic acid (%)
1		0	0
2	20 mol% $NaNO_3$	5	93
3	20 mol% CuO	8	4
4	20 mol% $Cu(OAc)_2$	3	0
5	5 mol% PdO	14	0

Supplementary Figure 27. Testing the activity of Cu, Pd and $NaNO_3$ in C=C bond activation. Reaction conditions: styrene (0.25 mmol), catalyst, biphenyl (0.2 mmol, internal standard), DMSO (2 mL), O_2 (3 bar), 140 ºC, 4 h. $NaNO_3$ is the most efficient catalyst for C=C bond activation.

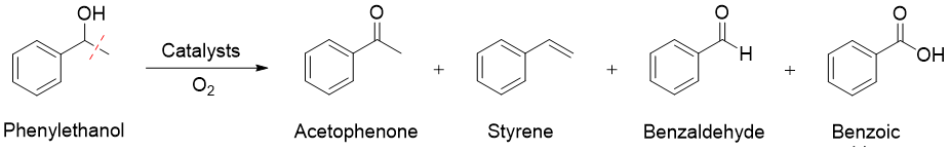

Entry	Catalyst	Acetophenone (%)	Styrene (%)	Benzaldehyde (%)	Benzoic acid (%)
1		2	1	0	0
2	20 mol% $NaNO_3$	1	0	5	90
3	20 mol% CuO	10	0	0	0
4	20 mol% $Cu(OAc)_2$	7	0	0	0
5	5 mol% PdO	90	2	2	3

Supplementary Figure 28. Testing the activity of Cu, Pd and $NaNO_3$ in C(OH)−C bond activation. Reaction conditions: 1-phenylethanol (0.25 mmol), catalyst, biphenyl (0.2 mmol, internal standard), DMSO (2 mL), O_2 (3 bar), 140 ºC, 4 h. PdO promotes the oxidation of 1-phenylethanol to acetophenone.[32-35] However, $NaNO_3$ was found to be the most efficient catalyst for C(OH)−C bond activation, as reported previously.[36] The mechanism of $NaNO_3$ catalyzed C=C/C(OH)−C bond activation is described below.

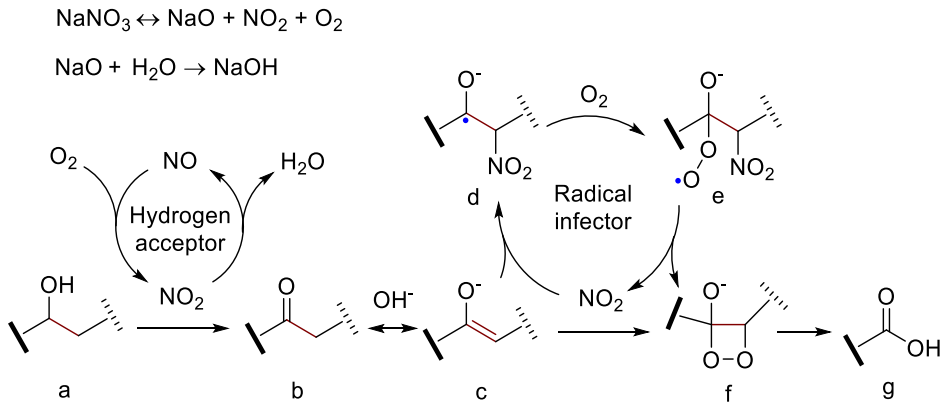

Supplementary Figure 29. Tentative reaction pathway for $NaNO_3$ catalyzed C=C/C(OH)−C bond activation of the alkene and alkanol intermediates. $NaNO_3$ catalyzed C=C/C(OH)−C bond activation was reported in previously.[36] Decomposition of $NaNO_3$ provides NO_2 gas and ^-OH that catalyze the cleavage of C=C/C(OH)−C bonds. Specifically, for the activation of C(OH)−C bond, NO_2 acts as hydrogen acceptor promoting the conversion of alcohol **a** to carbonyl **b**. ^-OH promotes the tautomerization of **b** to enol **c**. The addition of a NO_2 radical to enol **c** generates corresponding carbon centered radical **d**. Radical **d** may capture O_2 resulting in the formation of peroxyl radical intermediate **e**. Following the release of NO_2 radical from **e**, dioxetane intermediate **f** is generated, which undergoes thermal cleavage yielding the carboxylic acid product **g**. The reaction pathway of $NaNO_3$ catalyzed C=C bond activation is similar to the transformation of enol **c** to the carboxylic acid product **g**. Using chlorinated waste, alkene (dominant) and alkanol (minor) intermediates are formed, which can transfer into the carboxylic acid product (i.e. formic acid and other alkyl carboxylic acids) after the $NaNO_3$ catalyzed cleavage of C=C/C(OH)−C bonds. Formic acid can decompose into CO_x gas and H_2O, leading to the total mineralization of the hydrocarbon component.

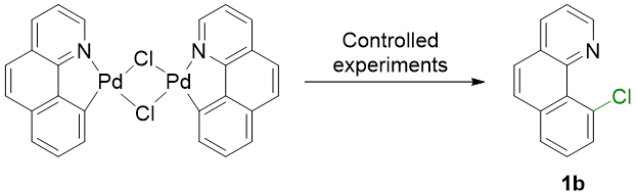

Entry	Reaction condition	Yield of **1b** (%)
1	O_2	0
2	$NaNO_3 + O_2$	33
3	$CuCl_2 + O_2$	0
4	$CuCl_2 + NaNO_3 + O_2$	99

Supplementary Figure 30. Chlorinated product **1b** generated from model benzo[h]quinolinyl Pd(II) chloride intermediate. Reaction conditions: benzo[h]quinolinyl Pd(II) chloride (0.1 mmol), $CuCl_2$ (20 mol%, 0.02 mmol), $NaNO_3$ (20 mol%, 0.02 mmol), biphenyl (0.1 mmol), DMSO (2 mL), O_2 (3 bar), 140 ºC, 1 h. Only with the combination of the $CuCl_2$ and $NaNO_3$ catalysts, benzo[h]quinolinyl Pd(II) chloride affords the chlorinated product **1b** in near-quantitative yield.

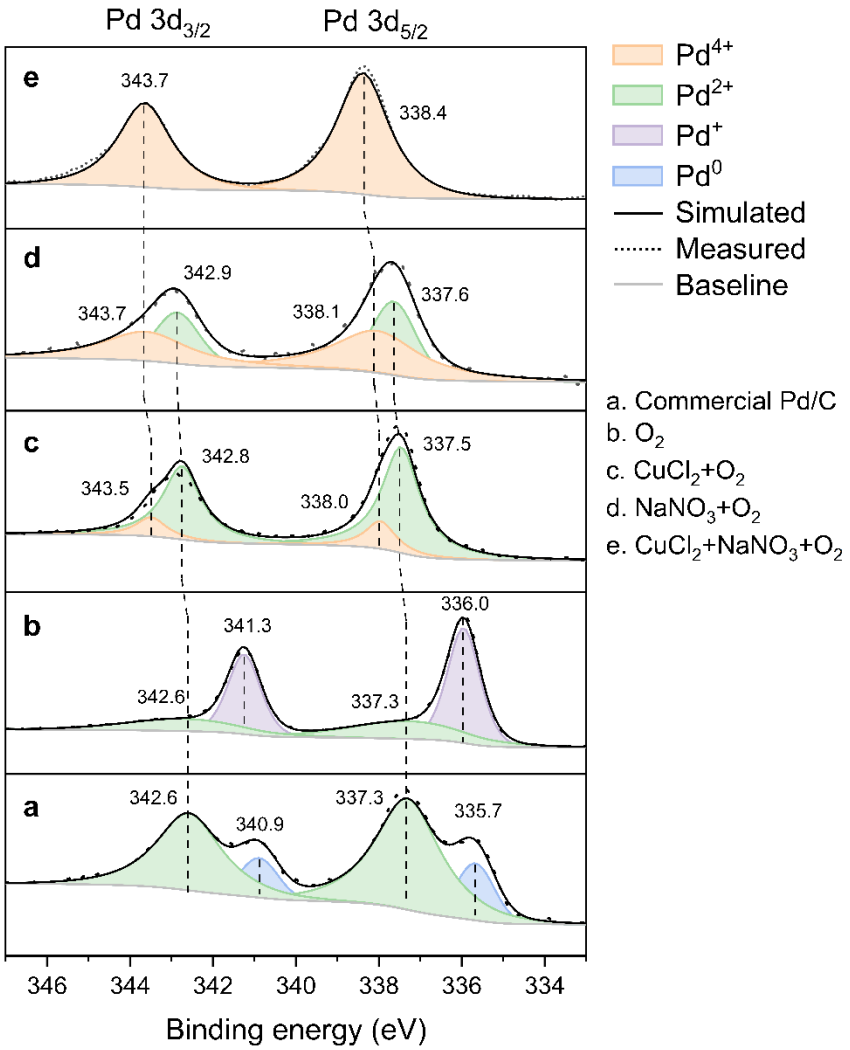

Supplementary Figure 31. X-ray photoelectron spectroscopy (XPS) of the Pd/C catalyst under different reaction conditions in the absence of a substrate. In order to monitor the evolution of the surface species, 10% Pd/C catalyst was used instead of PdO (Pd/C from Sigma-Aldrich has the same catalytic activity as PdO, see Supplementary Table 2, entry 14). After reaction, the Pd/C catalyst was purified by washing with water (3×10 mL), acetone (3×10 mL), ethyl acetate (3×10 mL) and diethyl ether (3×10 mL) and drying under vacuum (30 ºC, 18 h) prior to XPS. (**a**) XPS of commercial 10% Pd/C under anaerobic conditions, peaks with binding energy values E_b ($Pd3d_{5/2}$ and $Pd3d_{5/2}$) of 335.7 and 340.9 eV correspond to Pd^0 species and peaks with E_b ($Pd3d_{5/2}$ and $Pd3d_{5/2}$) of 337.3 and 342.6 eV correspond to Pd^{2+} species, indicating that the Pd/C catalyst is partially oxidized with PdO surface species. (**b**) XPS of the Pd/C catalyst after treatment under aerobic reactions (10% Pd/C (0.0125 mmol), DMSO (2 mL), O_2 (3 bar), 140 ºC, 15 h), peaks corresponding to Pd^0 and Pd^{2+} species nearly disappear and new peaks with E_b ($Pd3d_{5/2}$ and $Pd3d_{5/2}$) at 336.0 and 341.3 eV appear, which may be attributed to Pd^+ species. Thus, the surface species on the Pd/C catalyst undergo synproportionation in O_2 rather than further oxidation. (**c**) XPS of the Pd/C catalyst after treatment under Cu catalyzed aerobic reaction conditions ($Cu(NO_3)_2$•$3H_2O$ (0.05 mmol), 10% Pd/C (0.0125 mmol), DMSO (2 mL), O_2 (3 bar), 140 ºC, 15 h). Peaks with E_b ($Pd3d_{5/2}$ and $Pd3d_{5/2}$) at 337.5 and 342.8 eV correspond to Pd^{2+} species. The new component with highest E_b ($Pd3d_{5/2}$ and $Pd3d_{5/2}$) at 338.0 and 343.5 eV may be assigned to Pd^{4+} species. (**d**) XPS of the Pd/C catalyst following treatment under $NaNO_3$ catalyzed aerobic reaction conditions ($NaNO_3$ (0.05 mmol), 10% Pd/C (0.0125 mmol), DMSO (2 mL), O_2 (3 bar), 140 ºC, 15 h). Peaks with E_b ($Pd3d_{5/2}$ and $Pd3d_{5/2}$) at 337.6 and 342.9 eV correspond to Pd^{2+} species.

The new component with highest E_b ($Pd3d_{5/2}$ and $Pd3d_{5/2}$) at 338.1 and 343.7 eV corresponds to Pd^{4+} species. These results suggest that $CuCl_2$ or $NaNO_3$ act as redox mediator,[37] with O_2 acting as the final oxidant to promote the full oxidation of Pd^0 to Pd^{2+} species and partial oxidation of Pd^{2+} to Pd^{4+} species. (**e**) XPS of the Pd/C catalyst following treatment under aerobic reaction conditions in the presence of both $CuCl_2$ and $NaNO_3$ ($Cu(NO_3)_2$•$3H_2O$ (0.05 mmol), 10% Pd/C (0.0125 mmol), $NaNO_3$ (0.05 mmol), DMSO (2 mL), O_2 (3 bar), 140 ºC, 15 h). Peaks indicative of Pd^0 and Pd^{2+} species are not observed. The only component with highest E_b ($Pd3d_{5/2}$ and $Pd3d_{5/2}$) at 338.4 and 343.7 eV may be assigned Pd^{4+} species, indicating that using both $CuCl_2$ and $NaNO_3$ as redox mediators, oxidation of Pd^0 and Pd^{2+} species to Pd^{4+} is favored. Pd(IV) species formed under the standard reaction conditions are consequently expected to be the key intermediates that afford C−Cl bonds via reductive elimination.[38-39] These results agree with the observation that the chlorination reaction cannot proceed without either Cu or $NaNO_3$ catalyst (Extended Data Fig. 3).

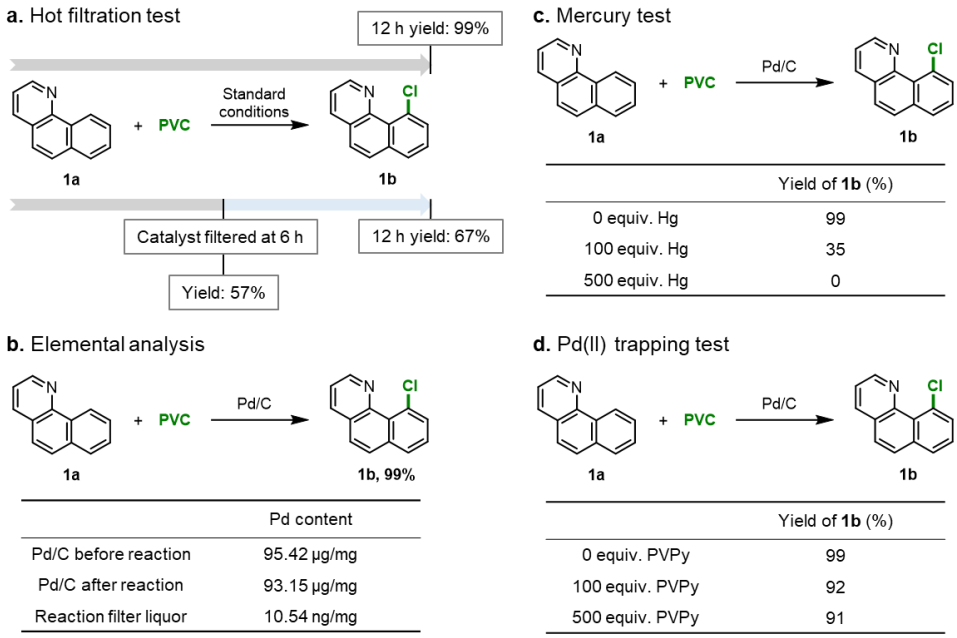

Supplementary Figure 32. Experiments to probe the nature of the active PdO catalyst. (**a**) Hot filtration test under the standard reaction conditions.[40] The hot reaction mixture was filtered to remove all heterogenous PdO catalyst after 6 h reaction, and the reaction was continued for a further 6 h, no further reaction was observed, suggesting all active heterogenous species were removed by filtration. This observation is consistent with the homogeneous Pd catalysts studied being less active than the heterogenous Pd catalysts studied (see Supplementary Figure 2 and Supplementary Table 2). (**b**) Elemental analysis of the heterogenous Pd/C catalyst and liquid reaction mixture. In order to determine if the heterogenous Pd catalyst leaches, Pd/C catalyst was used (Pd/C transforms into PdO/C under the reaction conditions and shows the same catalytic activity as PdO, see Supplementary Table 2). Inductively Coupled Plasma (ICP) mass spectrometry was used to determine the Pd content of the reaction mixture before and after reaction, as well as the filtered solution after reaction, suggesting very little leaching of Pd takes place. (**c**) Mercury poisoning test. Pd/C was used instead of PdO. Mercury acts as a selective poison for nanoparticle catalysts to form a catalytically inactive Hg amalgam. Addition of Hg was found to inhibit the reaction, suggesting that the catalyst is not homogeneous.[41] (**d**) Pd(II) trapping test using insoluble poly(4-vinylpyridine) (PVPy).[42] The pyridine ligands in PVPy strongly coordinates to homogeneous Pd species, trapping them within the insoluble polymer. Since PVPy does not suppress the reaction it suggests that homogeneous Pd species are not the active catalyst.[42]

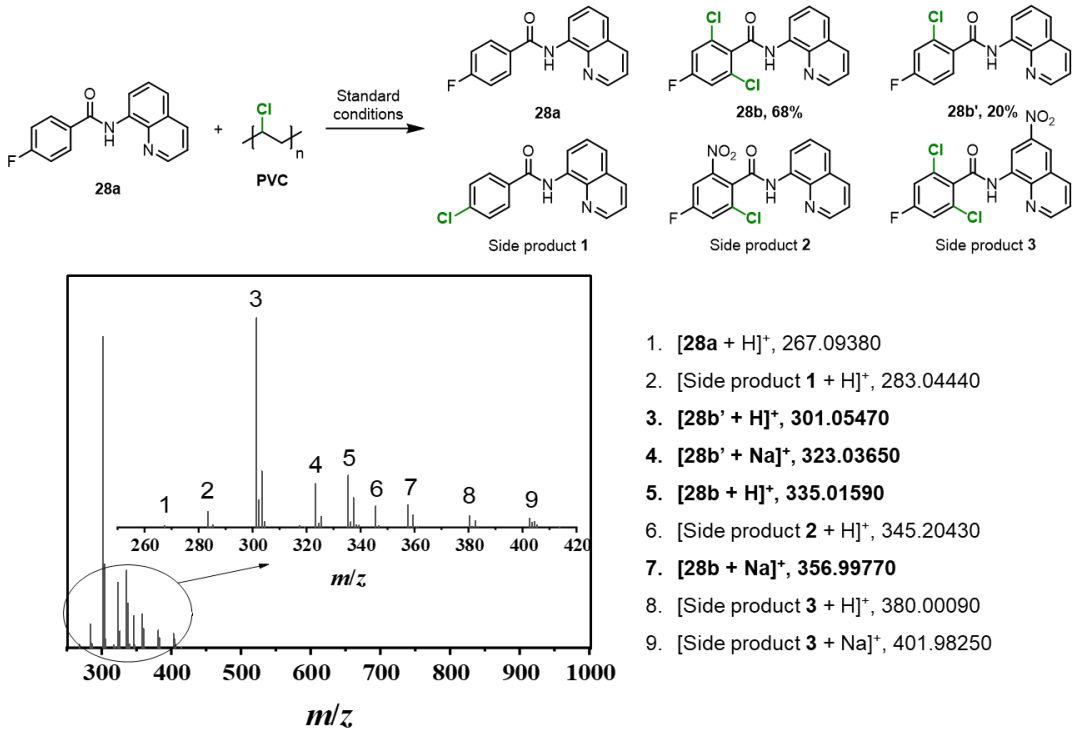

Supplementary Figure 33. Electrospray ionization mass spectrometry (ESI-MS) of the reaction mixture after filtration. In order to obtain strong mass signals **28a** was used as the substrate. Heterogeneous PdO was filtered and the DMSO reaction mixture solution was diluted with THF (DMSO : THF, 1 : 20, v/v). Pd species were not detected. Peak assignments are listed and correspond to the substrate and products.

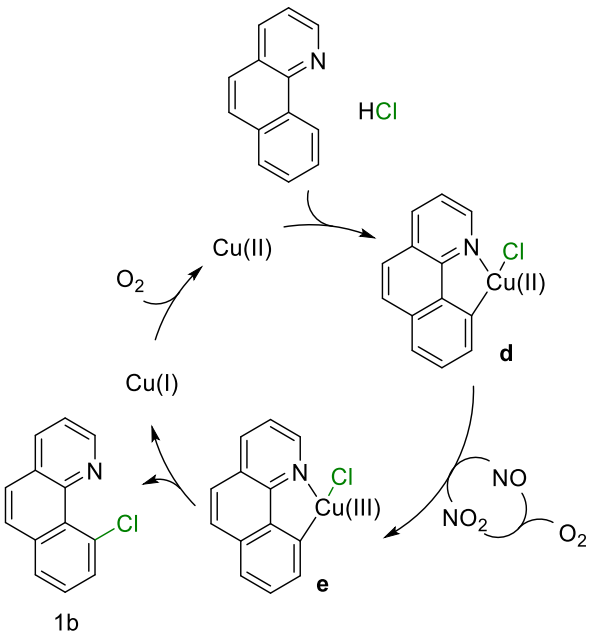

Supplementary Figure 34. Proposed reaction pathway for Cu catalyzed C−H chlorination with $NaNO_3$ promoter. Without Pd catalyst, Cu also can catalyze C−H chlorination with $NaNO_3$ as promoter, but less efficiently (Extended Data Fig. 3, entry 5). The Cu catalyst also will activate C−H bond of substrate **1a** to generate the Cu(II) complex **d**.[43-45] After oxidation with NO_2 (derived from the decomposition of $NaNO_3$), the Cu(III) complex **c** is formed. Although less favorable, Cu(III) complex **c** can also undergo reductive elimination to afford product **1b**.[45]

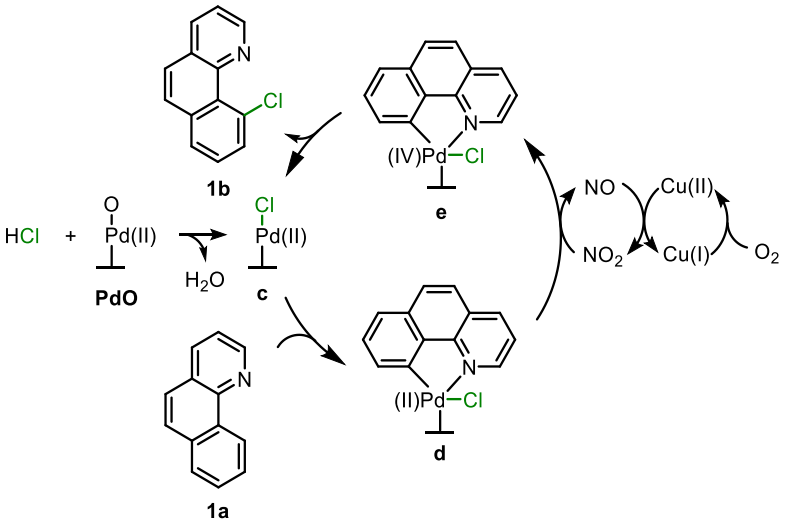

Supplementary Figure 35. Proposed reaction pathway for PdO catalyzed C−H chlorination with Cu and $NaNO_3$ promotor. Using HCl as chlorination reagent, PdO, $Cu(NO_3)_2$, $NaNO_3$ and O_2 are indispensable for the chlorination of 7,8-benzoquinoline **1a** to 10-chlorobenzoquinoline **1b**. A bimetallic pathway might be in operation as reported elsewhere for catalytic C–C or C–X bond formation.[46-47] Ion exchange of HCl with PdO generates the Pd(II) intermediate **c**.[48] The Pd catalyst **c** will activate C−H bond of substrate **1a** to generate the Pd(II) complex **d**.[43-45] After oxidation with Cu and NO_2 (derived from the decomposition of $NaNO_3$), the Pd(IV) complex **e** is formed.[45] Reductive elimination of Pd(IV) complex **e** gives product **1b**.[45]

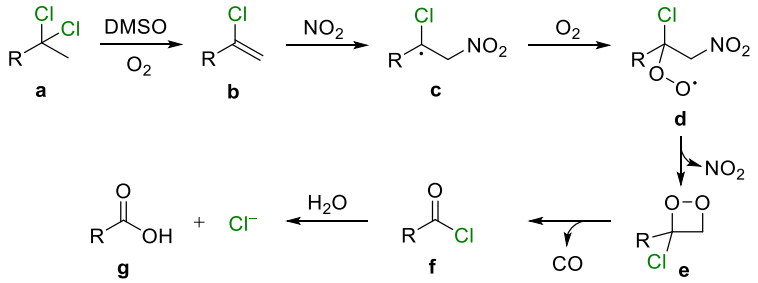

Supplementary Figure 36. Proposed pathway for the dechlorination and depolymerization of PVDC-type model compounds, i.e. containing two Cl atoms at the α-position. The Cl atoms undergo DMSO/O_2 catalyzed dechlorination to afford alkene intermediate **b** (see Supplementary Figure 26 for further details), followed by $NaNO_3$ catalyzed C=C bond cleavage and depolymerization to generate CO and acyl chloride **f** (Supplementary Figure 29). Hydrolysis of acyl chloride **f** affords Cl^- and carboxylic acid **g**.

Life cycle assessment (LCA)

Methods

The Life Cycle Assessment (LCA) approach implemented is a gate-to-gate analysis exclusively focused on the manufacturing phase of aryl chlorides. The production process for each scenario is synthetically represented in Supplementary Figs. 37-40. Analysis starts from the acquisition of raw materials, encompassing the synthetic process of aryl chlorides and it ends with waste disposal. LCA using PVC as chlorination reagent (scenario 1) is compared with a typical chlorination method using N-chlorosuccinimide (NCS) as chlorination reagent (scenario 2),[49] affording 2-(2-chloro-5-nitrophenyl)pyridine **12b**, an intermediate in the synthesis of the anticancer drug vismodegib. LCA of this work (scenario 3) is also compared with electrochemical method using PVC as chlorination reagent,[50] for the generation of 1-(2-chlorophenyl)-pyrazole **19b** (scenario 4)**.** LCA was performed using OpenLCA 1.11, with the Ecoinvent v3.8 database.[51] The scope of the LCA is to compare the 100-year global warming potential (GWP 100a) for the production of aryl chlorides of using PVC waste as chlorination reagent with other chlorination methods. Impact assessment is based on IPCC 2013 GWP 100a.[50, 52] Reaction details and LCA results are summarized in Supplementary Tables S5-7.

Assumptions

1. All scenarios are scaled to afford 1 kg of product.
2. In all scenarios, reactions are performed in sealed batch reactors and the energy consumption of each scenario was assumed to be constant.
3. In scenario 1 the equivalent PVC is considered to be incinerated, i.e. if the PVC is not used as a chlorination reagent.
4. In scenario 3 unreacted PVC is incinerated and the impact of DEHP is not included.
5. In scenarios 2 and 4 the production of valuable CO is not included.
6. Repeated reagents, solvents, energy consumption during product isolation, equipment required and waste effluent treatment and disposal, are deemed constant and are therefore not included.

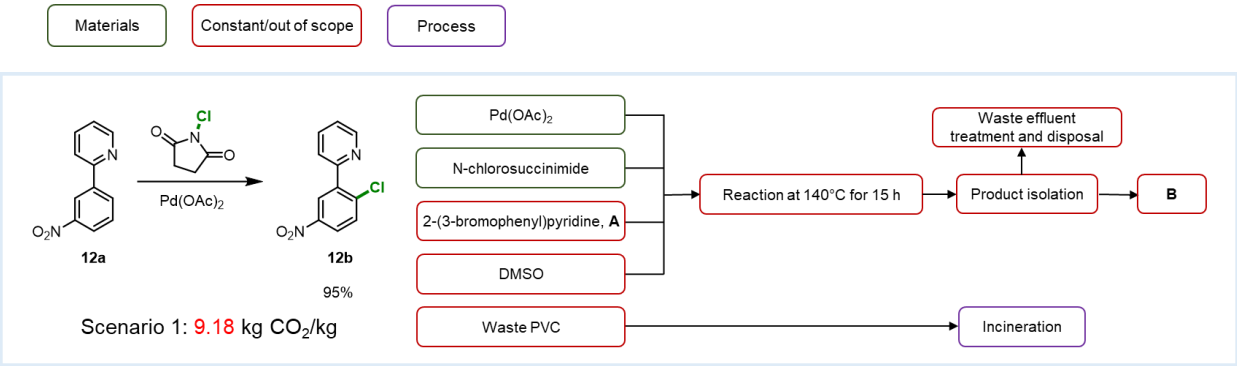

Supplementary Figure 37. LCA diagram for scenario 1.

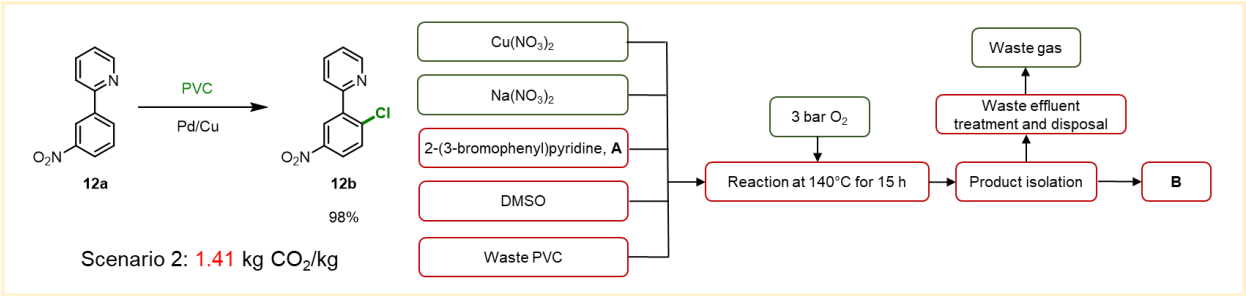

Supplementary Figure 38. LCA diagram for scenario 2.

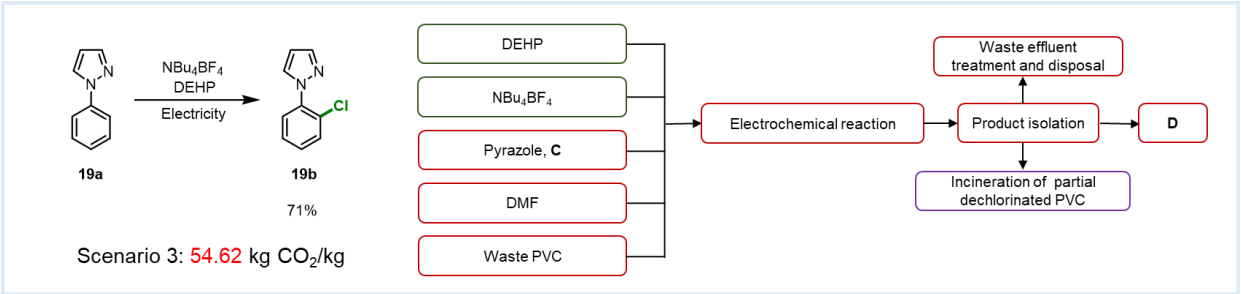

Supplementary Figure 39. LCA diagram for scenario 3.

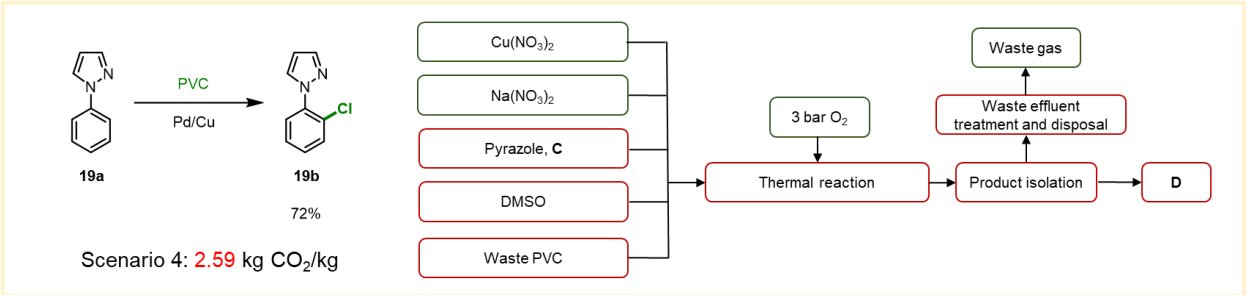

Supplementary Figure 40. LCA diagram for scenario 4.

Supplementary Table 5. Reaction details of scenarios 1-4.

Scenario	Substrate	Product	Materials	Yield (%)	Source
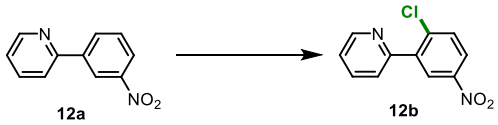					
1	**12a** (0.90 kg)	**12b** (1.00 kg)	$Pd(OAc)_2$ (5 mol%, 0.05 kg), N-chlorosuccinimide (1.5 equiv., 0.90 kg)	95	Ref. 7
2	**12a** (0.87 kg)	**12b** (1.00 kg)	PVC water pipe (1.5 equiv., 0.27 kg), $Cu(NO_3)_2{\bullet}3H_2O$ (20 mol%, 0.21 kg), PdO (5 mol%, 0.03 kg), $NaNO_3$ (20 mol%, 0.07 kg)	98	This work
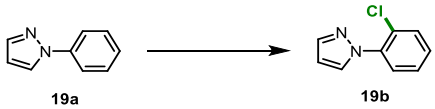					
3	**19a** (1.14 kg)	**19b** (1.00 kg)	PVC (~8 equiv., 3.95 kg), NBu_4BF_4 (~7.3 equiv., 5.15 kg), DEHP (1 equiv., 3.04 kg)	71	Ref. 8
4	**19a** (1.12 kg)	**19b** (1.00 kg)	PVC water pipe (1.5 equiv., 0.73 kg), $Cu(NO_3)_2{\bullet}3H_2O$ (20 mol%, 0.37 kg), PdO (5 mol%, 0.05 kg), $NaNO_3$ (20 mol%, 0.13 kg)	72	This work

Supplementary Table 6. LCA results for scenarios 1-2.

Item	**Impact (kg CO_2 per eq/kg)**	**Scenario 1**		**Scenario 2**	
		Amounts (kg)	*Impact (kg CO_2 per eq/kg)*	*Amounts (kg)*	*Impact (kg CO_2 per eq/kg)*
Materials production					
N-chlorosuccinimide	4.59	0.90	4.13	0	0
Palladium(II) acetate	92.97	0.05	4.65	0	0
Copper(II) nitrate	4.50	0	0	0.21	0.95
Sodium nitrate	0.52	0	0	0.07	0.04
Oxygen	1.07	0	0	0.02	0.02
Distribution and use life/end of life					
PVC incineration	1.47	0.27	0.40	0	0
CO_2 from reaction	1	0	0	0.40	0.40

LCA–GWP (kg CO_2 per eq/kg)	**9.18**	**1.41**

Supplementary Table 7. LCA results for scenarios 3-4.

Item	**Impact (kg CO_2 per eq/kg)**	**Scenario 3**		**Scenario 4**	
		Amounts (kg)	*Impact (kg CO_2 per eq/kg)*	*Amounts (kg)*	*Impact (kg CO_2 per eq/kg)*
Materials production					
DEHP	802.39	0	0	0	0
NBu_4BF_4	9.48	5.15	48.82	0	0
Copper(II) nitrate	4.50	0	0	0.37	1.67
Sodium nitrate	0.52	0	0	0.14	0.07
Oxygen	1.07	0	0	0.02	0.02
Distribution and use life/end of life					
PVC incineration	1.47	3.95	5.80	0	0
CO_2 from reaction	1	0	0	0.83	0.83
LCA–GWP (kg CO_2 per eq/kg)		**54.62**		**2.59**	

NMR spectra

Substrate

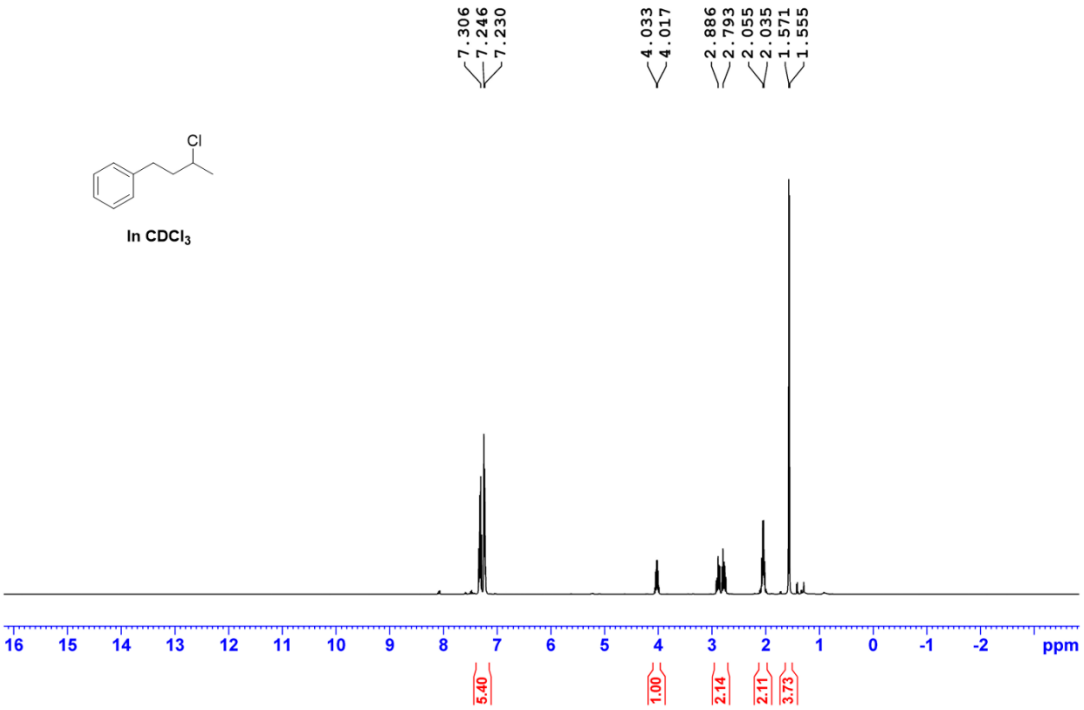

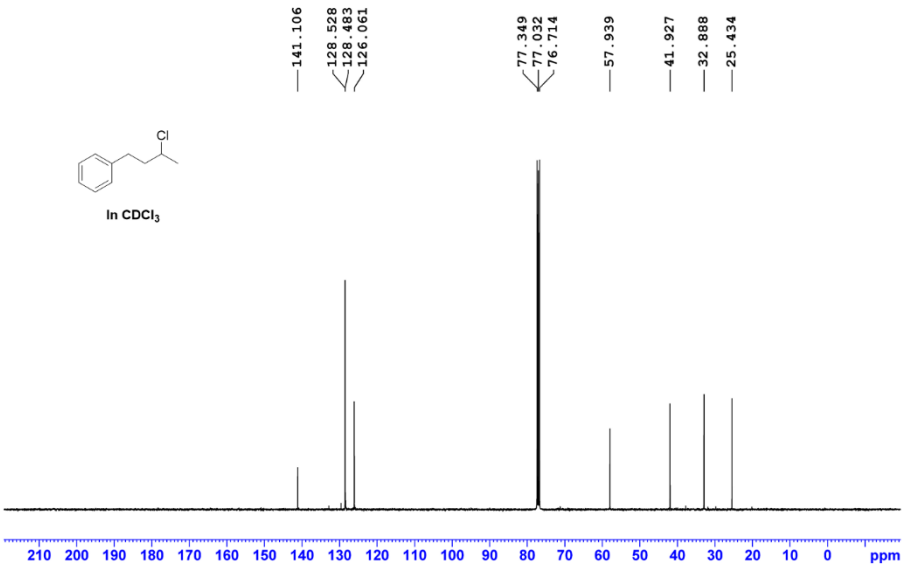

Supplementary Information

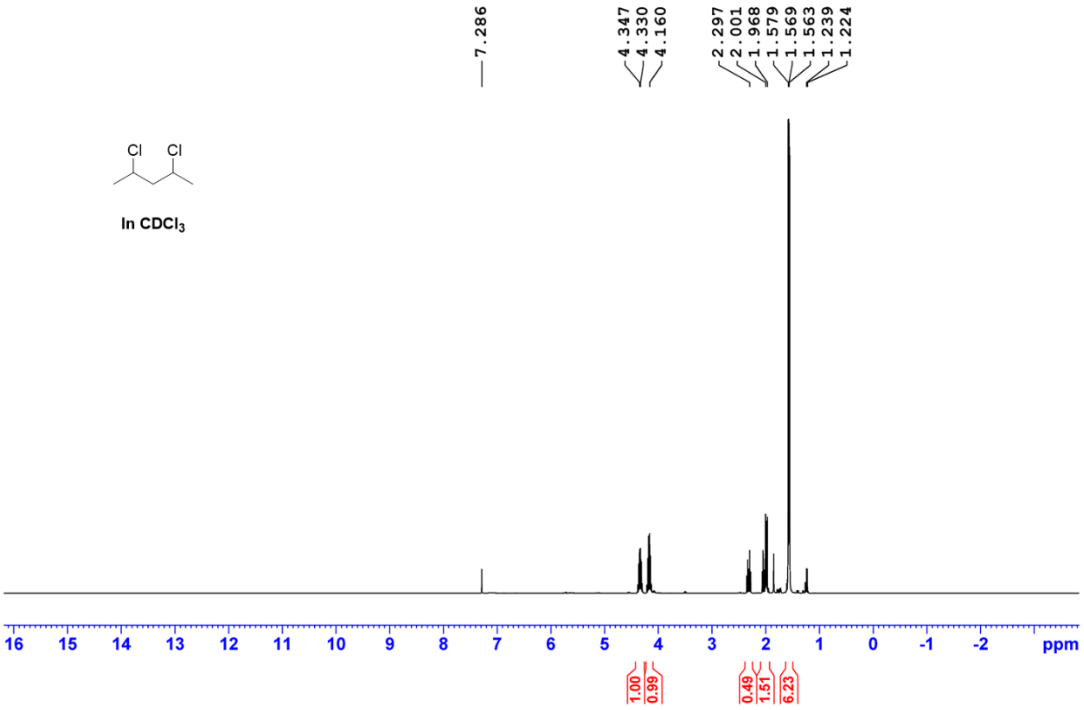

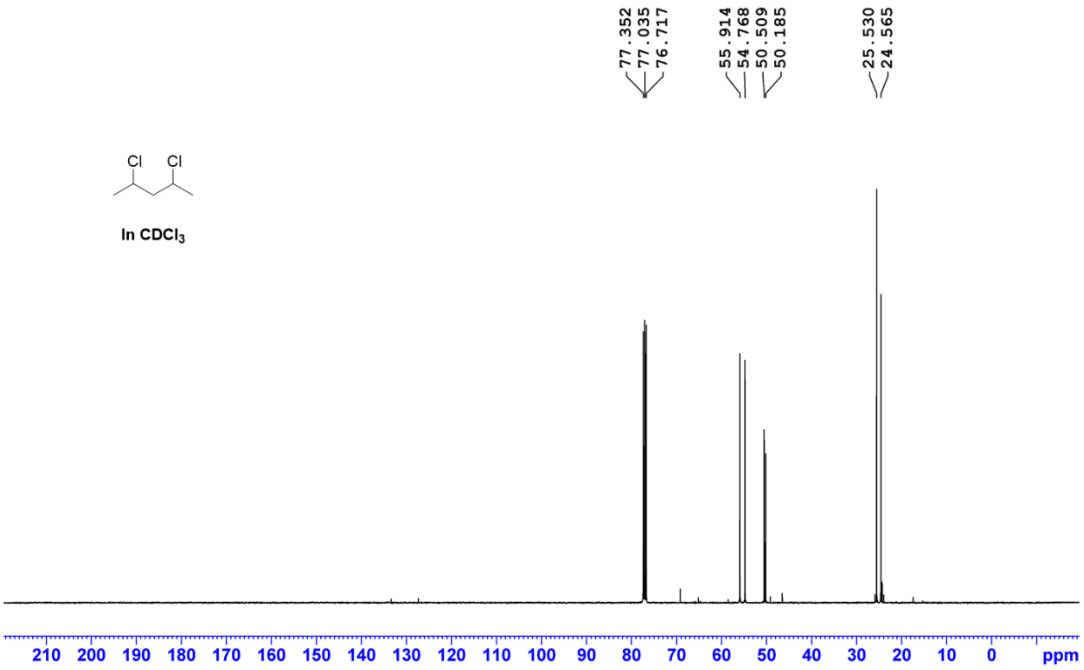

Supplementary Information

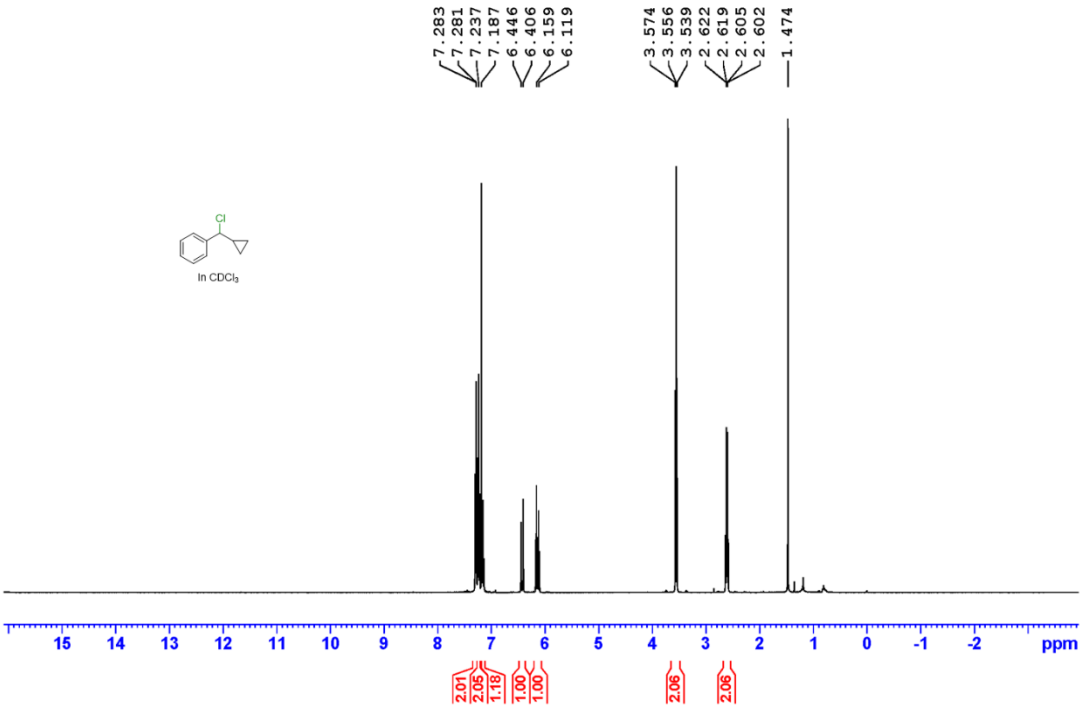

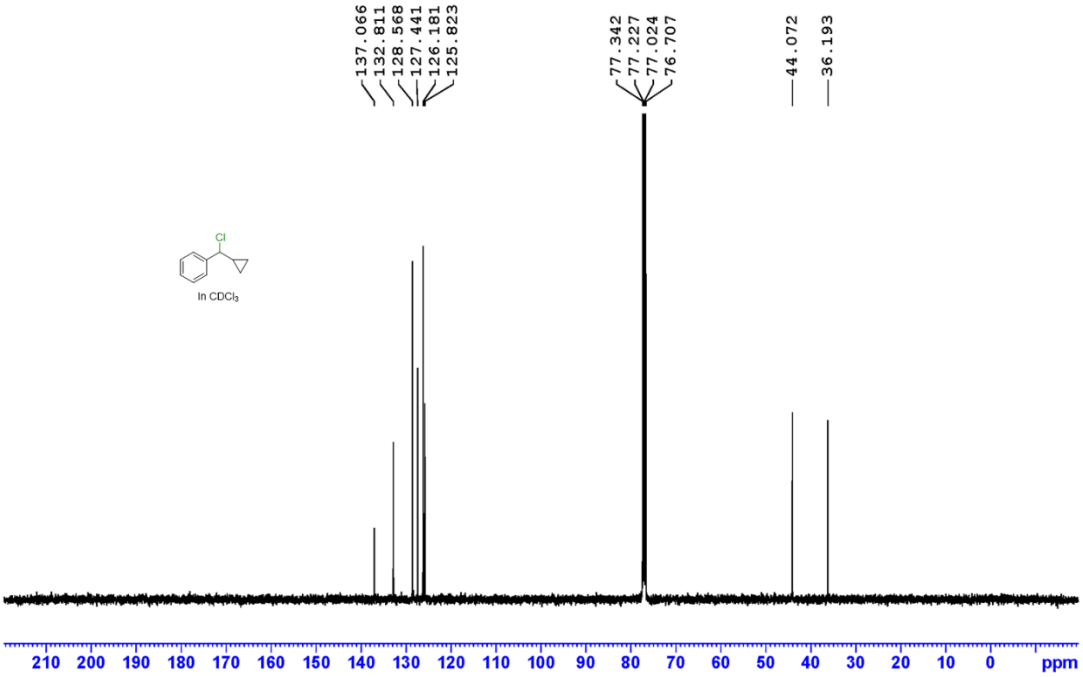

Supplementary Information

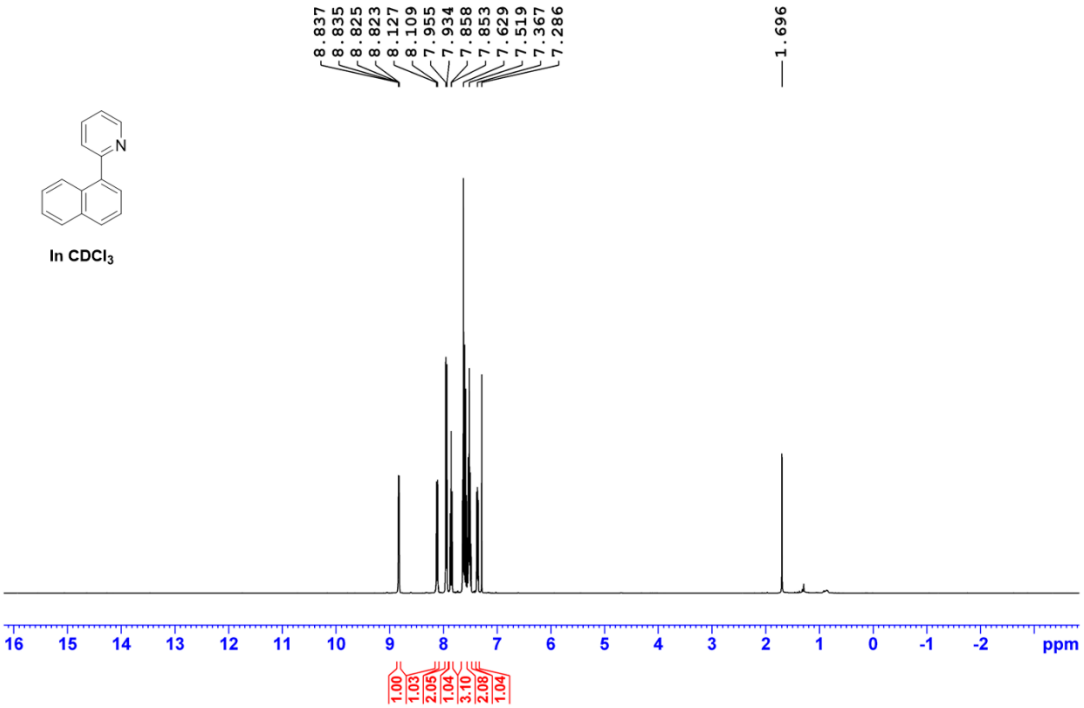

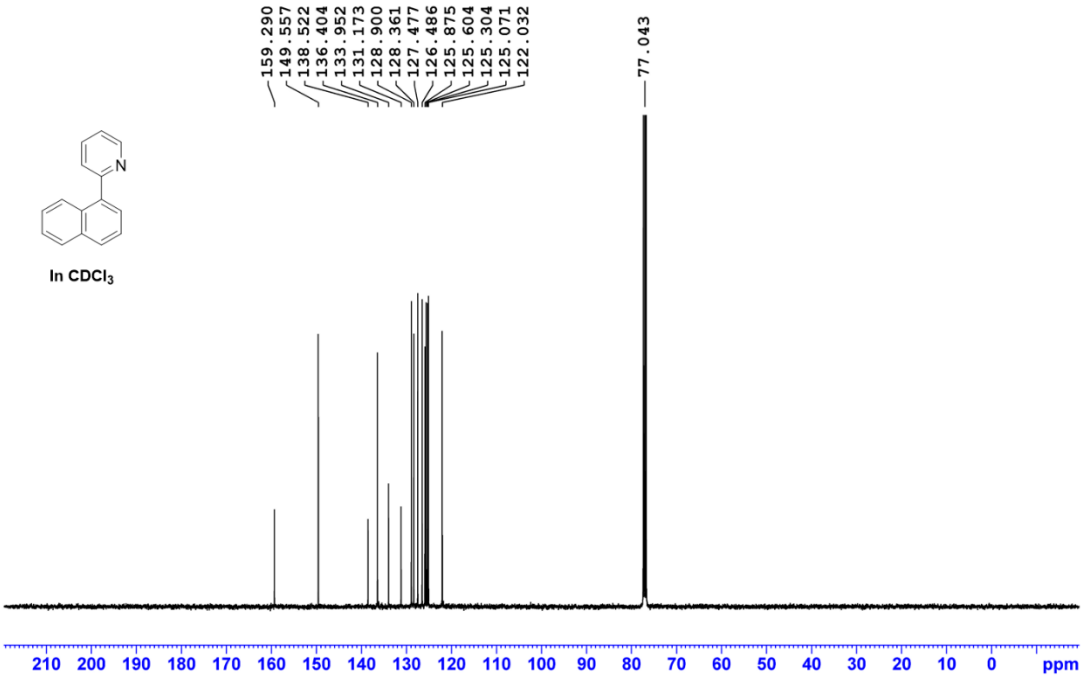

Supplementary Information

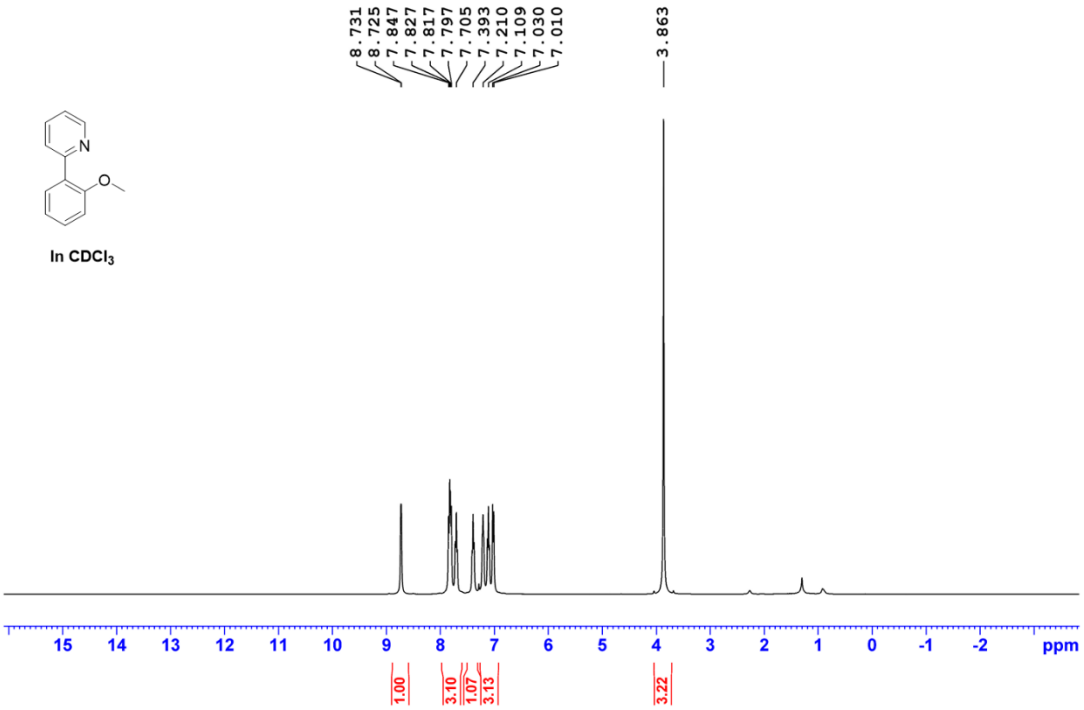

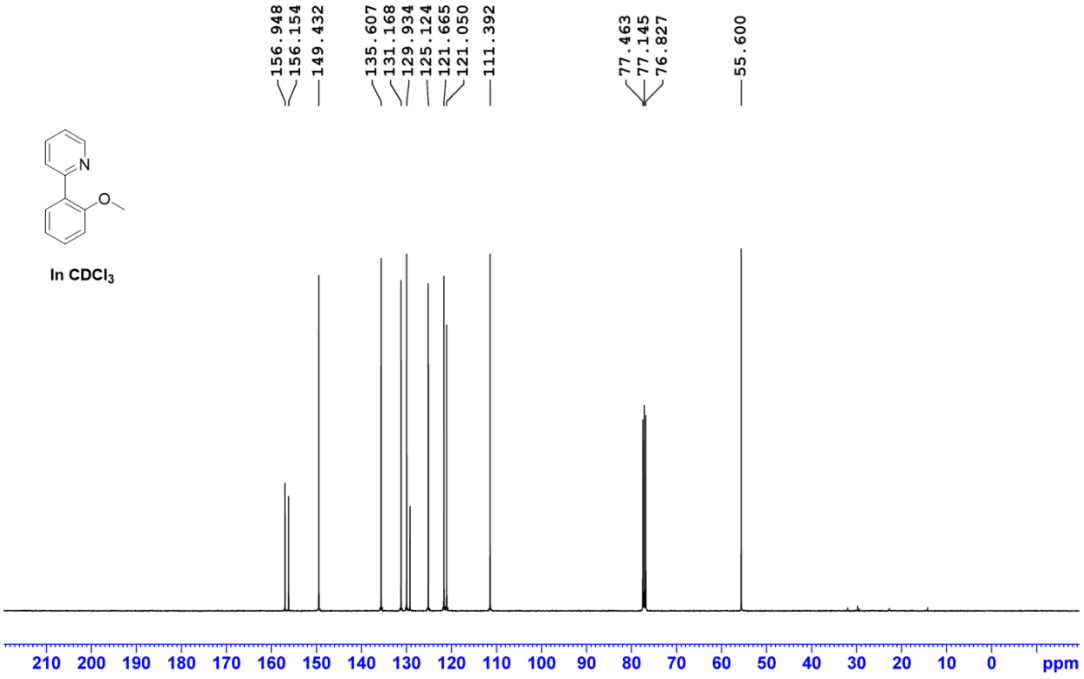

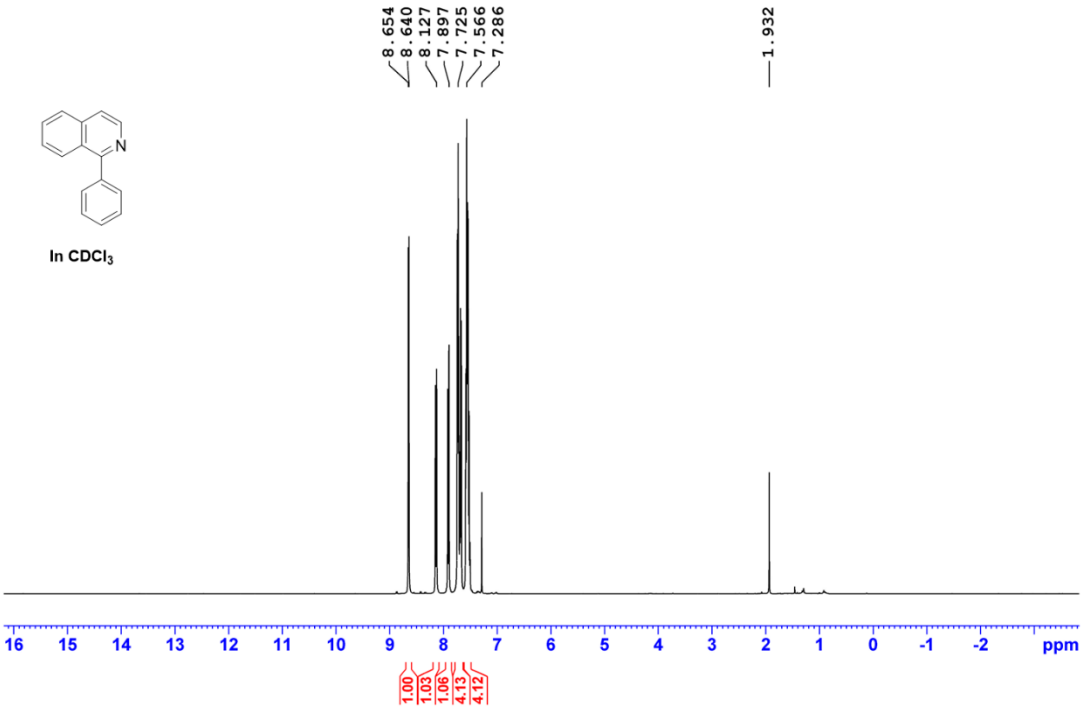
8.654
8.640
8.127
7.897
7.725
7.566
7.286
1.932
N
In CDCl3
16 15 14 13 12 11 10 9 8 7 6 5 4 3 2 1 0 -1 -2 ppm
1.00
1.03
1.06
4.13
4.12

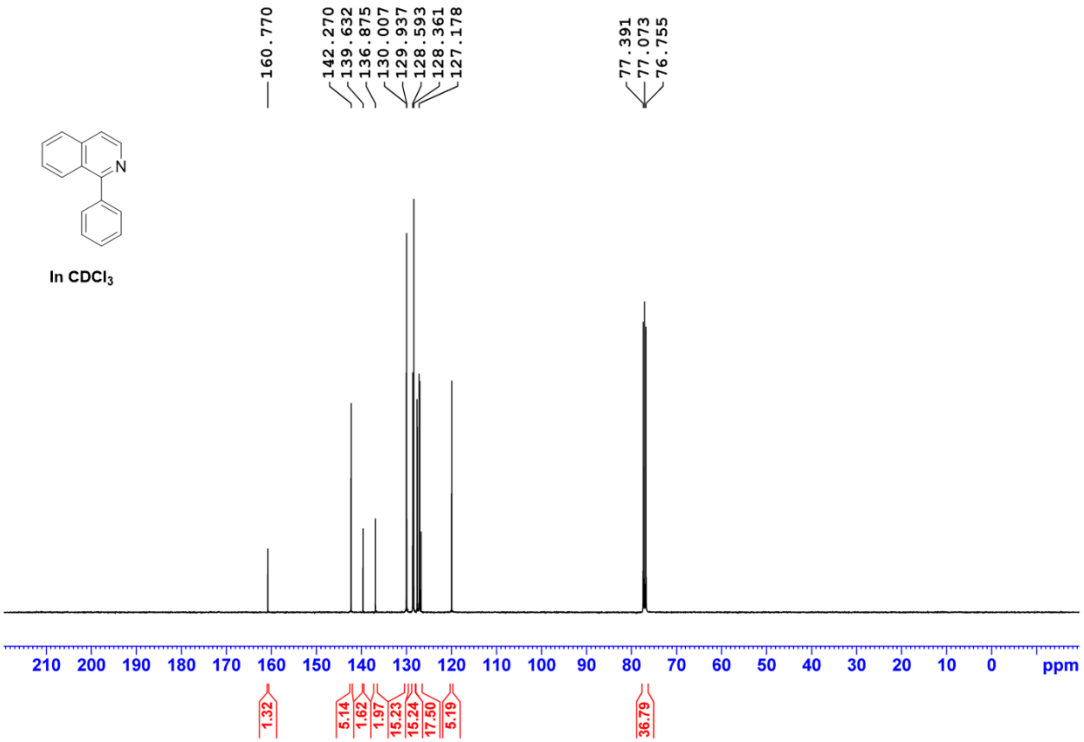
160.770
142.270
139.632
136.875
130.007
129.937
128.593
128.361
127.178
77.391
77.073
76.755
N
In CDCl3
210 200 190 180 170 160 150 140 130 120 110 100 90 80 70 60 50 40 30 20 10 0 ppm
1.32
5.14
1.62
1.97
15.23
15.24
17.50
5.19
36.79

Supplementary Information

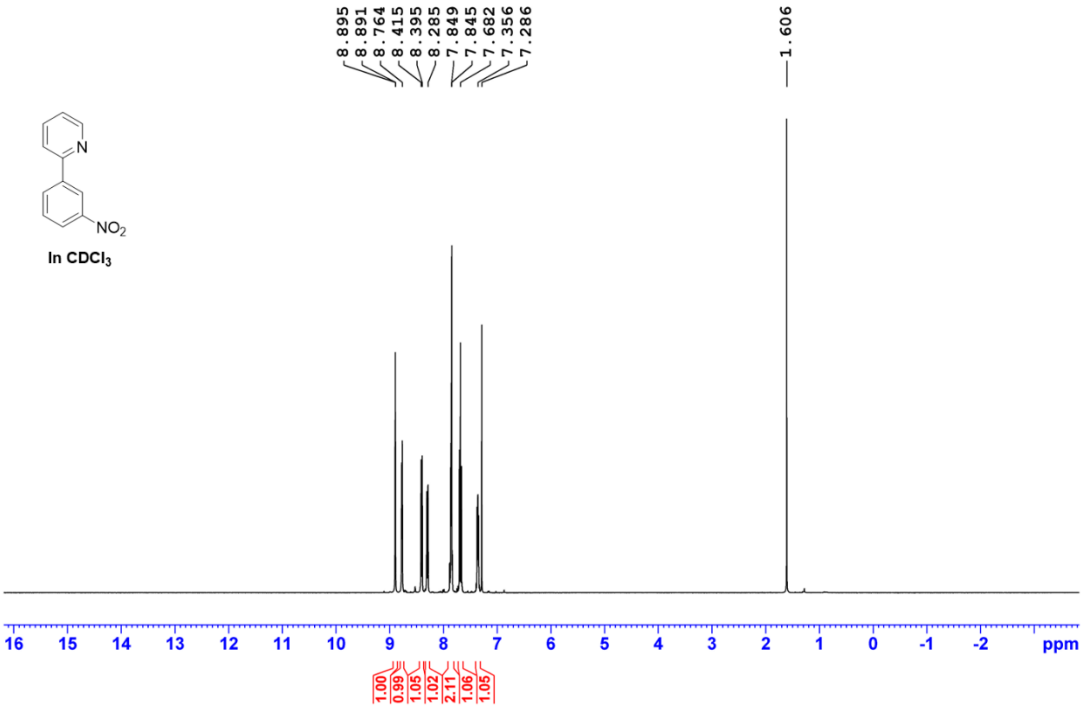

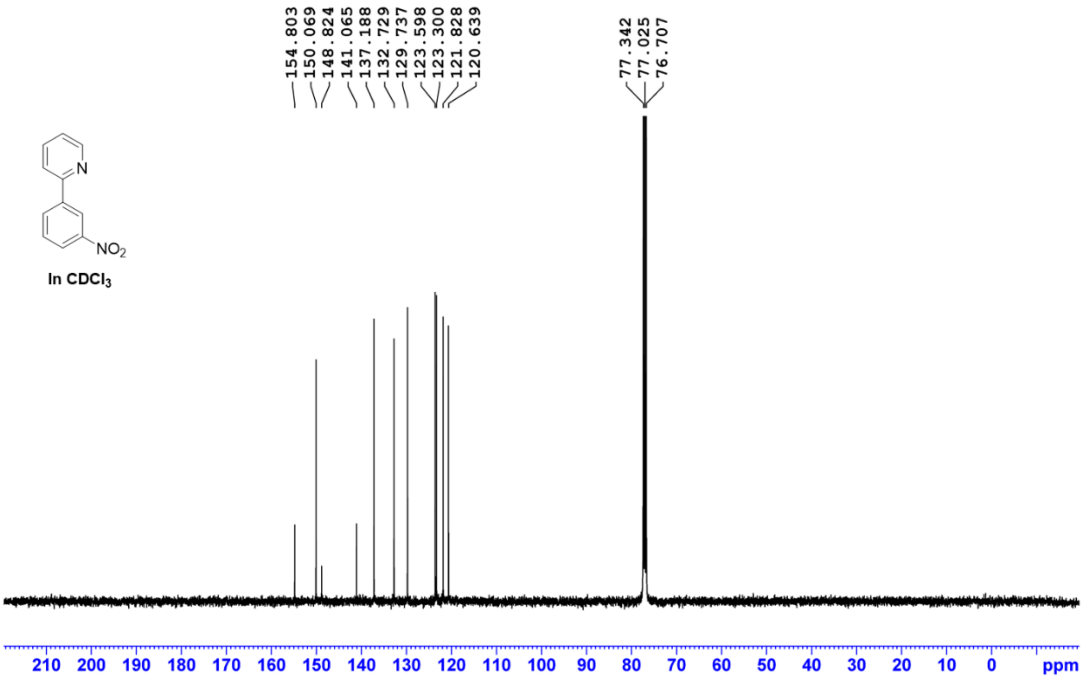

Supplementary Information

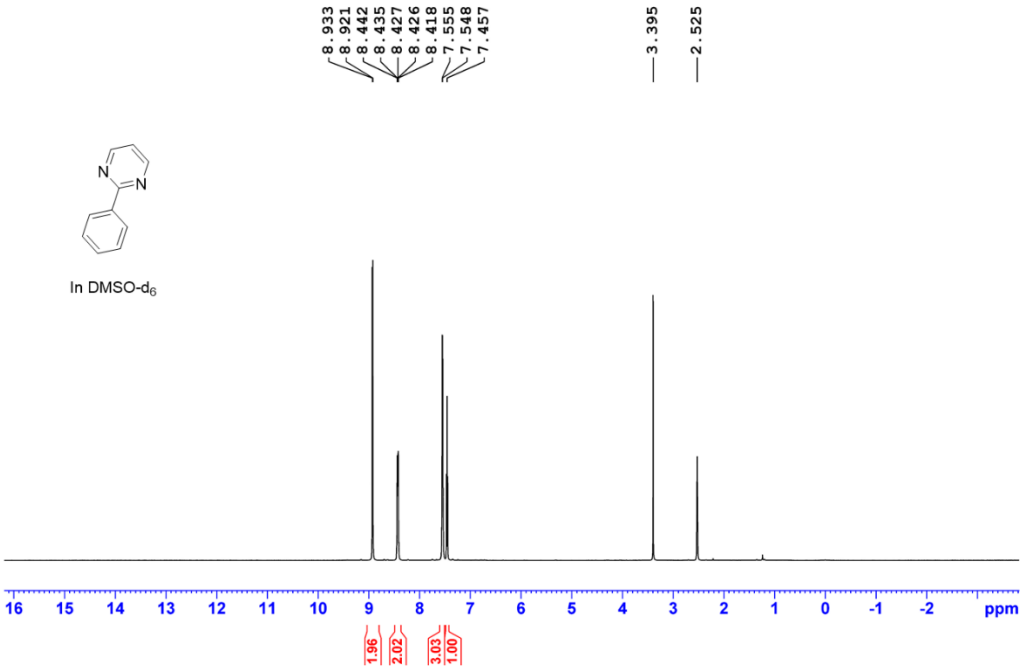

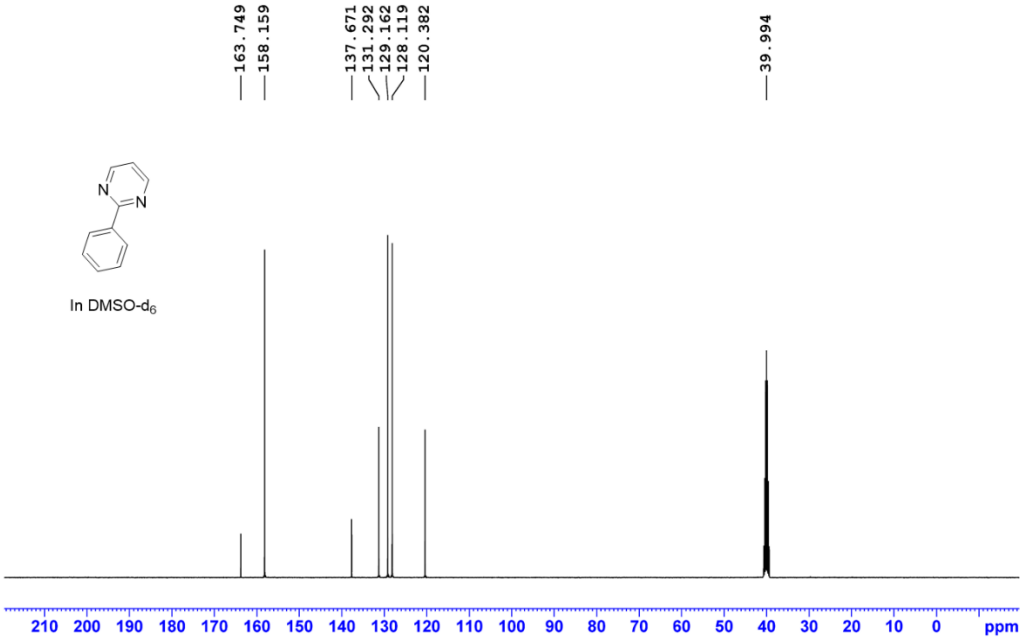

Supplementary Information

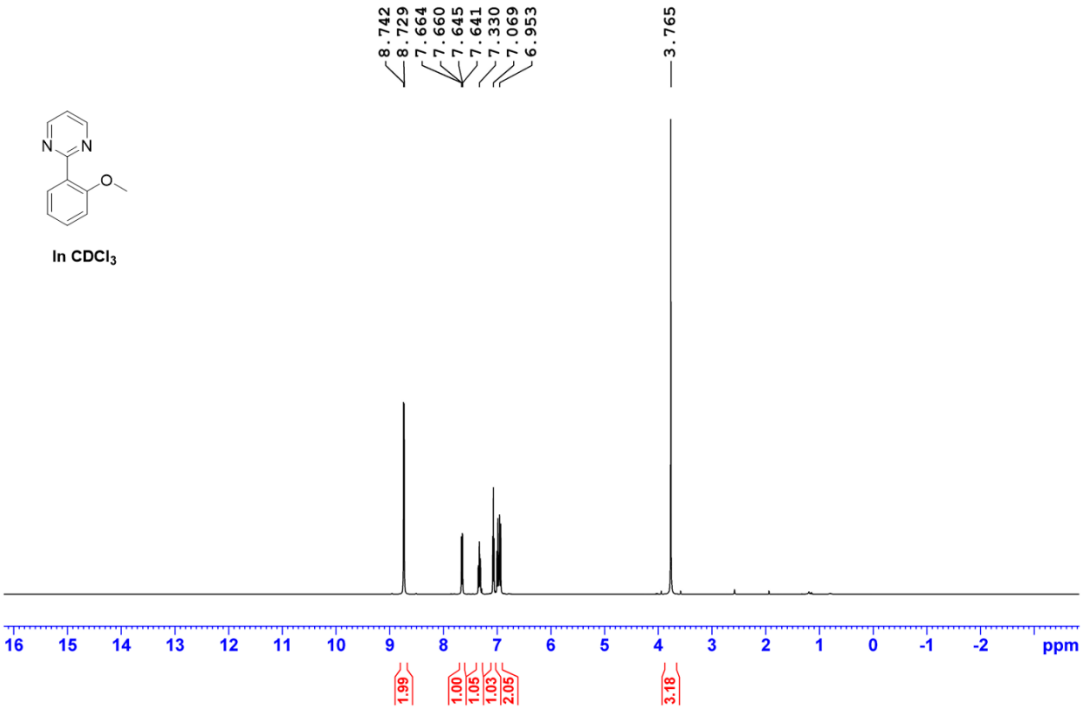

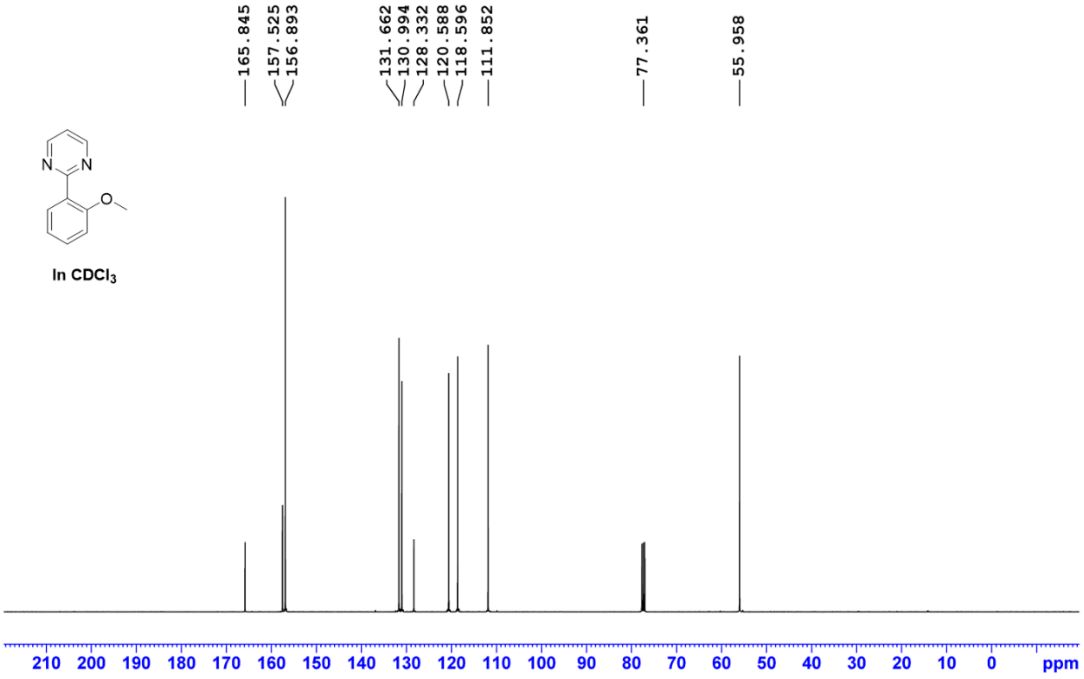

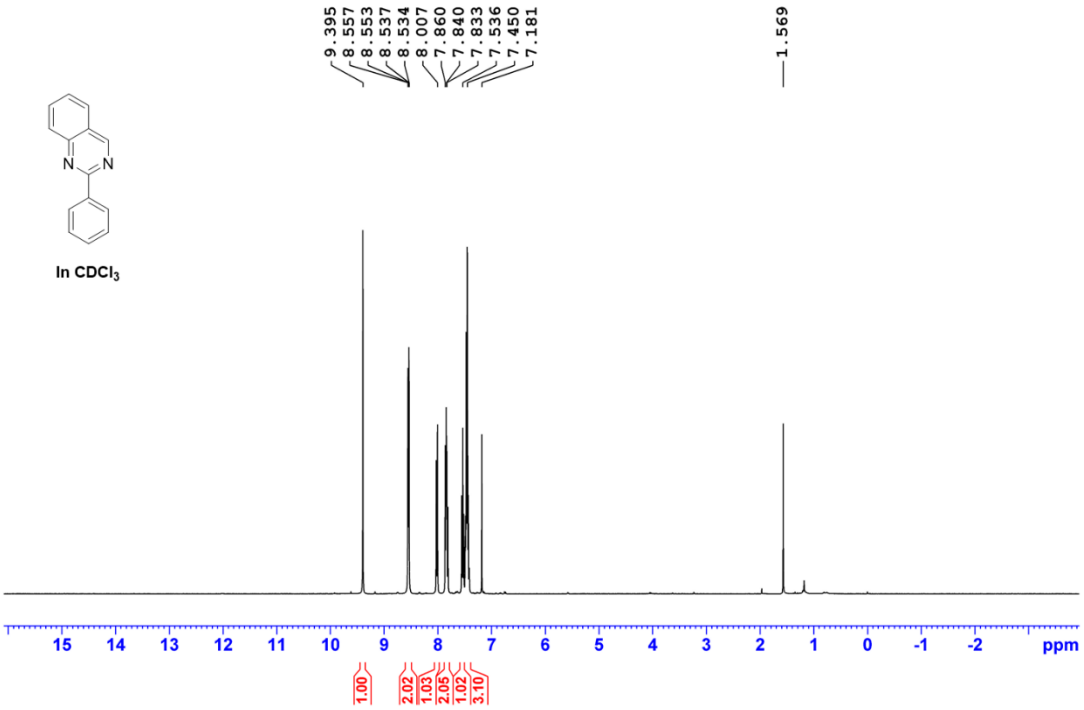
9.395
8.557
8.553
8.537
8.534
8.007
7.860
7.840
7.833
7.536
7.450
7.181
1.569
N
N
In CDCl3
15 14 13 12 11 10 9 8 7 6 5 4 3 2 1 0 -1 -2 ppm
1.00
2.02
1.03
2.05
1.02
3.10

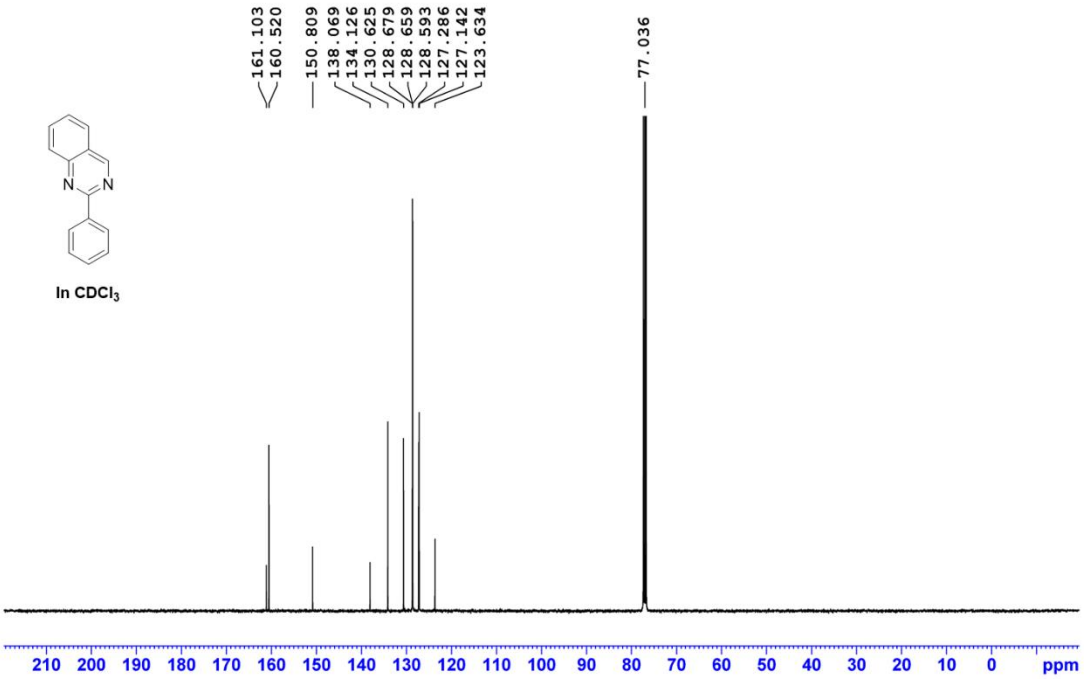
161.103
160.520
150.809
138.069
134.126
130.625
128.679
128.659
128.593
127.286
127.142
123.634
77.036
N
N
In CDCl3
210 200 190 180 170 160 150 140 130 120 110 100 90 80 70 60 50 40 30 20 10 0 ppm

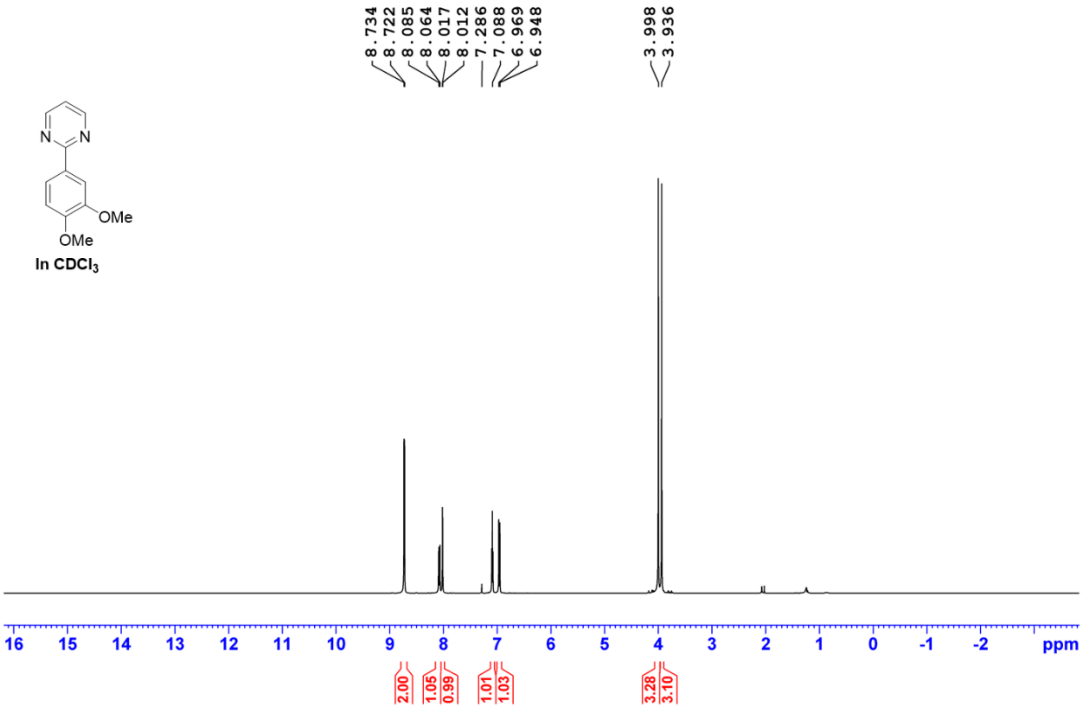
8.734
8.722
8.085
8.064
8.017
8.012
7.286
7.088
6.969
6.948
3.998
3.936
N
N
OMe
OMe
In CDCl3
16 15 14 13 12 11 10 9 8 7 6 5 4 3 2 1 0 -1 -2 ppm
2.00
1.05
0.99
1.01
1.03
3.28
3.10

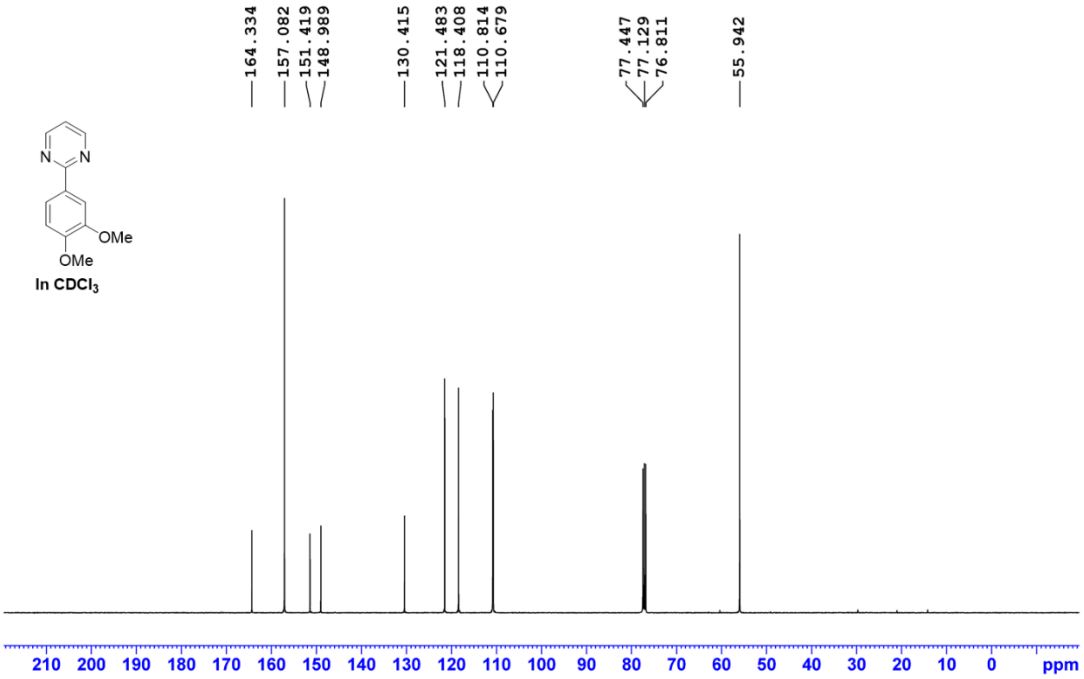
164.334
157.082
151.419
148.989
130.415
121.483
118.408
110.814
110.679
77.447
77.129
76.811
55.942
N
N
OMe
OMe
In CDCl3
210 200 190 180 170 160 150 140 130 120 110 100 90 80 70 60 50 40 30 20 10 0 ppm

Supplementary Information

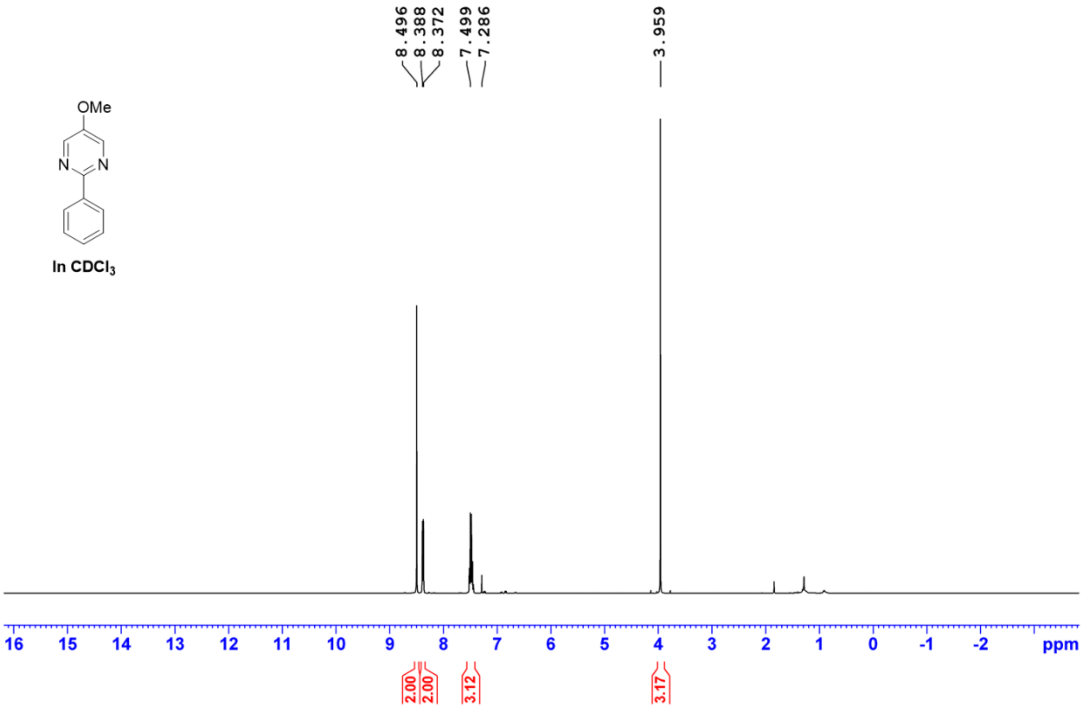

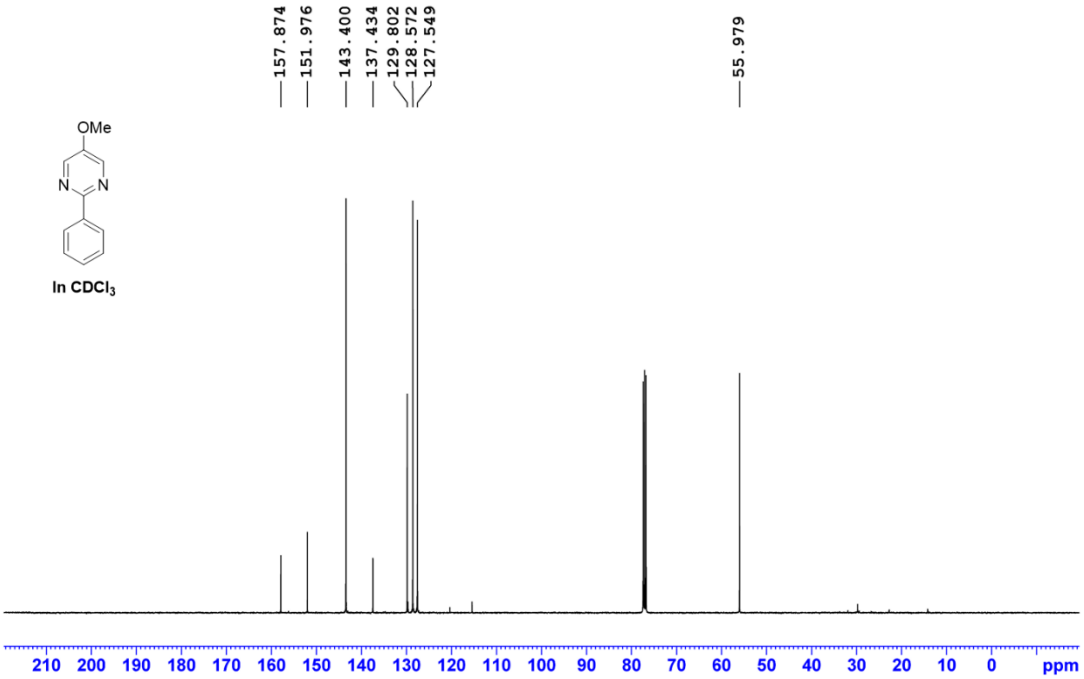

Supplementary Information

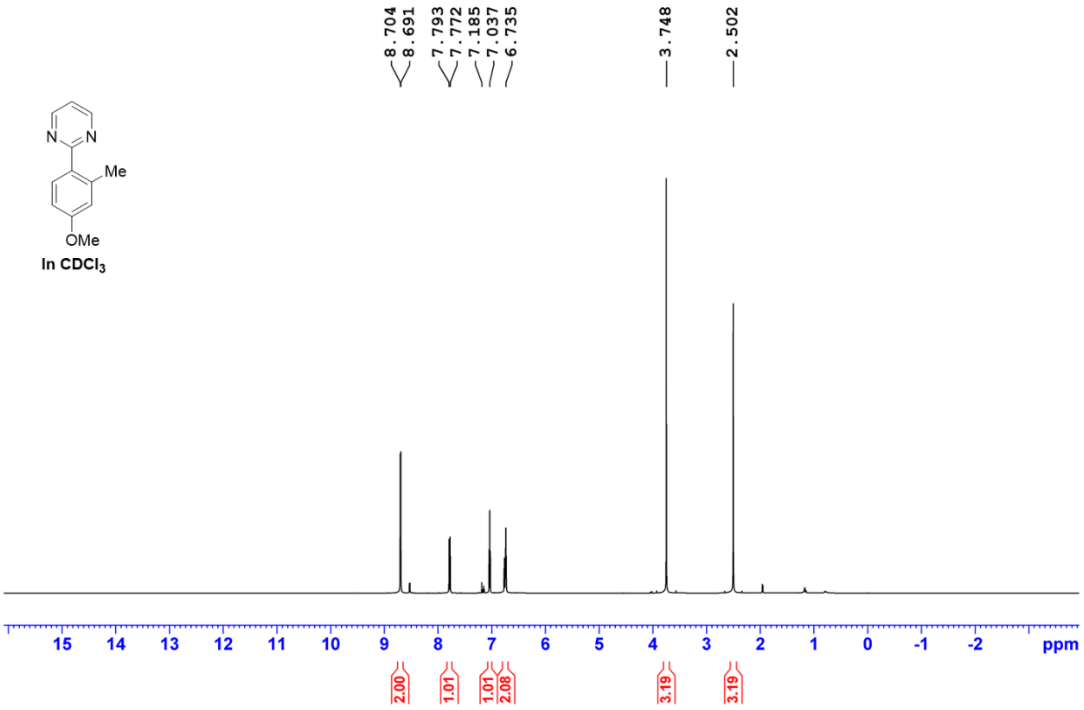

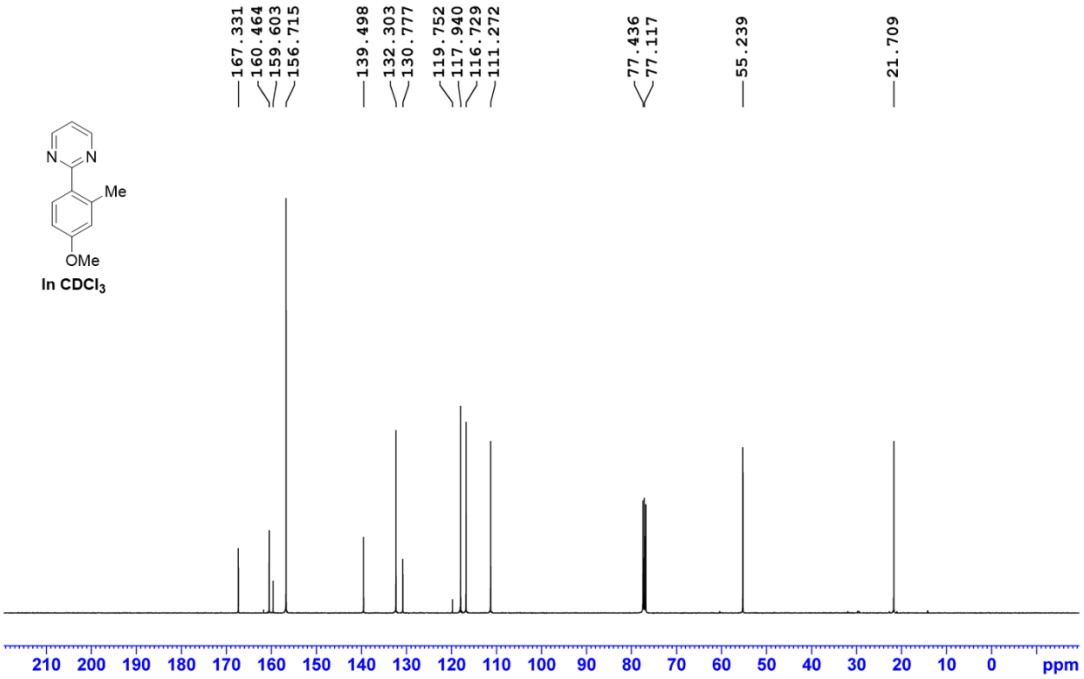

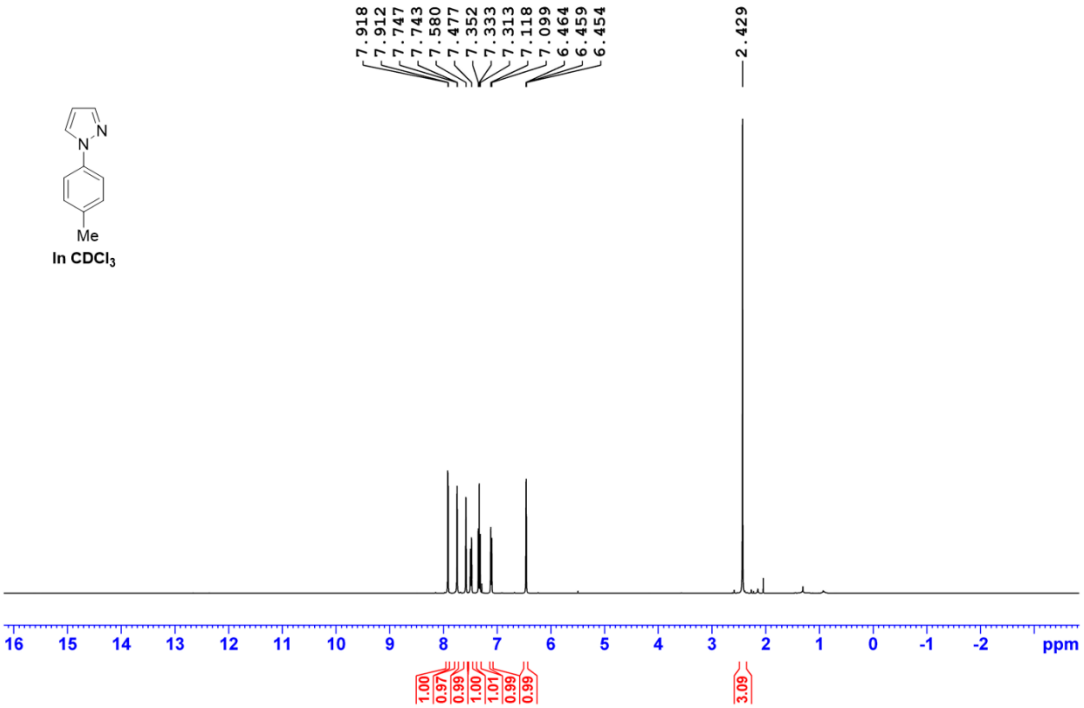
7.918
7.912
7.747
7.743
7.580
7.477
7.352
7.333
7.313
7.118
7.099
6.464
6.459
6.454
2.429
Me
In CDCl3
16 15 14 13 12 11 10 9 8 7 6 5 4 3 2 1 0 -1 -2 ppm
1.00
0.97
0.99
1.00
1.01
0.99
0.99
3.09

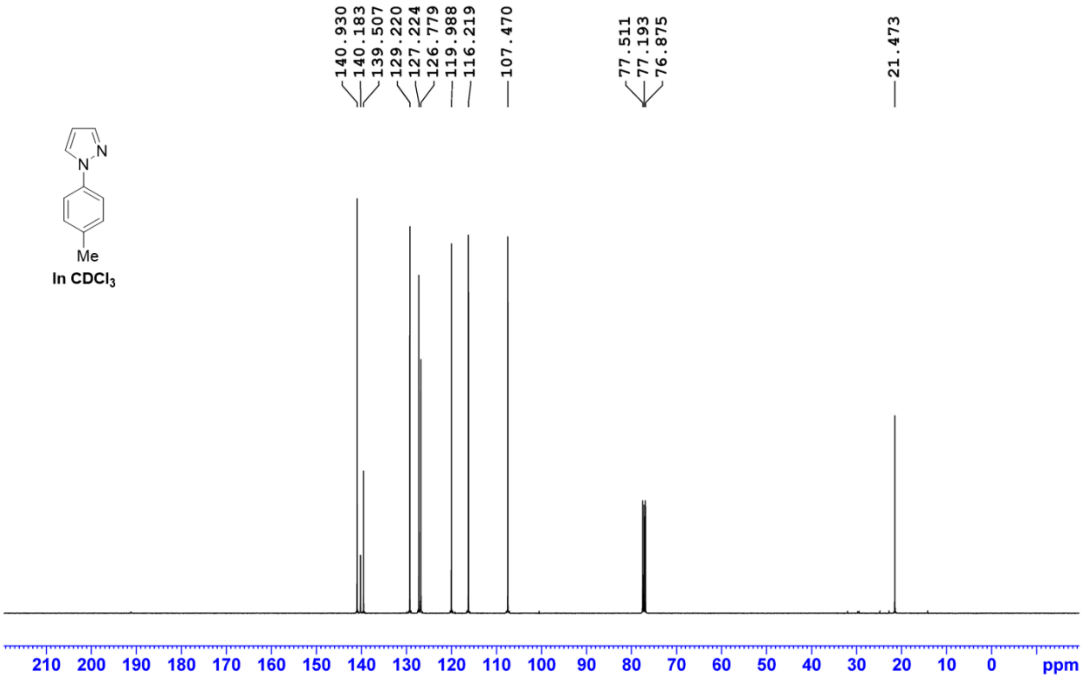
140.930
140.183
139.507
129.220
127.224
126.779
119.988
116.219
107.470
77.511
77.193
76.875
21.473
Me
In CDCl3
210 200 190 180 170 160 150 140 130 120 110 100 90 80 70 60 50 40 30 20 10 0 ppm

Supplementary Information

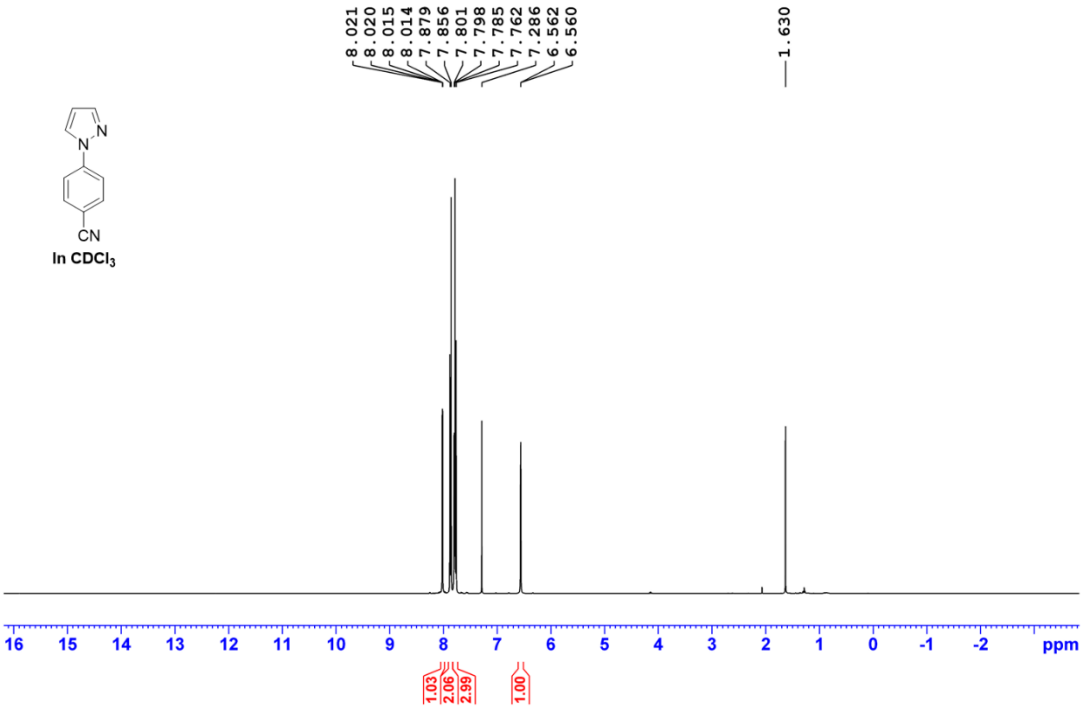

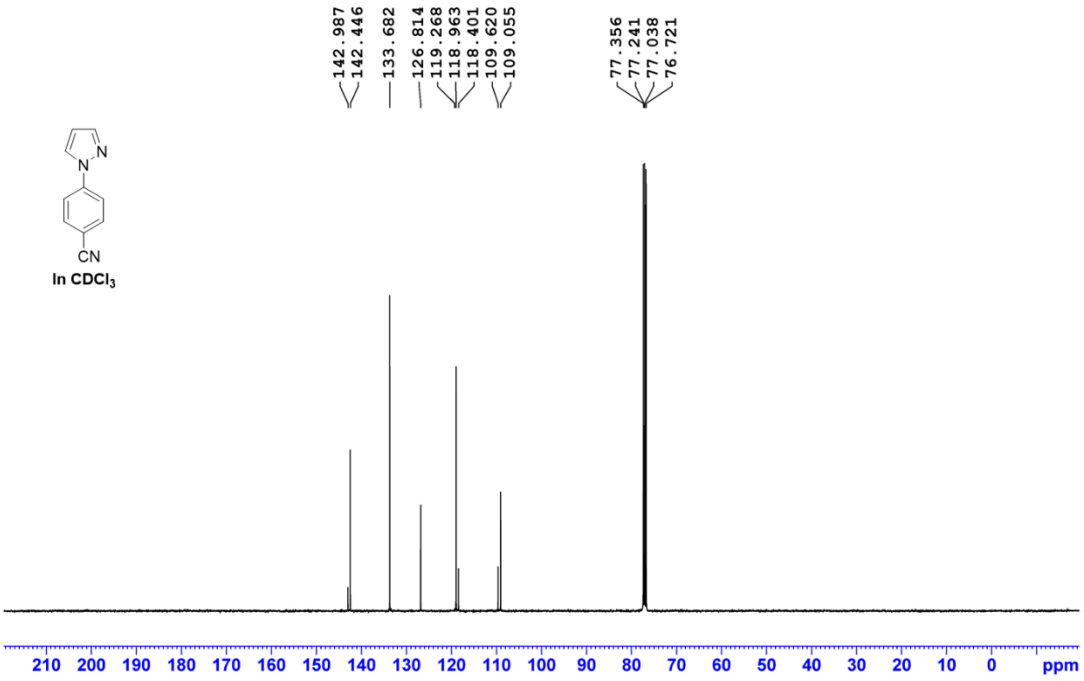

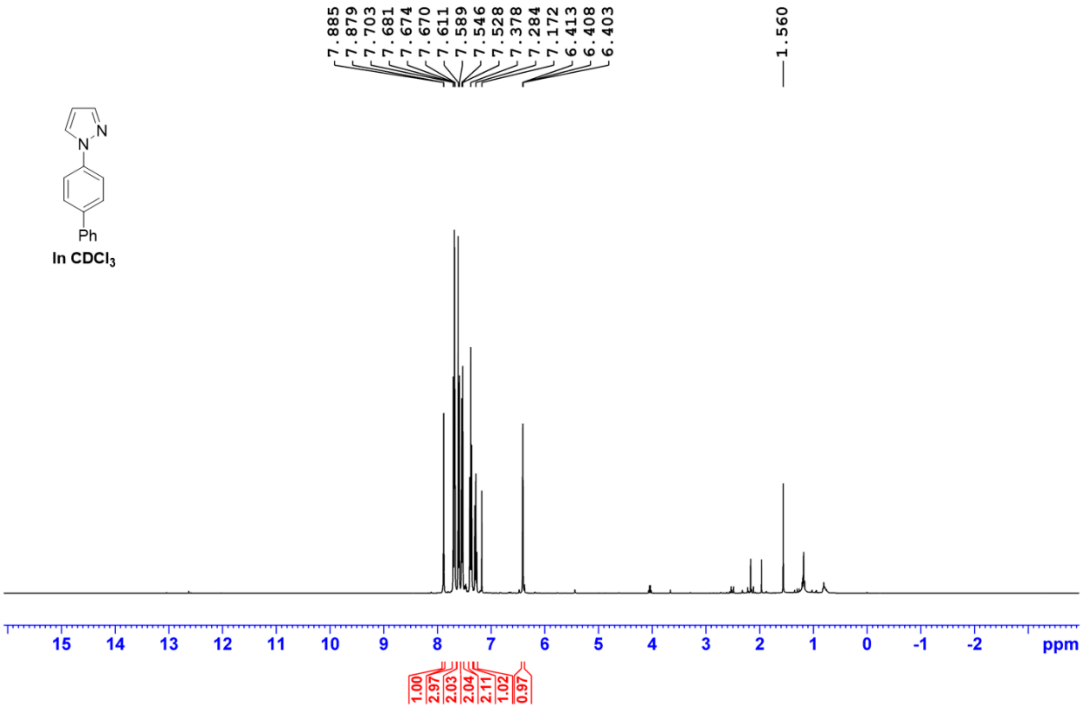
7.885
7.879
7.703
7.681
7.674
7.670
7.611
7.589
7.546
7.528
7.378
7.284
7.172
6.413
6.408
6.403
1.560
N
N
Ph
In CDCl3
15 14 13 12 11 10 9 8 7 6 5 4 3 2 1 0 -1 -2 ppm
1.00
2.97
2.03
2.04
2.11
1.02
0.97

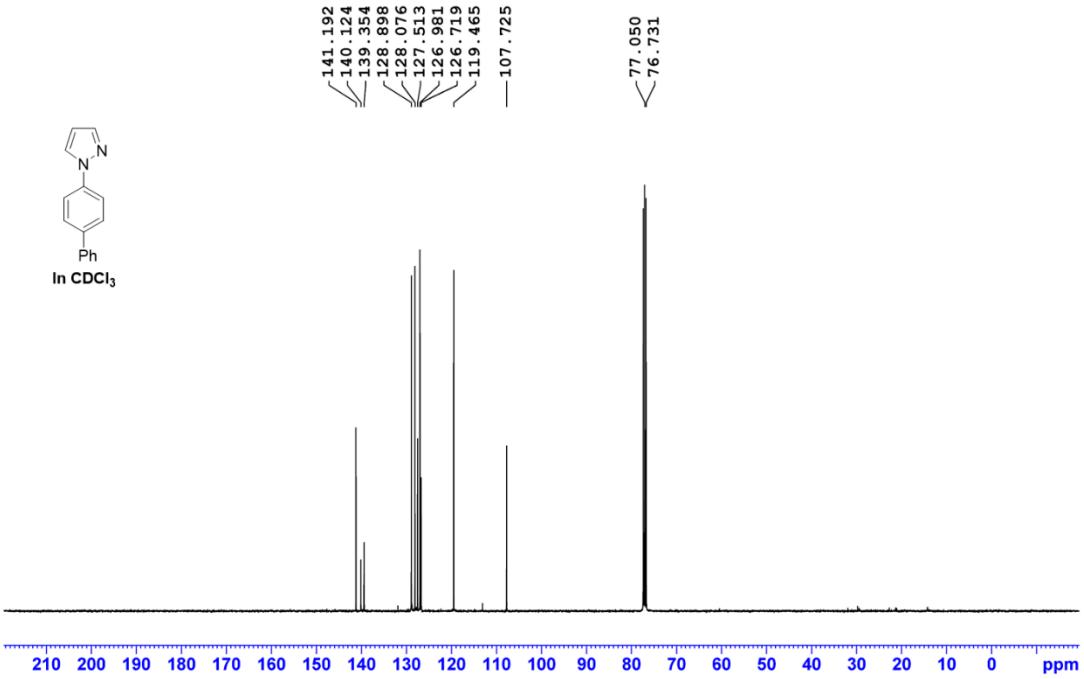
141.192
140.124
139.354
128.898
128.076
127.513
126.981
126.719
119.465
107.725
77.050
76.731
N
N
Ph
In CDCl3
210 200 190 180 170 160 150 140 130 120 110 100 90 80 70 60 50 40 30 20 10 0 ppm

Supplementary Information

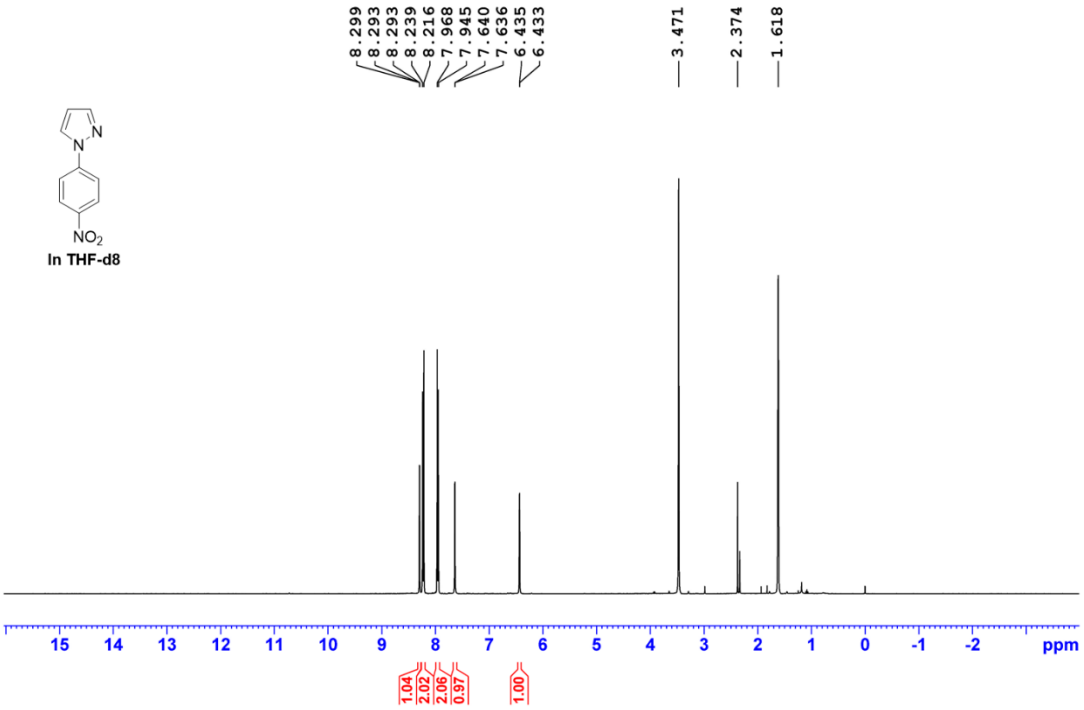

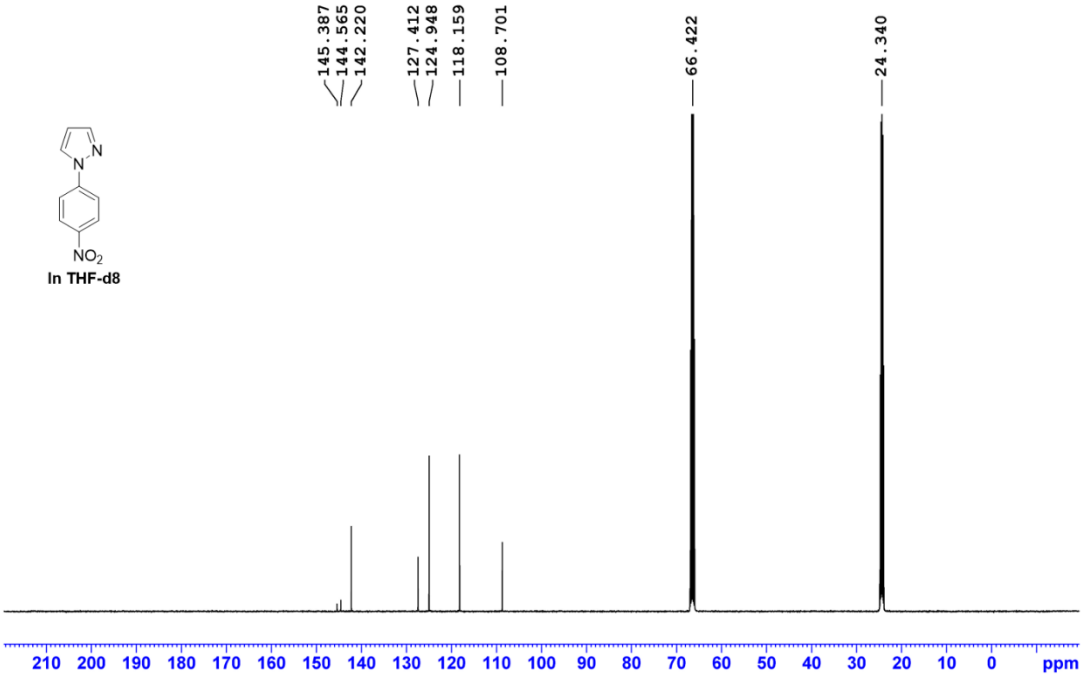

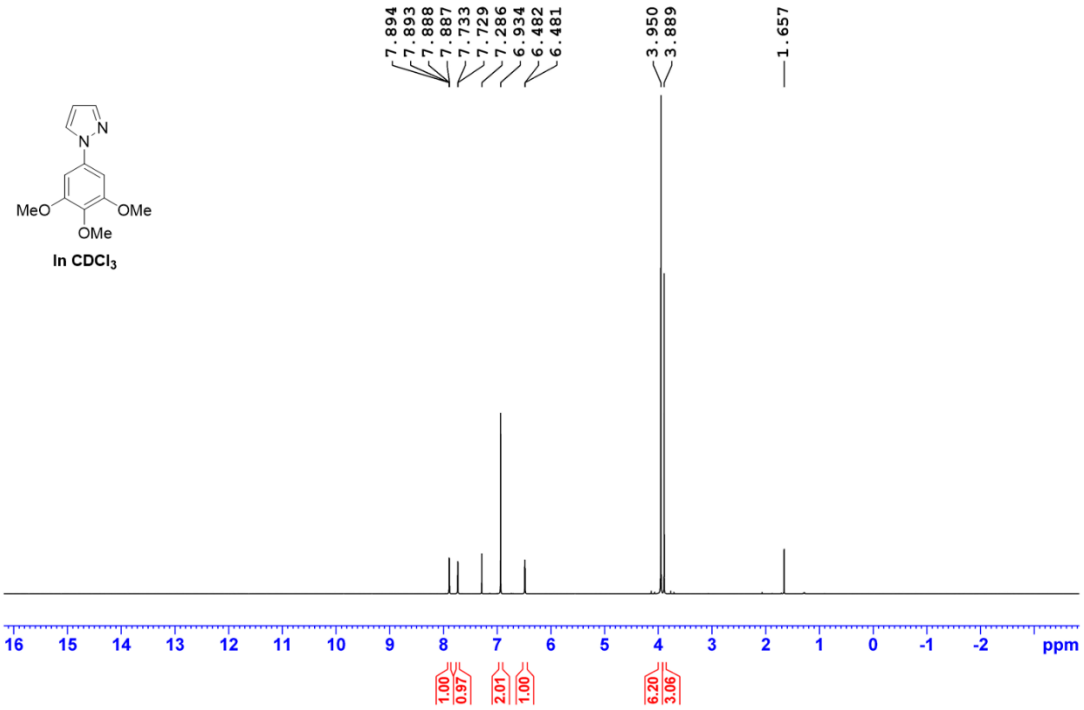
7.894
7.893
7.888
7.887
7.733
7.729
7.286
6.934
6.482
6.481
3.950
3.889
1.657
MeO
OMe
OMe
In CDCl3
16 15 14 13 12 11 10 9 8 7 6 5 4 3 2 1 0 -1 -2 ppm
1.00
0.97
2.01
1.00
6.20
3.06

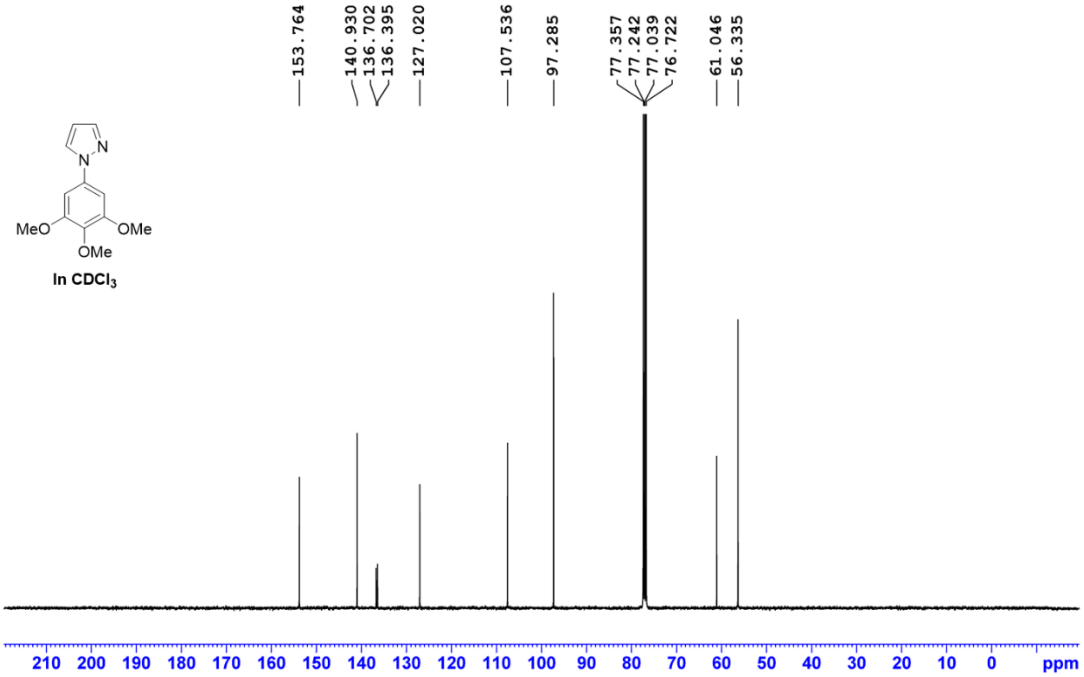
153.764
140.930
136.702
136.395
127.020
107.536
97.285
77.357
77.242
77.039
76.722
61.046
56.335
MeO
OMe
OMe
In CDCl3
210 200 190 180 170 160 150 140 130 120 110 100 90 80 70 60 50 40 30 20 10 0 ppm

Supplementary Information

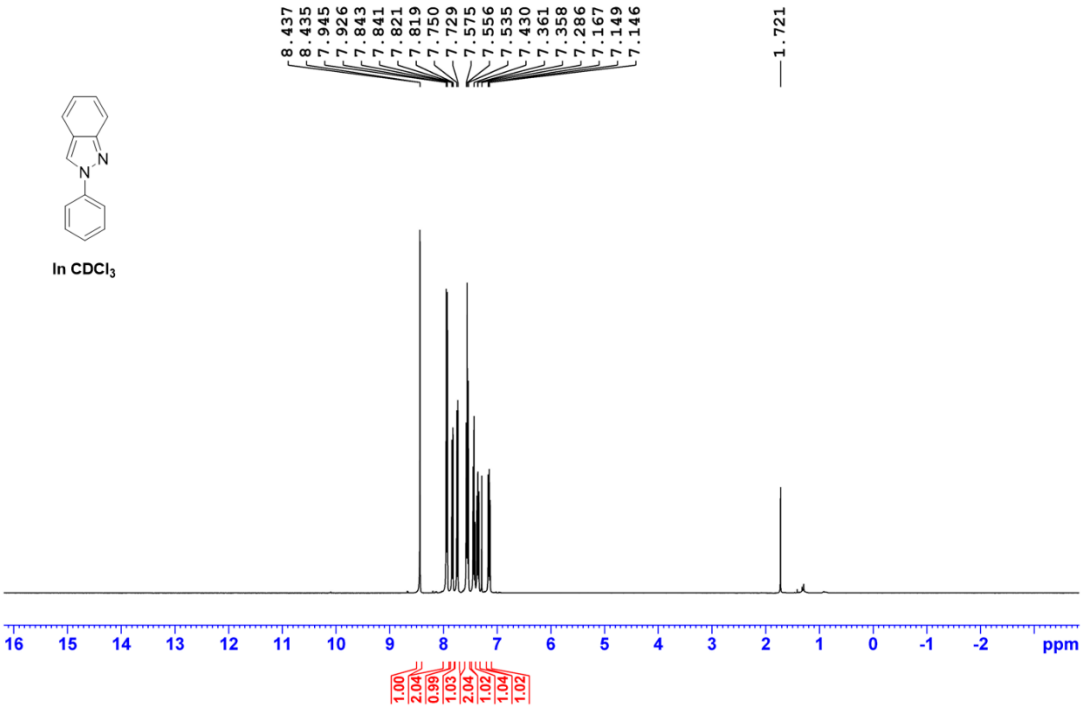

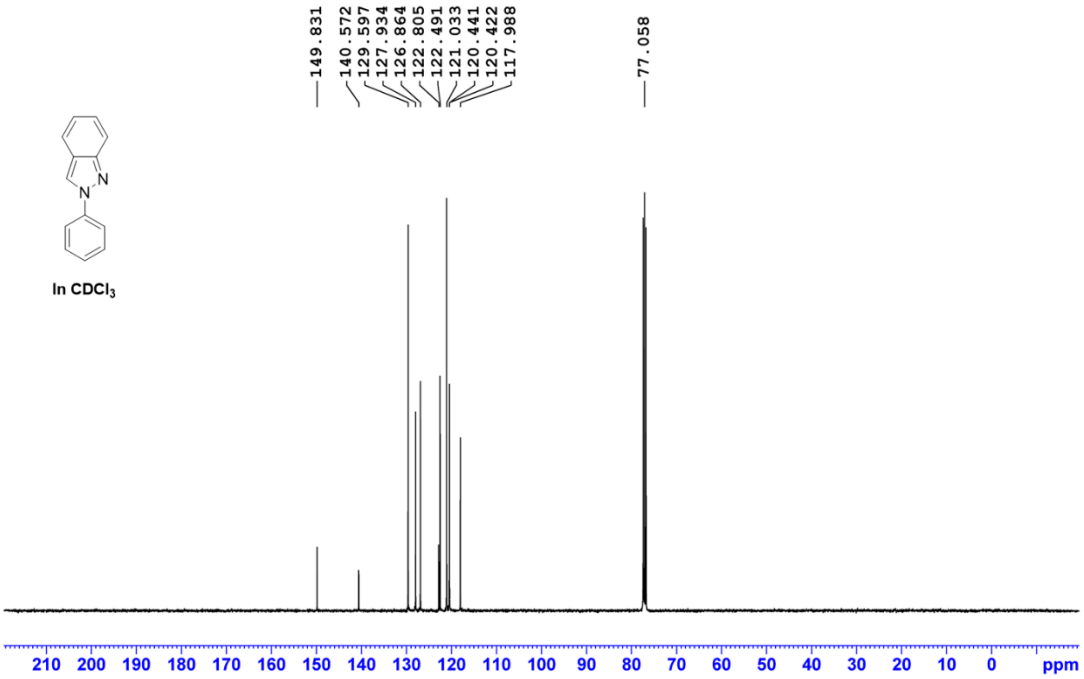

Supplementary Information

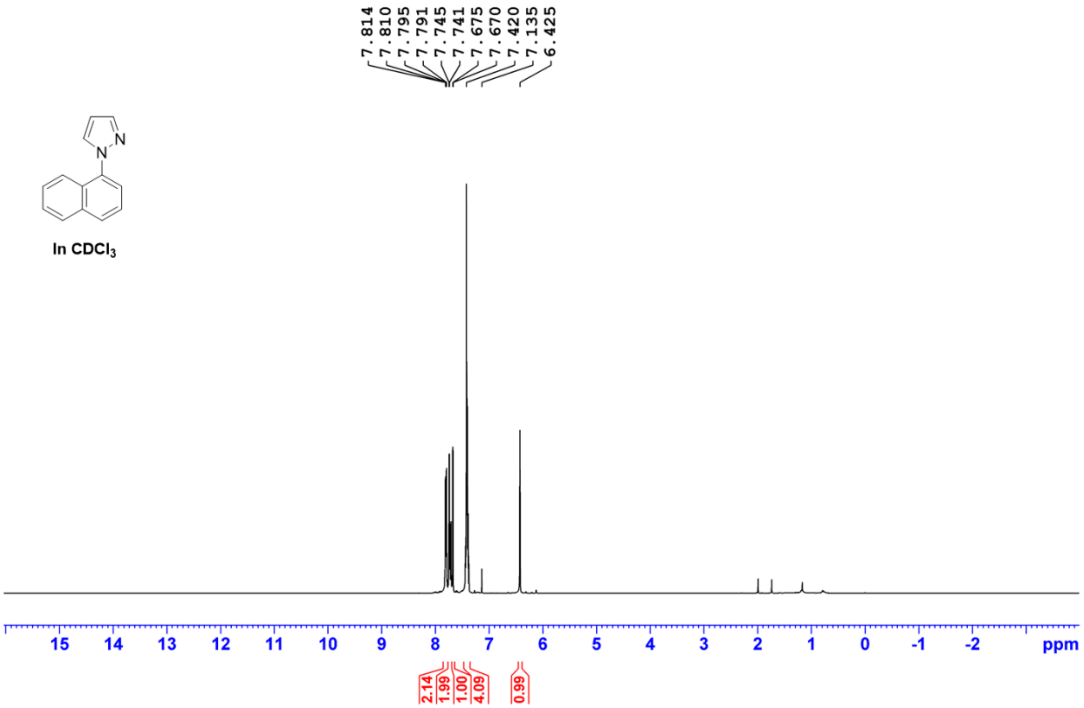

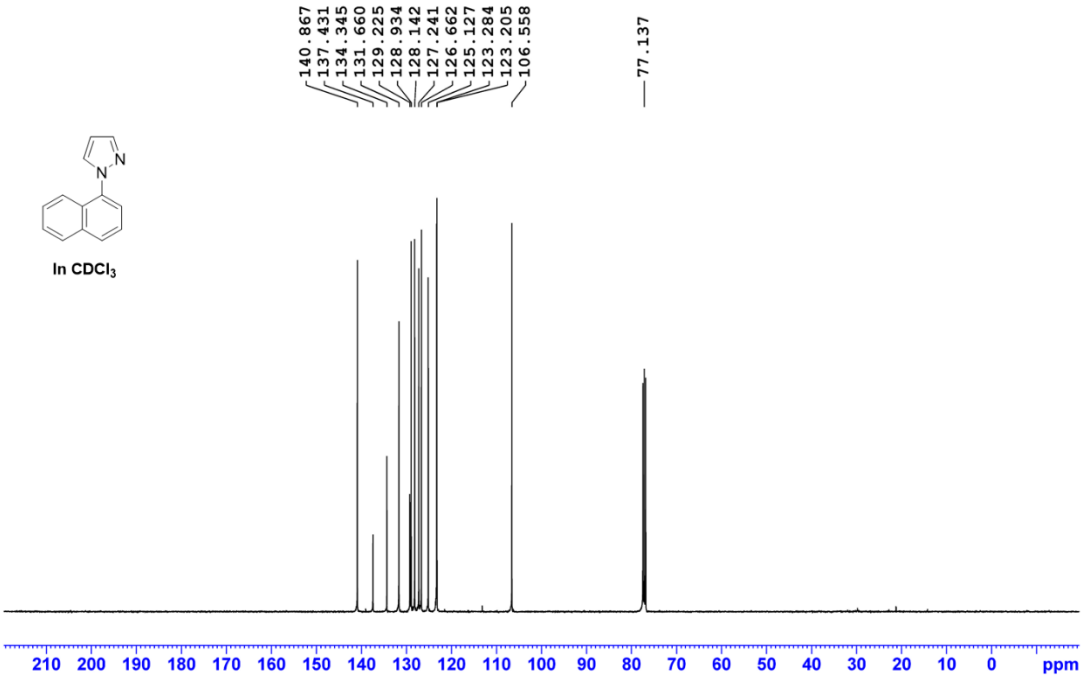

Supplementary Information

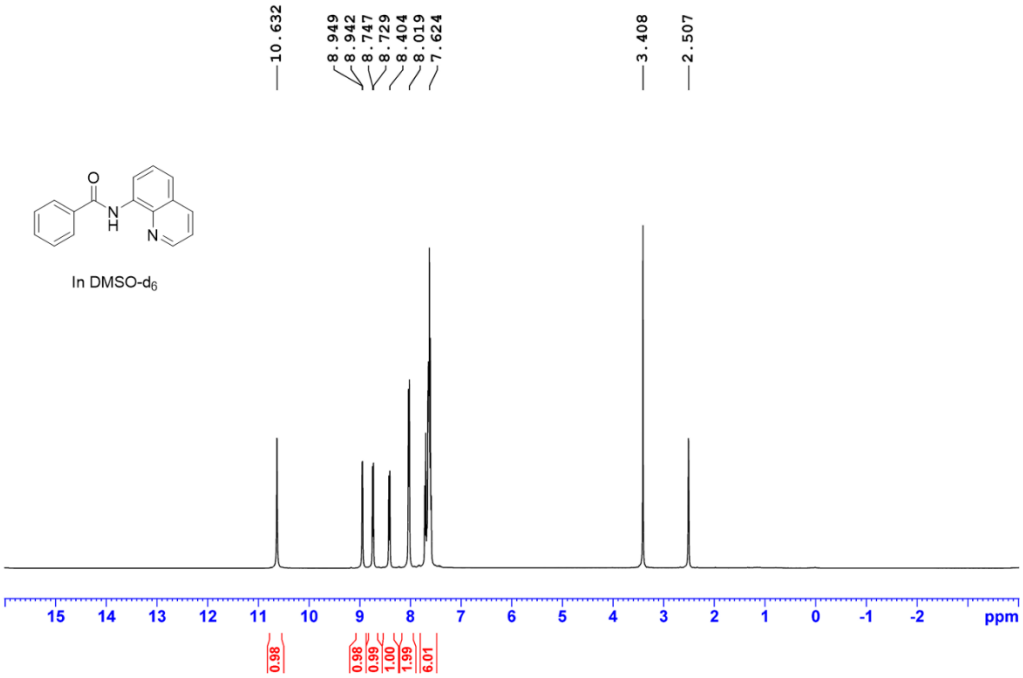

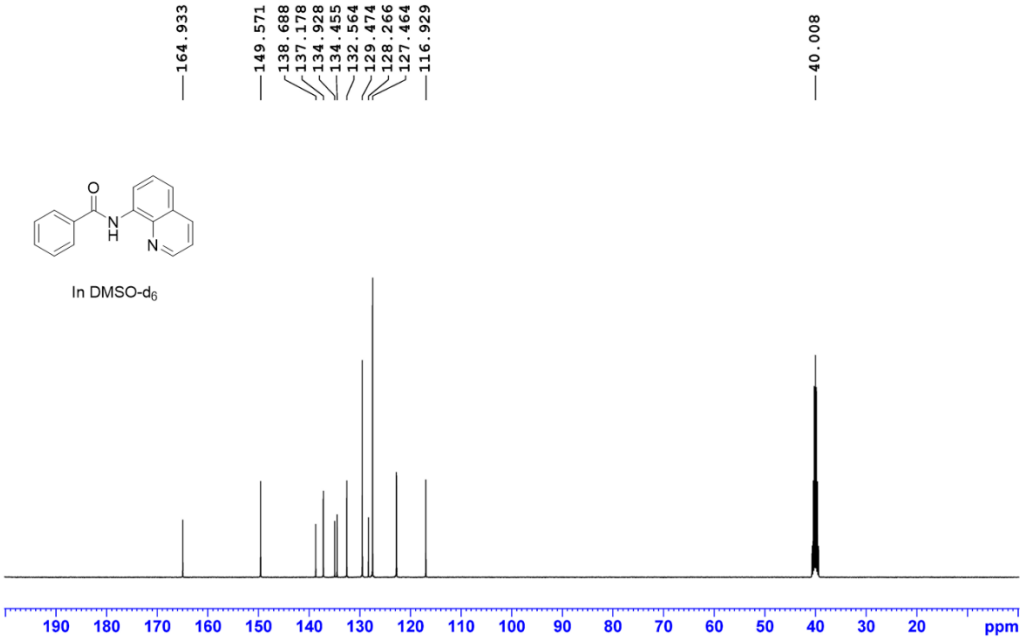

Supplementary Information

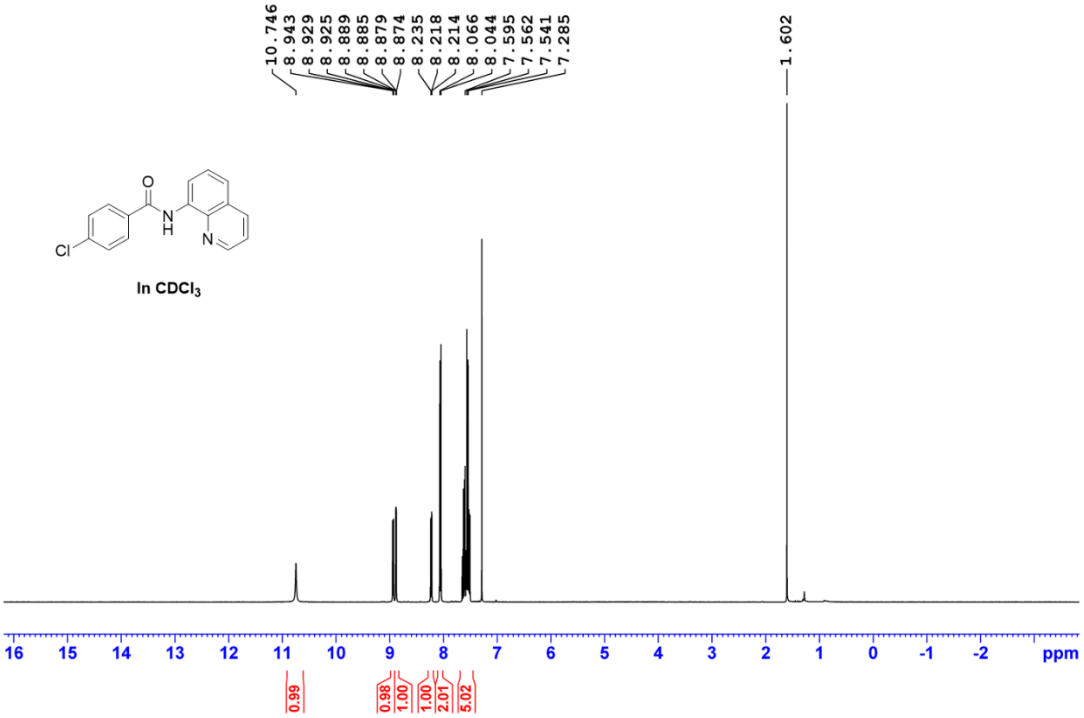

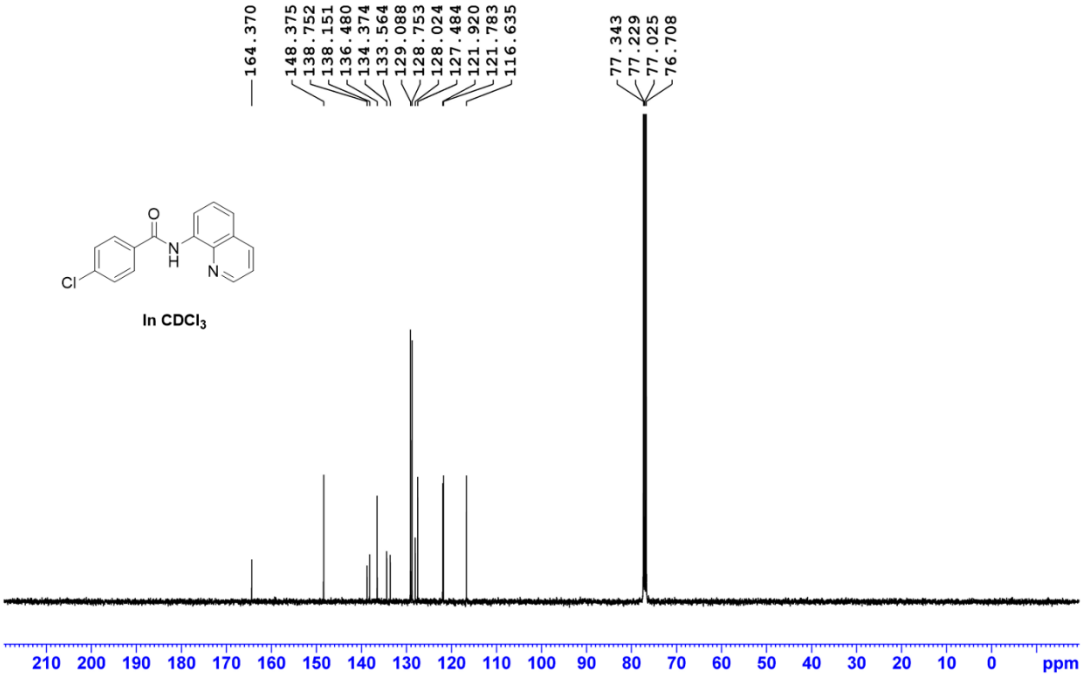

Supplementary Information

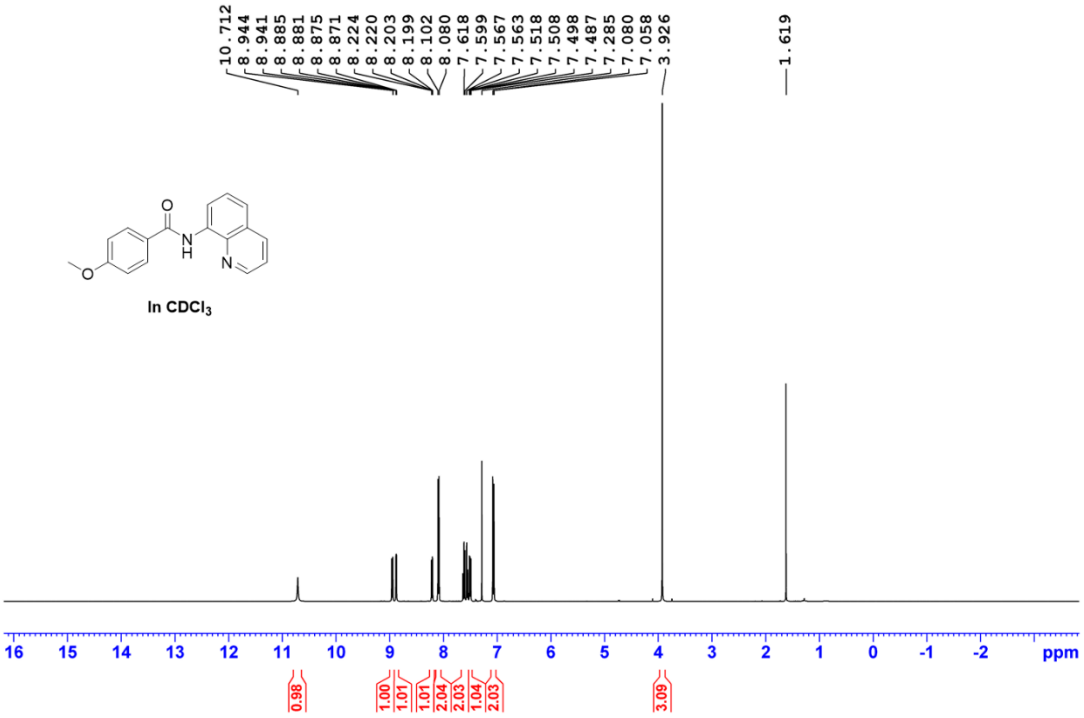

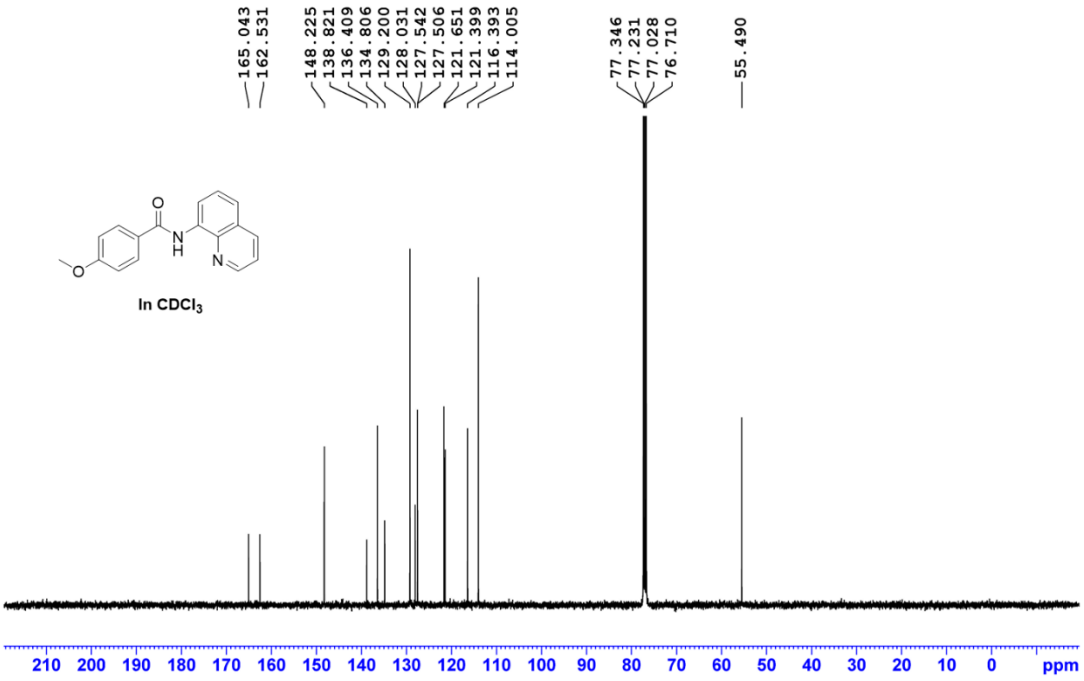

Supplementary Information

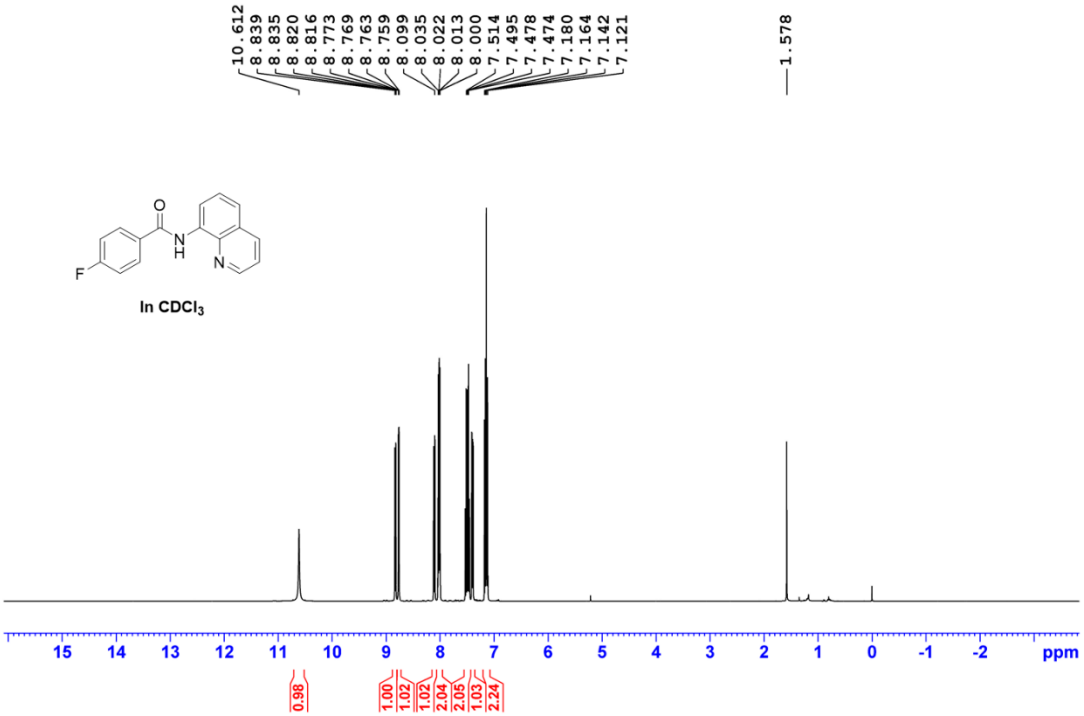

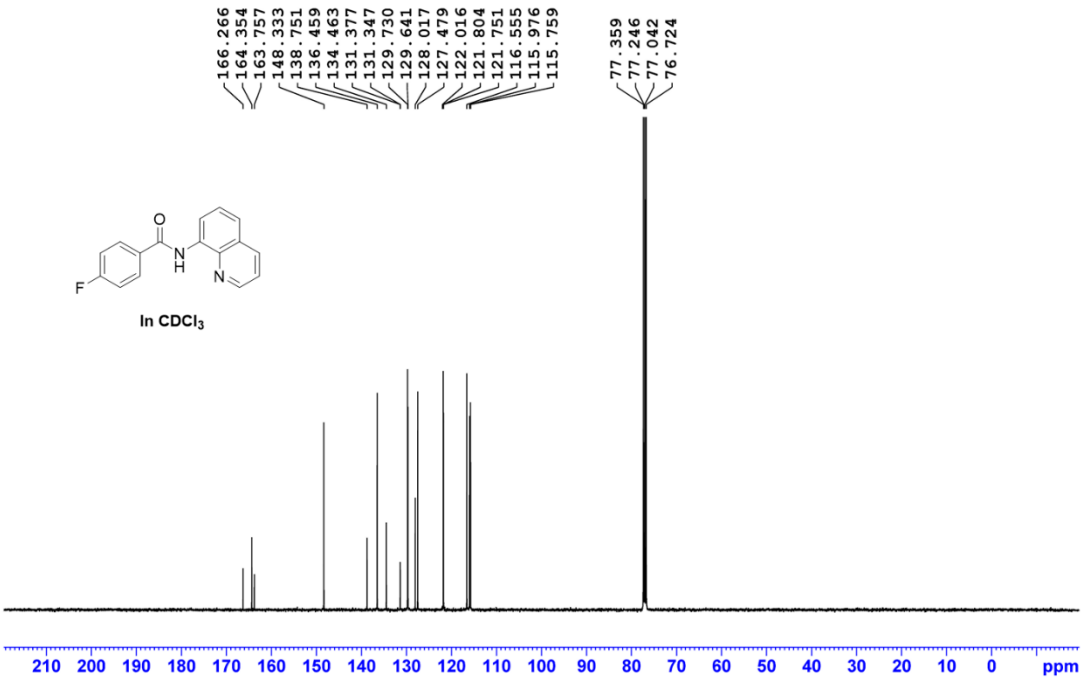

Supplementary Information

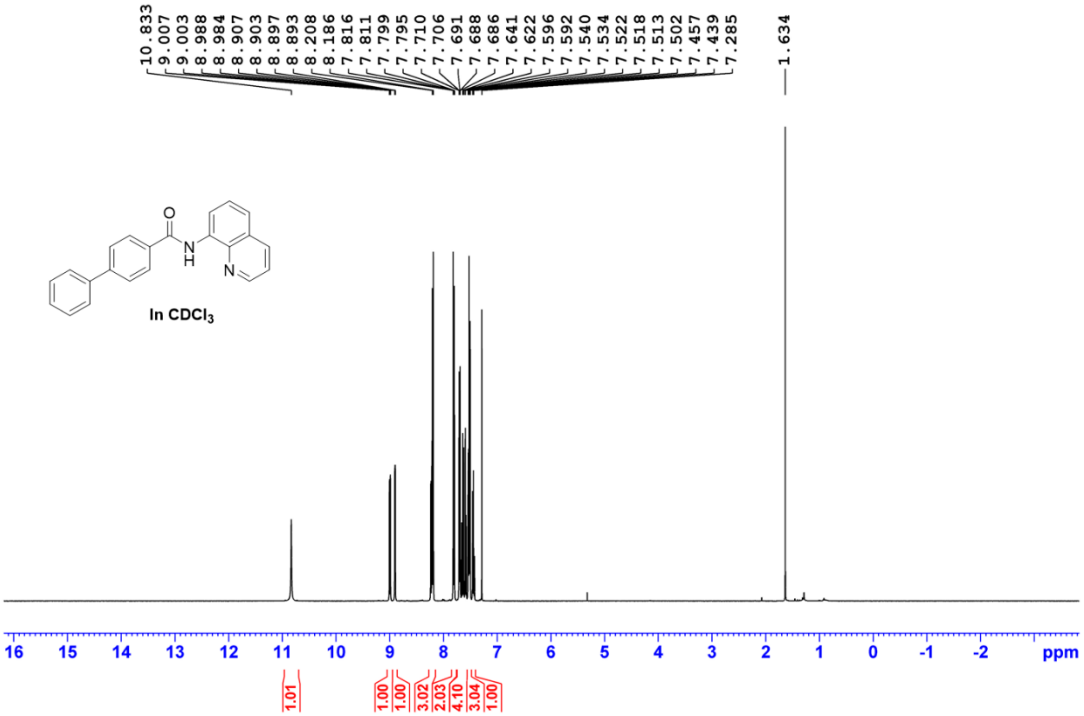

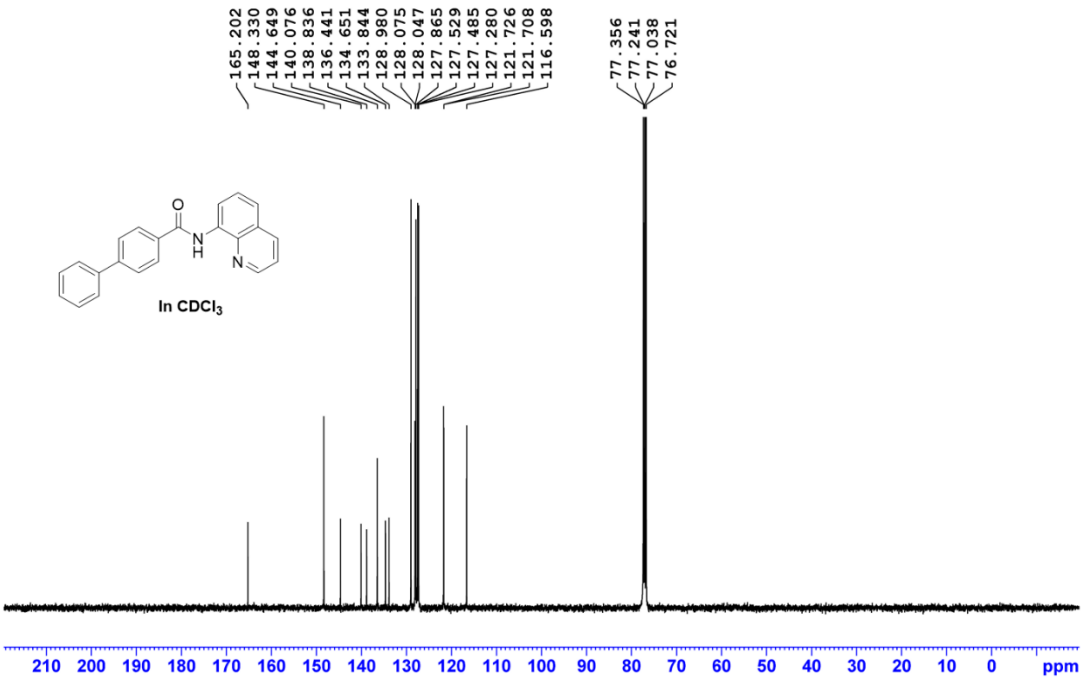

Supplementary Information

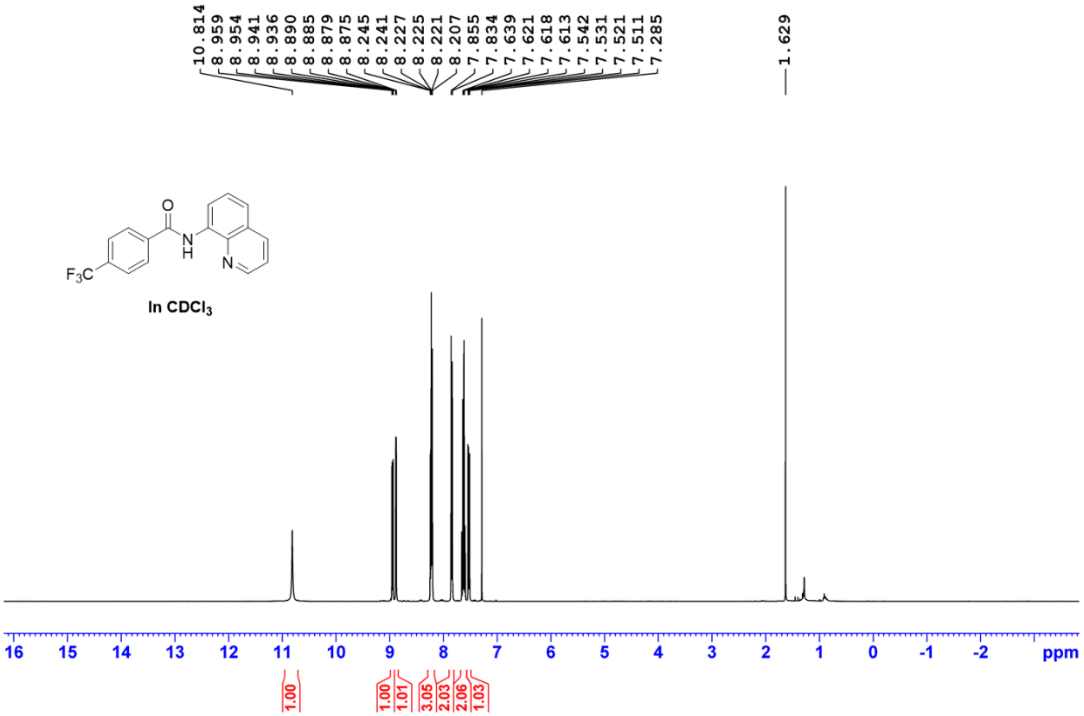

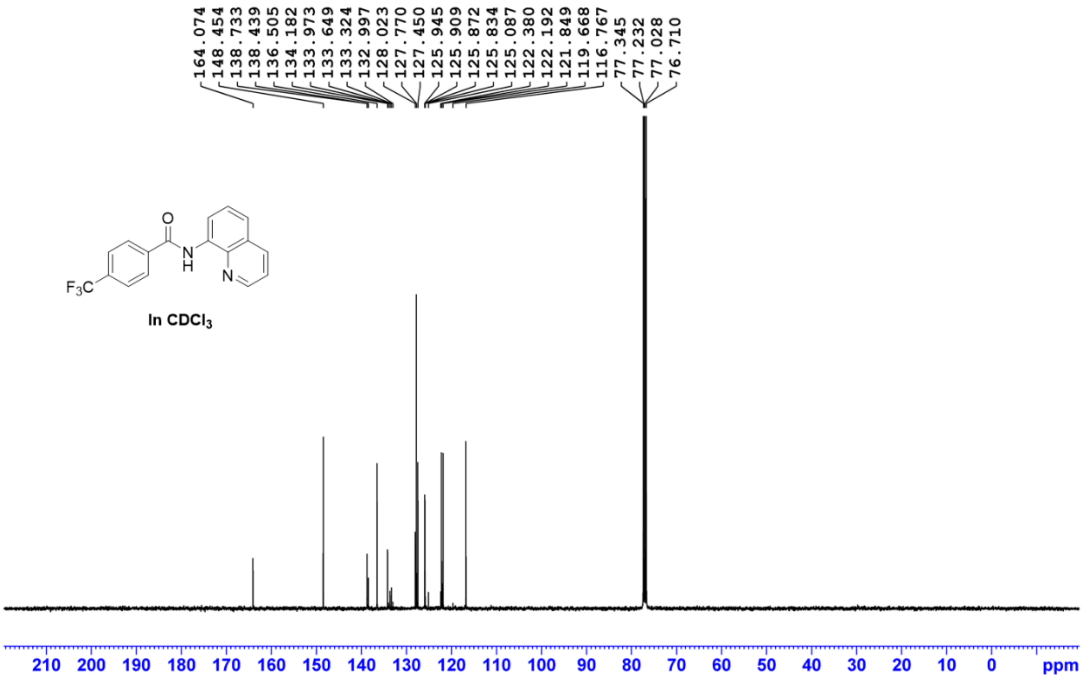

Supplementary Information

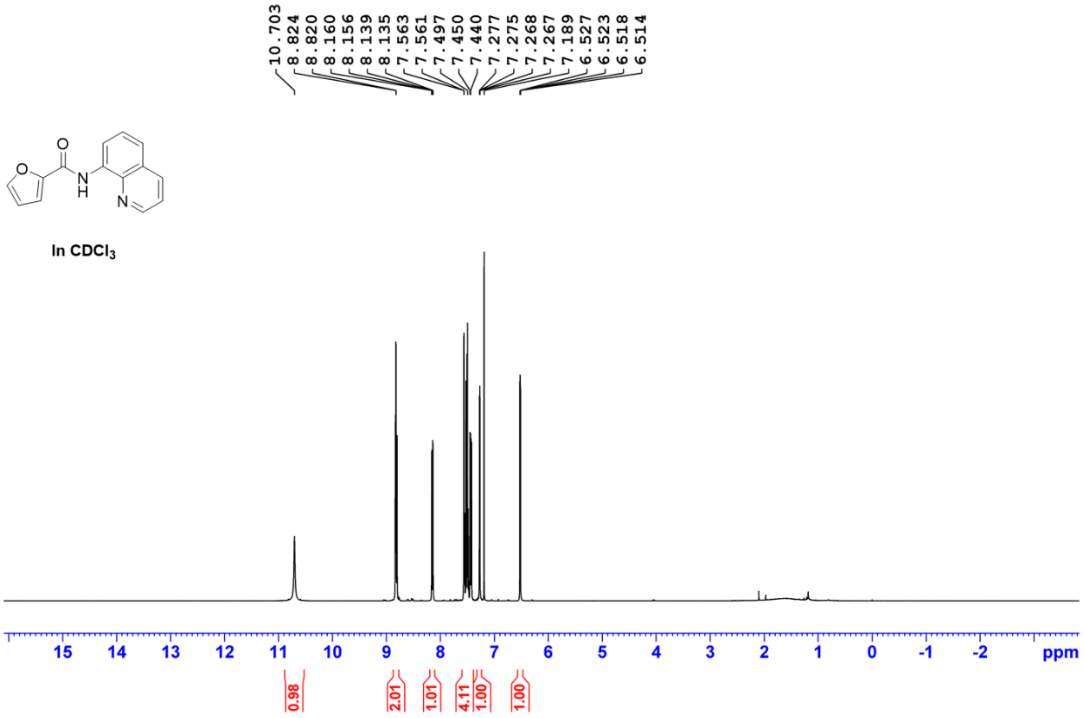

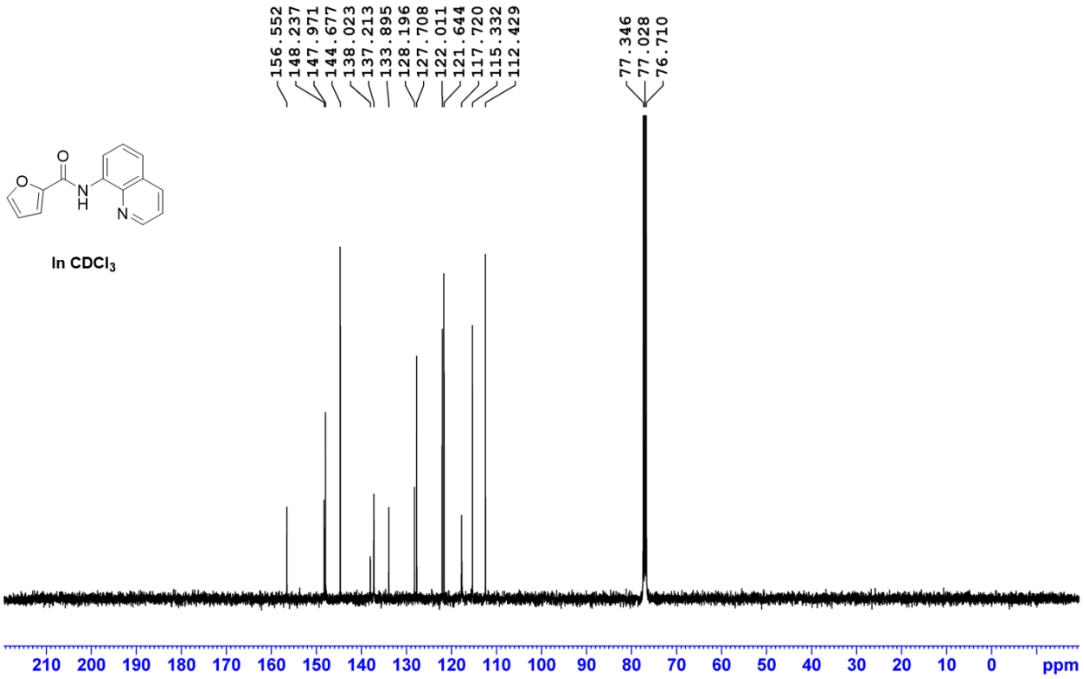

Supplementary Information

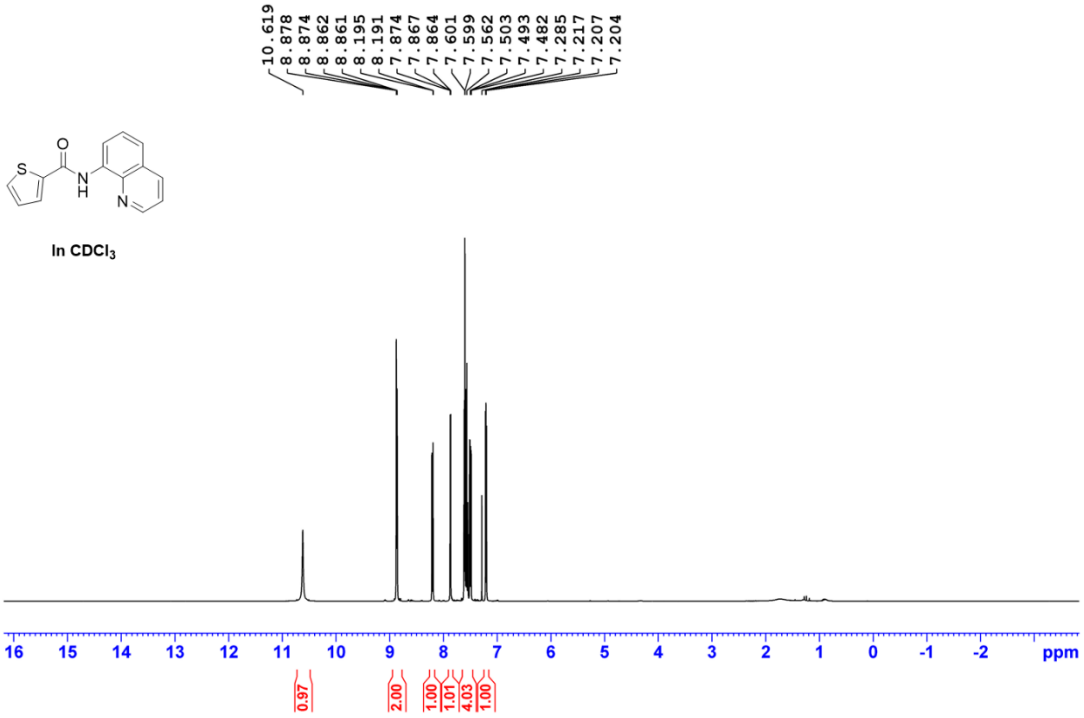

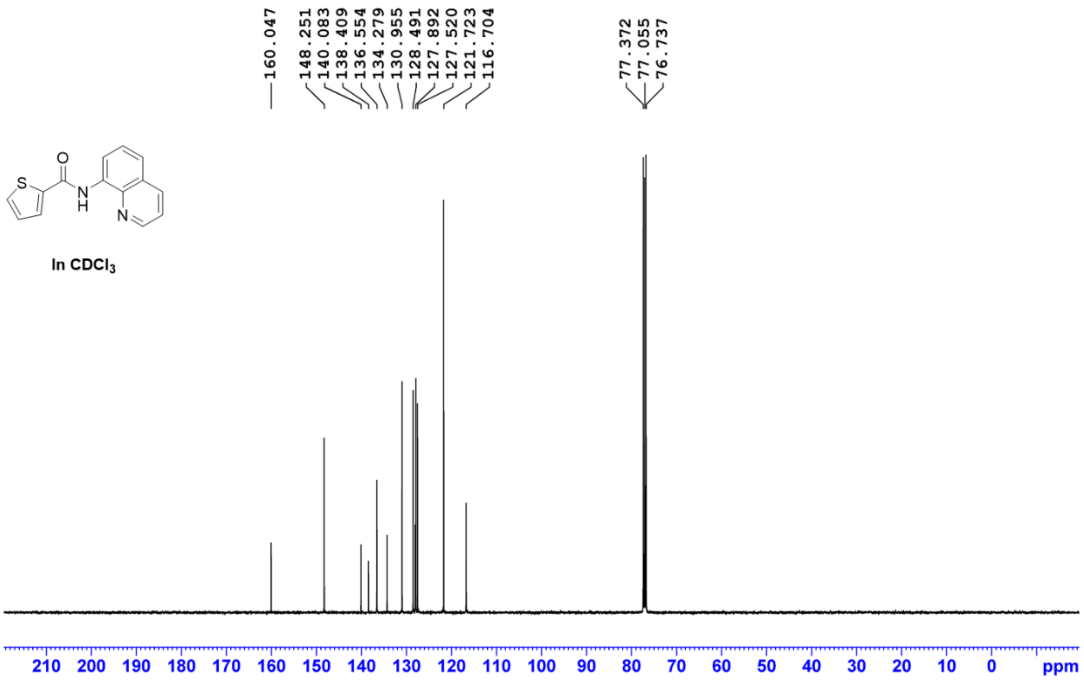

Supplementary Information

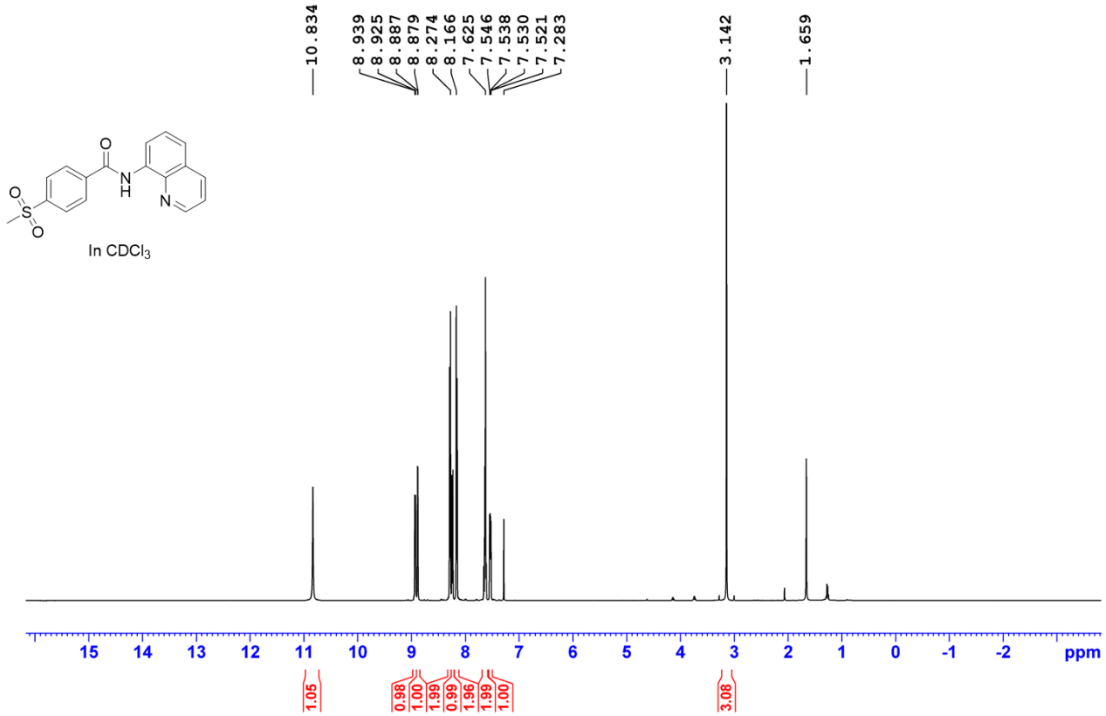

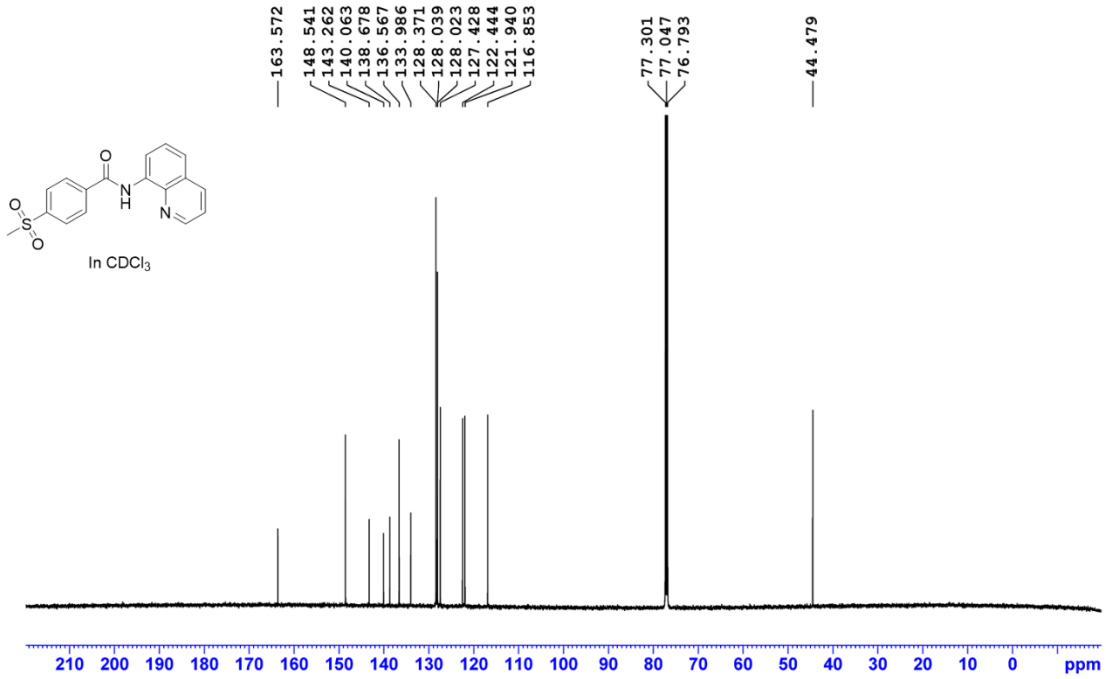

Supplementary Information

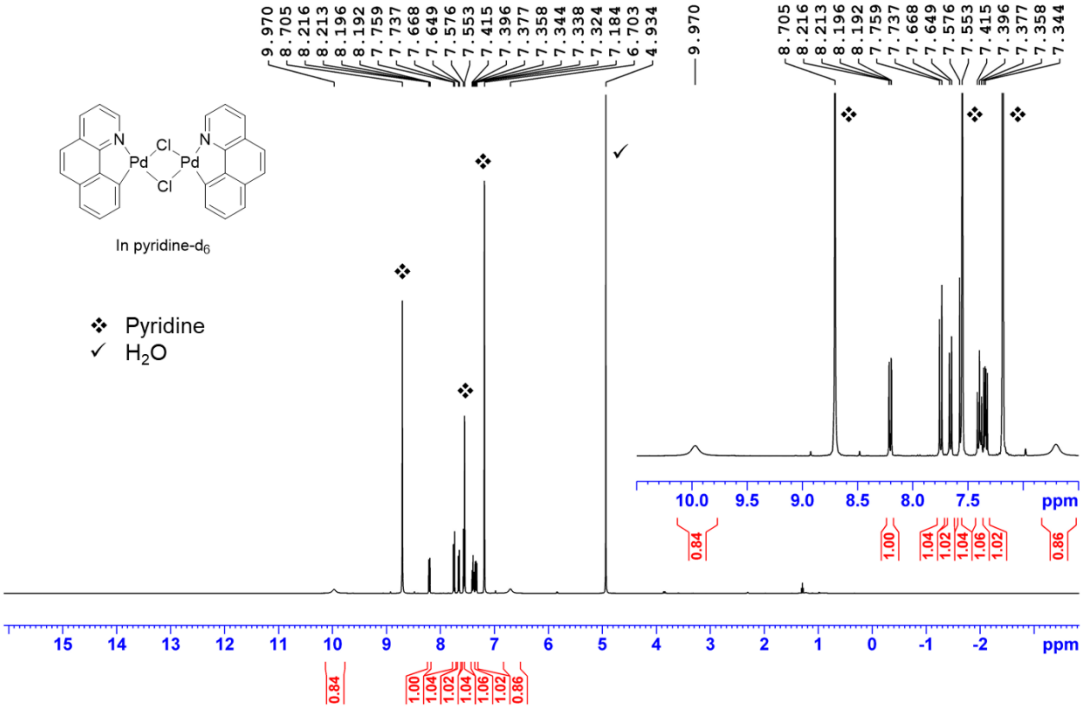

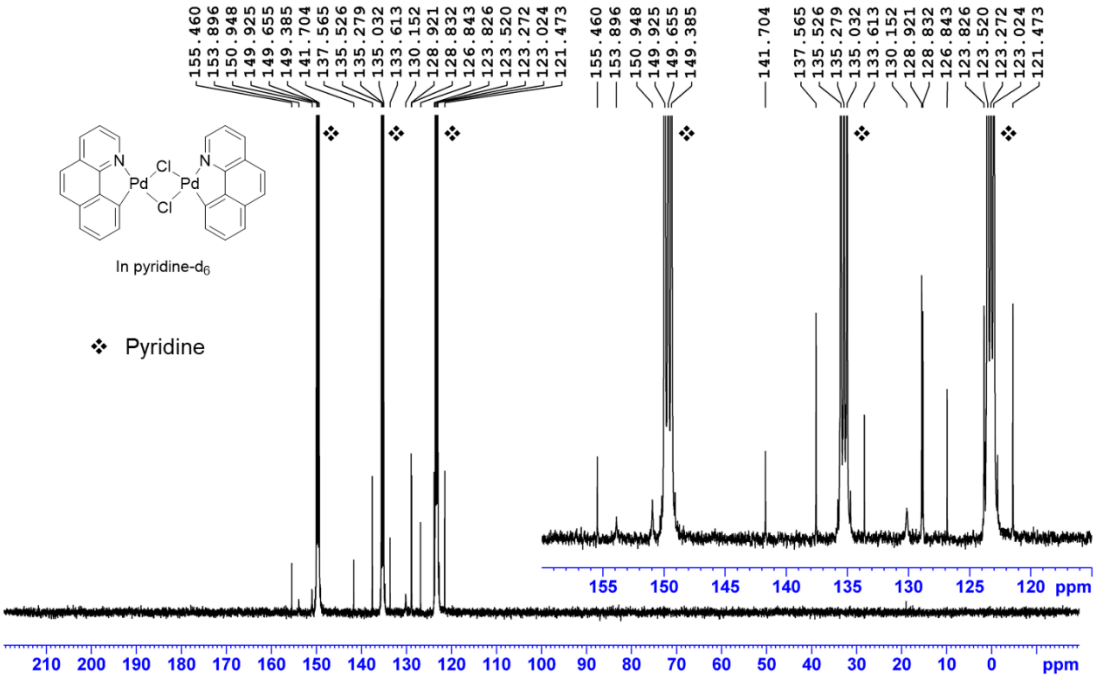

Supplementary Information

Product

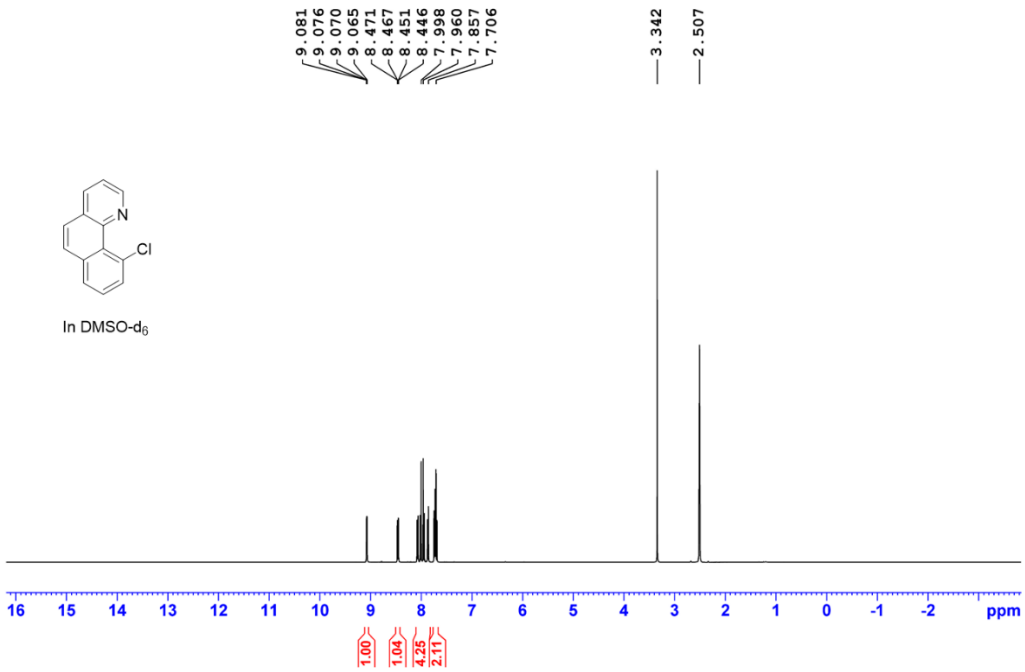

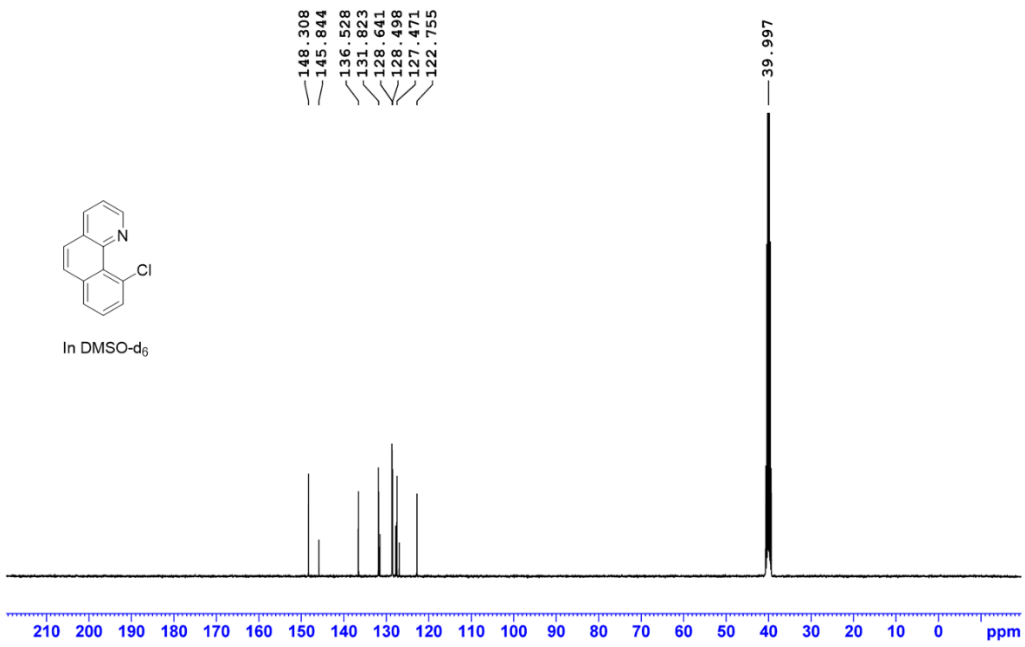

Supplementary Information

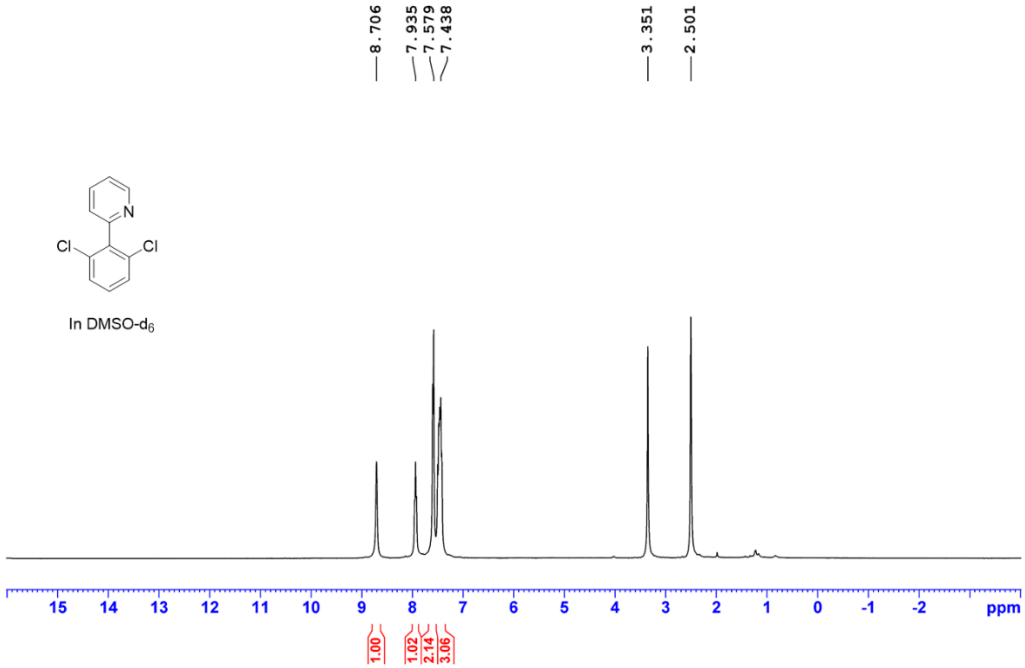

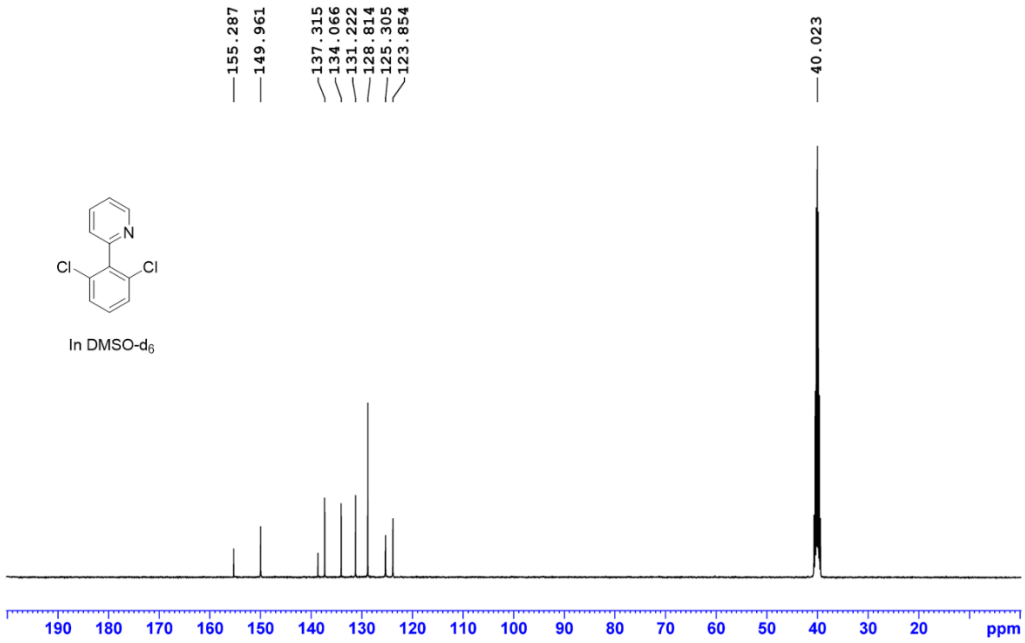

Supplementary Information

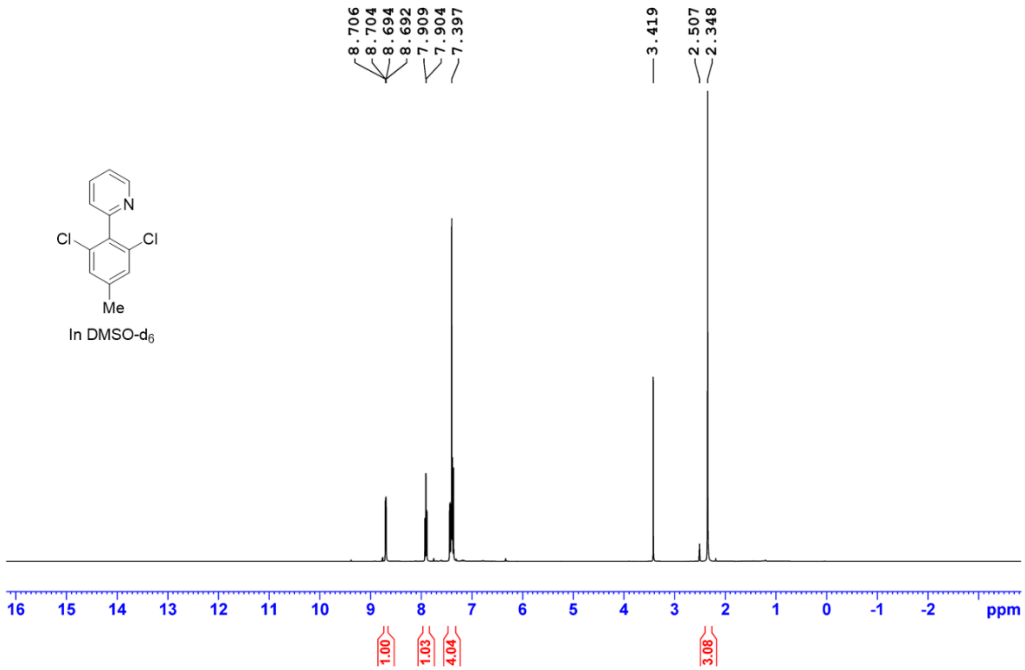

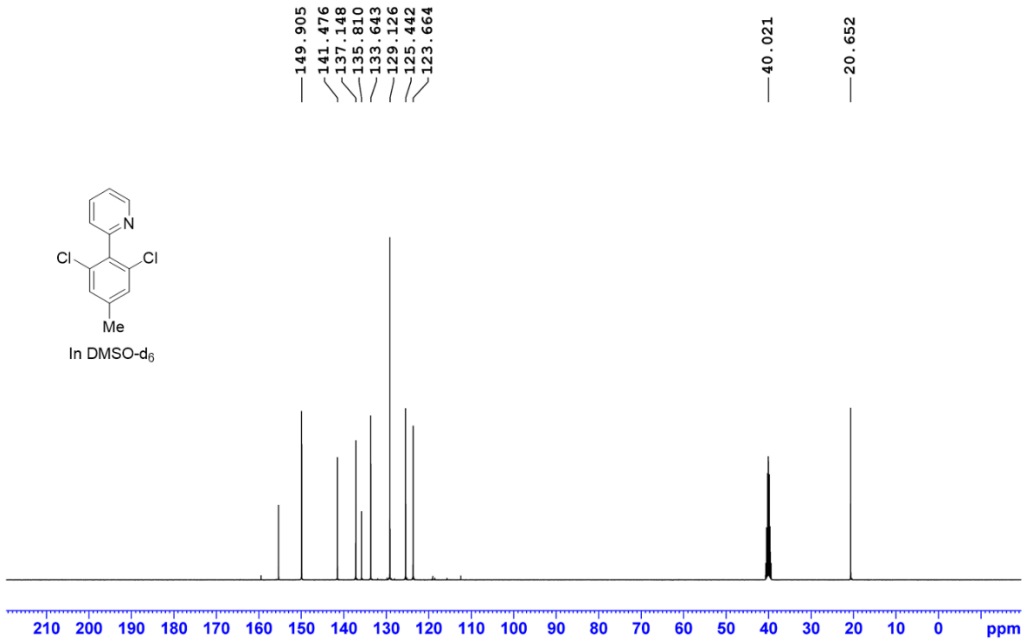

Supplementary Information

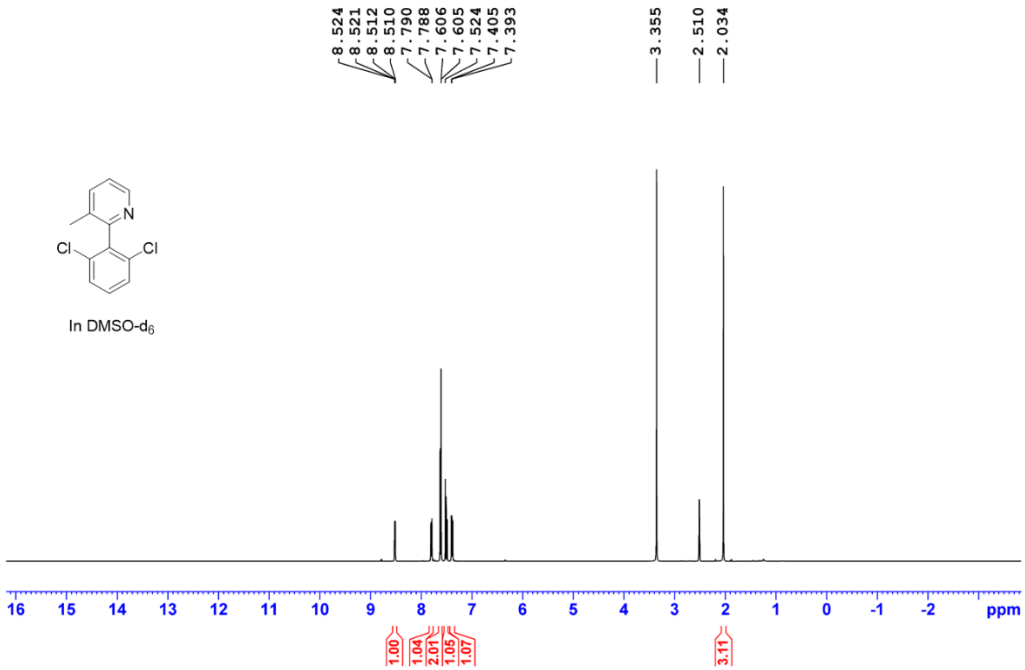

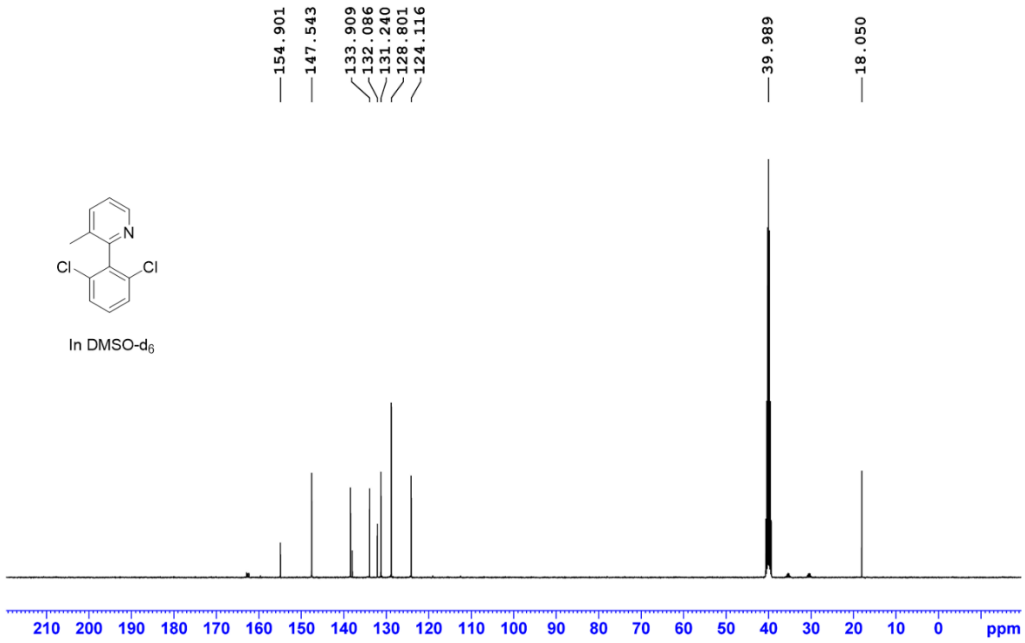

Supplementary Information

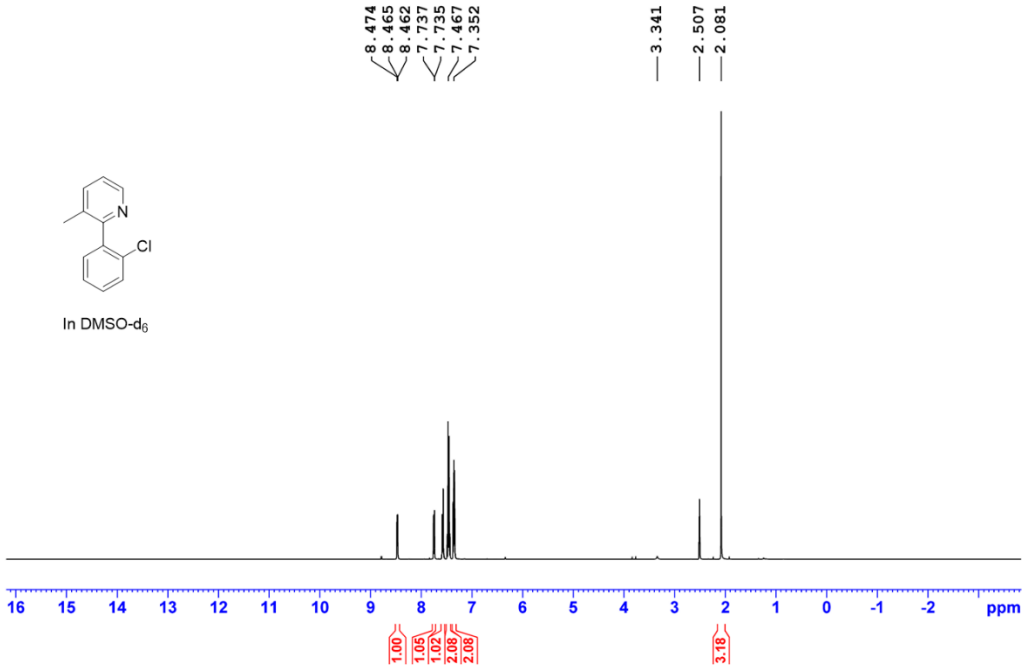

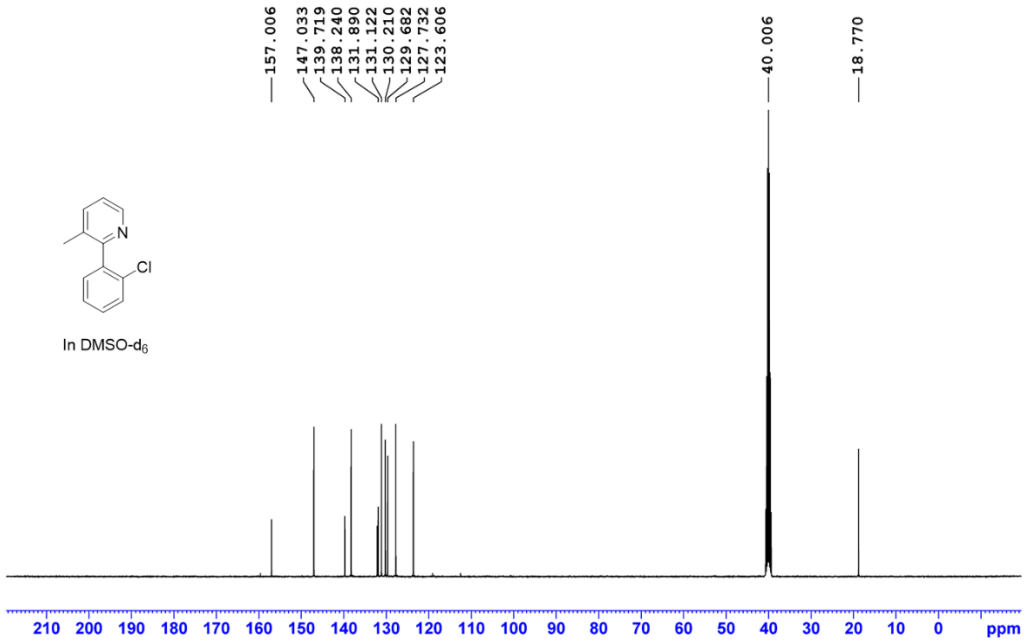

Supplementary Information

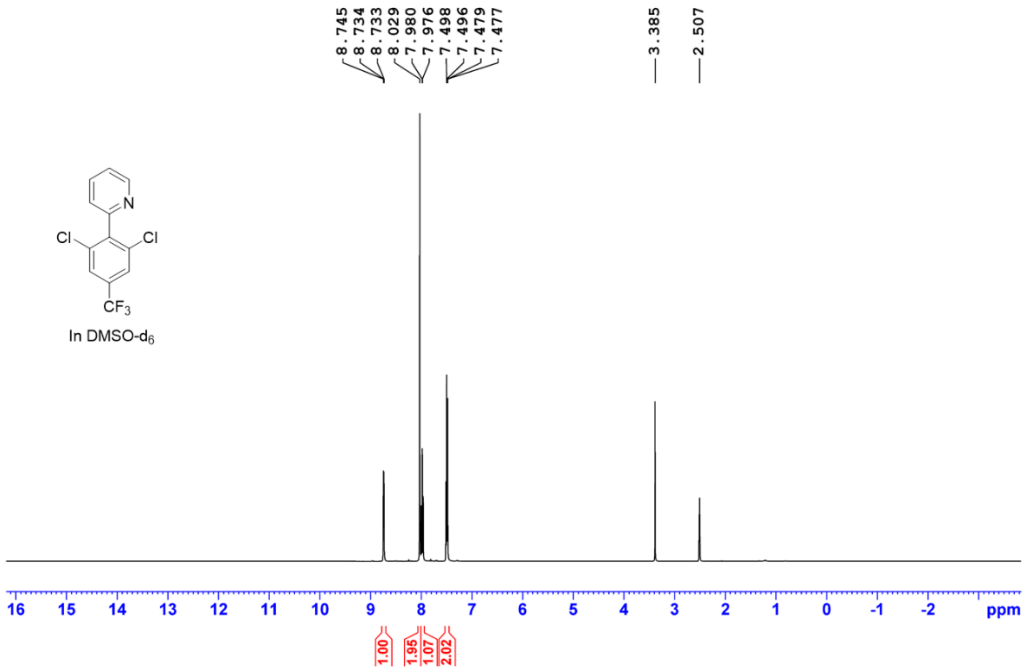

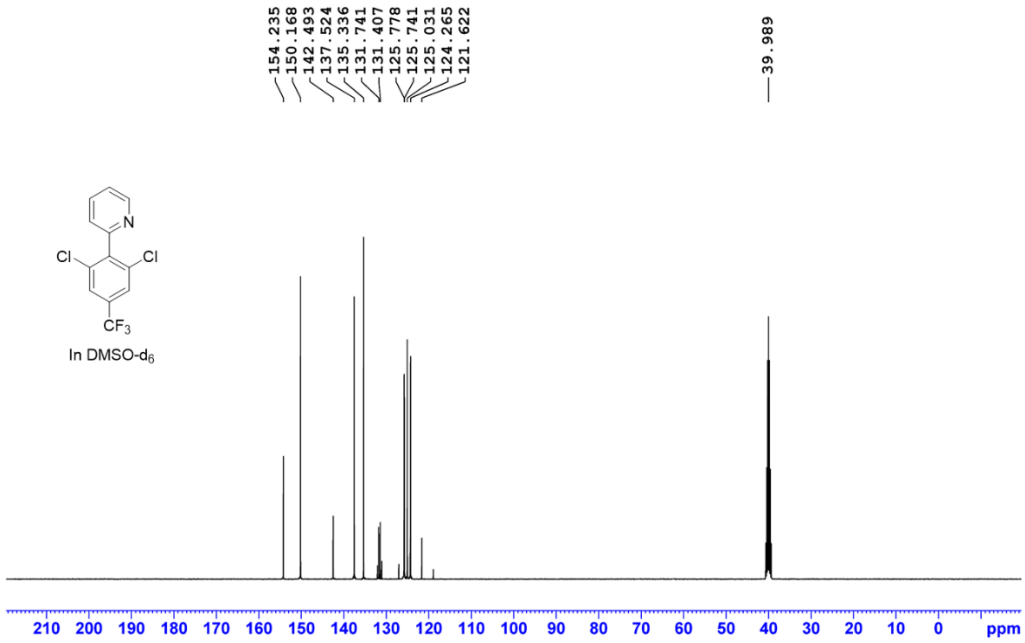

Supplementary Information

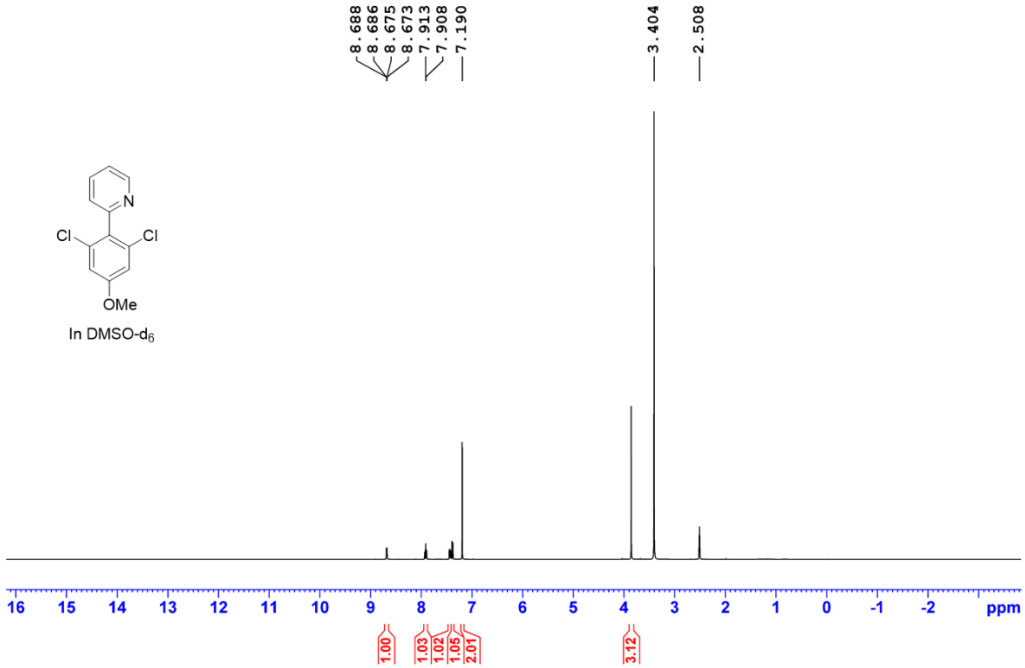

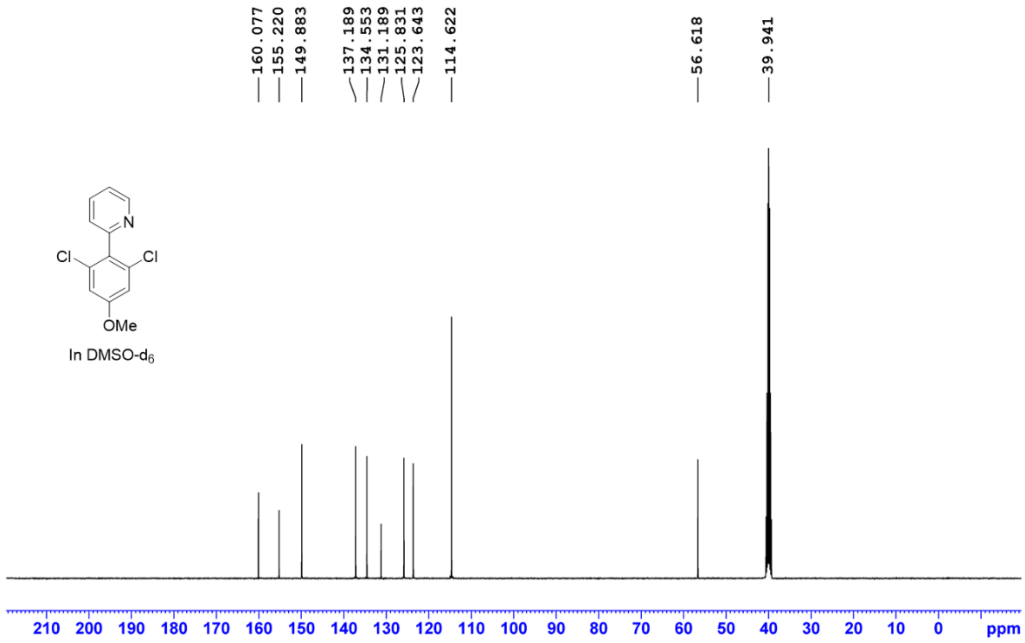

Supplementary Information

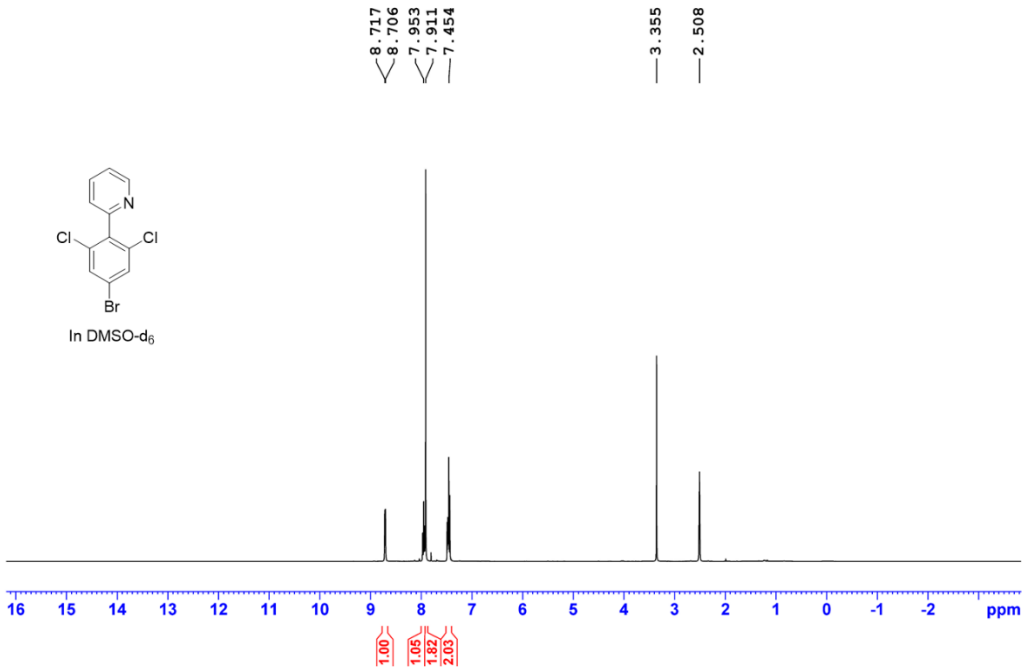

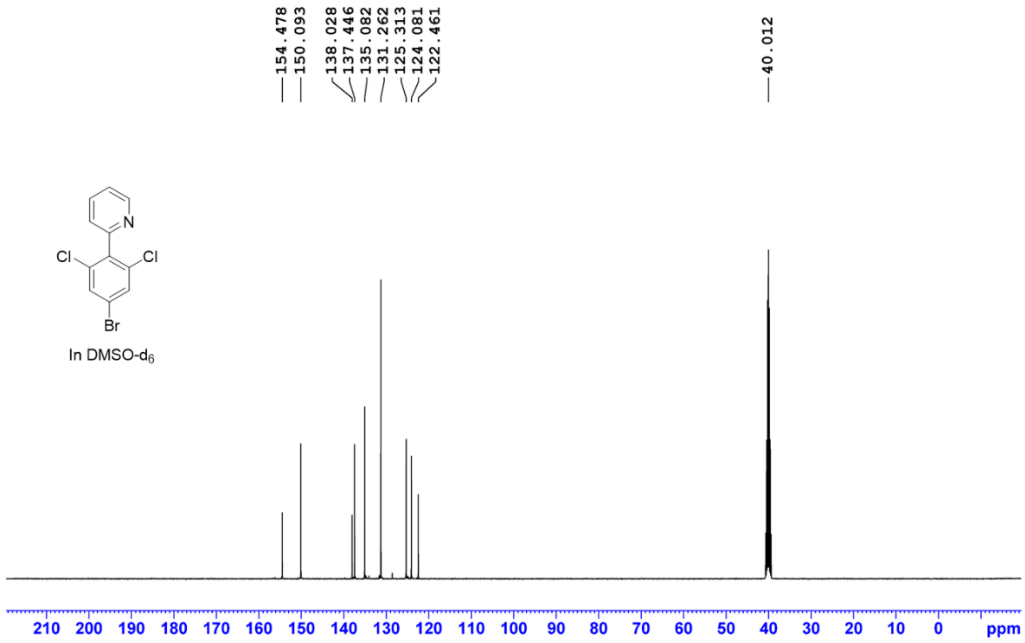

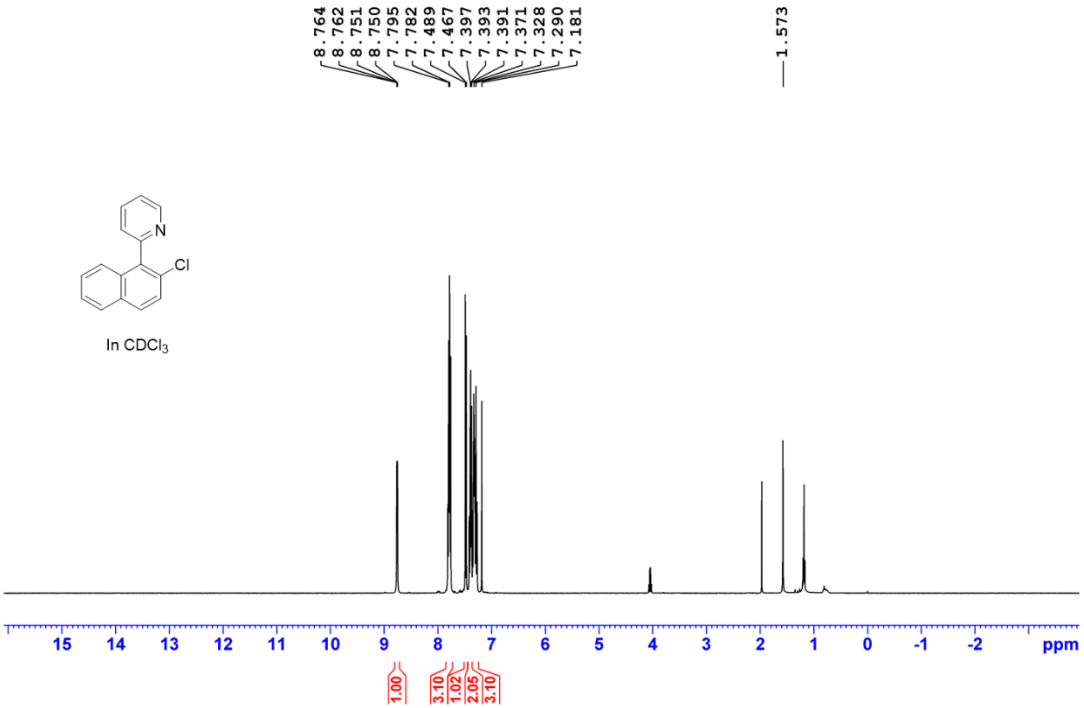
8.764
8.762
8.751
8.750
7.795
7.782
7.489
7.467
7.397
7.393
7.391
7.371
7.328
7.290
7.181
1.573
N
Cl
In CDCl3
15 14 13 12 11 10 9 8 7 6 5 4 3 2 1 0 -1 -2 ppm
1.00
3.10
1.02
2.05
3.10

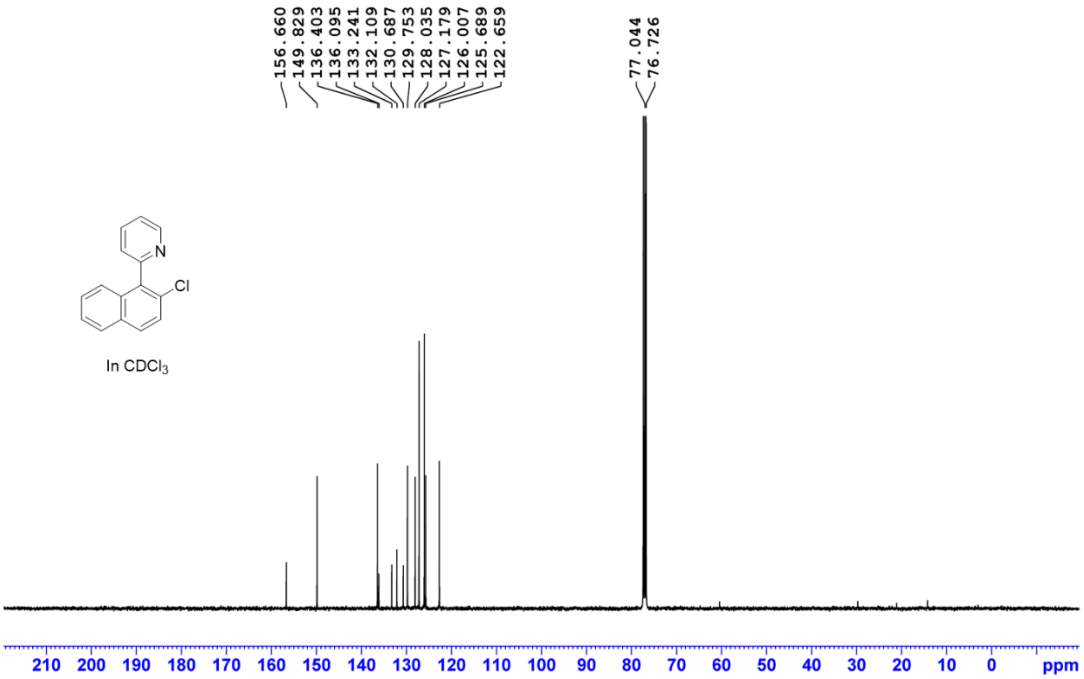
156.660
149.829
136.403
136.095
133.241
132.109
130.687
129.753
128.035
127.179
126.007
125.689
122.659
77.044
76.726
N
Cl
In CDCl3
210 200 190 180 170 160 150 140 130 120 110 100 90 80 70 60 50 40 30 20 10 0 ppm

Supplementary Information

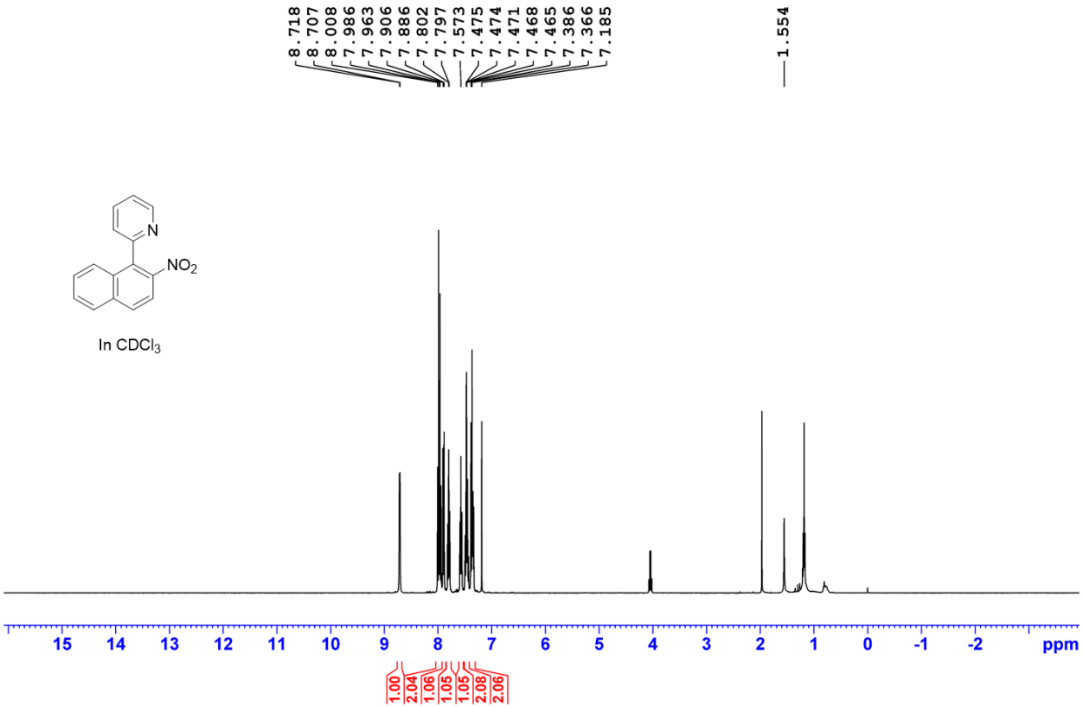

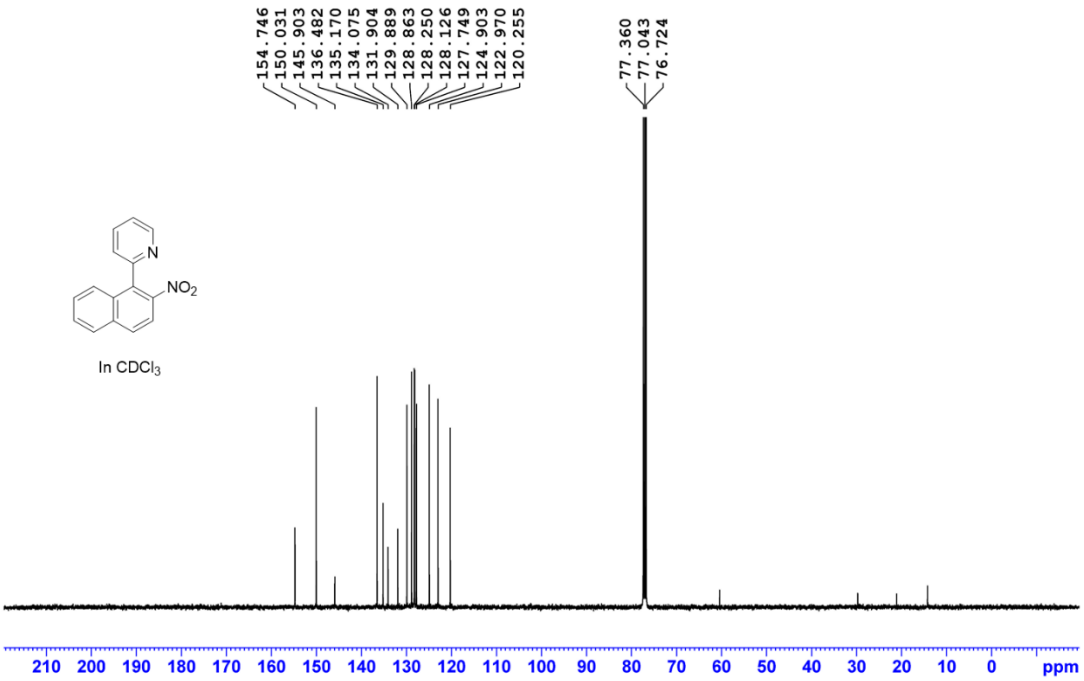

Supplementary Information

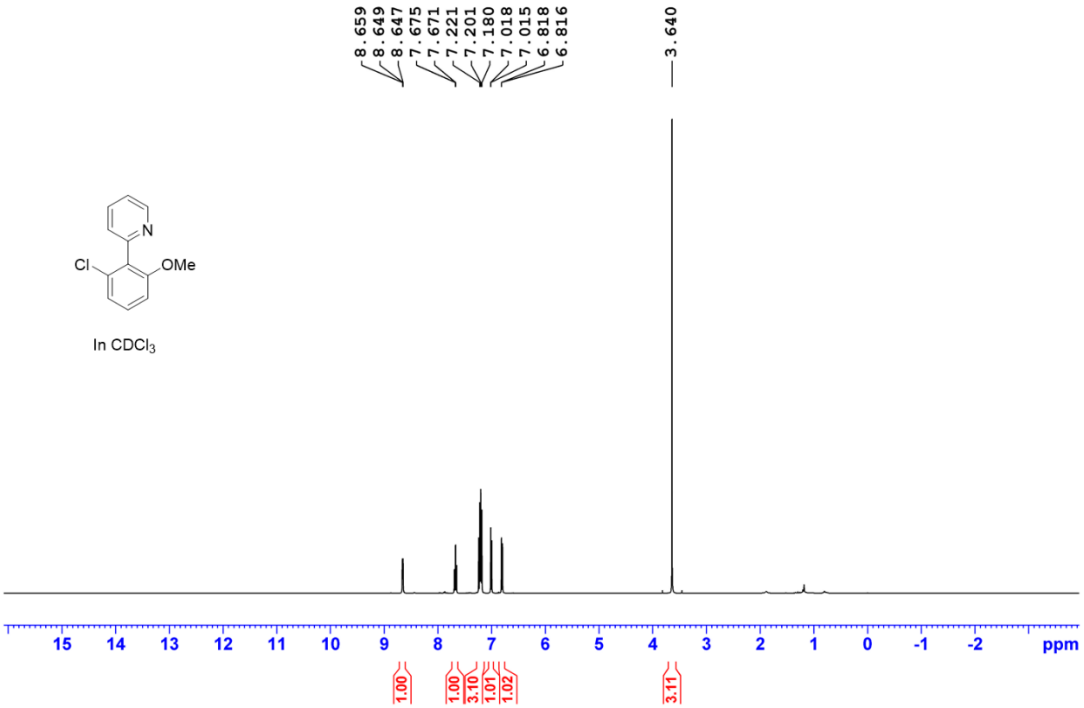

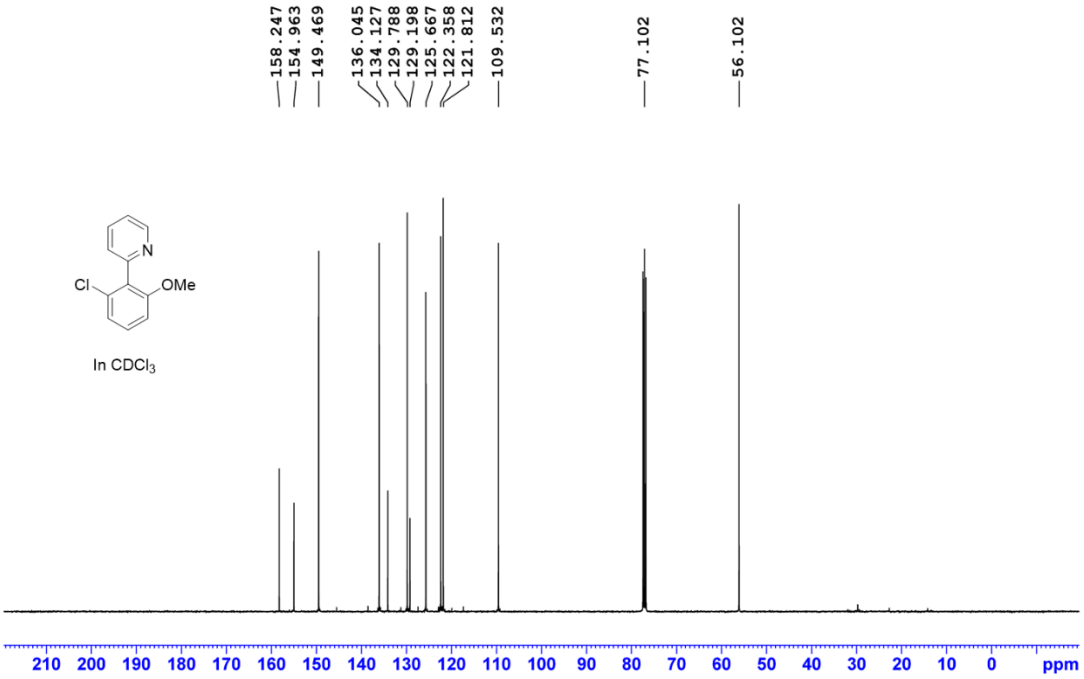

Supplementary Information

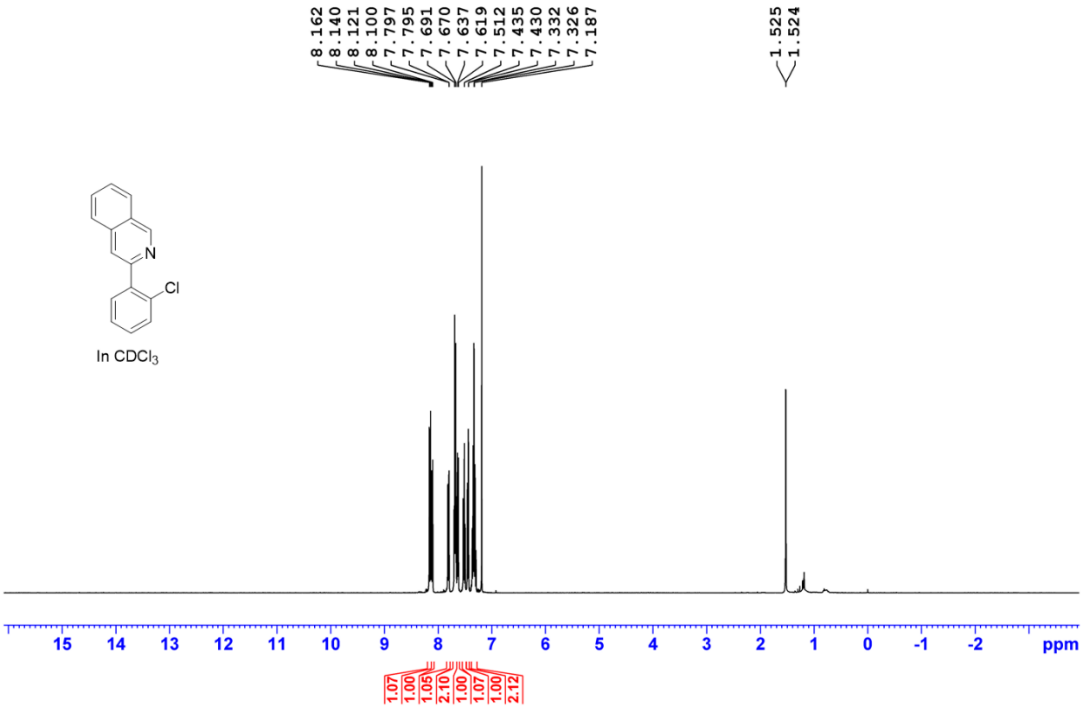

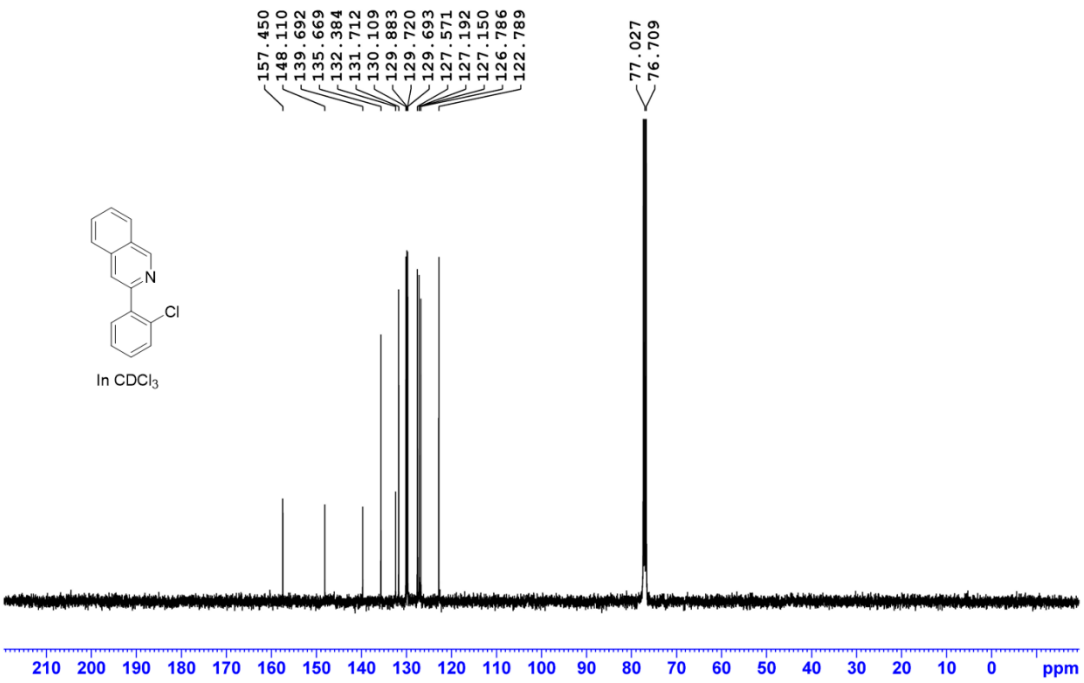

Supplementary Information

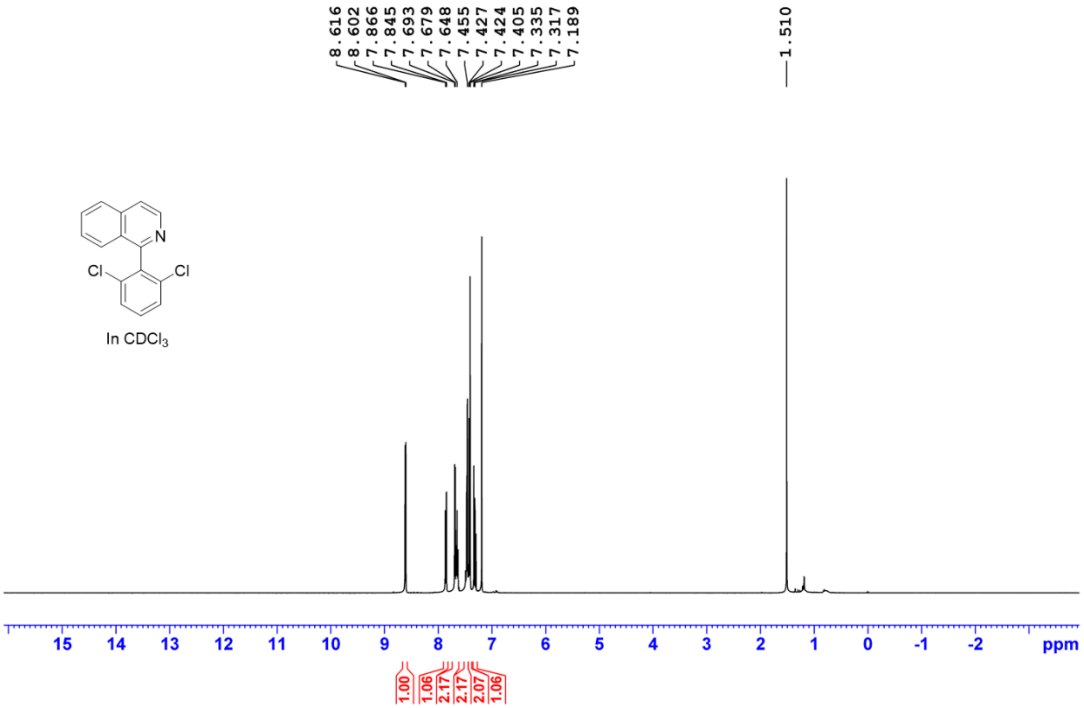

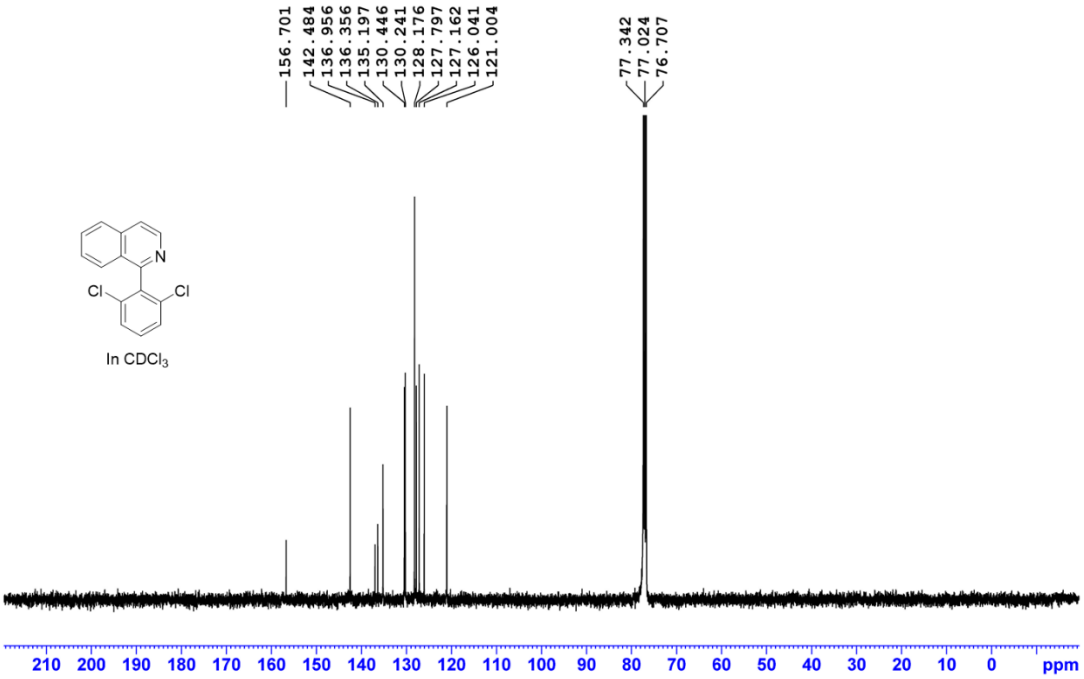

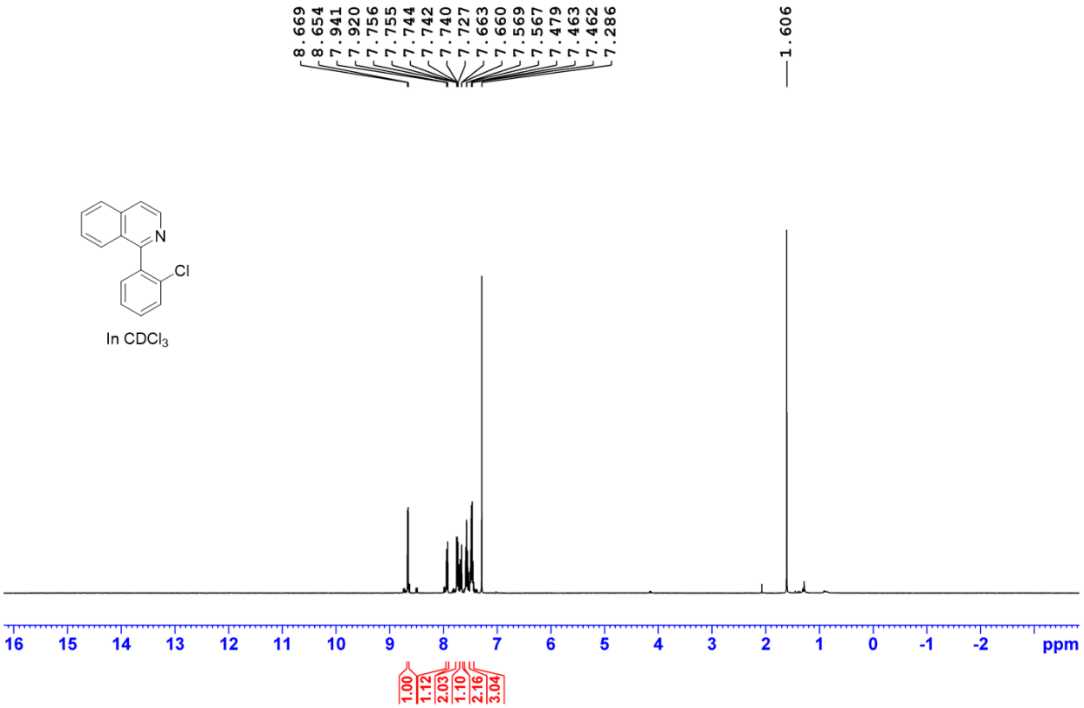
8.669
8.654
7.941
7.920
7.756
7.755
7.744
7.742
7.740
7.727
7.663
7.660
7.569
7.567
7.479
7.463
7.462
7.286
1.606
N
Cl
In CDCl3
16 15 14 13 12 11 10 9 8 7 6 5 4 3 2 1 0 -1 -2 ppm
1.00
1.12
2.03
1.10
2.16
3.04

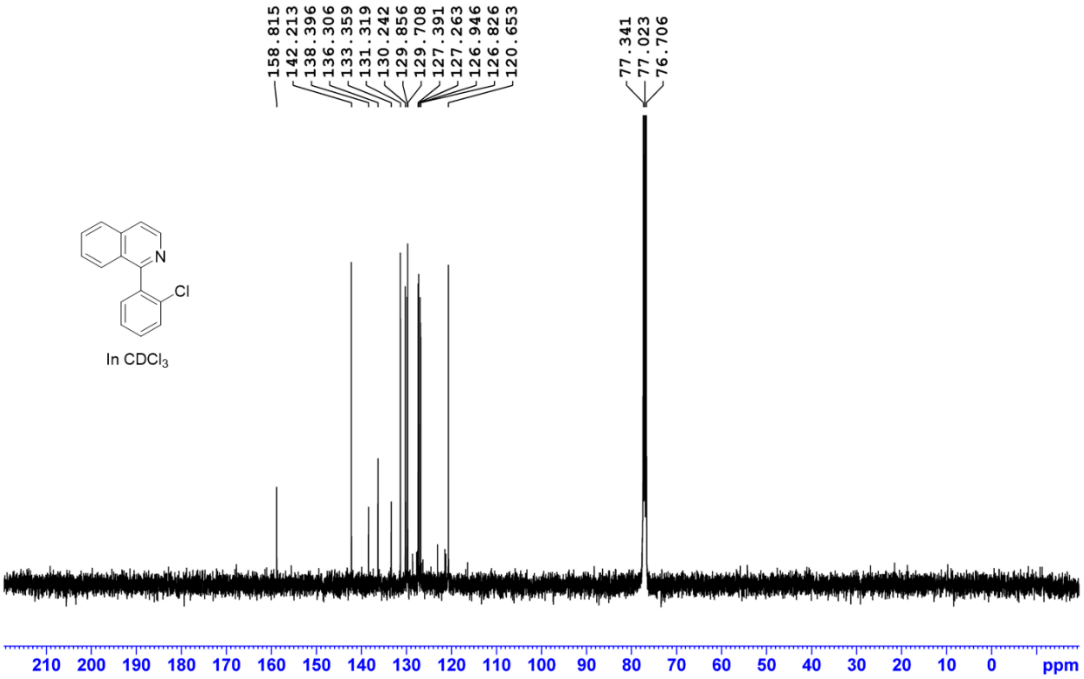
158.815
142.213
138.396
136.306
133.359
131.319
130.242
129.856
129.708
127.391
127.263
126.946
126.826
120.653
77.341
77.023
76.706
N
Cl
In CDCl3
210 200 190 180 170 160 150 140 130 120 110 100 90 80 70 60 50 40 30 20 10 0 ppm

Supplementary Information

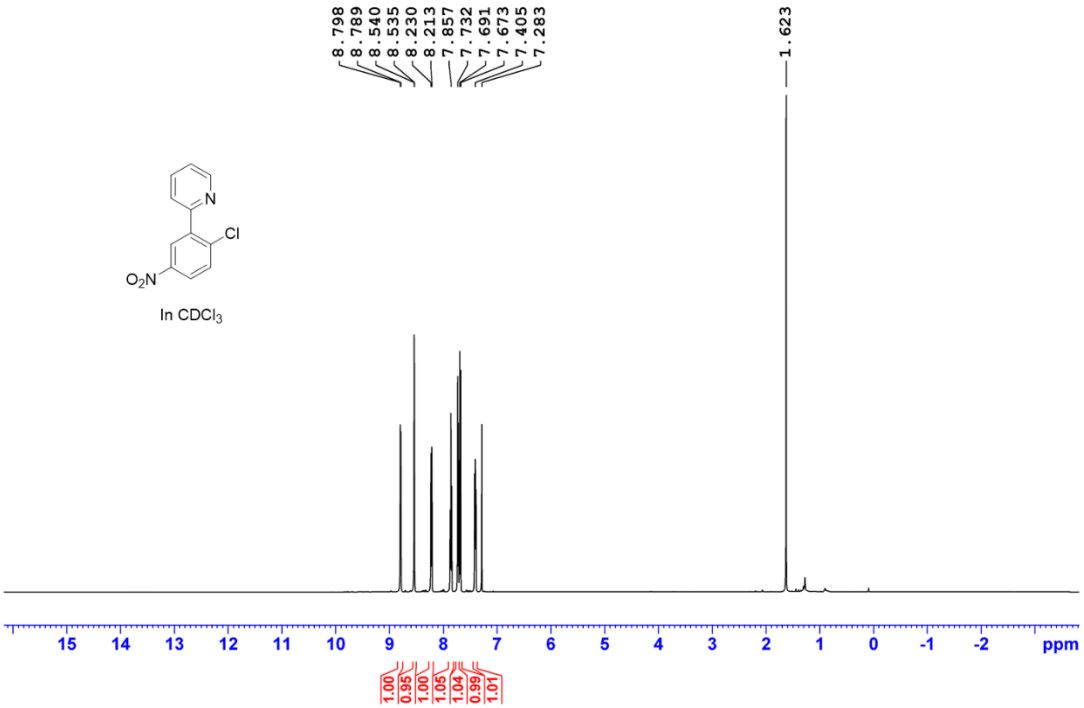

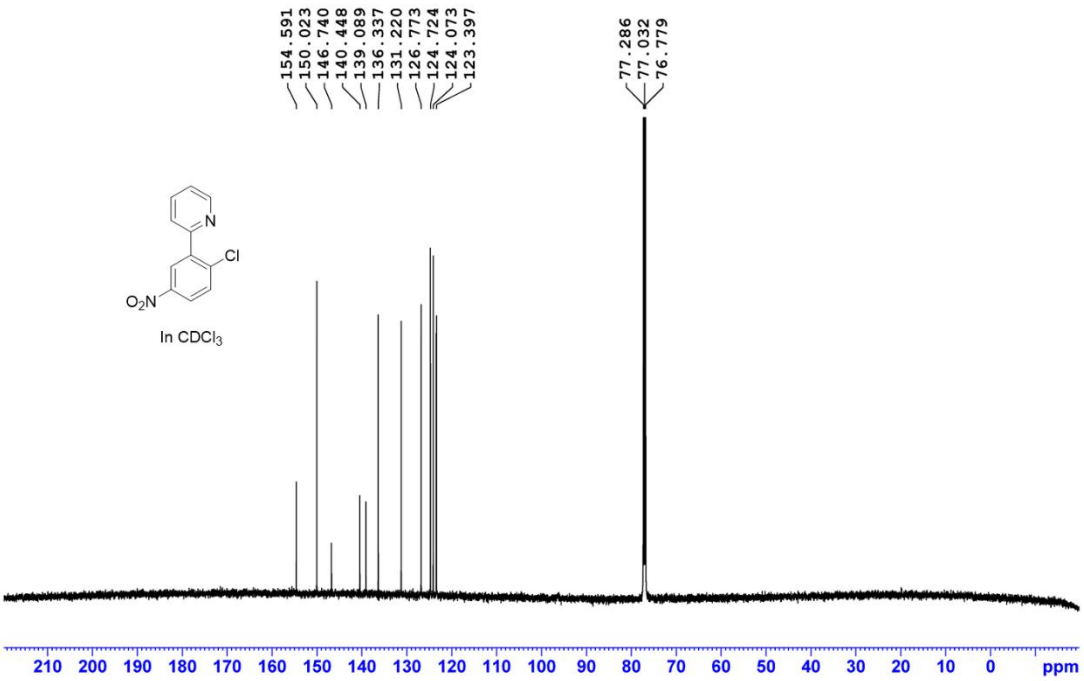

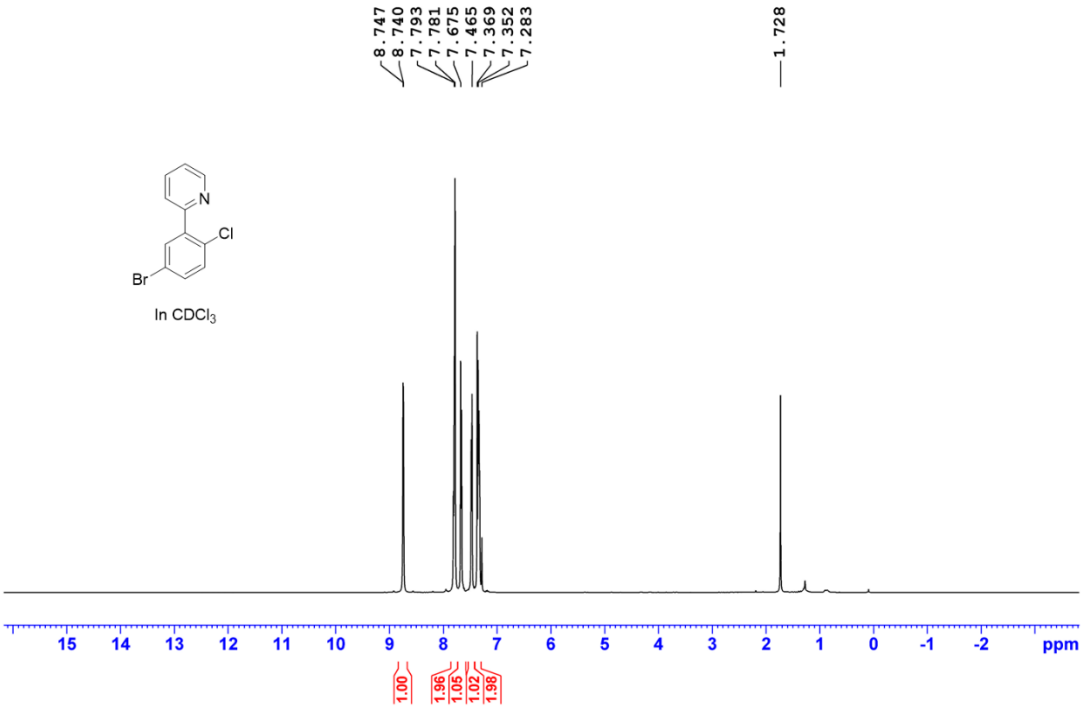
8.747
8.740
7.793
7.781
7.675
7.465
7.369
7.352
7.283
1.728
N
Cl
Br
In CDCl3
15 14 13 12 11 10 9 8 7 6 5 4 3 2 1 0 -1 -2 ppm
1.00
1.96
1.05
1.02
1.98

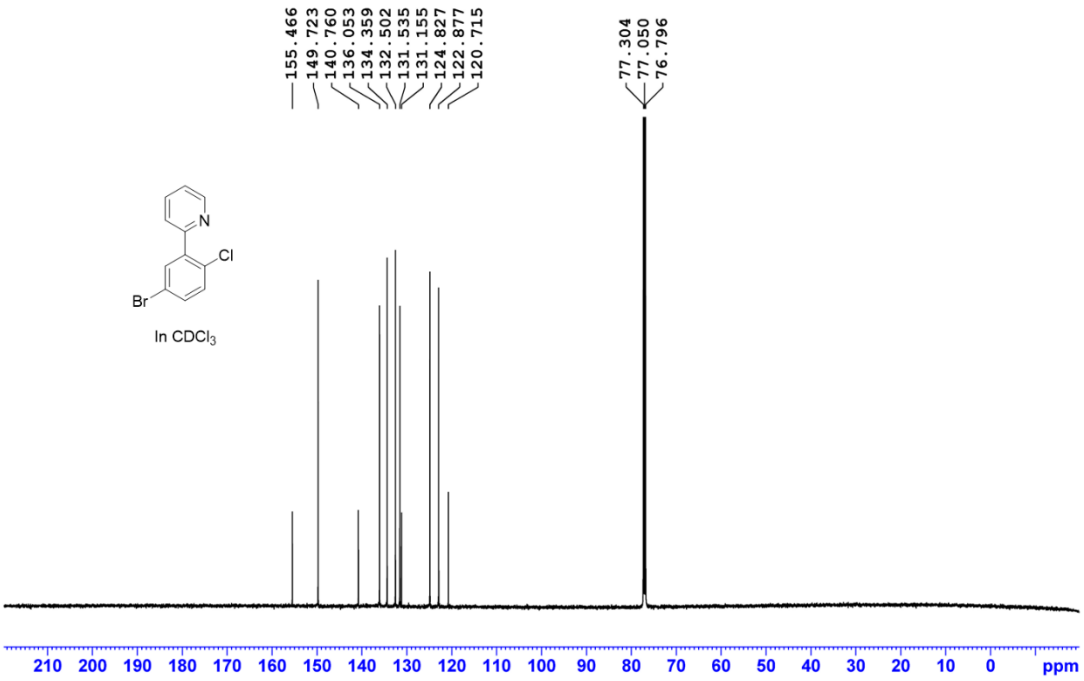
155.466
149.723
140.760
136.053
134.359
132.502
131.535
131.155
124.827
122.877
120.715
77.304
77.050
76.796
N
Cl
Br
In CDCl3
210 200 190 180 170 160 150 140 130 120 110 100 90 80 70 60 50 40 30 20 10 0 ppm

Supplementary Information

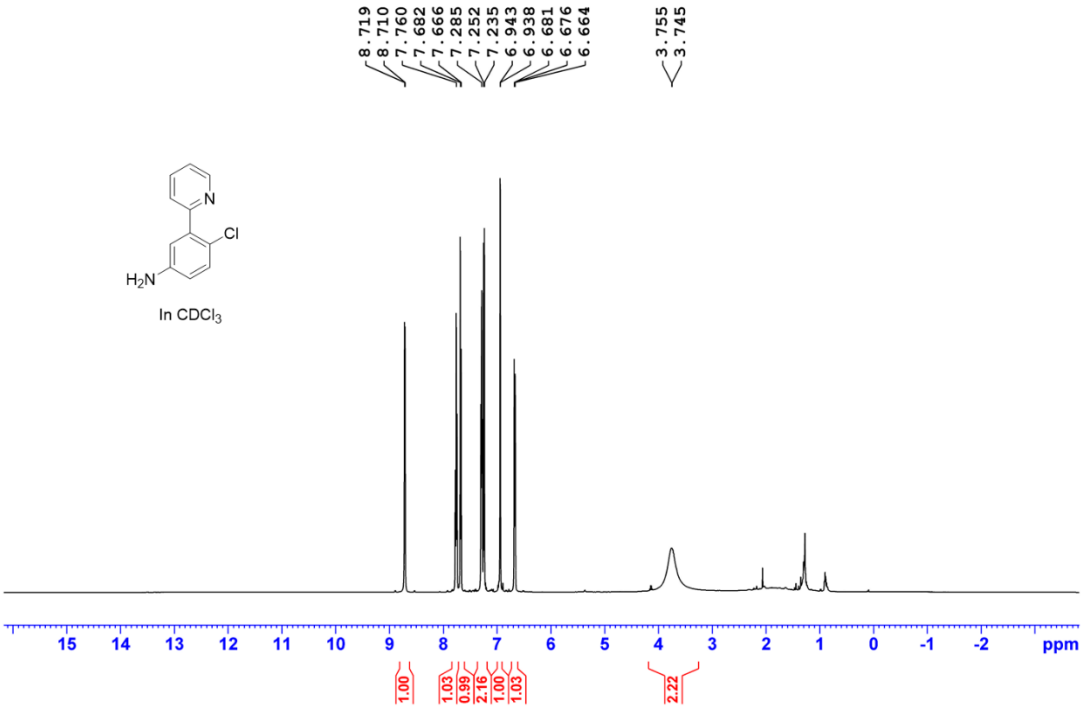

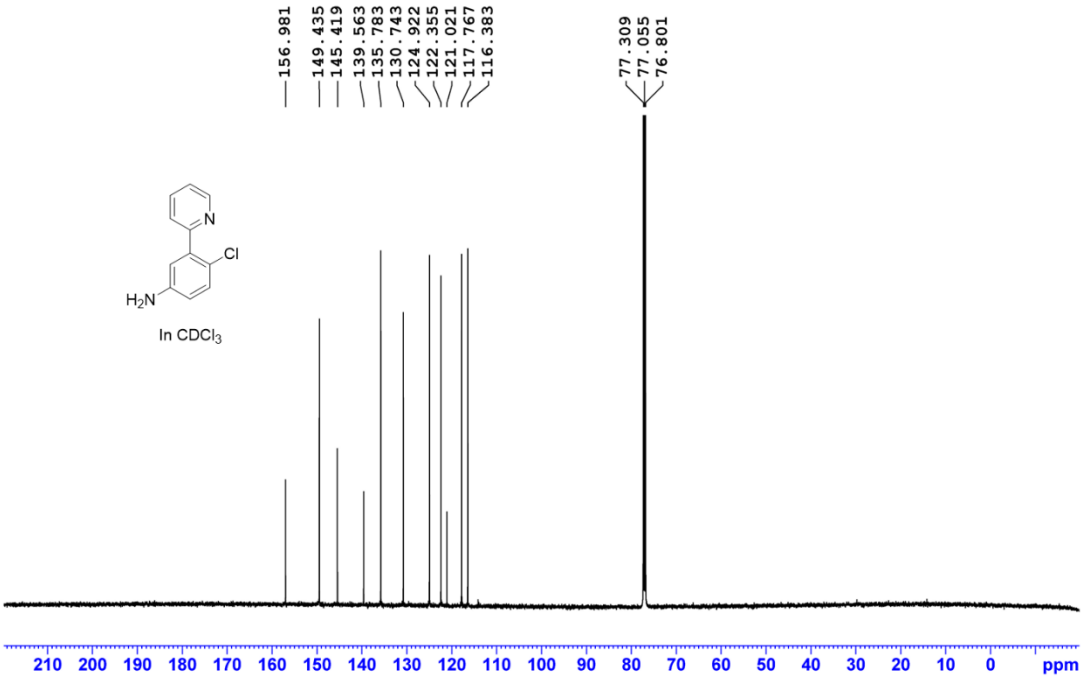

Supplementary Information

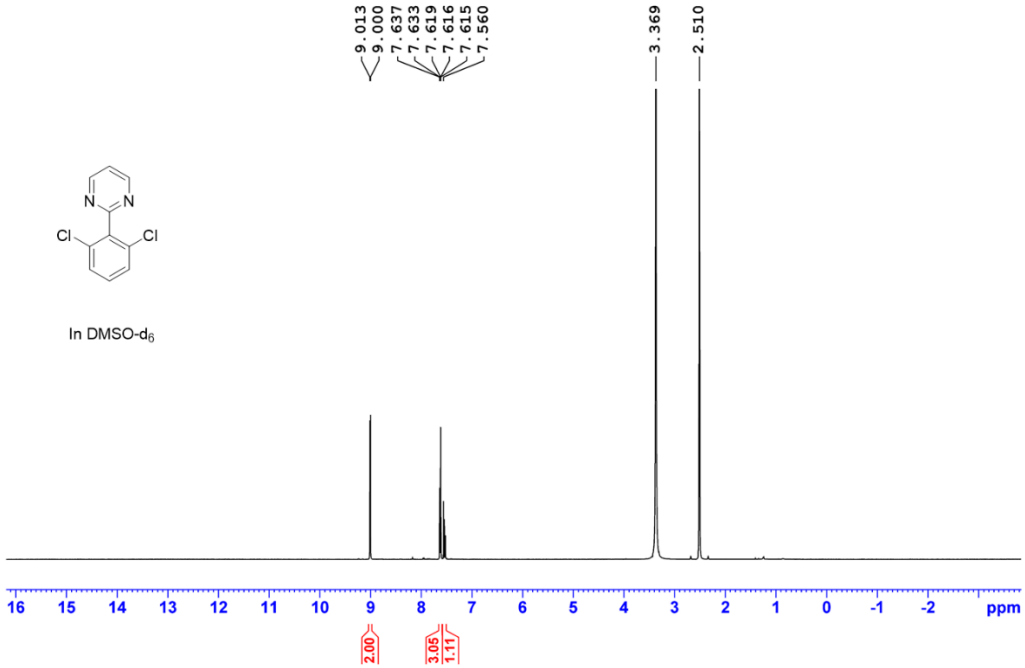

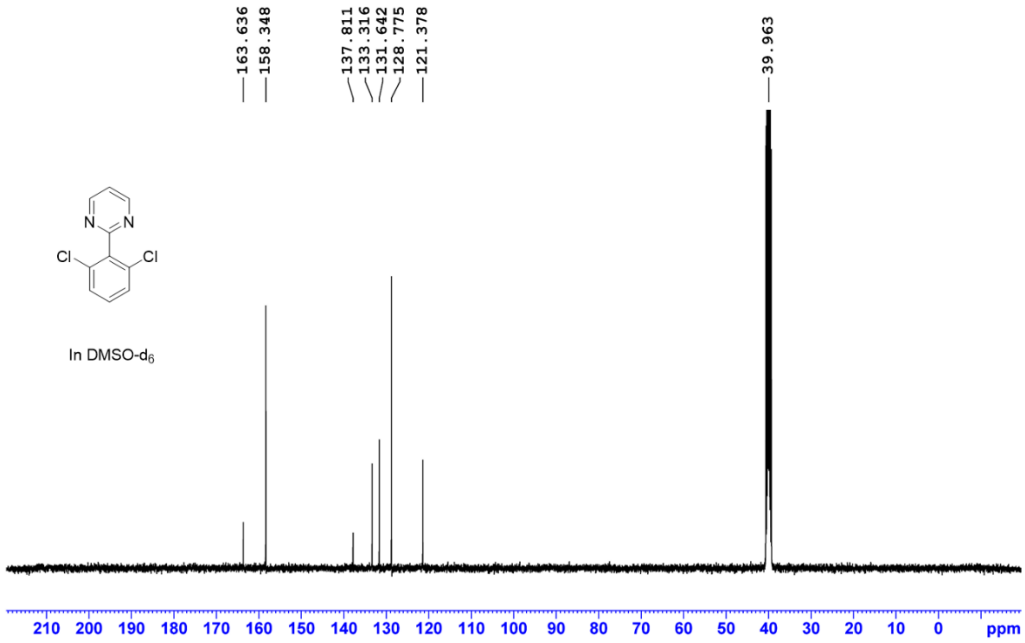

Supplementary Information

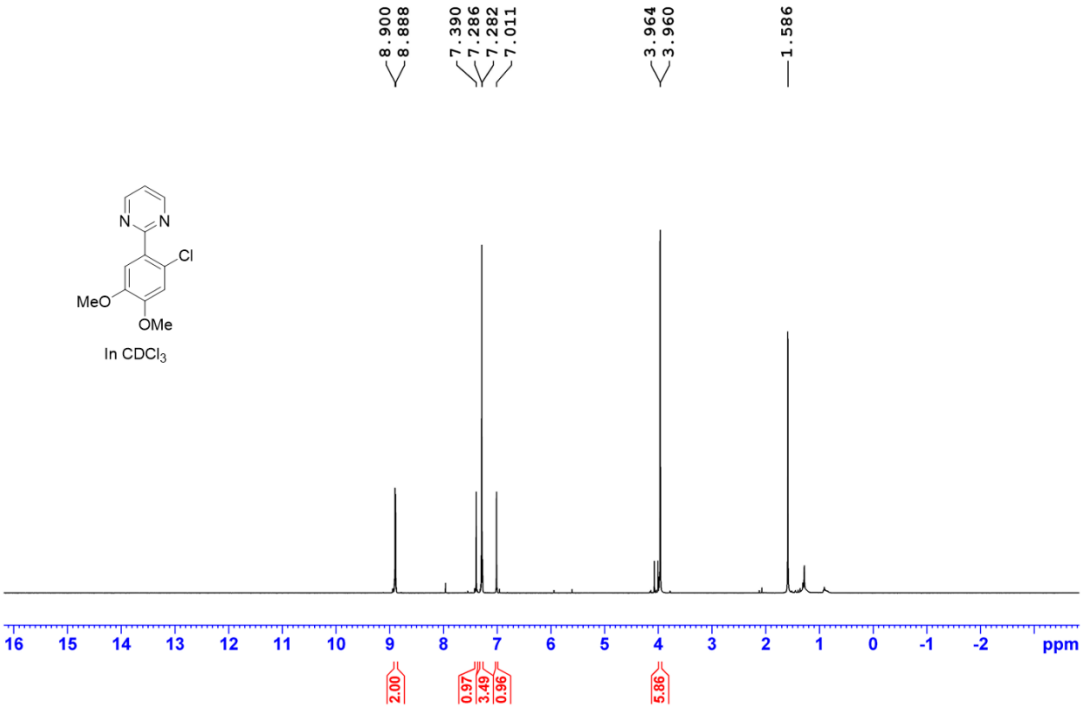

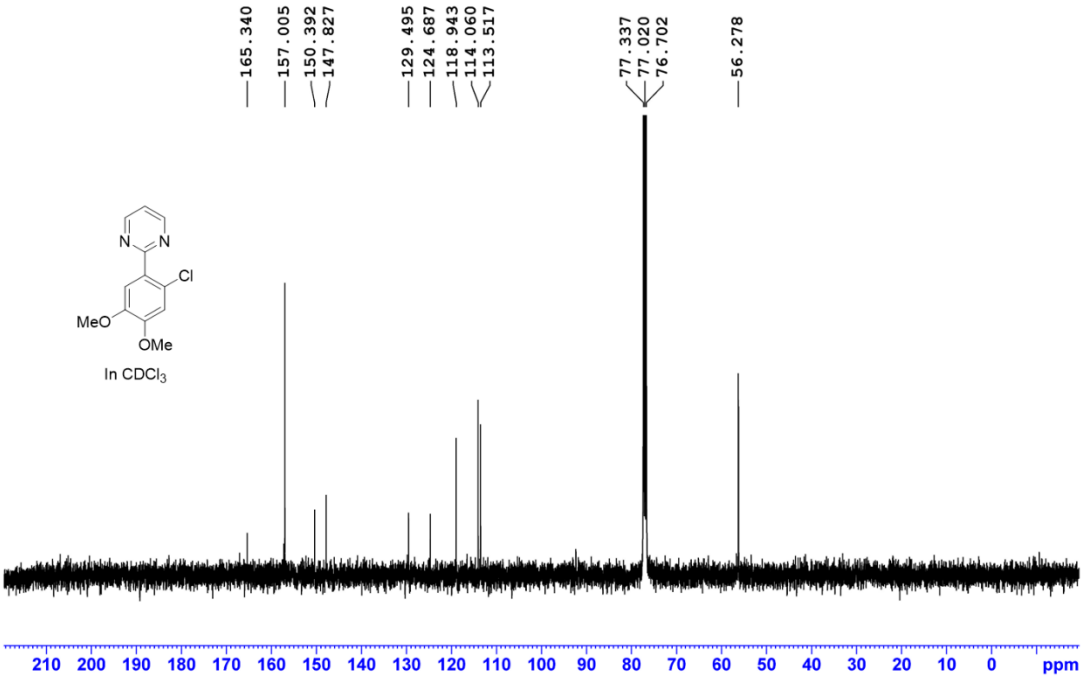

Supplementary Information

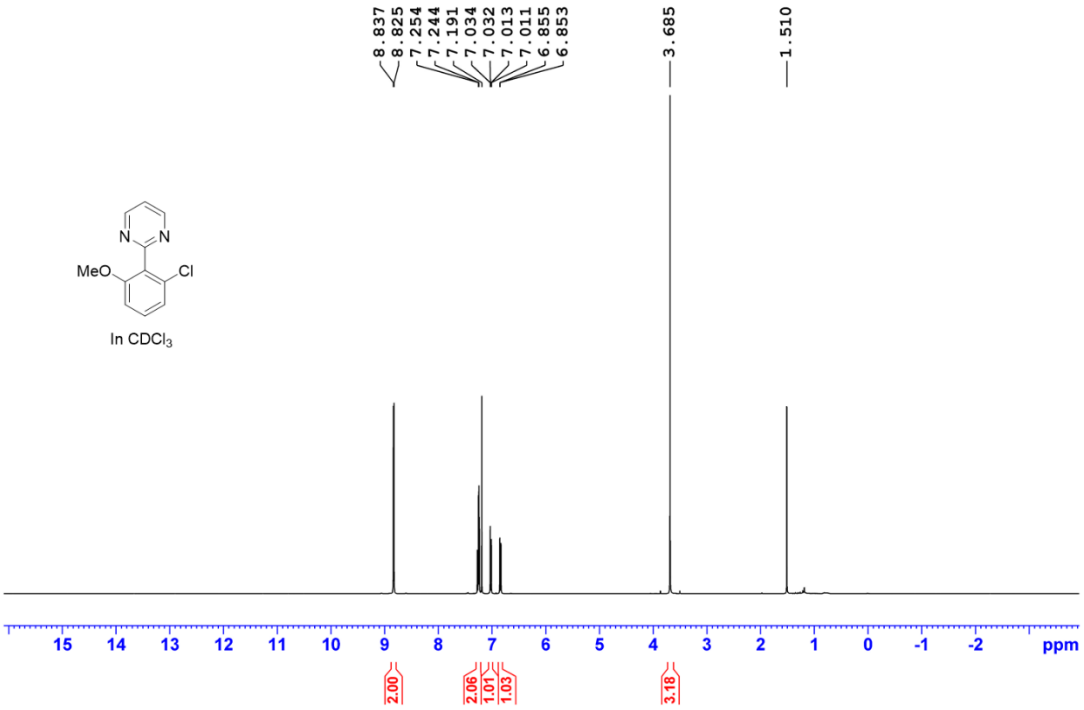

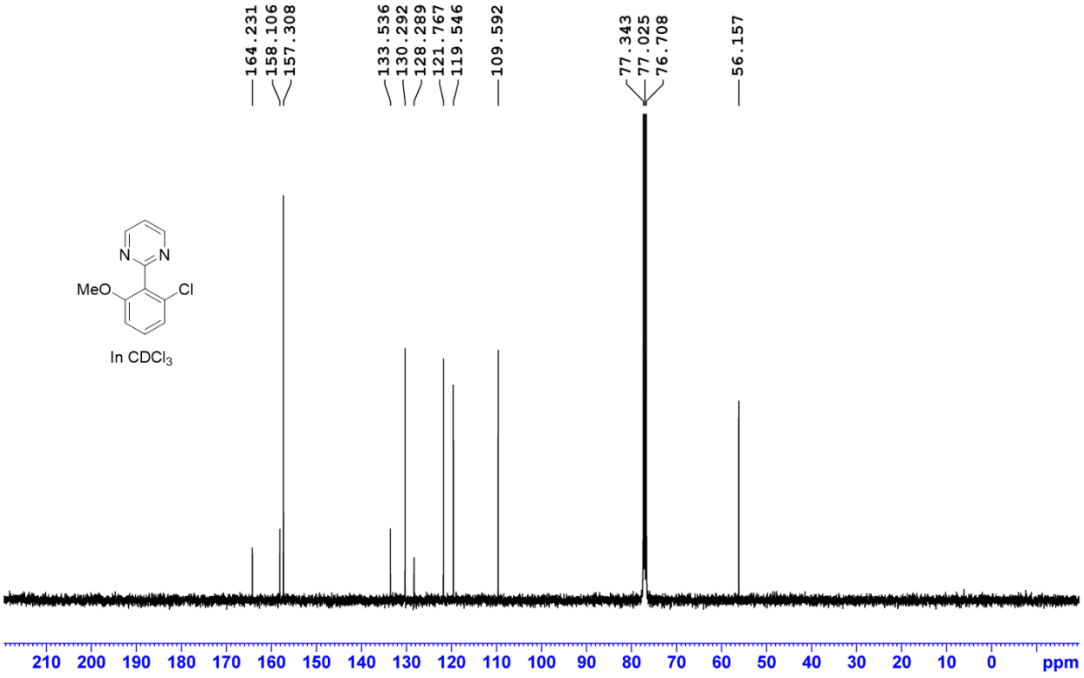

Supplementary Information

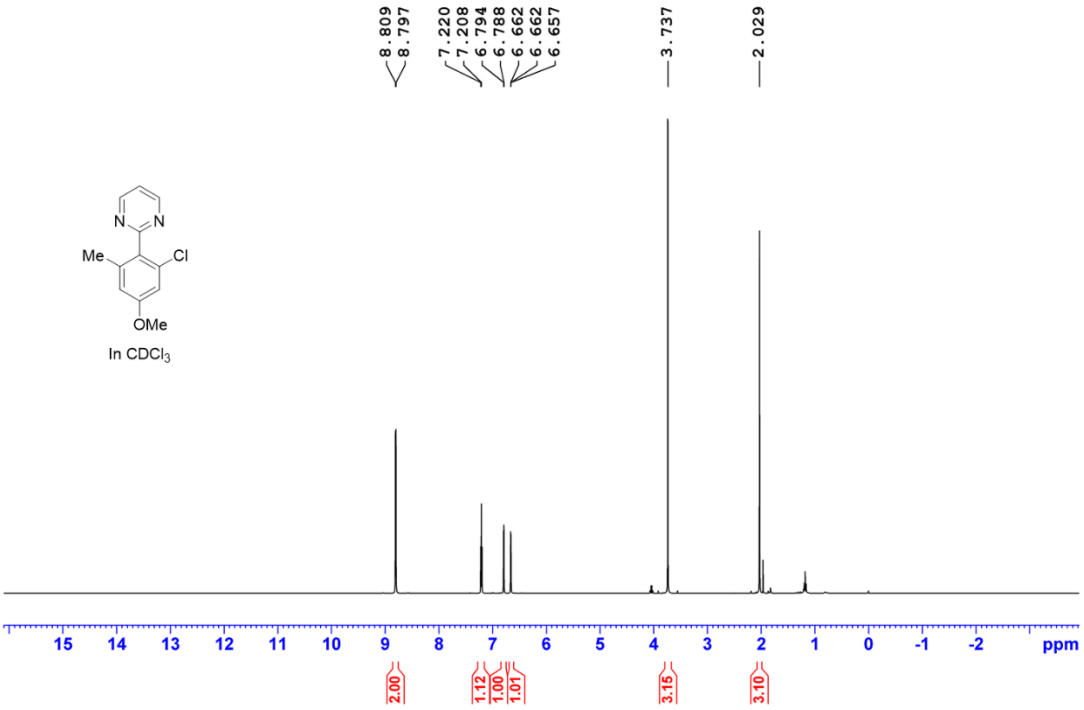

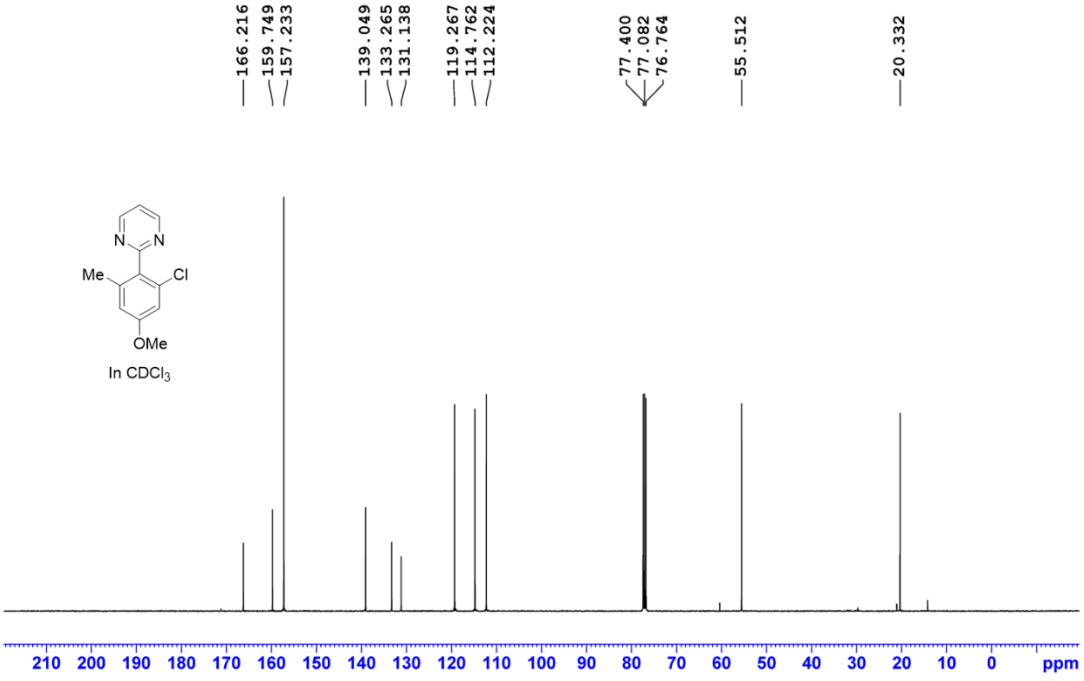

Supplementary Information

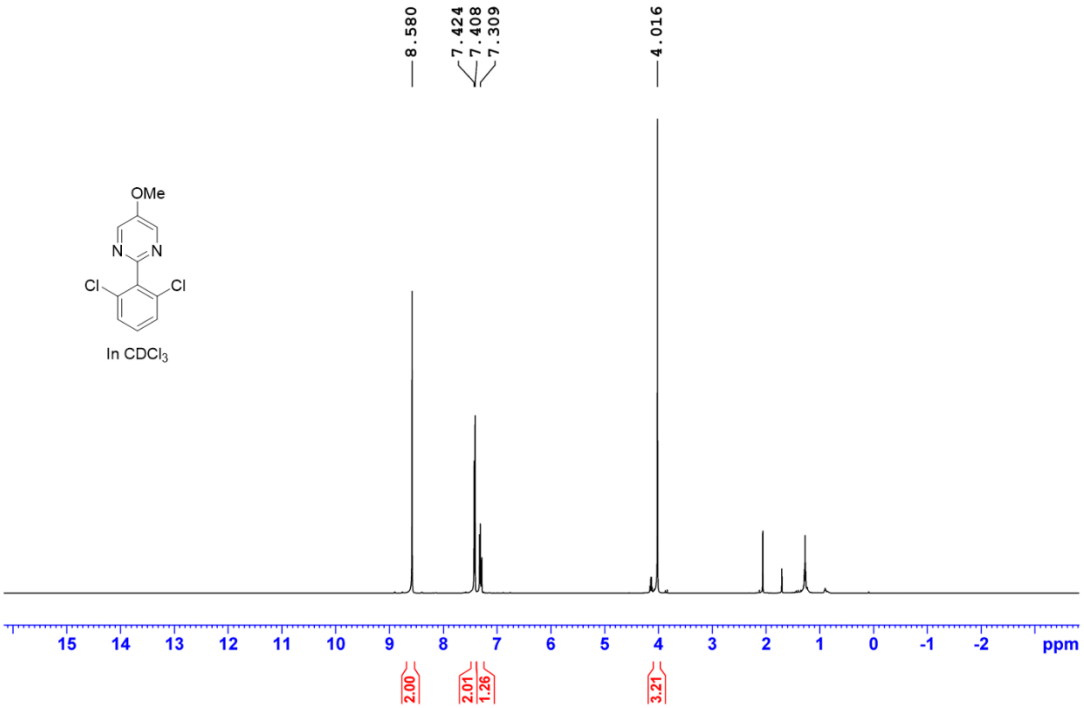

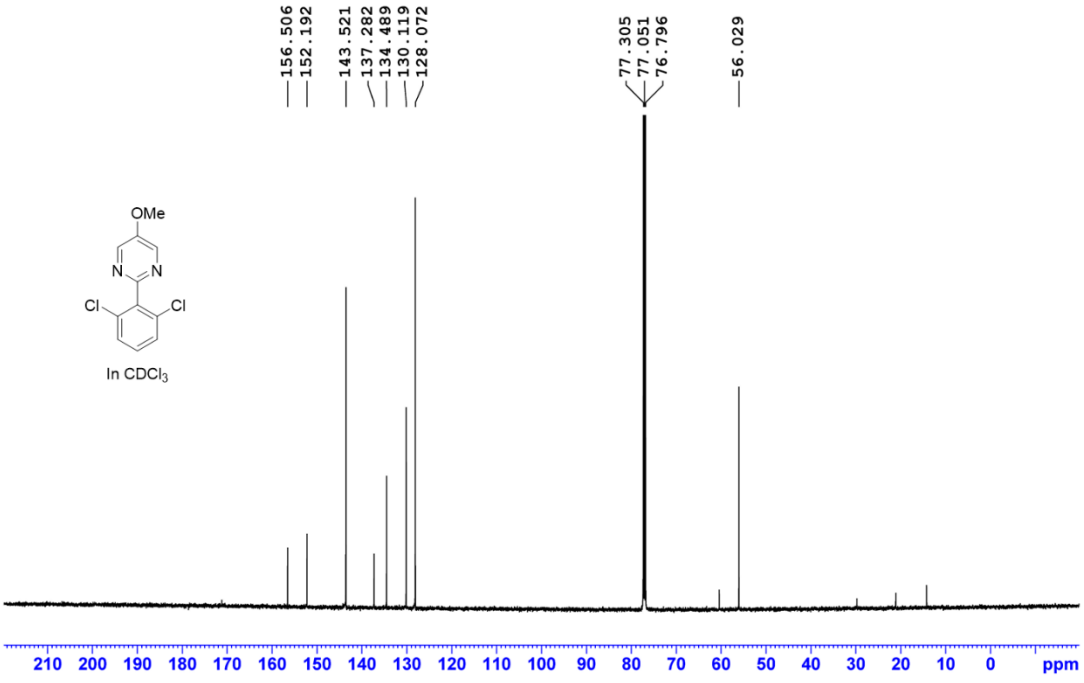

Supplementary Information

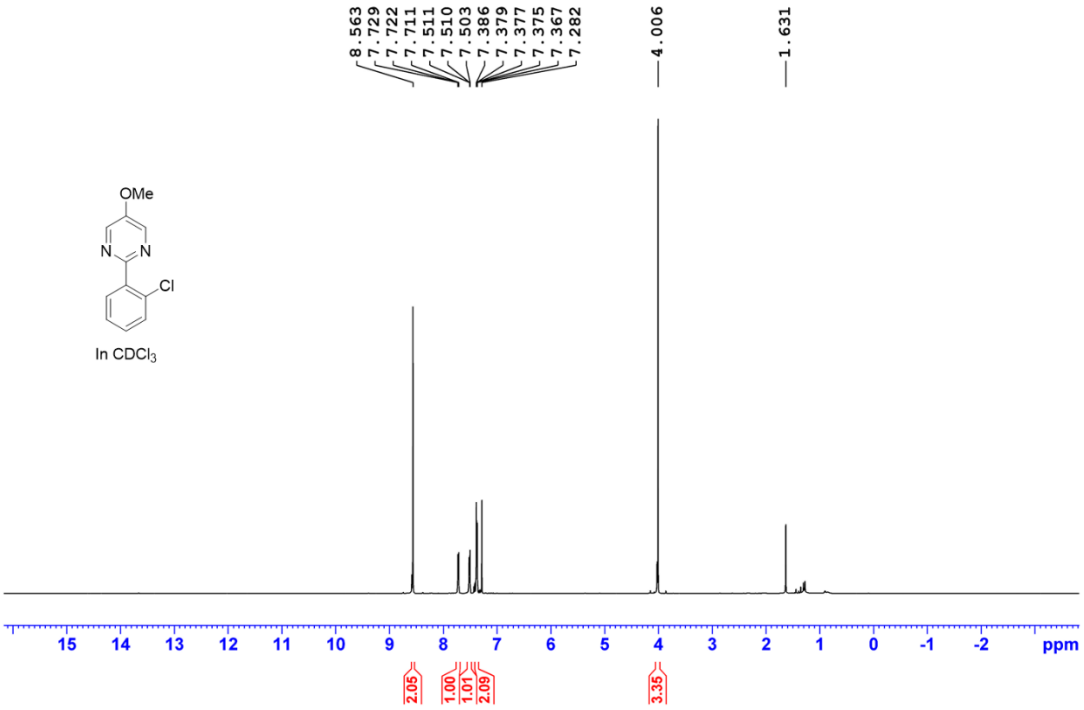

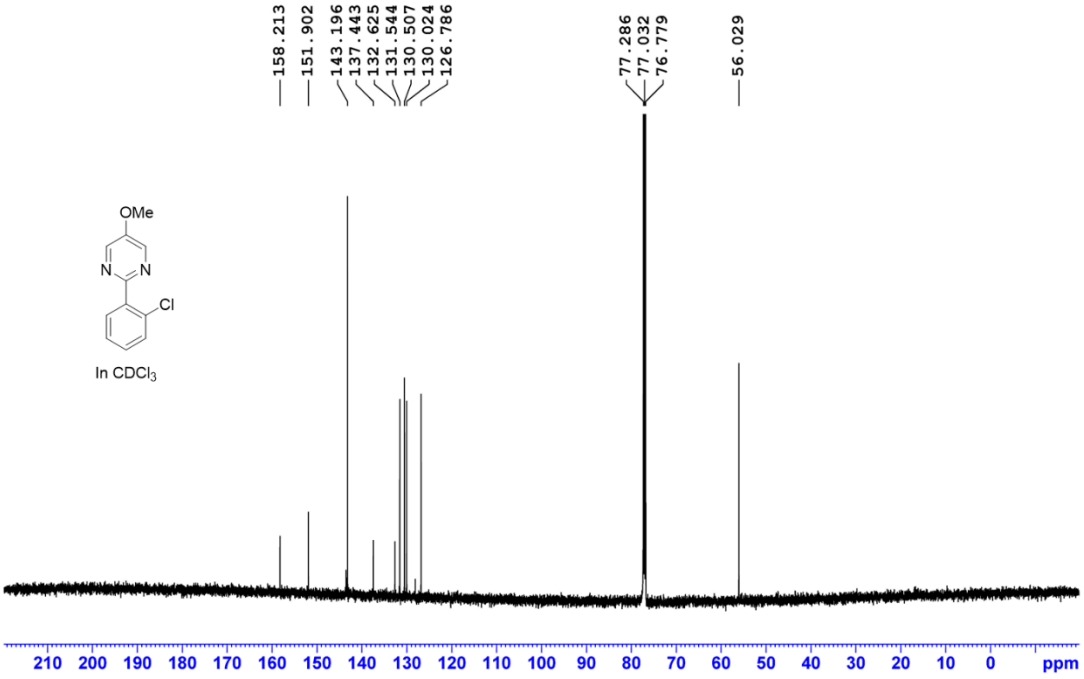

Supplementary Information

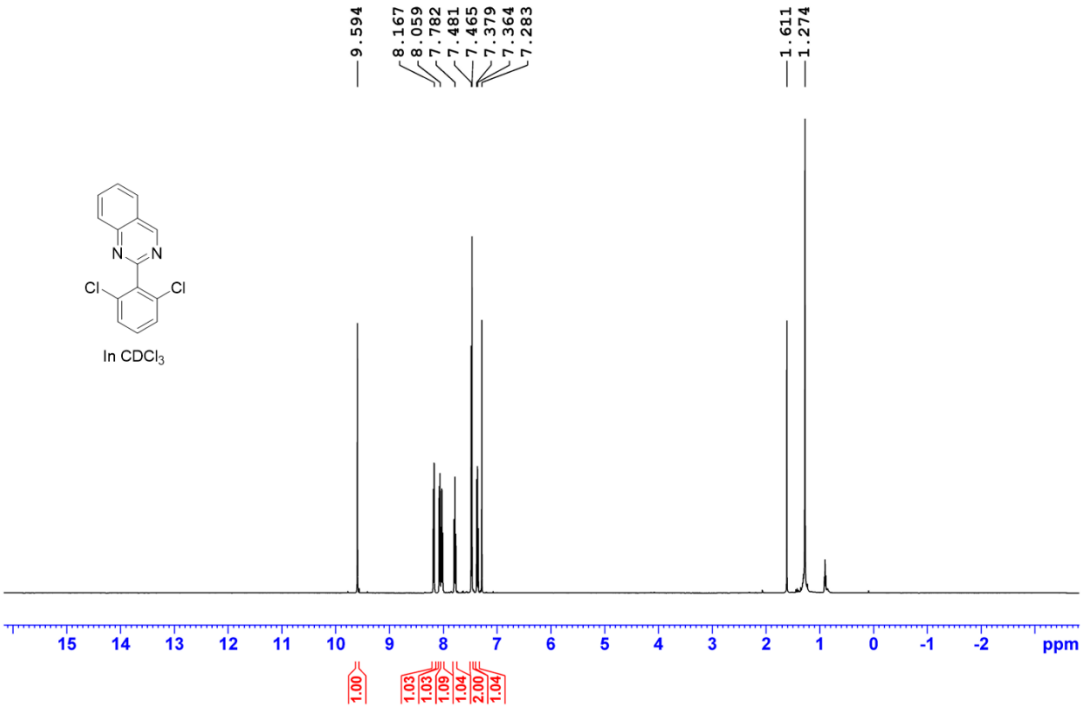

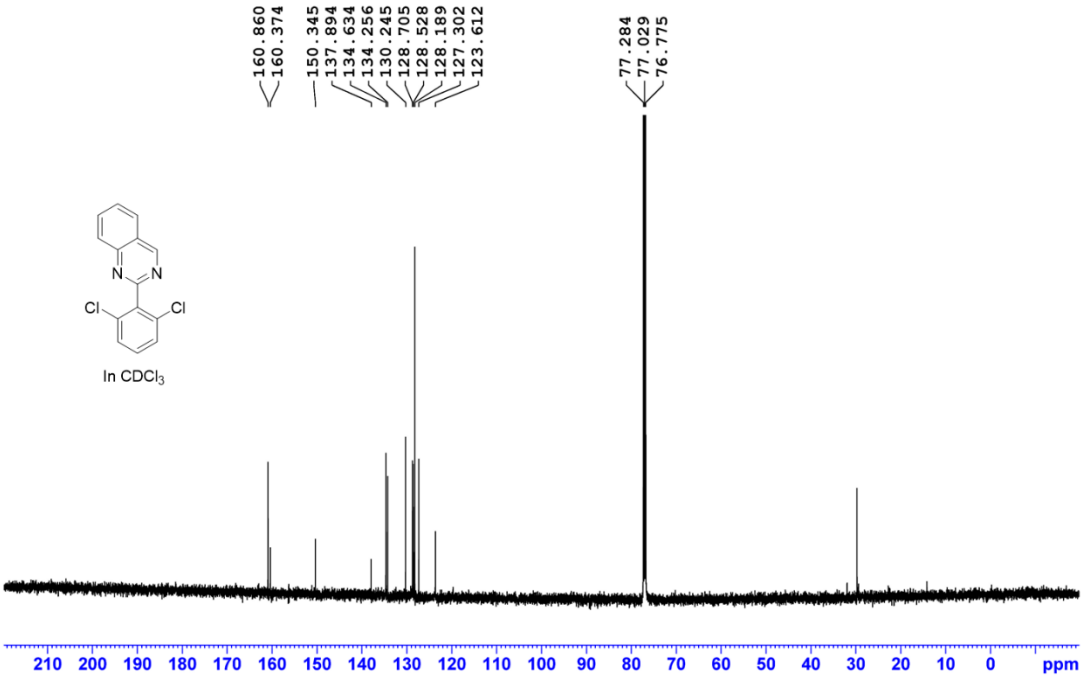

Supplementary Information

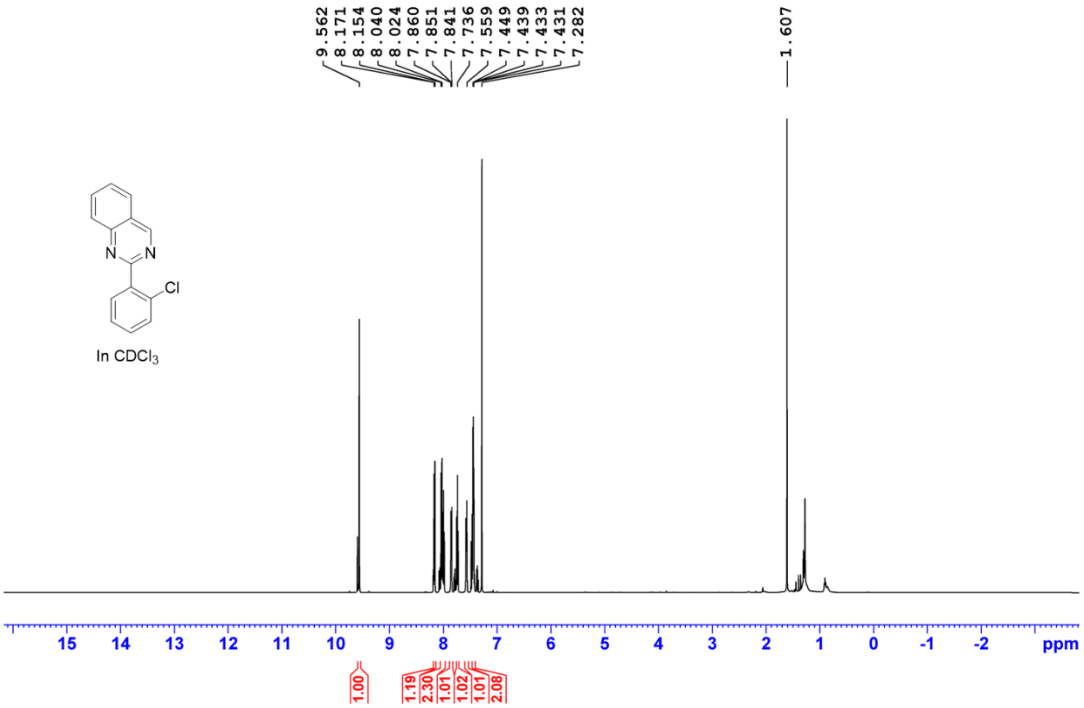

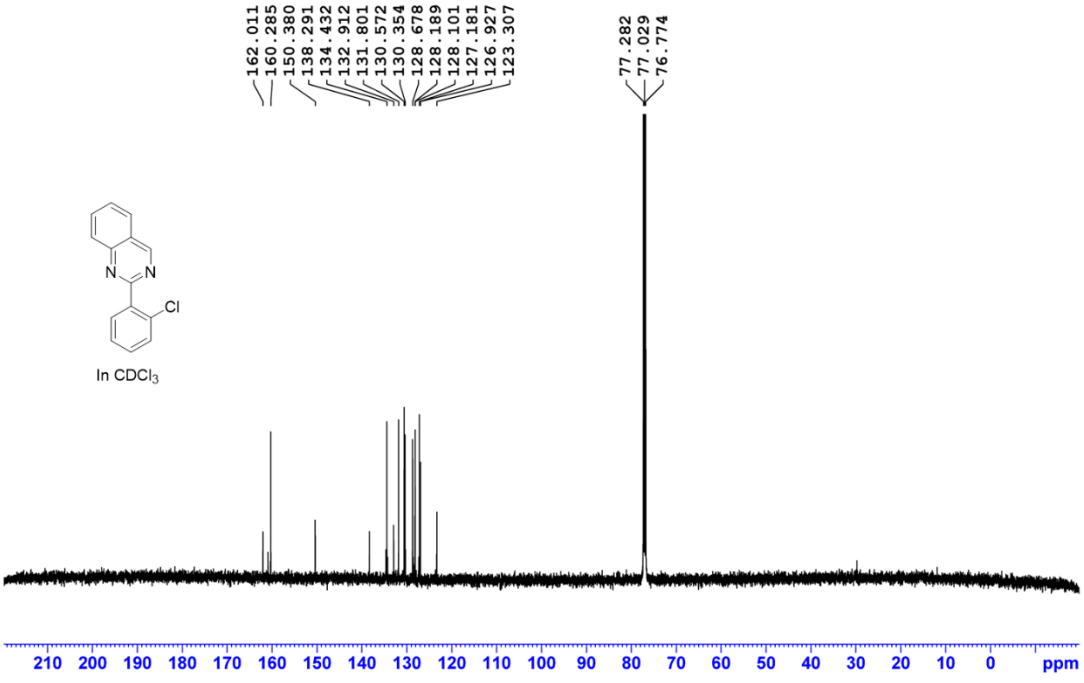

Supplementary Information

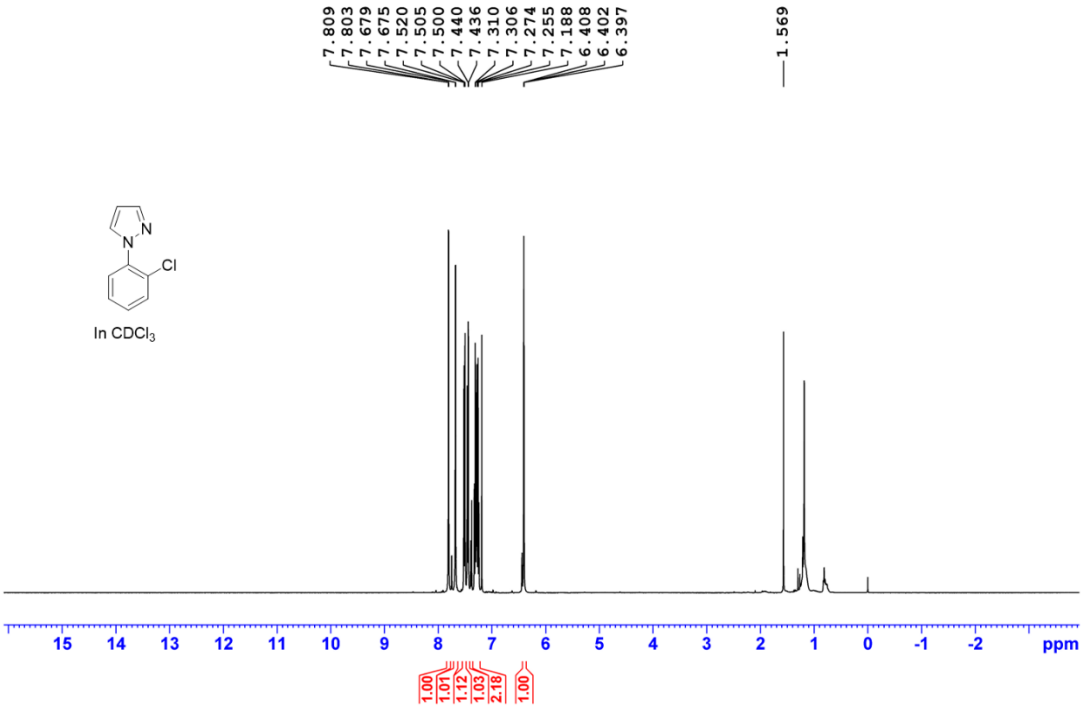

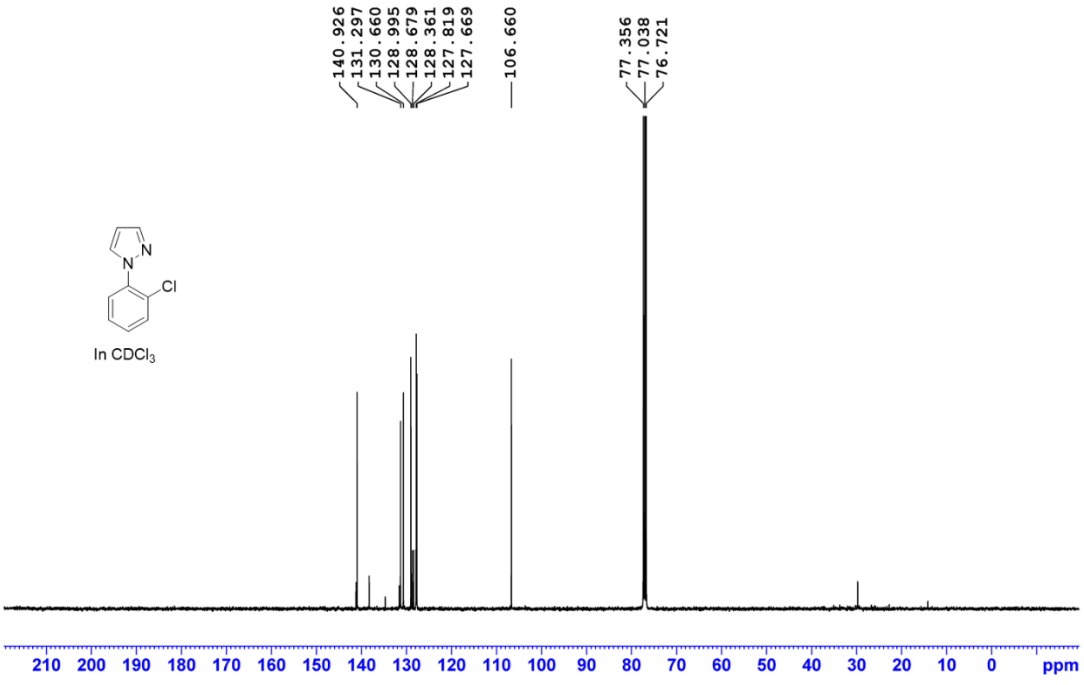

Supplementary Information

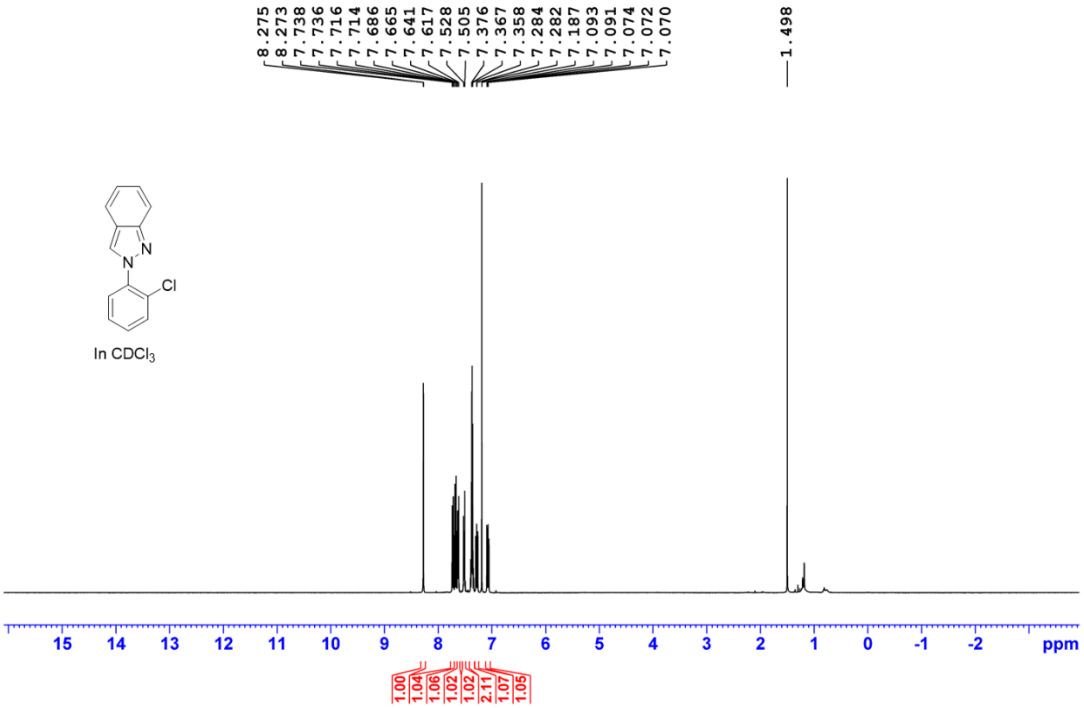

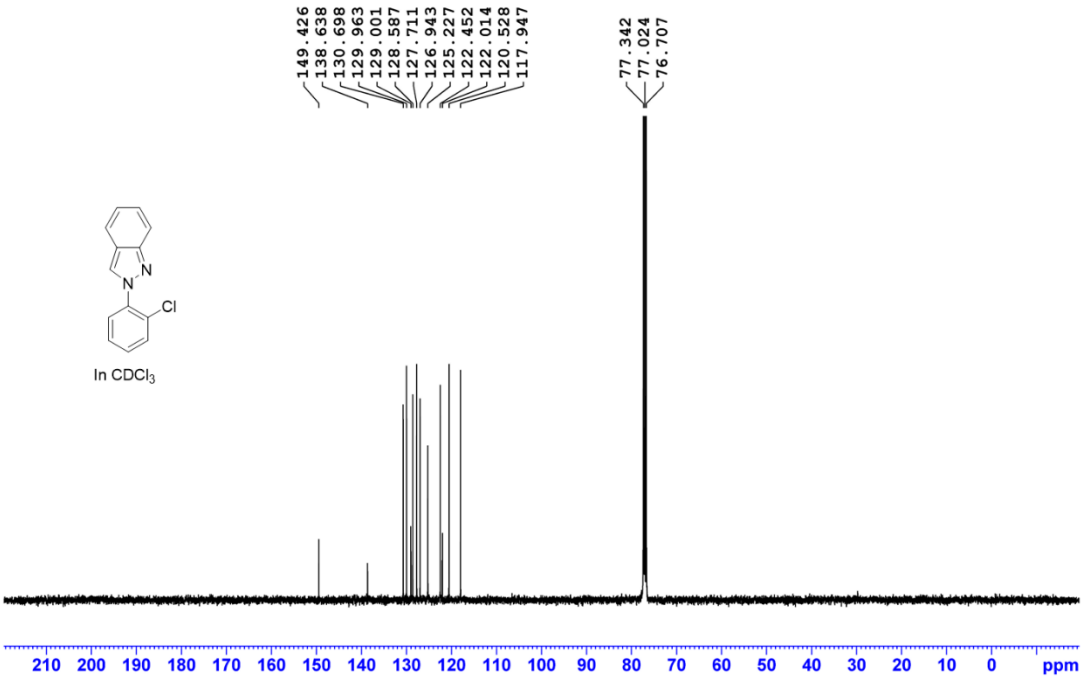

Supplementary Information

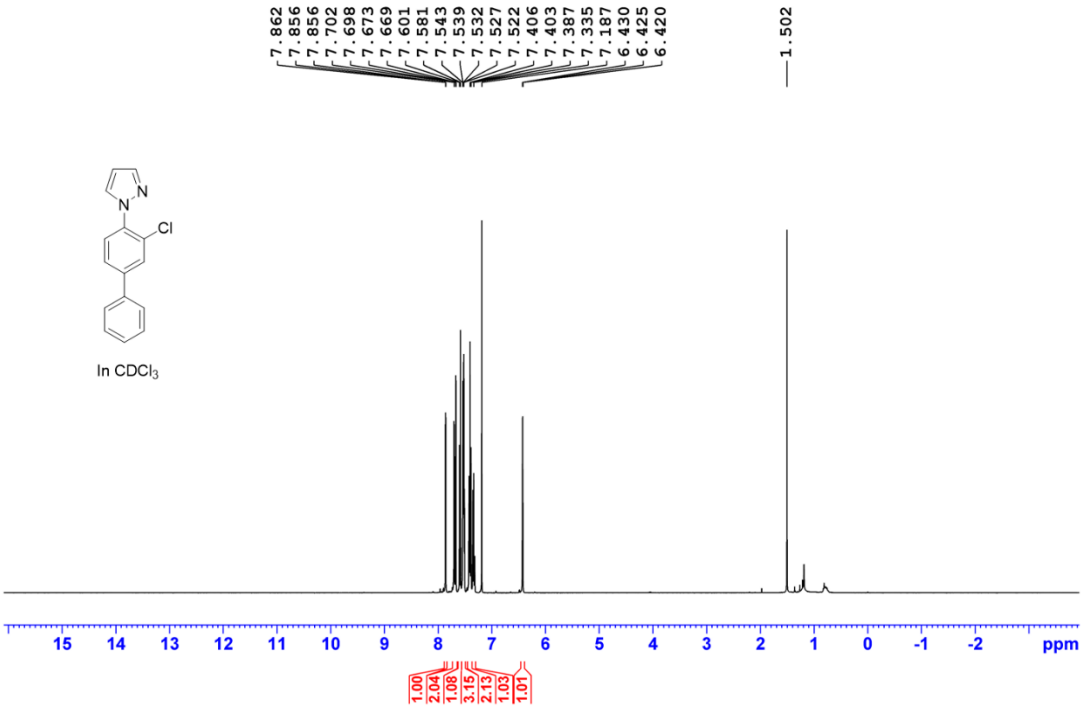

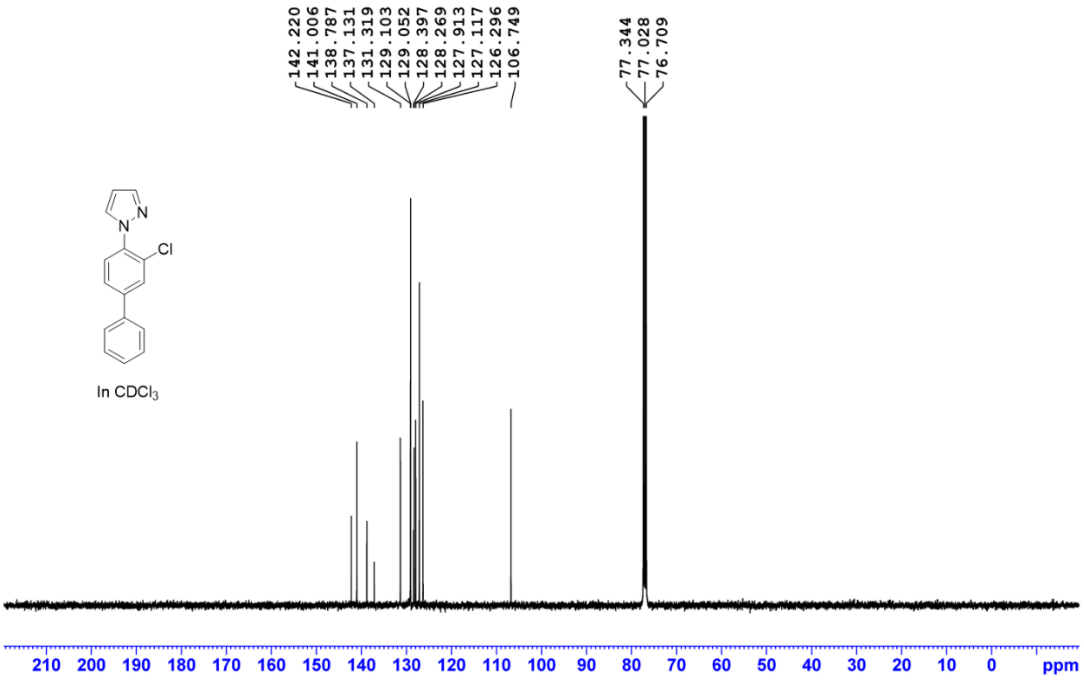

Supplementary Information

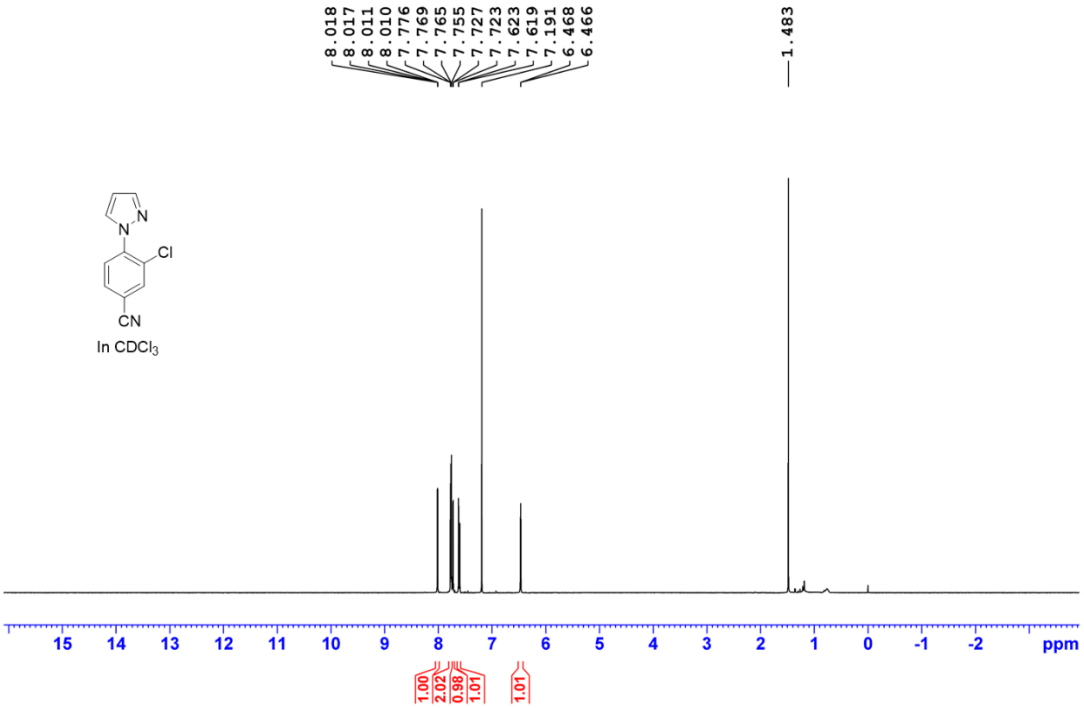

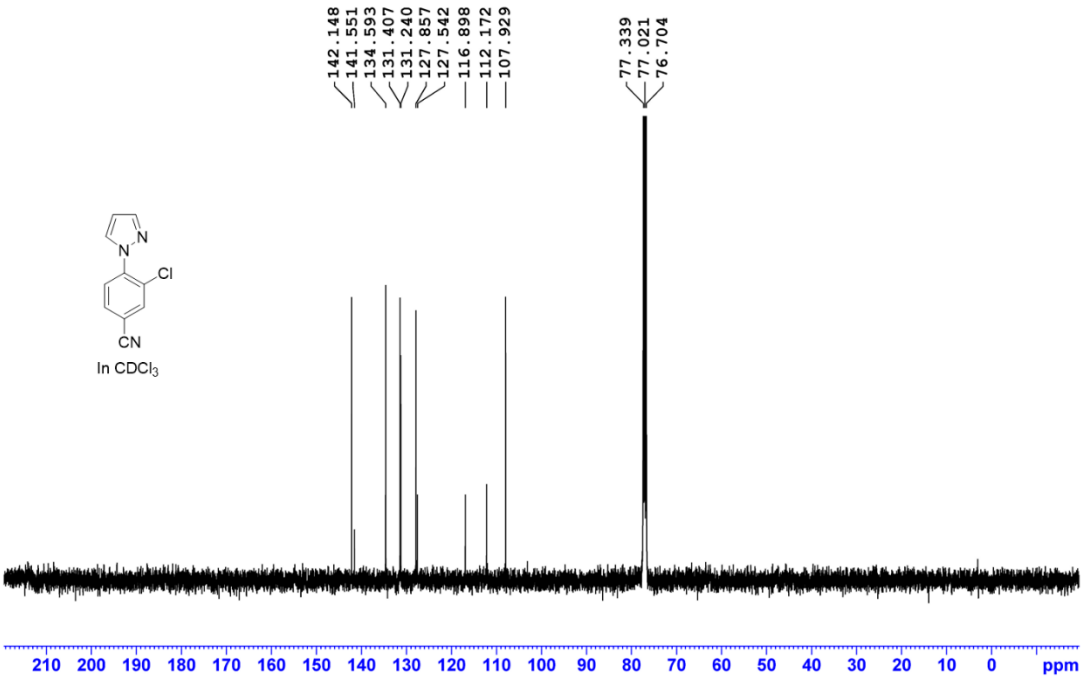

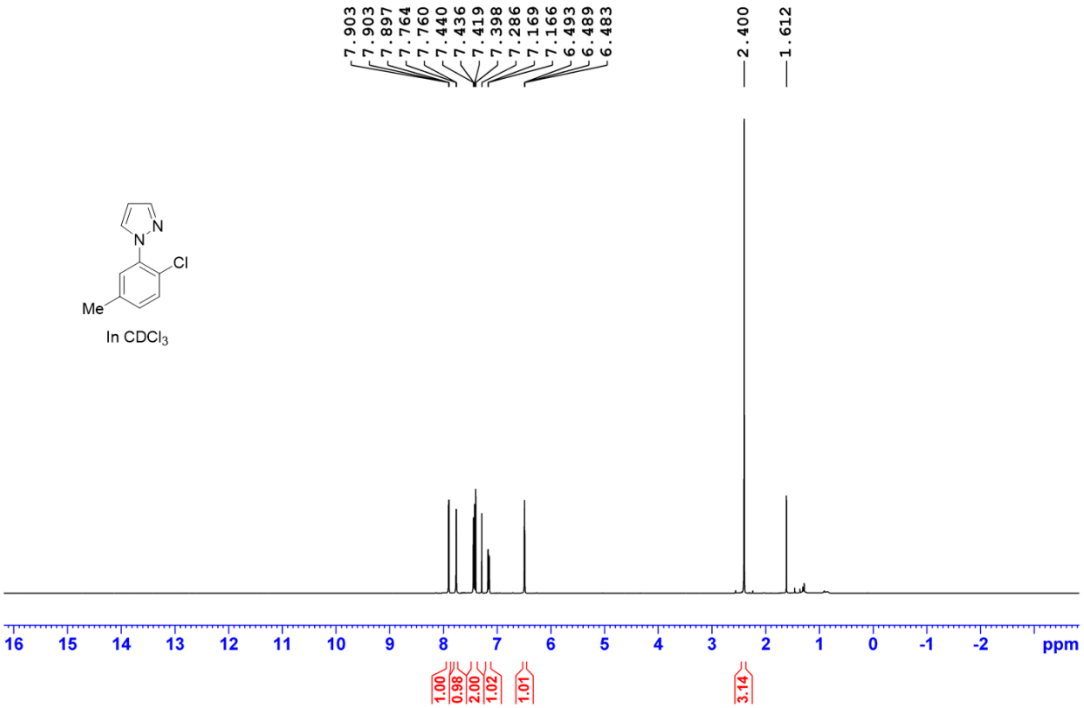
7.903
7.903
7.897
7.764
7.760
7.440
7.436
7.419
7.398
7.286
7.169
7.166
6.493
6.489
6.483
2.400
1.612
N
N
Cl
Me
In CDCl3
16 15 14 13 12 11 10 9 8 7 6 5 4 3 2 1 0 -1 -2 ppm
1.00
0.98
2.00
1.02
1.01
3.14

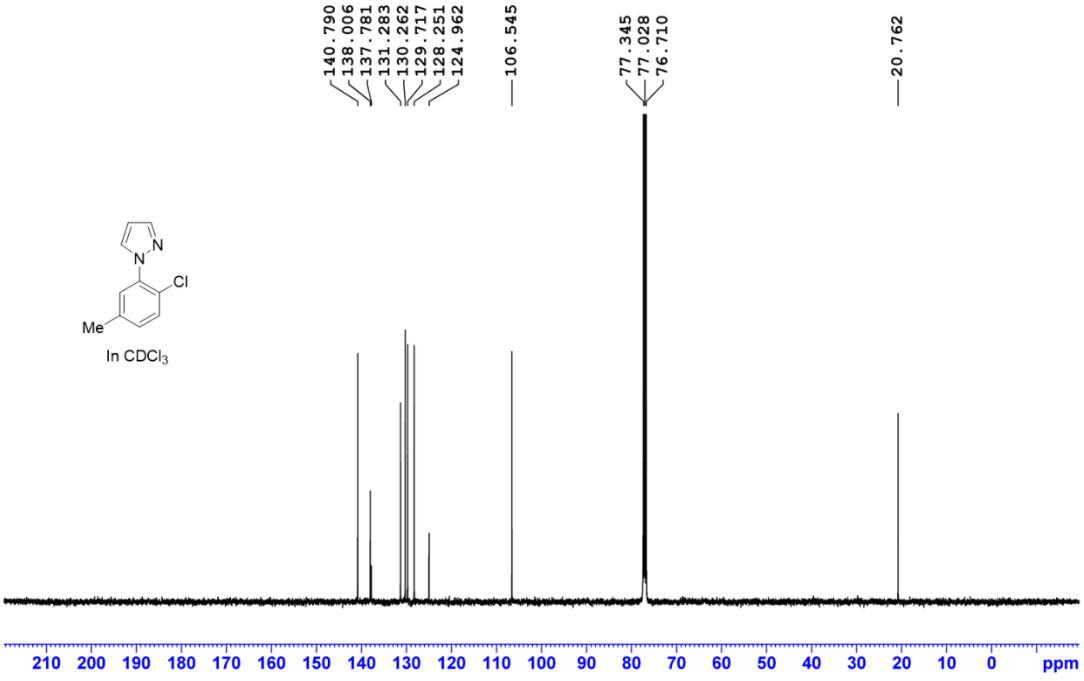
140.790
138.006
137.781
131.283
130.262
129.717
128.251
124.962
106.545
77.345
77.028
76.710
20.762
N
N
Cl
Me
In CDCl3
210 200 190 180 170 160 150 140 130 120 110 100 90 80 70 60 50 40 30 20 10 0 ppm

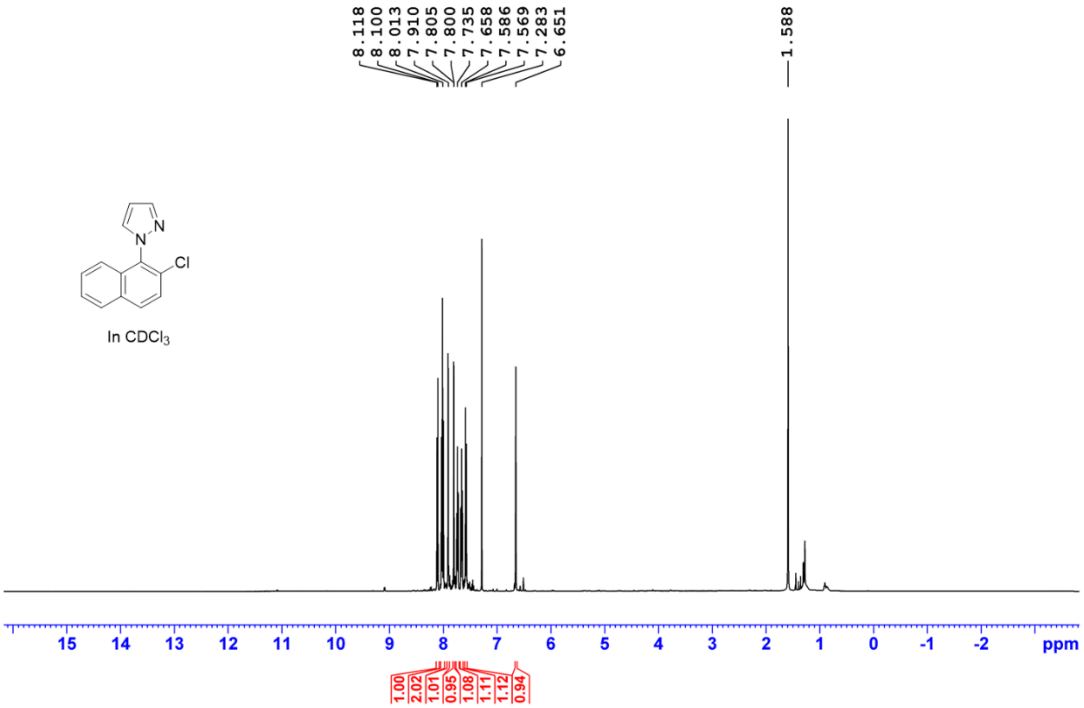
8.118
8.100
8.013
7.910
7.805
7.800
7.735
7.658
7.586
7.569
7.283
6.651
1.588
N
N
Cl
In CDCl3
15 14 13 12 11 10 9 8 7 6 5 4 3 2 1 0 -1 -2 ppm
1.00
2.02
1.01
0.95
1.08
1.11
1.12
0.94

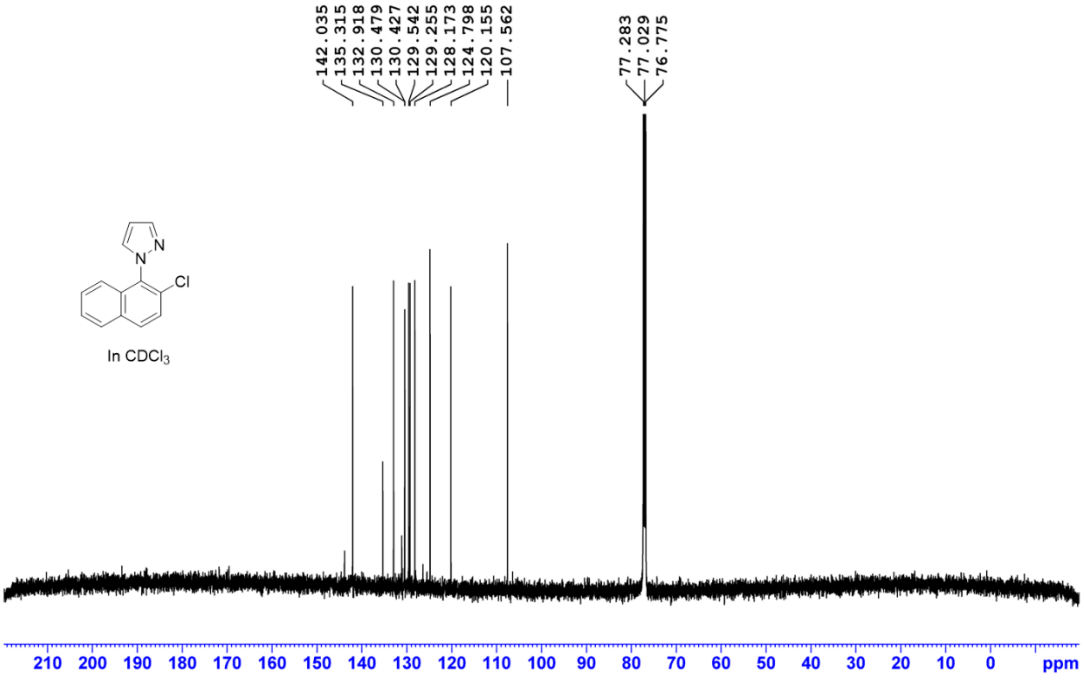
142.035
135.315
132.918
130.479
130.427
129.542
129.255
128.173
124.798
120.155
107.562
77.283
77.029
76.775
N
N
Cl
In CDCl3
210 200 190 180 170 160 150 140 130 120 110 100 90 80 70 60 50 40 30 20 10 0 ppm

Supplementary Information

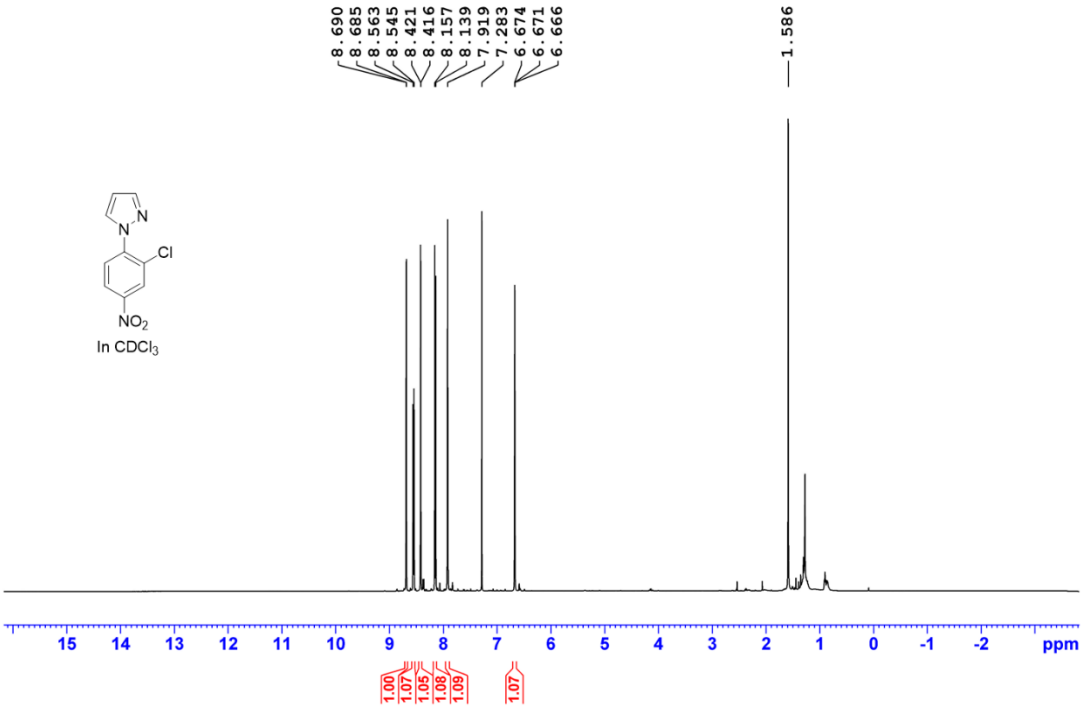

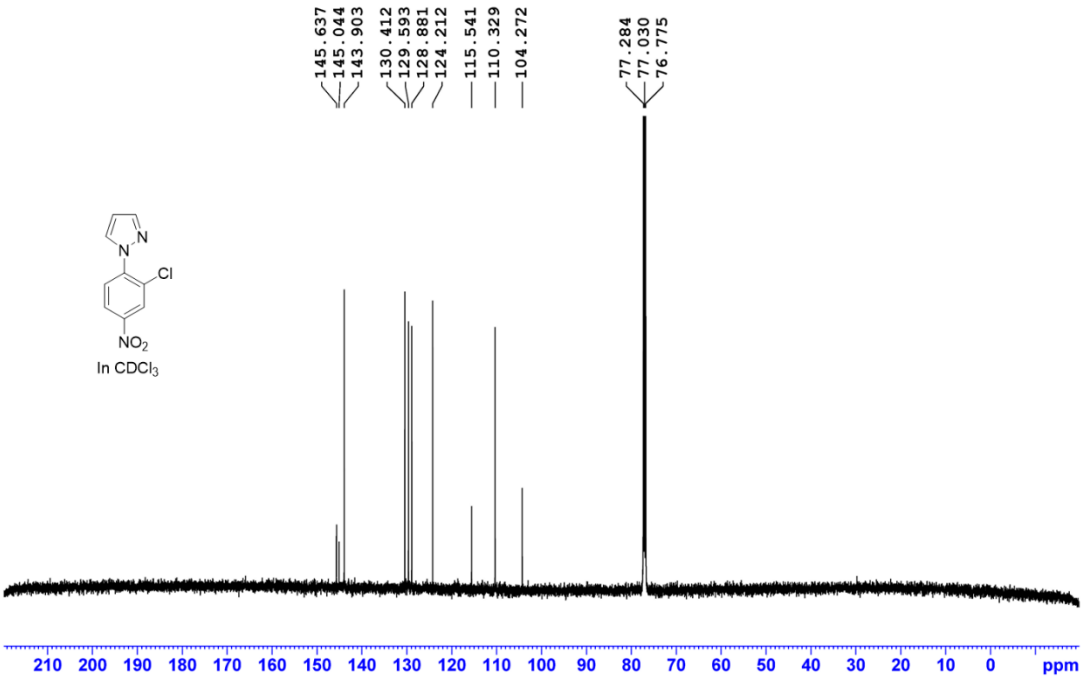

Supplementary Information

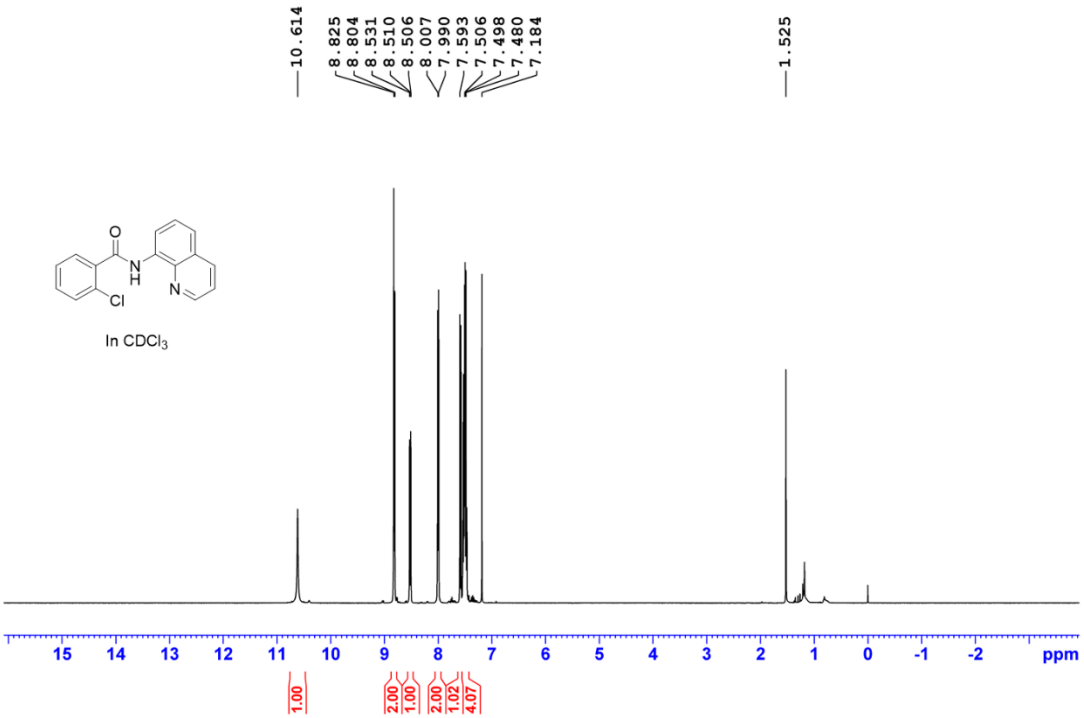

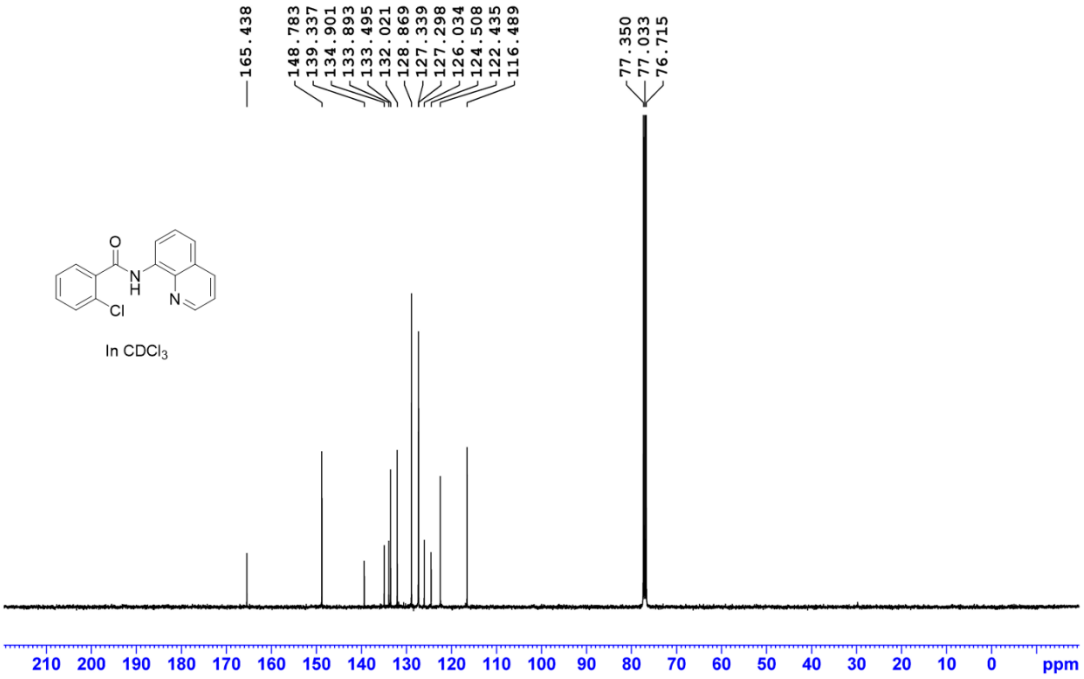

Supplementary Information

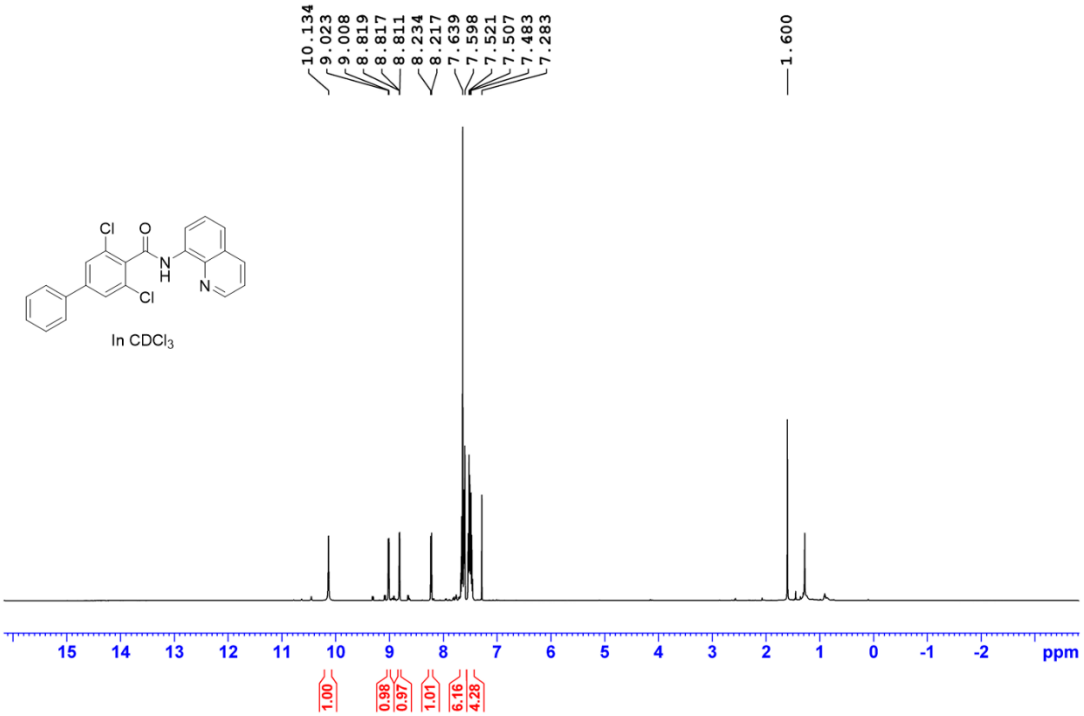

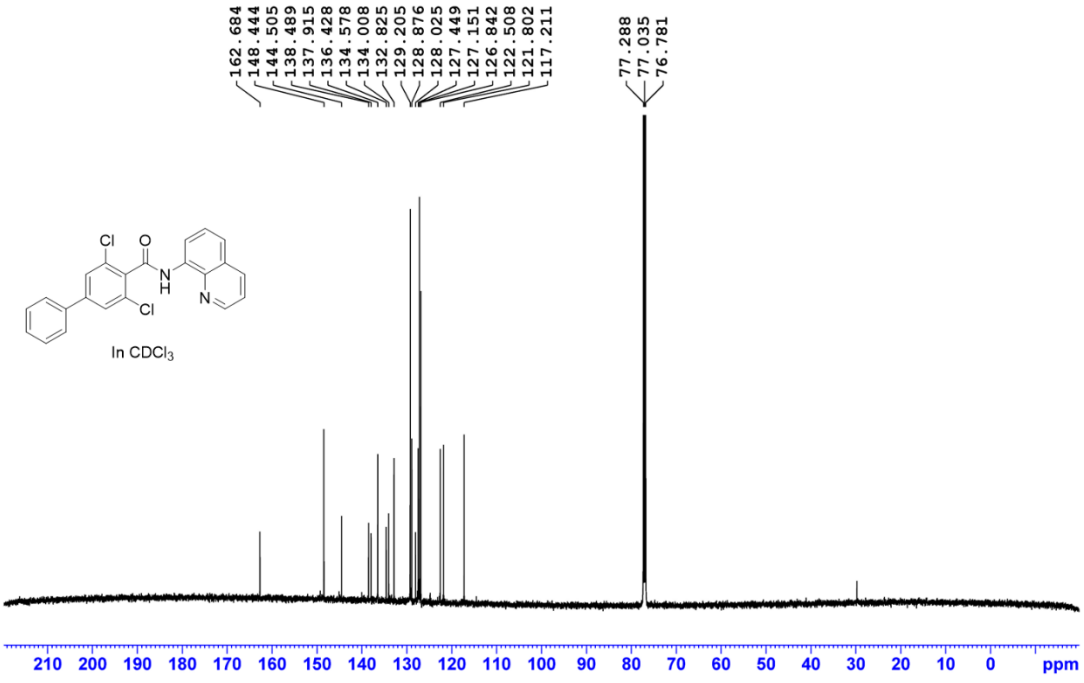

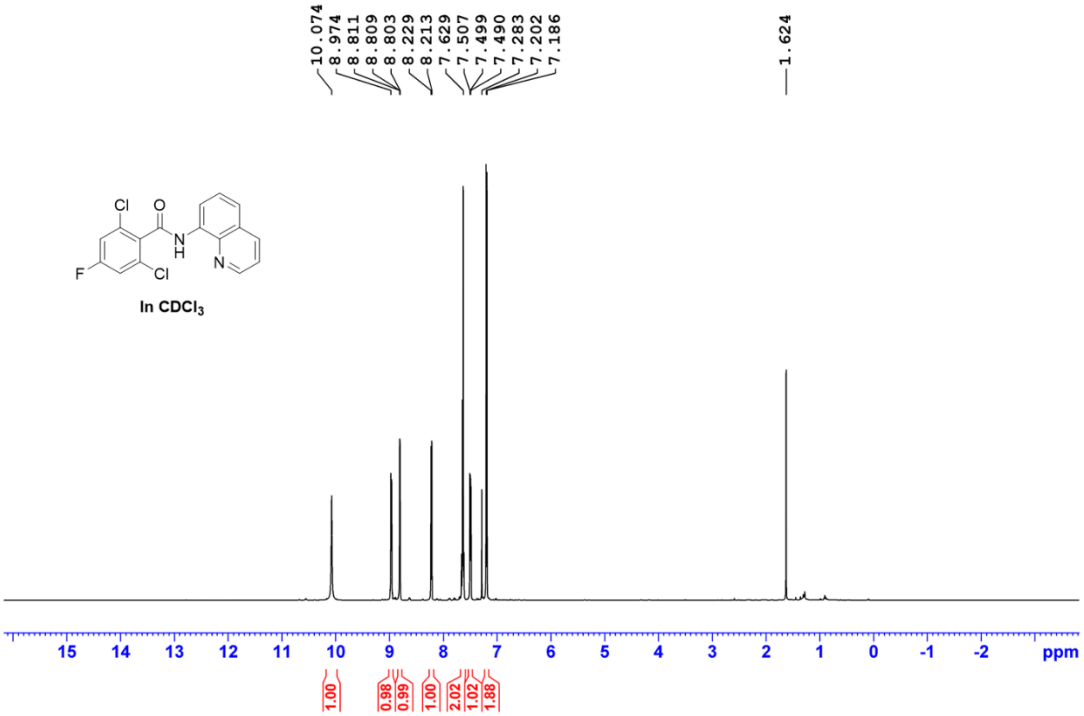
10.074
8.974
8.811
8.809
8.803
8.229
8.213
7.629
7.507
7.499
7.490
7.283
7.202
7.186
1.624
Cl
O
N
H
N
F
Cl
In CDCl3
15 14 13 12 11 10 9 8 7 6 5 4 3 2 1 0 -1 -2 ppm
1.00
0.98
0.99
1.00
2.02
1.02
1.88

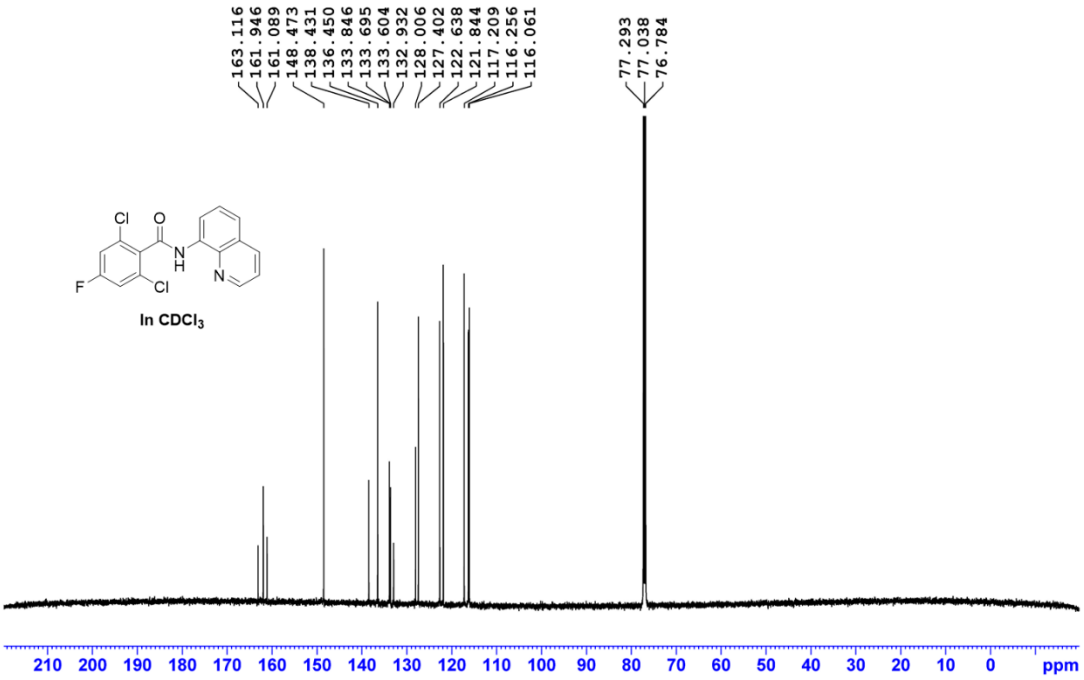
163.116
161.946
161.089
148.473
138.431
136.450
133.846
133.695
133.604
132.932
128.006
127.402
122.638
121.844
117.209
116.256
116.061
77.293
77.038
76.784
Cl
O
N
H
N
F
Cl
In CDCl3
210 200 190 180 170 160 150 140 130 120 110 100 90 80 70 60 50 40 30 20 10 0 ppm

Supplementary Information

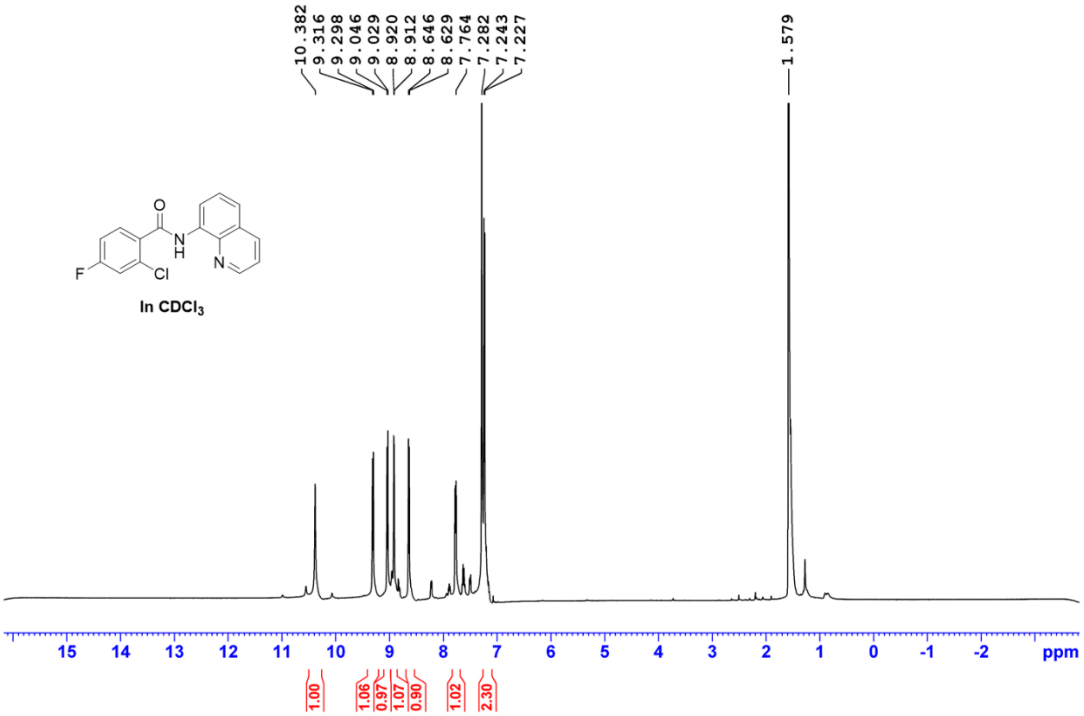

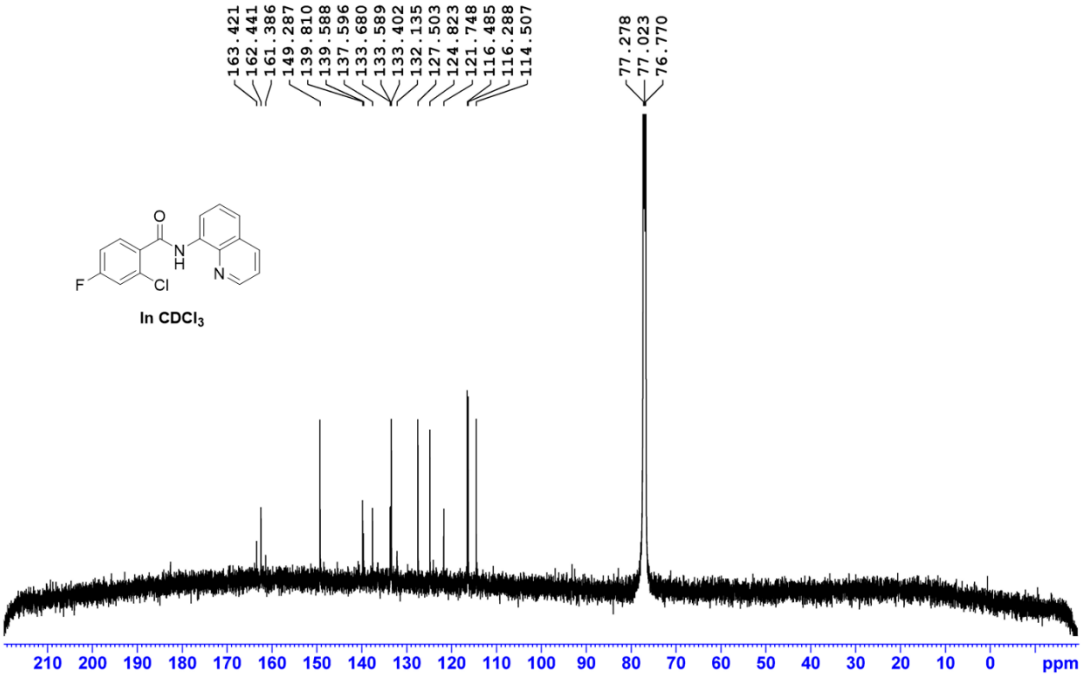

Supplementary Information

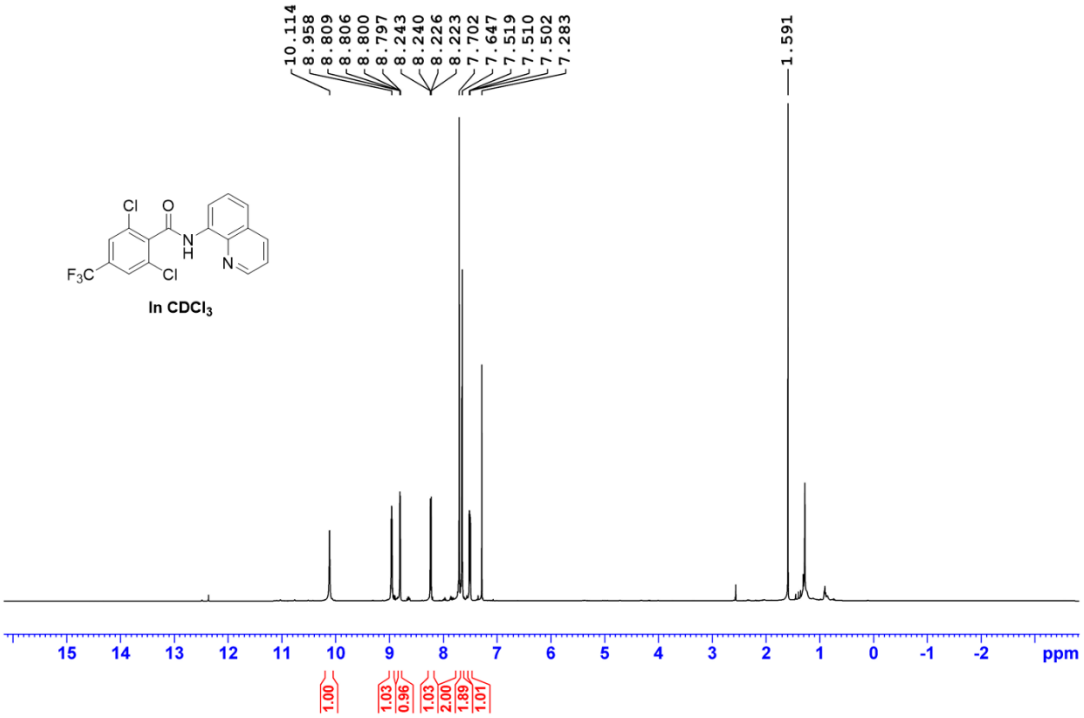

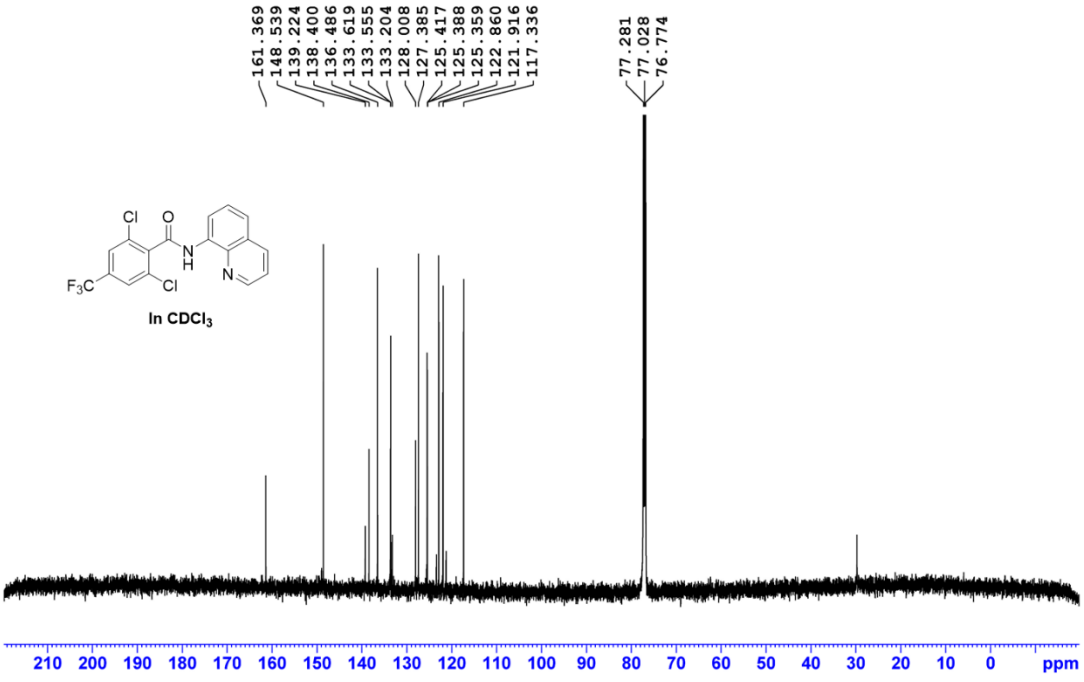

Supplementary Information

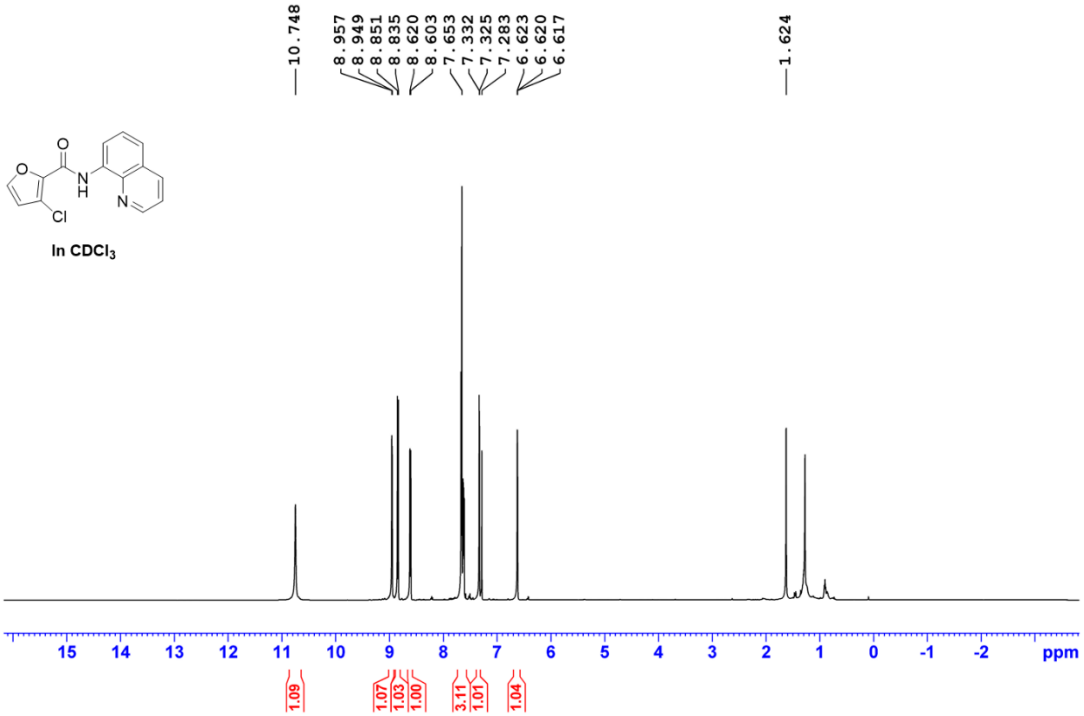

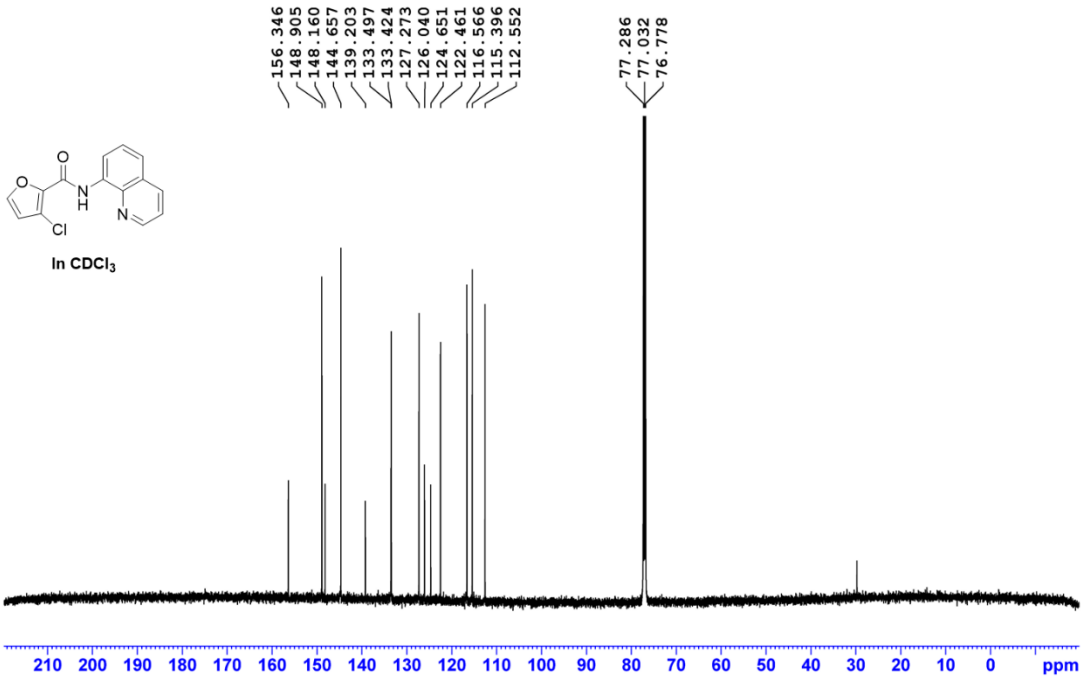

Supplementary Information

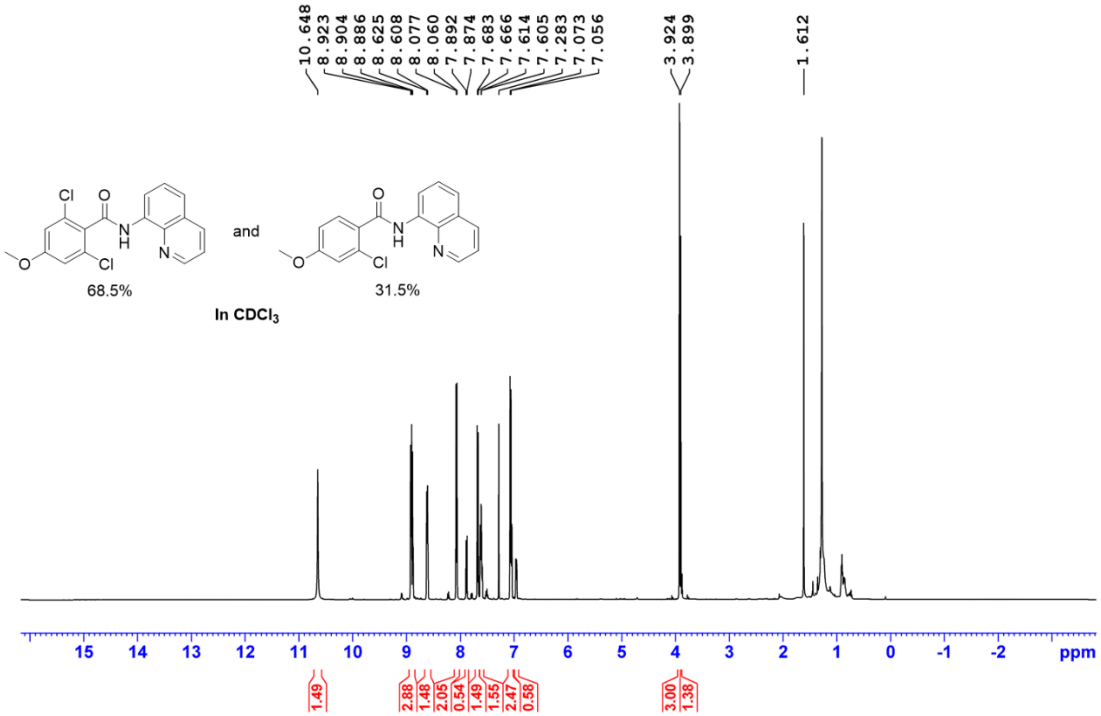

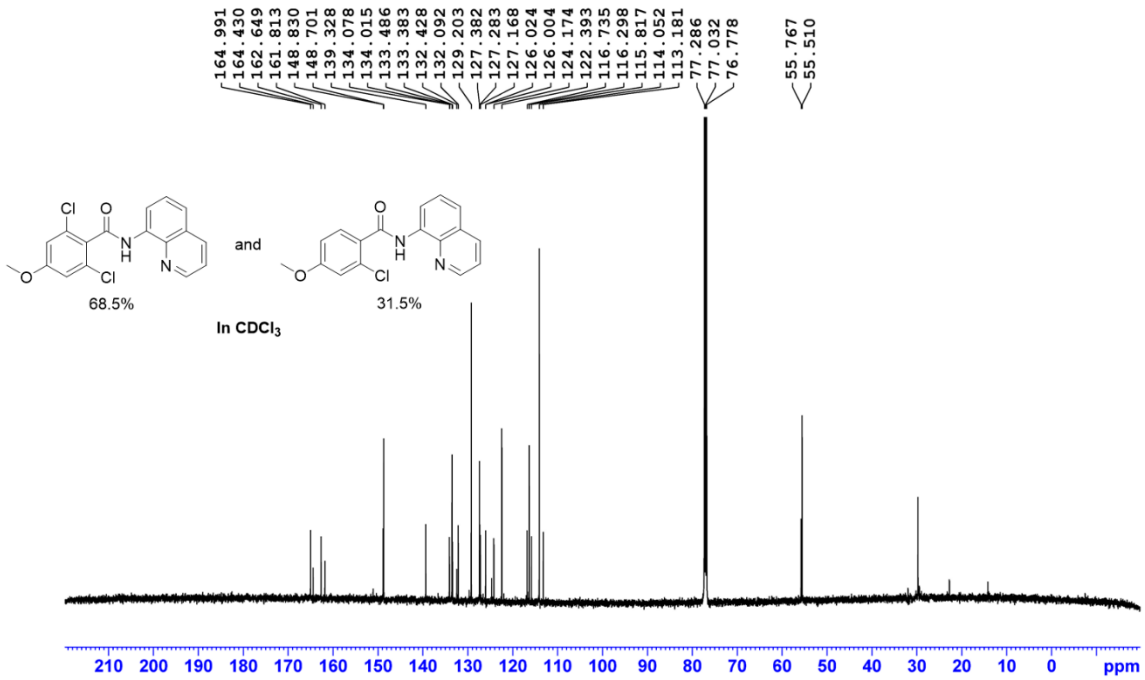

Supplementary Information

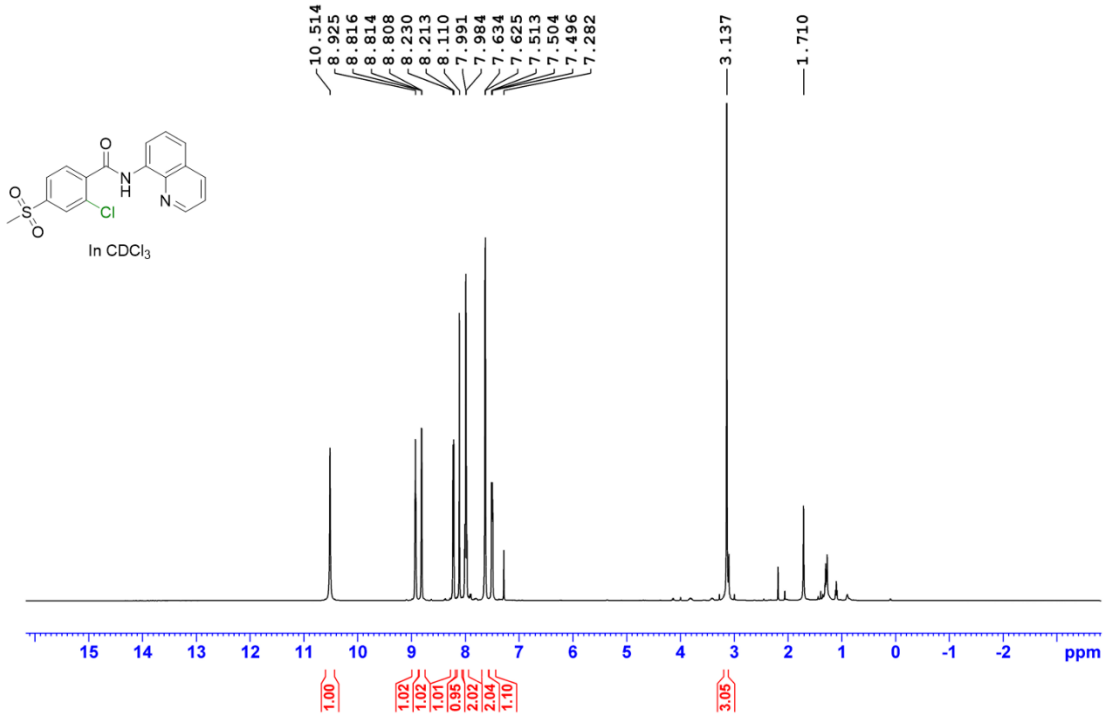

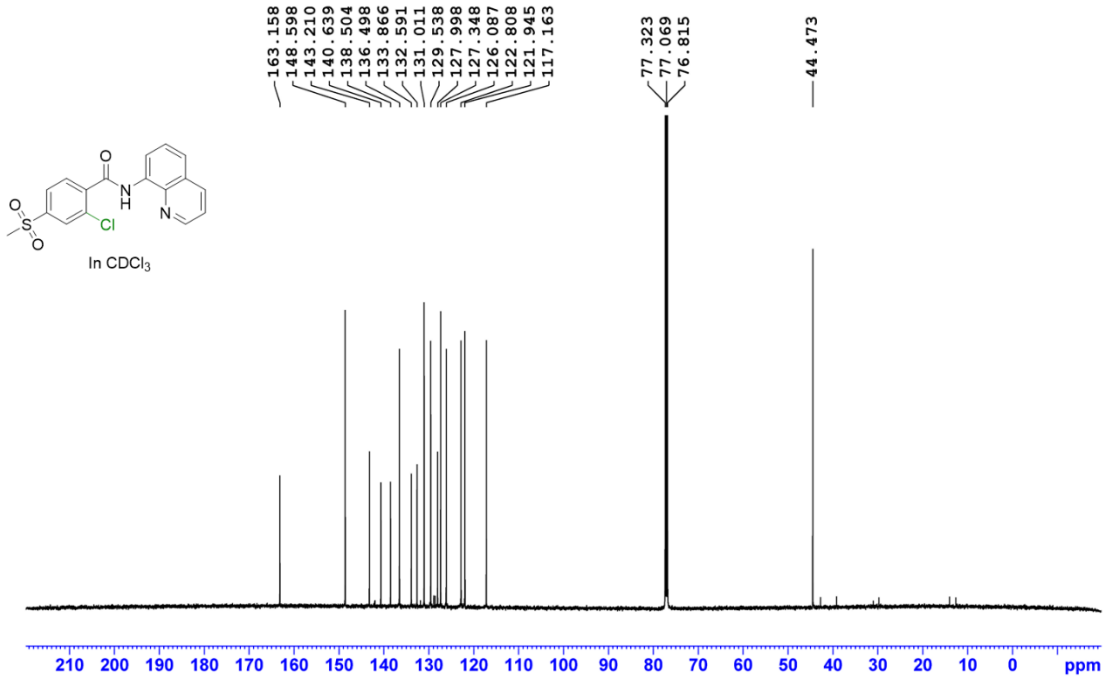

Supplementary Information

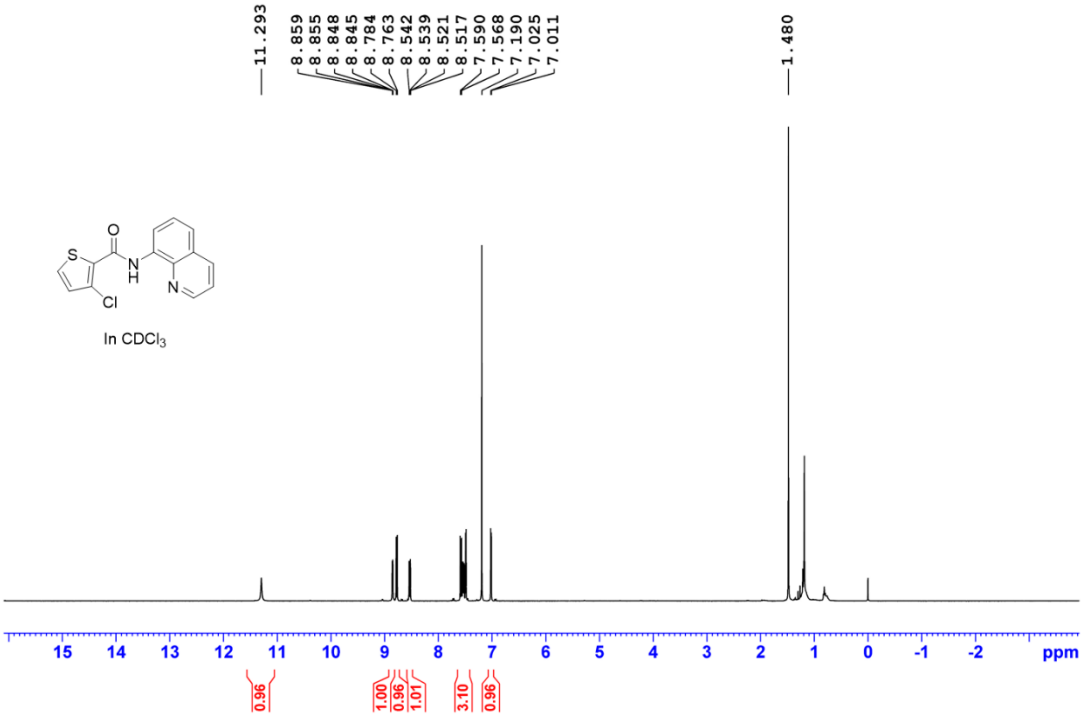

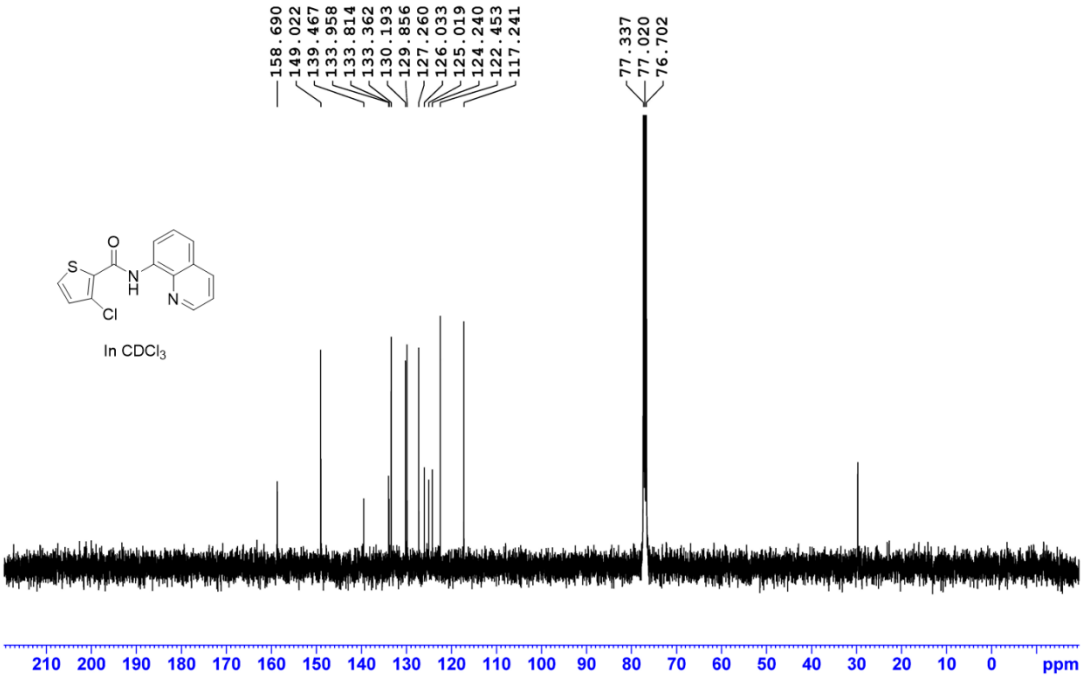

References

1. Huy, P. H.; Motsch, S.; Kappler, S. M., Formamides as Lewis Base Catalysts in SN Reactions—Efficient Transformation of Alcohols into Chlorides, Amines, and Ethers. *Angew. Chem., Int. Ed.* **2016**, *55*, 10145-10149.
2. Pritchard, J. G.; Vollmer, R. L., The meso and Racemic Forms of 2,4-Pentanediol and Certain of Their Derivatives. *J. Org. Chem.* **1963**, *28*, 1545-1549.
3. Dong, X.-Y.; Zhang, Y.-F.; Ma, C.-L.; Gu, Q.-S.; Wang, F.-L.; Li, Z.-L.; Jiang, S.-P.; Liu, X.-Y., A general asymmetric copper-catalysed Sonogashira C(sp3)–C(sp) coupling. *Nat. Chem.* **2019**, *11*, 1158-1166.
4. Littke, A. F.; Fu, G. C., A Convenient and General Method for Pd-Catalyzed Suzuki Cross-Couplings of Aryl Chlorides and Arylboronic Acids. *Angew. Chem., Int. Ed.* **1998**, *37*, 3387-3388.
5. Xu, Z.-L.; Li, H.-X.; Ren, Z.-G.; Du, W.-Y.; Xu, W.-C.; Lang, J.-P., Cu(OAc)2·H2O-catalyzed N-arylation of nitrogen-containing heterocycles. *Tetrahedron* **2011**, *67*, 5282-5288.
6. Thrimurtulu, N.; Dey, A.; Maiti, D.; Volla, C. M. R., Cobalt-Catalyzed sp2-C−H Activation: Intermolecular Heterocyclization with Allenes at Room Temperature. *Angew. Chem., Int. Ed.* **2016**, *55*, 12361-12365.
7. Powers, D. C.; Benitez, D.; Tkatchouk, E.; Goddard, W. A., III; Ritter, T., Bimetallic Reductive Elimination from Dinuclear Pd(III) Complexes. *J. Am. Chem. Soc.* **2010**, *132*, 14092-14103.
8. Yoshioka, T.; Furukawa, K.; Okuwaki, A., Chemical recycling of rigid-PVC by oxygen oxidation in NaOH solutions at elevated temperatures. *Polym. Degrad. Stab.* **2000**, *67*, 285-290.
9. Hashimoto, K.; Suga, S.; Wakayama, Y.; Funazukuri, T., Hydrothermal dechlorination of PVC in the presence of ammonia. *J. Mater. Sci.* **2008**, *43*, 2457-2462.
10. Zhao, T.; Zhou, Q.; He, X.-L.; Wei, S.-D.; Wang, L.; van Kasteren, J. M. N.; Wang, Y.-Z., A highly efficient approach for dehydrochlorinating polyvinyl chloride: catalysis by 1-butyl-3-methylimidazolium chloride. *Green Chem.* **2010**, *12*, 1062-1065.
11. Yoshihara, M.; Grause, G.; Kameda, T.; Yoshioka, T., Upgrading of poly(vinyl chloride) by chemical modifications using sodium sulfide. *J. Mater. Cycles Waste Manag.* **2010**, *12*, 264-270.
12. Kameda, T.; Wachi, S.; Grause, G.; Mizoguchi, T.; Yoshioka, T., Dehydrochlorination of poly(vinyl chloride) with Ca(OH)2 in ethylene glycol and the effect of ball milling. *J. Polym. Res.* **2011**, *18*, 1687-1691.
13. Glas, D.; Hulsbosch, J.; Dubois, P.; Binnemans, K.; De Vos, D. E., End-of-Life Treatment of Poly(Vinyl Chloride) and Chlorinated Polyethylene by Dehydrochlorination in Ionic Liquids. *ChemSusChem* **2014**, *7*, 610-617.
14. Oster, K.; Tedstone, A.; Greer, A. J.; Budgen, N.; Garforth, A.; Hardacre, C., Dehydrochlorination of PVC in multi-layered blisterpacks using ionic liquids. *Green Chem.* **2020**, *22*, 5132-5142.
15. Assefa, M. K.; Fieser, M. E., Divergent silylium catalysis enables facile poly(vinyl chloride) upcycling to poly(ethylene-co-styrene) derivatives. *J. Mater. Chem. A* **2023**, *11*, 2128-2132.
16. O'Rourke, G.; Hennebel, T.; Stalpaert, M.; Skorynina, A.; Bugaev, A.; Janssens, K.; Van Emelen, L.; Lemmens, V.; De Oliveira Silva, R.; Colemonts, C.; Gabriels, P.; Sakellariou, D.; De Vos, D., Catalytic tandem dehydrochlorination–hydrogenation of PVC towards valorisation of chlorinated plastic waste. *Chem. Sci.* **2023**, *14*, 4401-4412.
17. Zhou, Q.; Lan, W.; Du, A.; Wang, Y.; Yang, J.; Wu, Y.; Yang, K.; Wang, X., Lanthania promoted MgO: Simultaneous highly efficient catalytic degradation and dehydrochlorination of polypropylene/polyvinyl chloride. *Appl. Catal. B: Environ.* **2008**, *80*, 141-146.
18. Bae, S. Y.; Jeon, S.; Lee, Y. H.; Lee, D. H.; Kye, H.; Bae, J. W., Dehydrochlorination of polyvinylchloride using Al-modified graphitic-C3N4. *RSC Advances* **2016**, *6*, 20728-20733.
19. Chen, Y.; Zhang, S.; Han, X.; Zhang, X.; Yi, M.; Yang, S.; Yu, D.; Liu, W., Catalytic Dechlorination and Charring Reaction of Polyvinyl Chloride by CuAl Layered Double Hydroxide. *Energy Fuels* **2018**, *32*, 2407-2413.

20. Gao, Z.; Lu, L.; Shi, C.; Qian, X.; Wang, X.; Zhang, G.; Zhou, M.; Pan, Y., The study of ZnAl and ZnFe layered double hydroxide on the catalytic dechlorination and fire safety of polyvinyl chloride. *J. Therm. Anal. Calorim.* **2020**, *140*, 115-123.
21. Jin, D.; Khanal, S.; Xu, S., Effects of ZnAl layered double hydroxide and benzimidazole derivative on the dechlorination of poly(vinyl chloride). *Appl. Clay Sci.* **2021**, *208*, 106114.
22. Kots, P. A.; Vance, B. C.; Quinn, C. M.; Wang, C.; Vlachos, D. G., A two-stage strategy for upcycling chlorine-contaminated plastic waste. *Nature Sustainability* **2023**, *6*, 1258-1267.
23. Pearson, D. M.; Conley, N. R.; Waymouth, R. M., Palladium-Catalyzed Carbonylation of Diols to Cyclic Carbonates. *Adv. Synth. Catal.* **2011**, *353*, 3007-3013.
24. Eytel, L. M.; Fargher, H. A.; Haley, M. M.; Johnson, D. W., The road to aryl CH⋯anion binding was paved with good intentions: fundamental studies, host design, and historical perspectives in CH hydrogen bonding. *Chem. Commun.* **2019**, *55*, 5195-5206.
25. Wang, L.; Zhang, R.-z.; Deng, R.; Luo, Y.-h., Oxygen-Induced Enhancement in Low-Temperature Dechlorination of PVC: An Experimental and DFT Study on the Oxidative Pyrolysis Process. *ACS Sustain. Chem. Eng.* **2021**, *9*, 2835-2843.
26. Zhang, R.-z.; Wang, L.-z.; Deng, R.-q.; Luo, Y.-h., Inhibition on Chloroaromatics during thermal conversion processes of Municipal Solid Waste by oxygen-induced low-temperature pre-dechlorination and hydrogen-assisted in-situ Cl capture. *Fuel Process. Technol.* **2022**, *237*, 107445.
27. Song, S.; Li, X.; Wei, J.; Wang, W.; Zhang, Y.; Ai, L.; Zhu, Y.; Shi, X.; Zhang, X.; Jiao, N., DMSO-catalysed late-stage chlorination of (hetero)arenes. *Nat. Catal.* **2020**, *3*, 107-115.
28. Nizovtsev, A. S.; Bogdanchikov, G. A.; Baklanov, A. V., The computational study of the "inversion substitution" reactions CX3Br+O2→CX3O2+Br (X=H, F). *Combust. Flame* **2010**, *157*, 1382-1389.
29. Richard, J. P.; Jencks, W. P., Concerted bimolecular substitution reactions of 1-phenylethyl derivatives. *J. Am. Chem. Soc.* **1984**, *106*, 1383-1396.
30. Hasan, T.; Sims, L. B.; Fry, A., Heavy atom isotope effect studies of elimination reaction mechanisms. 1. A kinetic and carbon-14 kinetic isotope effect study of the base-promoted dehydrochlorination of substituted 1-phenylethyl-2-14C chlorides. *J. Am. Chem. Soc.* **1983**, *105*, 3967-3975.
31. Wang, Z.; Bachman, S.; Dudnik, A. S.; Fu, G. C., Nickel-Catalyzed Enantioconvergent Borylation of Racemic Secondary Benzylic Electrophiles. *Angew. Chem., Int. Ed.* **2018**, *57*, 14529-14532.
32. Mueller, J. A.; Goller, C. P.; Sigman, M. S., Elucidating the Significance of β-Hydride Elimination and the Dynamic Role of Acid/Base Chemistry in a Palladium-Catalyzed Aerobic Oxidation of Alcohols. *J. Am. Chem. Soc.* **2004**, *126*, 9724-9734.
33. Schultz, M. J.; Park, C. C.; Sigman, M. S., A convenient palladium-catalyzed aerobic oxidation of alcohols at room temperature. *Chem. Commun.* **2002**, 3034-3035.
34. Schultz, M. J.; Adler, R. S.; Zierkiewicz, W.; Privalov, T.; Sigman, M. S., Using Mechanistic and Computational Studies To Explain Ligand Effects in the Palladium-Catalyzed Aerobic Oxidation of Alcohols. *J. Am. Chem. Soc.* **2005**, *127*, 8499-8507.
35. Wang, D.; Weinstein, A. B.; White, P. B.; Stahl, S. S., Ligand-Promoted Palladium-Catalyzed Aerobic Oxidation Reactions. *Chem. Rev.* **2018**, *118*, 2636-2679.
36. Liu, M.; Zhang, Z.; Song, J.; Liu, S.; Liu, H.; Han, B., Nitrogen Dioxide Catalyzed Aerobic Oxidative Cleavage of C(OH)–C Bonds of Secondary Alcohols to Produce Acids. *Angew. Chem., Int. Ed.* **2019**, *58*, 17393-17398.
37. Piera, J.; Bäckvall, J.-E., Catalytic Oxidation of Organic Substrates by Molecular Oxygen and Hydrogen Peroxide by Multistep Electron Transfer—A Biomimetic Approach. *Angew. Chem., Int. Ed.* **2008**, *47*, 3506-3523.
38. Whitfield, S. R.; Sanford, M. S., Reactivity of Pd(II) Complexes with Electrophilic Chlorinating Reagents: Isolation of Pd(IV) Products and Observation of C−Cl Bond-Forming Reductive Elimination. *J. Am. Chem. Soc.* **2007**, *129*, 15142-15143.
39. Song, B.; Zheng, X.; Mo, J.; Xu, B., Palladium-Catalyzed Monoselective Halogenation of C□H Bonds: Efficient Access to Halogenated Arylpyrimidines using Calcium Halides. *Adv. Synth. Catal.* **2010**, *352*, 329-335.

40. Phan, N. T. S.; Van Der Sluys, M.; Jones, C. W., On the Nature of the Active Species in Palladium Catalyzed Mizoroki–Heck and Suzuki–Miyaura Couplings – Homogeneous or Heterogeneous Catalysis, A Critical Review. *Adv. Synth. Catal.* **2006**, *348*, 609-679.
41. Chernyshev, V. M.; Astakhov, A. V.; Chikunov, I. E.; Tyurin, R. V.; Eremin, D. B.; Ranny, G. S.; Khrustalev, V. N.; Ananikov, V. P., Pd and Pt Catalyst Poisoning in the Study of Reaction Mechanisms: What Does the Mercury Test Mean for Catalysis? *ACS Catal.* **2019**, *9*, 2984-2995.
42. Ji, Y.; Jain, S.; Davis, R. J., Investigation of Pd Leaching from Supported Pd Catalysts during the Heck Reaction. *J. Phys. Chem. B* **2005**, *109*, 17232-17238.
43. Chen, X.; Hao, X.-S.; Goodhue, C. E.; Yu, J.-Q., Cu(II)-Catalyzed Functionalizations of Aryl C−H Bonds Using O2 as an Oxidant. *J. Am. Chem. Soc.* **2006**, *128*, 6790-6791.
44. Yang, L.; Lu, Z.; Stahl, S. S., Regioselective copper-catalyzed chlorination and bromination of arenes with O2 as the oxidant. *Chem. Commun.* **2009**, 6460-6462.
45. Wang, W.; Pan, C.; Chen, F.; Cheng, J., Copper(ii)-catalyzed ortho-functionalization of 2-arylpyridines with acyl chlorides. *Chem. Commun.* **2011**, *47*, 3978-3980.
46. Pye, D. R.; Mankad, N. P., Bimetallic catalysis for C–C and C–X coupling reactions. *Chem. Sci.* **2017**, *8*, 1705-1718.
47. Kim, U. B.; Jung, D. J.; Jeon, H. J.; Rathwell, K.; Lee, S.-g., Synergistic Dual Transition Metal Catalysis. *Chem. Rev.* **2020**, *120*, 13382-13433.
48. Kakiuchi, F.; Kochi, T.; Mutsutani, H.; Kobayashi, N.; Urano, S.; Sato, M.; Nishiyama, S.; Tanabe, T., Palladium-Catalyzed Aromatic C−H Halogenation with Hydrogen Halides by Means of Electrochemical Oxidation. *J. Am. Chem. Soc.* **2009**, *131*, 11310-11311.
49. Dick, A. R.; Hull, K. L.; Sanford, M. S., A Highly Selective Catalytic Method for the Oxidative Functionalization of C−H Bonds. *J. Am. Chem. Soc.* **2004**, *126*, 2300-2301.
50. Fagnani, D. E.; Kim, D.; Camarero, S. I.; Alfaro, J. F.; McNeil, A. J., Using waste poly(vinyl chloride) to synthesize chloroarenes by plasticizer-mediated electro(de)chlorination. *Nat. Chem.* **2022**.
51. López Granados, M.; Moreno, J.; Alba-Rubio, A. C.; Iglesias, J.; Martín Alonso, D.; Mariscal, R., Catalytic transfer hydrogenation of maleic acid with stoichiometric amounts of formic acid in aqueous phase: paving the way for more sustainable succinic acid production. *Green Chem.* **2020**, *22*, 1859-1872.
52. Escobar-Hernandez, H. U.; Quan, Y.; Papadaki, M. I.; Wang, Q., Life Cycle Assessment of Metal–Organic Frameworks: Sustainability Study of Zeolitic Imidazolate Framework-67. *ACS Sustain. Chem. Eng.* **2023**, *11*, 4219-4225.